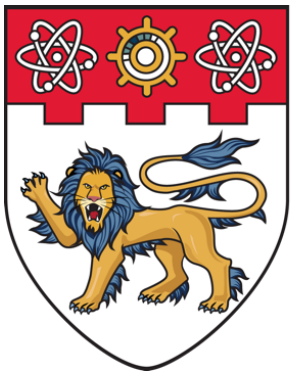

NANYANG TECHNOLOGICAL UNIVERSITY
SINGAPORE

TRANSFORMATIONS OF CYCLOPROPANOLS VIA ZINC HOMOENOLATE AND ENOLIZED HOMOENOLATE

SEKIGUCHI YOSHIYA

SCHOOL OF CHEMISTRY, CHEMICAL ENGINEERING AND BIOTECHNOLOGY

2023

TRANSFORMATIONS OF CYCLOPROPANOLS VIA ZINC HOMOENOLATE AND ENOLIZED HOMOENOLATE

SEKIGUCHI YOSHIYA

SCHOOL OF CHEMISTRY, CHEMICAL ENGINEERING AND BIOTECHNOLOGY

A thesis submitted to the Nanyang Technological University in partial fulfilment of the requirement for the degree of Doctor of Philosophy

2023

Statement of Originality

I hereby certify that the work embodied in this thesis is the result of original research done by me except where otherwise stated in this thesis. The thesis work has not been submitted for a degree or professional qualification to any other university or institution. I declare that this thesis is written by myself and is free of plagiarism and of sufficient grammatical clarity to be examined. I confirm that the investigations were conducted in accord with the ethics policies and integrity standards of Nanyang Technological University and that the research data are presented honestly and without prejudice.

01-Aug-2022

. . . . . .

Date

. . . . . .

Sekiguchi Yoshiya

Supervisor Declaration Statement

I have reviewed the content and presentation style of this thesis and declare it of sufficient grammatical clarity to be examined. To the best of my knowledge, the thesis is free of plagiarism and the research and writing are those of the candidate's except as acknowledged in the Author Attribution Statement. I confirm that the investigations were conducted in accord with the ethics policies and integrity standards of Nanyang Technological University and that the research data are presented honestly and without prejudice.

02-Aug-2022

. . . . . .
Date

. . . . . .
Professor Shunsuke Chiba

Authorship Attribution Statement

This thesis contains material from 4 papers published in the following peer-reviewed journals in which I am listed as an author.

Chapter 1 is published as Sekiguchi, Y.; Yoshikai, N., Metal-Catalyzed Transformations of Cyclopropanols via Homoenolates. *Bull. Chem. Soc. Jpn.* **2021,** *94*, 265-280. DOI: 10.1246/bcsj.20200270

The contributions of the co-authors are as follows:

- Prof. Yoshikai provided the initial project direction and edited the manuscript drafts.
- I prepared the manuscript drafts.

Chapter 2 is published as Sekiguchi, Y.; Yoshikai, N., Enantioselective Conjugate Addition of Catalytically Generated Zinc Homoenolate. *J. Am. Chem. Soc.* **2021,** *143*, 4775-4781. DOI: 10.1021/jacs.1c00869.

The contributions of the co-authors are as follows:

- Prof. Yoshikai provided the initial project direction and edited the manuscript drafts.
- I performed all the laboratory work and prepared the manuscript drafts.

Chapter 3 is published as Sekiguchi, Y.; Yoshikai, N., Zinc-Catalyzed *β*-Functionalization of Cyclopropanols via Enolized Homoenolate. *J. Am. Chem. Soc.* **2021,** *143*, 18400-18405. DOI: 10.1021/jacs.1c10109.

The contributions of the co-authors are as follows:

- Prof. Yoshikai provided the initial project direction and edited the manuscript drafts.
- I performed all the laboratory work and prepared the manuscript drafts.

Chapter 4 is published as Sekiguchi, Y.; Yoshikai, N., Zinc-Mediated Hydroxyallylation of Aldehydes with Cyclopropanols: Direct Access to Vicinal *anti-sec,tert*-Diols via Enolized Homoenolates. *Org. Lett.* **2022,** *24,* 960-965. DOI: 10.1021/acs.orglett.1c04331.

The contributions of the co-authors are as follows:

- Prof. Yoshikai provided the initial project direction, edited the manuscript drafts and conducted the DFT calculations.
- I performed all the laboratory work and prepared the manuscript drafts.

01-Aug-2022

. . . . . .
Date

. . . . . .
Sekiguchi Yoshiya

Abstract

Cyclopropanols have emerged as easily accessible precursors for the *in situ* generation of keto-homoenolates in the presence of metal catalysts and reagents. This thesis describes the discovery and development of three different transformations of a cyclopropanol that utilize a zinc homoenolate as a common intermediate. Chapter 1 provides a general introduction to the chemistry of metal homoenolate and its enolized species referred to as enolized homoenolate, followed by the design and summary of this thesis research. Chapter 2 describes the development of a zinc-catalyzed enantioselective ring-opening conjugate addition of a cyclopropanol to an enone. A catalyst generated from diethylzinc and a chiral *β*-aminoalcohol promotes ring-opening/1,4-addition of the cyclopropanol to the enone to give a 1,6-diketone, which then undergoes intramolecular aldol condensation to afford a cyclopentene derivatives in good yield and enantioselectivity. Chapter 3 describes a zinc-catalyzed *β*-allylation of a cyclopropanol with a Morita−Baylis−Hillman (MBH)-type allylic carbonate with retention of the cyclopropane ring. The key intermediate in this reaction is a catalytically generated enolized homoenolate, which is a bis-nucleophilic species generated through enolization of a zinc homoenolate intermediate. The enolized homoenolate reacts with the MBH carbonate at the *α*-position to generate the *β*-allylated zinc homoenolate, which then undergoes cyclization to afford the *β*-allylated cyclopropanol. Chapter 4 describes a zinc-mediated *α*-hydroxyallylation of an aldehyde with a cyclopropanol via an enolized homoenolate. In this reaction, the enolized homoenolate acts as a *γ*-oxyallyl nucleophile and reacts with the aldehyde to form a vicinal *anti-sec,tert*-diol in a diastereoselective manner.

Acknowledgements

I would like to express the most important acknowledgement of gratitude to my supervisor, Professor Naohiko Yoshikai for giving me a chance to conduct my Ph.D. study under him. I will always be grateful for his patient support and guidance. I wish to extend my thanks to my current supervisor Professor Shunsuke Chiba for his kind help and support in the last phase of the study.

My Ph.D. study was covered by the AcRF (Academic Research Fund) Research Scholarship. I sincerely appreciate the Ministry of Education and NTU for the financial support.

I am also thankful to all of Prof. Yoshikai's group members, Dr. Junfeng Yang, Dr. Wei Ding, Dr. Chang-Sheng Wang, Dr. Qiao Sun, Dr. Md. Shafiqur Rahman, Dr. Roshayed Ali Laskar, Ploypailin Tan Siew Ling, Yongqi Yu, Jinkui Chai, Yaquan Liang and Yan Ying Lee. Lastly, I would like to thank all people I met at NTU during my Ph.D. study.

Table of Contents

List of Abbreviations

12-crown-4	1,4,7,10-tetraoxacyclododecane
δ	chemical shift (ppm)
Ac	acetyl
acac	acetylacetonate
aq	aqueous
Ar	aryl (substituted aromatic ring)
bdpp	2,4-bis(diphenylphosphino)pentane
BINAP	(2,2'-bis(diphenylphosphino)-1,1'-binaphthyl
BINOL	1,1'-bi-2-naphthol
Bn	benzyl
Boc	*tert*-butyloxycarbonyl
bpy	2,2'-bipyridine
br	broad
Bz	benzoyl
c	g/100 mL (for specific rotation)
CA	conjugate addition
Calcd	calculated
cat.	catalytic
CCDC	The Cambridge Crystallographic Data Centre
cod	1,5-cyclooctadiene
Cp*	1,2,3,4,5-pentamethylcyclopentadienyl
Cy	cyclohexyl
d	doublet
DABCO	1,4-diazabicyclo[2.2.2]octane
DCM	dichloromethane
dd	doublet of doublet
DEPT	distorsionless enhancement by polarization transfer
DIBAL	diisobutylaluminum hydride
DMAP	4-dimethylaminopyridine
DMF	*N*,*N*-dimethylformamide
DMPU	*N*,*N*'-dimethylpropyleneurea
DMSO	dimethylsulfoxide

dppe	1,2-bis(diphenylphosphino)ethane
dppf	1,1'-bis(diphenylphosphino)ferrocene
dr	diastereomer ratio
dt	doublet of triplet
ECA	enantioselective conjugate addition
ee	enantiomeric excess
equiv.	equivalent
er	enantiomeric ratio
ESI	electrospray ionization
Et	ethyl
FTIR	fourier transform infrared spectroscopy
GC	gas chromatography
h	hour
HMDS	hexamethyldisilazane
HMPA	hexamethylphosphoric triamide
HPLC	high performance liquid chromatography
HRMS	high resolution mass spectrometry
*i*Pr	*iso*-propyl
J	coupling constants
m	multiple
M	concentration (mol/L)
M^+	parent ion peak (mass spectrum)
MBH	Morita–Baylis–Hillman
*m*CPBA	*meta*-chloroperoxybenzoic acid
Me	methyl
MHz	mega hertz
m.p.	melting point
MS	molecular sieves
m/z	mass per charge ratio
*n*Bu	normal butyl
NHC	N-heterocyclic carbene
NLE	nonlinear effect
NMP	*N*-methyl-2-pyrrolidone

NMR	nuclear magnetic resonance
o-Tol	*ortho*-tolyl
ppm	parts per million
q	quartet
quint	quintet
rac	racemic
R_f	retention factor value
rt	room temperature
s	singlet
Sat.	saturated
t	triplet
TBAF	tetra-*n*-butylammonium fluoride
*t*Bu	*tert*-butyl
td	triplet of doublet
Tf	trifluoromethyl
THF	tetrahydrofuran
TLC	thin layer chromatography
TM	transition metal
TMEDA	*N,N,N',N'*-tetramethylethylenediamine
TMS	trimethylsilyl
t_R	retention time
Ts	*para*-toluenesulfonyl
UV	ultraviolet
Xantphos	(9,9-dimethyl-9*H*-xanthene-4,5-diyl)bis(diphenylphosphane)

Chapter 1. Introduction

1.1 Cyclopropanol as Homoenolate Precursor

Enolate is one of the most well studied nucleophilic reactive species, and there is no doubt of its huge role in the field of organic synthesis. Thus, interception of enolate with electrophiles is arguably the most common approach to the synthesis of *α*-substituted ketones. On the other hand, homoenolate, a one-carbon-extended homolog of enolate, can also be attractive reactive species, as it could react with electrophiles to afford *β*-substituted ketones. While enolate can be accessed by deprotonating the *α*-position of the corresponding carbonyl compound with an appropriate base, the preparation of homoenolate cannot be performed in an analogous fashion because selective deprotonation of the *β*-C–H bond is difficult because it is less acidic than the *α*-C–H bond (Scheme 1.1).

Scheme 1.1. Access to Metal Enolate and Homoenolate

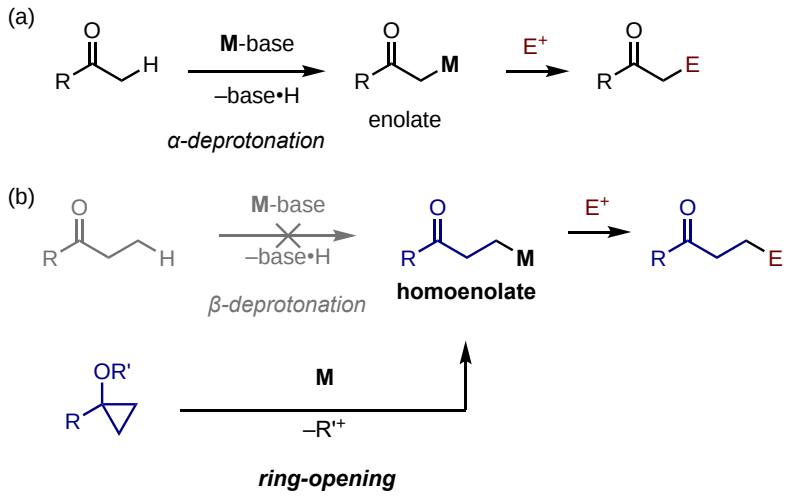

Cyclopropanol derivatives have been widely recognized as viable precursors to metal homoenolate, as the cleavage of the strained cyclopropane ring and the formation of a strong C=O bond constitute substantial driving forces.[1] Based on the reports of ring-opening reactions of cyclopropanol derivatives, here I propose that the mechanisms of homoenolate formation can be classified into two categories (Scheme 1.2). The first one is initiated by the interaction of an electrophilic metal species and the cyclopropane ring to cleave C−C bond and form oxonium cation intermediate, followed by the dissociation/departure of the original *O*-substituent on the

cyclopropanol derivative (Scheme 1.2a). The second involves the initial formation of a metal cyclopropoxide intermediate, which then undergoes β-carbon elimination to form homoenolate (Scheme 1.2b).

Scheme 1.2. Possible Pathways for Ring-Opening Homoenolate Formation

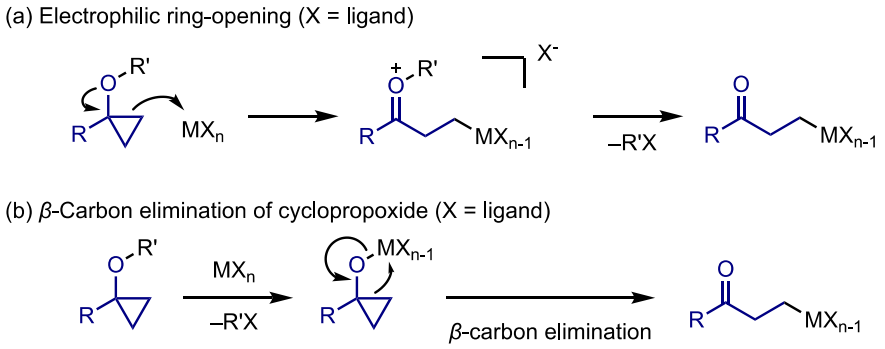

The cyclopropanol derivatives used as homoenolate precursors can be categorized into three types, that is, 1-alkoxy-1-siloxycyclopropanes (**A**) for ester-homoenolates and 1-alkyl/aryl-1-siloxycyclopropanes (**B**) and cyclopropanols (**C**) for keto-homoenolates (Scheme 1.3). The chemistry of homoenolate as β-carbonyl nucleophile has started in the late 1970s, when 1-alkoxy-1-siloxycyclopropane (**A**) and 1-alkyl/aryl-1-siloxycyclopropane (**B**) were used as precursors.[1a] On the other hand, the full appreciation of the utility of cyclopropanol (**C**) as a homoenolate precursor only begun in the 2010s.[1c-g] The upsurge of reports on using cyclopropanol (**C**) as homoenolate precursor in the 2010s could be partly attributed to the establishment of Kulinkovich reaction, which is now the most reliable and concise method to access a variety of cyclopropanols. While the synthetic procedures for 1-alkoxy-1-siloxycyclopropane (**A**) and 1-alkyl/aryl-1-siloxycyclopropane (**B**), such as reduction of β-halogenated esters,[2] Simmons-Smith reaction of silyl ketene acetals,[3] and enol silyl ethers,[4] were established in the 1970s, the first report of Kulinkovich reaction was made in 1989.[5] In the following sections, β-functionalization reactions of homoenolate are discussed based on the types of cyclopropanol derivatives used as homoenolate precursors.

Scheme 1.3. Cyclopropanol-Derivatives for Homoenolate Precursors

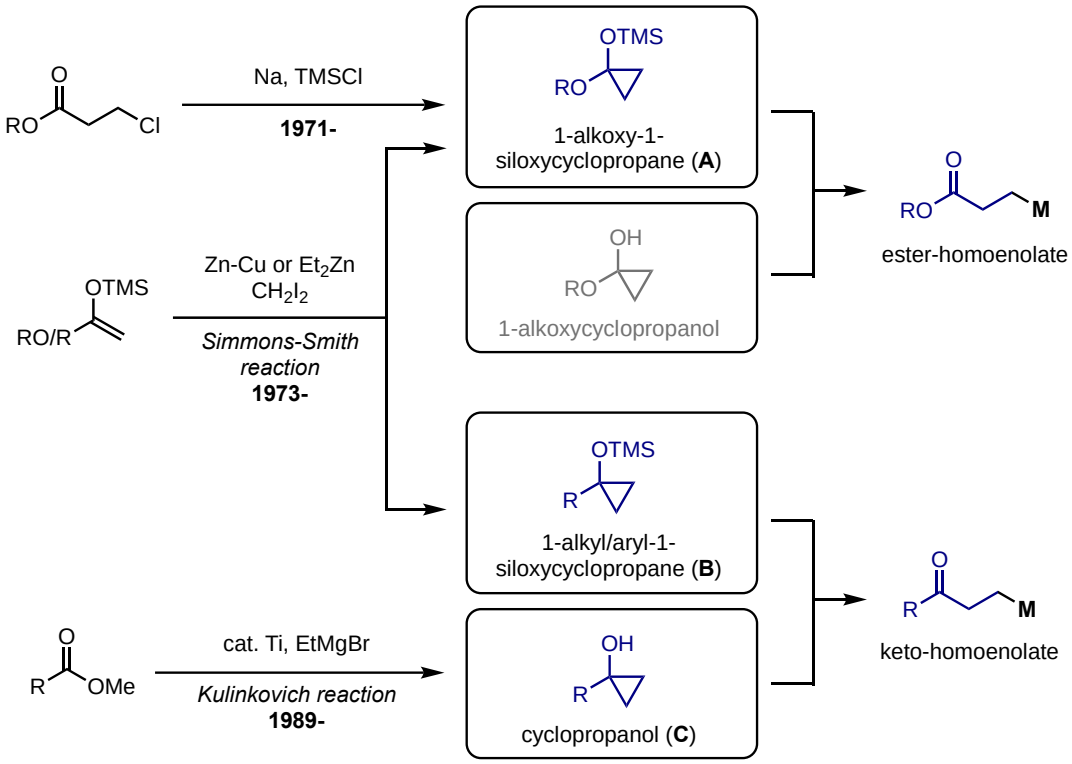

1.1.1 1-Alkoxy-1-Siloxycyclopropane (Ester-Homoenolate)

Starting from 1977, Nakamura and Kuwajima reported various ester-type metal homoenolates prepared by treating 1-alkoxy-1-siloxycyclopropane with metal salts.[6] Thus, various homoenolates containing metals such as Ti,[6a, 6b, 6d, 6g] Zn,[6c-f, 6h, 6i] Cd,[6d] Hg,[6d] Ga,[6d] Sn,[6d] Sb,[6d] Bi,[6d] and Te[6d] have been isolated by this approach (Scheme 1.4). Due to the lower electrophilicity of the carbonyl of ester than that of ketone, these metal ester-homoenolates are stable enough to be isolated and are not in equilibrium with their ring-closed tautomers, unlike the case with keto-homoenolates (*vide infra*). The extensive research by Nakamura and Kuwajima showed that the homoenolate was not generated via silicon-metal exchange to form metal cyclopropoxide, but was generated via direct cleavage of the strained C−C bond by the metal salts to form *β*-oxonium alkylmetal species as the intermediate (Scheme 1.2a).[6a, 6d]

Scheme 1.4. Ester-Homoenolates Derived from 1-Alkoxy-1-siloxycyclopropane

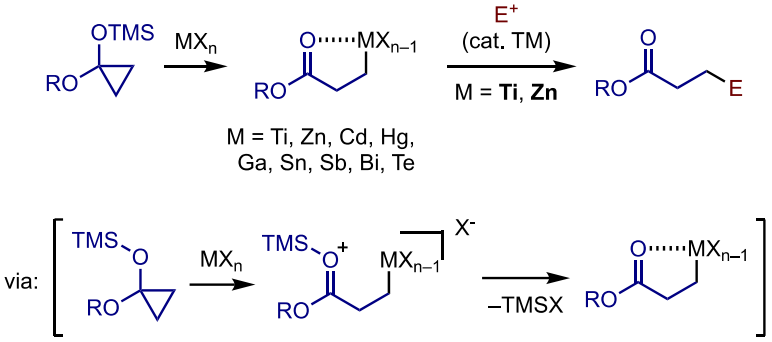

Among the aforementioned metal homoenolates, only titanium and zinc variants showed nucleophilicity towards electrophiles, with or without the aid of transition metals. The $TiCl_3$-homoenolate was an isolable compound, but its reactivity was low, reacting only with aldehydes to afford γ-chloroesters through *in situ* chlorination of the initial adducts but not with ketones (Scheme 1.5a).[6a, 6b] Meanwhile, exchange of the chloride ligand of this homoenolate with an alkoxide using 0.5 equivalent of $Ti(OR)_4$ was found to make the homoenolate more nucleophilic, thus reacting with ketones to give γ-lactones by intramolecular transesterification of the initial adducts.[6g] Later, Gleason developed a catalytic and enantioselective variant of this reaction in 2003 (Scheme 1.5b).[7] Titanium fluoride bearing (*R*)-BINOL catalyzed ring-opening addition of 1-alkoxy-1-siloxycyclopropane to aldehydes, and the products were isolated as γ-lactones with moderate ees after acid treatment. Since 1-alkoxy-1-siloxycyclopropane is considered as a one-methylene homolog of ketene silyl acetal, these reactions can be called enantioselective Mukaiyama homoaldol reaction.

Scheme 1.5. Reactions of Titanium Ester-Homoenolate

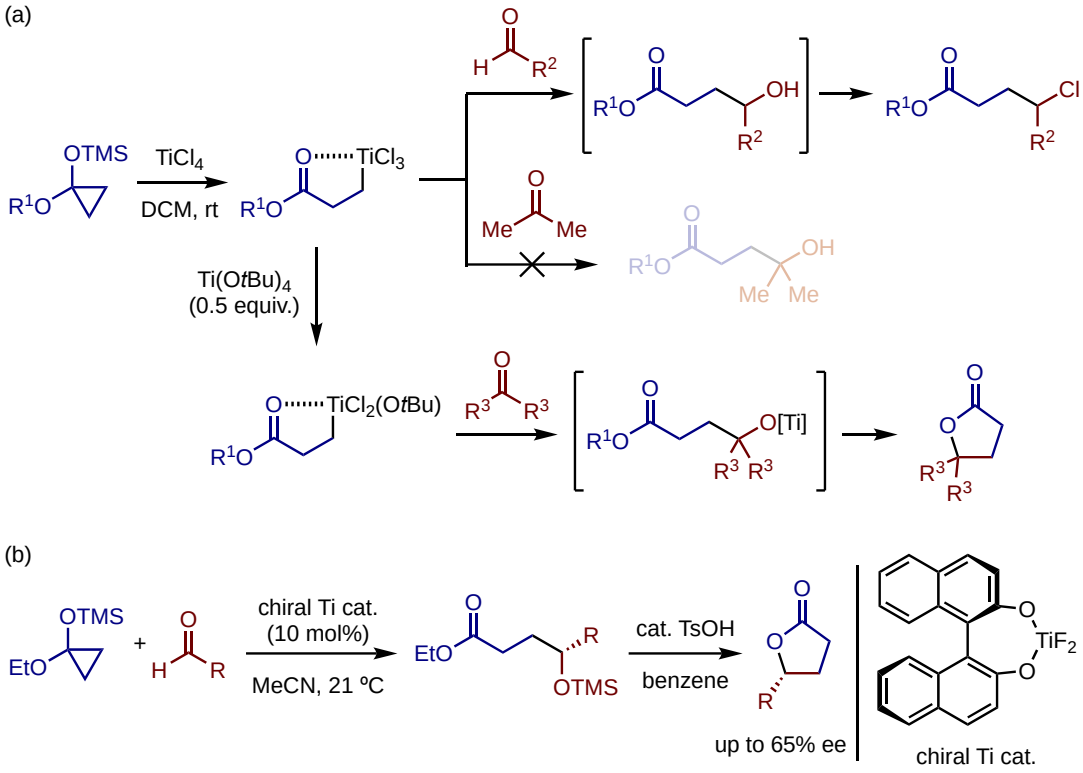

Like well-studied alkyl zinc reagents, the zinc homoenolate worked as a good alkyl nucleophile towards various electrophiles with or without transition metals.[6c-f, 6h, 6i] The thermally stable dialkyl-type Zn-homoenolate was easily isolated by mixing 1-alkoxy-1-siloxycyclopropane and $ZnCl_2$. A series of reactions reported by Nakamura and Kuwajima are shown in Scheme 1.6.[6c, 6h] A conjugate addition of the Zn-homoenolate to an enone was achieved using a copper catalyst. Allylation reactions with allyl halides were also promoted using copper and nickel catalysts with different regioselectivity. While branch products were obtained with the copper catalyst through S_N2'-type allylation, linear products were obtained with the nickel catalyst through S_N2-type allylation. Negishi cross-coupling with aryl or vinyl halides was achieved using a palladium catalyst to afford *β*-arylated/vinylated esters. Interestingly, the ring-opening addition of 1-alkoxy-1-siloxycyclopropane to aldehydes and ketones proceeded using a catalytic amount of Zn salts without pre-formation of the zinc homoenolate.[6e]

Scheme 1.6. Reactions of Zinc Ester-Homoenolate

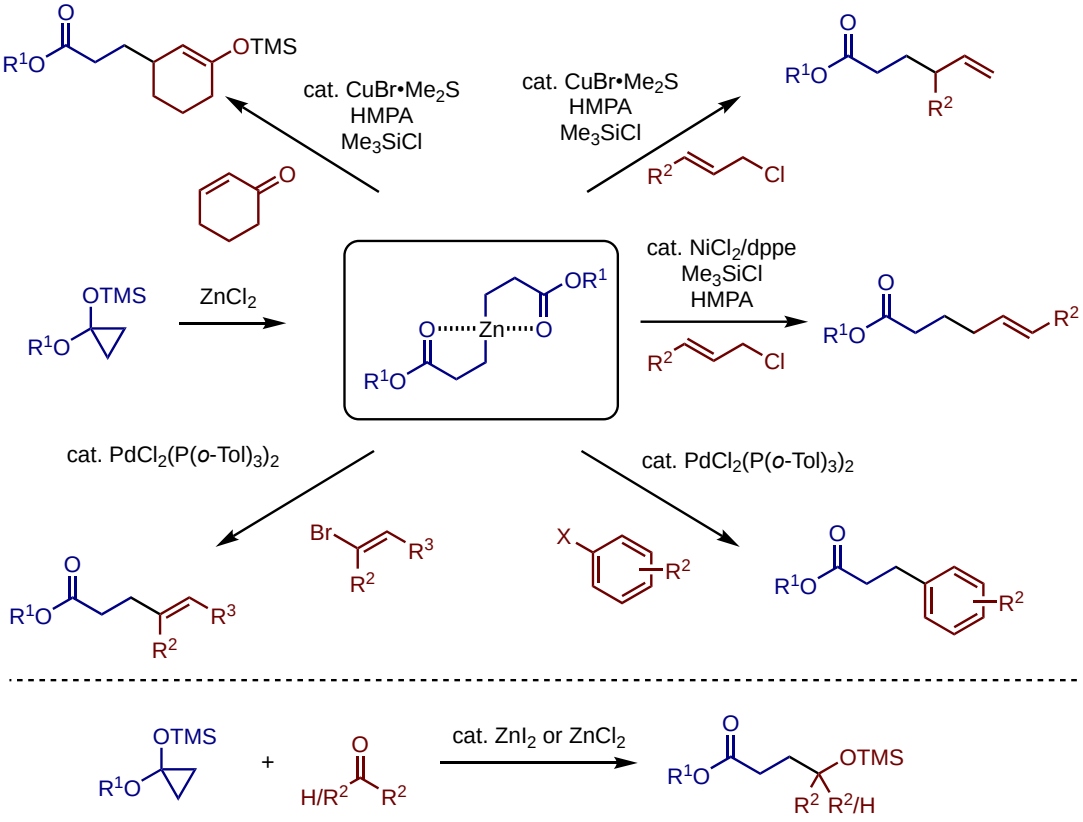

A catalytic transformation of 1-alkoxy-1-siloxycyclopropane was also achieved by the same group using a palladium catalyst (Scheme 1.7).[6j] Ring-opening *β*-arylation with aryl triflates was promoted by a catalytic system comprised of $[PdCl(\eta^3\text{-}C_3H_5)]_2$ and PPh_3 in benzene or HMPA at 100 °C to afford *β*-arylated esters. The reaction system was also applicable to 1-alkyl/aryl-1-siloxycyclopropane to give *β*-arylated ketones. In these reactions, the use of aryl triflate is essential for generating a cationic Pd species, which interacts with the cyclopropane ring to form the homoenolate intermediate (see Scheme 1.2a).

Scheme 1.7. Pd-Catalyzed Ring-Opening *β*-Arylation of 1-Alkoxy-1-siloxycyclopropane and 1-Alkyl/aryl-1-siloxycyclopropane

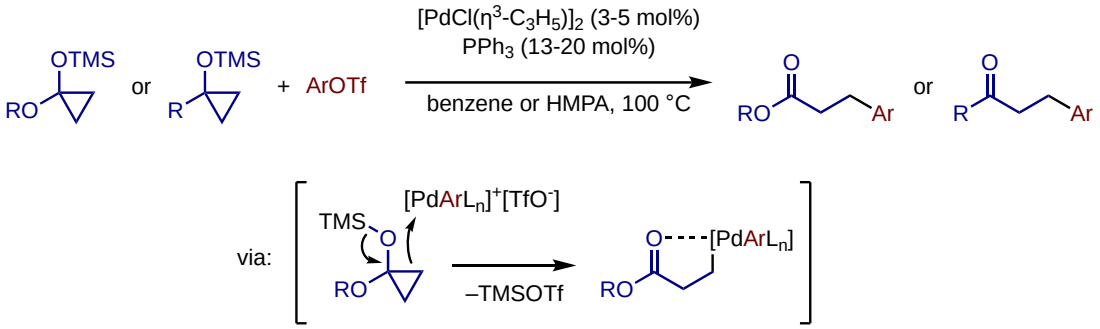

The aforementioned titanium and zinc ester-homoenolates have been applied for total syntheses of complex natural products.[8] The examples which employed copper-catalyzed conjugate addition[9] of zinc ester-homoenolate are shown in Scheme 1.8. In 1986, Nakamura and Kuwajima achieved total synthesis of cortisone using their developed conjugate addition of ester-homoenolate to a cyclohexenone derivative as one of the key steps.[8b] The diastereoselectivity was greatly improved (>95:5 dr) in the presence of $BF_3 \cdot OEt_2$.[10] In 1990, Crimmins used this reaction system for the synthesis of cyclopentenone derivatives by a formal [3+2] cycloaddition with acetylenic esters,[11] and this reaction has been used in the total synthesis of ginkgolide B.[8f, 8g] The conjugate addition of zinc ester-homoenolate to the acetylenic ester would afford a metal allenoate intermediate, which then would be trapped with TMSCl as a ketene acetal. This ketene acetal would then undergo intramolecular acylation to afford the cyclopentenone product.

Scheme 1.8. Application of Cu-Catalyzed Conjugate Addition of Zn Homoenolate to Synthesize Natural Products

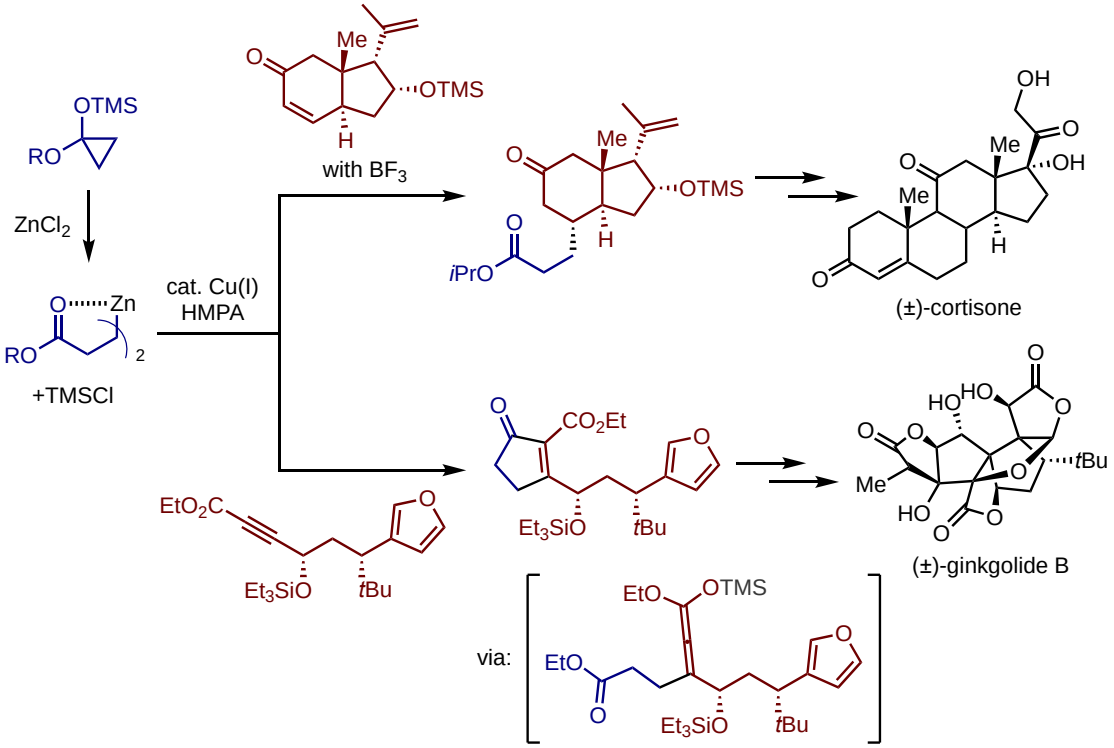

In the recent years, reports on new synthetic methods based on the transformation of 1-alkoxy-1-siloxycyclopropane-derived ester-homoenolate are rare. That said, Shen and Han recently reported alkynylation of *in situ*-generated stoichiometric copper homoenolates with terminal alkynes (Scheme 1.9).[12] Interestingly, the standard reaction conditions using 2 equivalents of $Cu(OAc)_2$ could be used for not only a 1-alkoxy-1-siloxycyclopropane to afford the *β*-alkynyl esters, but also 1-phenyl-1-siloxycyclopropane and cyclopropanols to afford *β*-alkynyl ketones.

Scheme 1.9. Cu-Mediated Ring-Opening Sonogashira Coupling of Cyclopropanol Derivatives

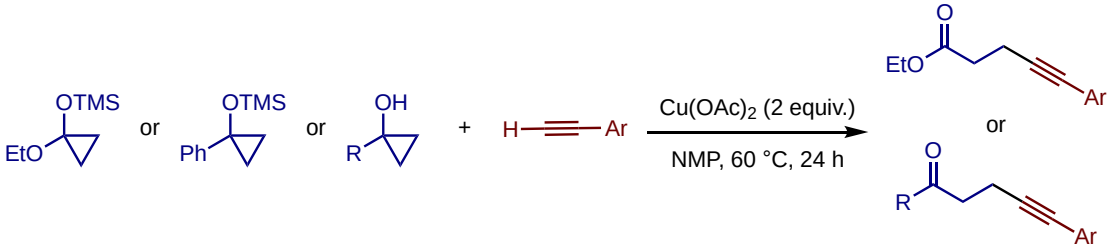

1.1.2 1-Alkyl/Aryl-1-Siloxycyclopropane (Keto-Homoenolate)

1-Alkyl/aryl-1-siloxycyclopropanes have not been used as widely as 1-alkoxy-1-siloxycyclopropanes as homoenolate precursors despite their good accessibility by Simmons-Smith reaction. A possible reason for this would be the difficulty of isolation of the resulting keto-homoenolate due to its propensity of intramolecular cyclization (Scheme 1.10). Unlike ester-homoenolate, most of metal keto-homoenolates exist in equilibrium with the corresponding metal cyclopropoxide tautomers, and the balance of this equilibrium depends on the metal.

Scheme 1.10. Keto-Homoenolate Derived from 1-Alkyl/aryl-1-siloxycyclopropane

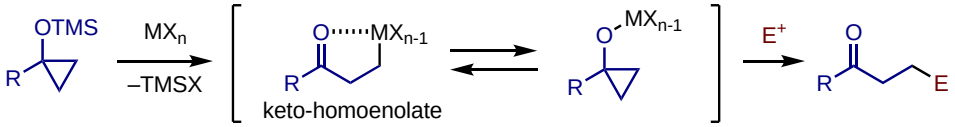

In addition to the above mentioned palladium-catalyzed *β*-arylation reported by Nakamura and Kuwajima,[6j] in 2011, Orellana reported the same type of palladium-catalyzed *β*-arylation, but using tetra-*n*-butylammonium fluoride (TBAF) as an additive (Scheme 1.11).[13] Unlike the original reaction system, this reaction system is proposed to involve a palladium cyclopropoxide formed via fluoride-mediated desilylation, which undergoes *β*-carbon elimination, which is the reaction pathway for cyclopropanol (see 1.1.3), to generate the palladium homoenolate.

Scheme 1.11. Pd-Catalyzed, Fluoride-Mediated Ring-Opening *β*-Arylation of 1-Alkyl/aryl-1-siloxycyclopropane

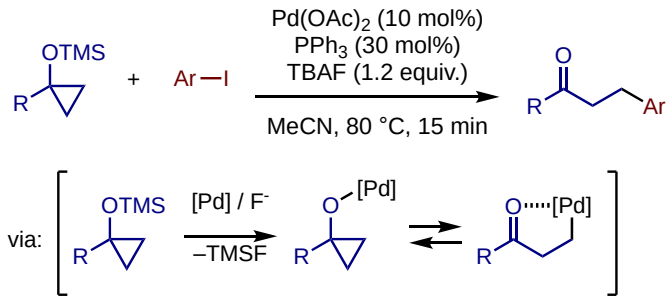

Murai, Ryu and Sonoda reported generation of homoenolates via ring-opening of siloxycyclopropanes using stoichiometric amounts of Hg,[14] Sn,[15] Te,[16] Pt,[17] Ag[18] and Cu[18-19]. Among them, copper homoenolates were found to react with electron-deficient

alkynes such as dimethyl acetylenedicarboxylate (Scheme 1.12).[19] As was the case with the generation of palladium homoenolate from 1-alkoxy-1-siloxycyclopropane, the copper homoenolate was proposed to form by ring-opening of siloxycyclopropane via electrophilic attack of a cationic copper species. The authors also mentioned that the counter anion, BF_4^-, played an important role for the ring-opening by promoting the elimination of silyl group as fluorosilane.

Scheme 1.12. Ring-Opening Addition of 1-Alkyl/aryl-1-siloxycyclopropane to an Electron-Deficient Alkyne

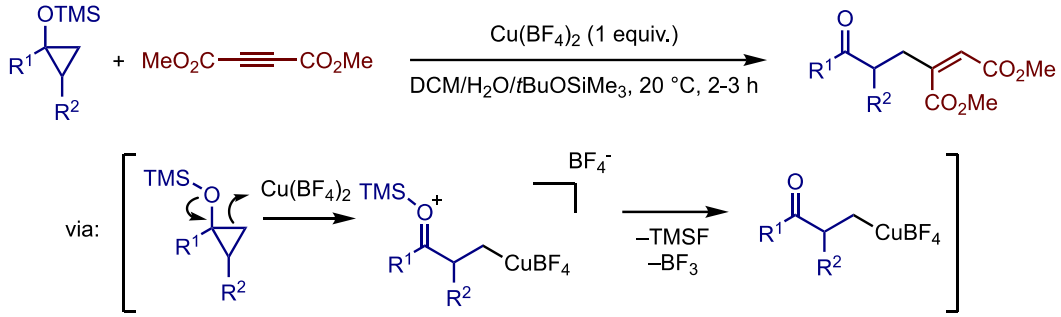

1.1.3 Cyclopropanol (Keto-Homoenolate)

While 1-alkoxy-1-siloxycyclopropane and 1-alkyl/aryl-1-siloxycyclopropane have been used as homoenolate precursors since 1970s, unprotected cyclopropanols have escaped attention as homoenolate precursors for a long period of time, even after the first report of Kulinkovich reaction in 1989.[1b, 1d-g] In fact, the development of transformations cyclopropanols via homoenolate has begun in earnest only in the 2010s. A problem specific to the use of cyclopropanol is protonation of the resultant homoenolate with another molecule of cyclopropanol, affording a ring-opened ketone (Scheme 1.13).

Scheme 1.13. Ring-Opening Homoenolate Formation of Cyclopropanol

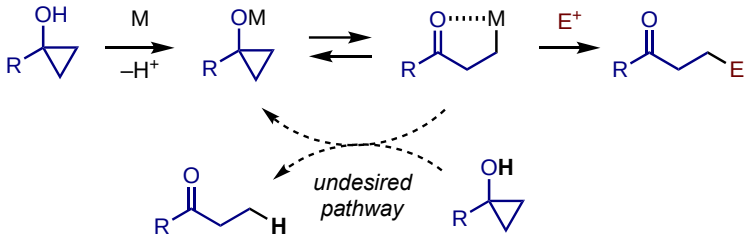

Despite the above pitfall, the ease of preparation of variously substituted cyclopropanols makes them attractive homoenolate precursors. Over the last decade, a variety of (transition) metals have been found to promote the reaction between cyclopropanols and a wide range of electrophiles via the corresponding homoenolates to afford *β*-substituted ketones. In the following sections, the ring-opening reactions of cyclopropanols are introduced in two parts, namely, stoichiometric reaction and catalytic reaction.

1.1.3.1 Stoichiometric Reaction

The first example of intermolecular *β*-functionalization of cyclopropanol-derived homoenolate was reported by Cha and coworkers in 2012 (Scheme 1.14a).[20] A cyclopropanol was firstly treated with a stoichiometric amount of Et_2Zn, and then CuCN and allyl,[20a] propagyl and alkynyl electrophiles[20b] were added to afford *β*-allylated, allenylated and alkynylated ketones in an S_N2' fashion. The authors argued that the zinc keto-homoenolate would be less favored in the equilibrium with the cyclopropoxide, while copper keto-homoenolate, generated upon transmetalation, could be stable as well as nucleophilic enough to react with the electrophile. *β*-Acylation of zinc homoenolate with an acid chloride was also achieved in the presence of a palladium catalyst to afford a 1,4-diketone (Scheme 1.14b).[21] The Zn/Cu homoenolate conditions were successfully applied for the key step of the total synthesis of an alkaloid natural product (–)-205B, using a densely functionalized cyclopropanol and an enantioenriched propargyl tosylate (Scheme 1.14c).[22]

Scheme 1.14. Transformations of Zinc Keto-Homoenoalte

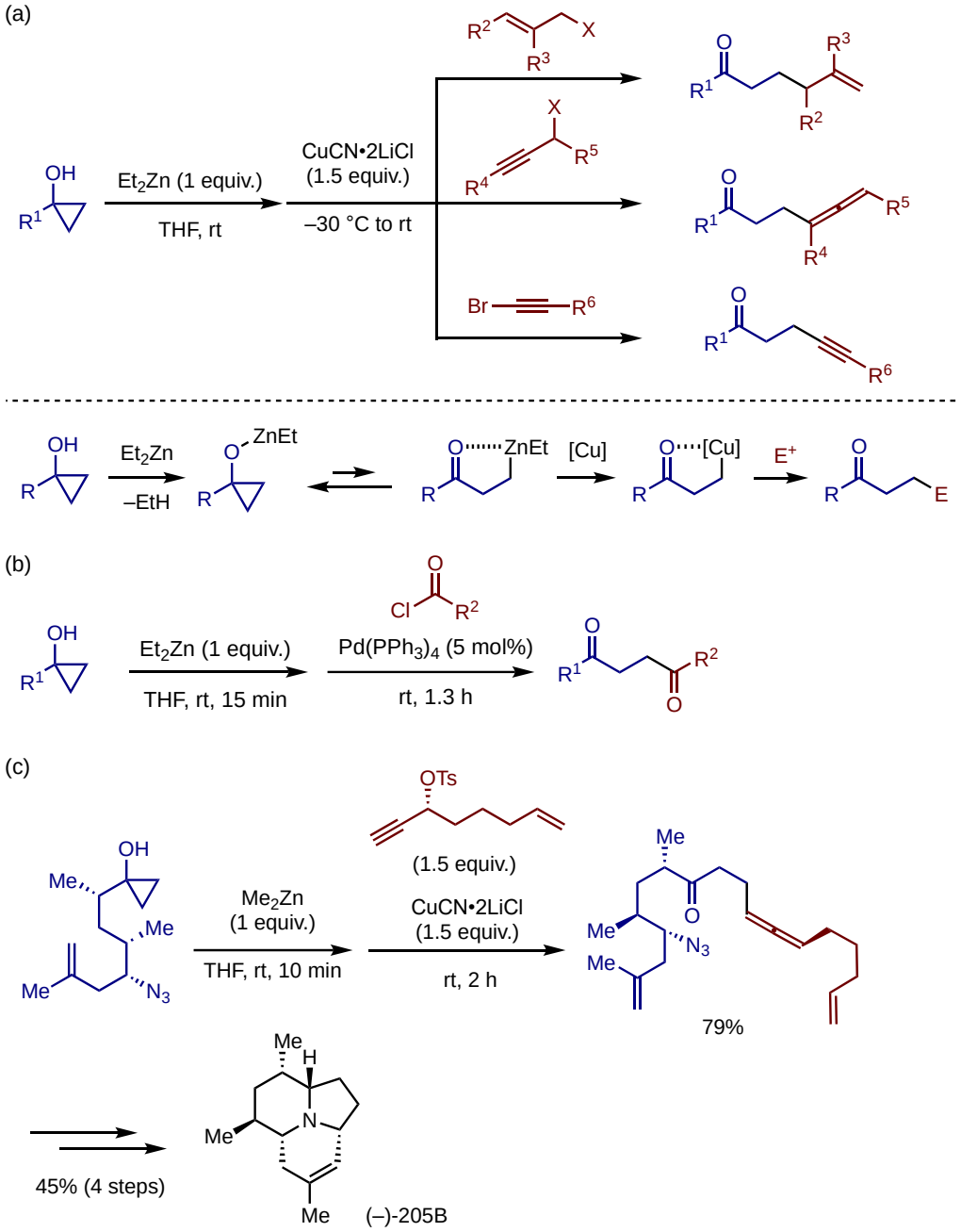

Very recently, Trost and coworkers reported enantioselective S_N2' allylic alkylation of allyl phosphate with zinc homoenolate using a Cu/Zn heterobimetallic catalyst (Scheme 1.15).[23] The ligand is designed based on the proline-derived ligand known as ProPhenol developed by their group,[24] where one of the proline moiety of the original ligand was replaced by an NHC moiety so that it can accommodate both Cu and Zn. The authors proposed that the zinc moiety of the catalyst worked as a Lewis acid coordinated by the carbonyl of the copper homoenolate.

Scheme 1.15. Enantioselective Allylation of Zinc Keto-Homoenolate

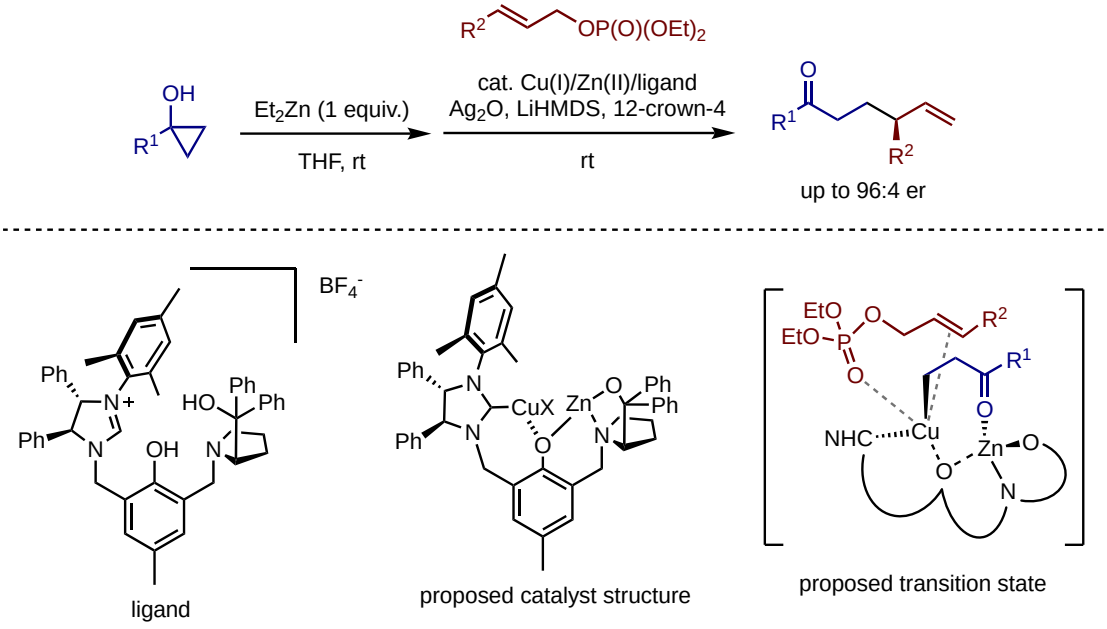

Although it is not *β*-functionalization, Rousseaux reported an interesting Zn-mediated transformation of cyclopropanol to cyclopropyl amine, by utilizing the electrophilic nature of the carbonyl of zinc aldehyde-homoenolate (Scheme 1.16).[25] In this reaction, the aldehyde-homoenolate derived from *trans*-2-substituted cyclopropanol, $Zn(CN)_2$ and a base is trapped with an amine to form an iminium intermediate, which then undergoes ring-closing to form the cyclopropyl amine.

Scheme 1.16. Zn-Mediated Conversion of Cyclopropanols to Cyclopropylamines

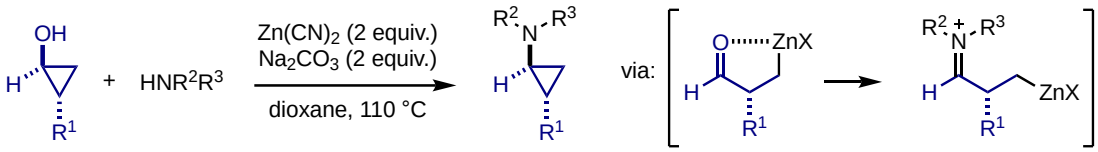

1.1.3.2 Catalytic Reaction

The recent reports on ring-opening reactions of cyclopropanols to afford *β*-substituted ketones mostly employ transition metal-catalysts (Scheme 1.17a, path A). Transition metals can mediate not only heterolytic cleavage of the cyclopropane ring to give a homoenolate but also homolytic ring-opening process to give a *β*-keto radical (path B),[26] while reactions involving the latter pathway will not be discussed here. The homoenolate pathway (path A) could be distinguished from the *β*-keto radical pathway (path B) by the regioselectivity of cleavage of unsymmetric cyclopropanols. Thus, the

less substituted C−C bond would be cleaved to a give homoenolate, while the more substituted C−C bond would be homolytically cleaved to generate a more stable radical. A major problem specific to transition metal homoenolates is *β*-hydride elimination to generate *α*,*β*-unsaturated ketones.[27] Although this reaction is often reported as an undesired pathway, in some reactions, *α*,*β*-unsaturated ketones are proposed to be the key intermediates to give *β*-substituted ketones (path C). For example, rhodium(III)-catalyzed oxidative arylation via C−H activation fits this case (Scheme 1.17b).[28] The rhodium(III) catalyst undergoes chelation-assisted C−H activation of the aryl oxime ether, ligand exchange with the cyclopropanol, and ring-opening to afford an arylrhodium(III) homoenolate. Mechanistic experiments suggested that this intermediate would undergo *β*-hydride elimination rather than reductive elimination, which would be followed by insertion of the *α*,*β*-unsaturated ketone into the Rh−aryl bond to afford the product.

Scheme 1.17. General Mechanistic Consideration for Catalytic Transformation of Cyclopropanols

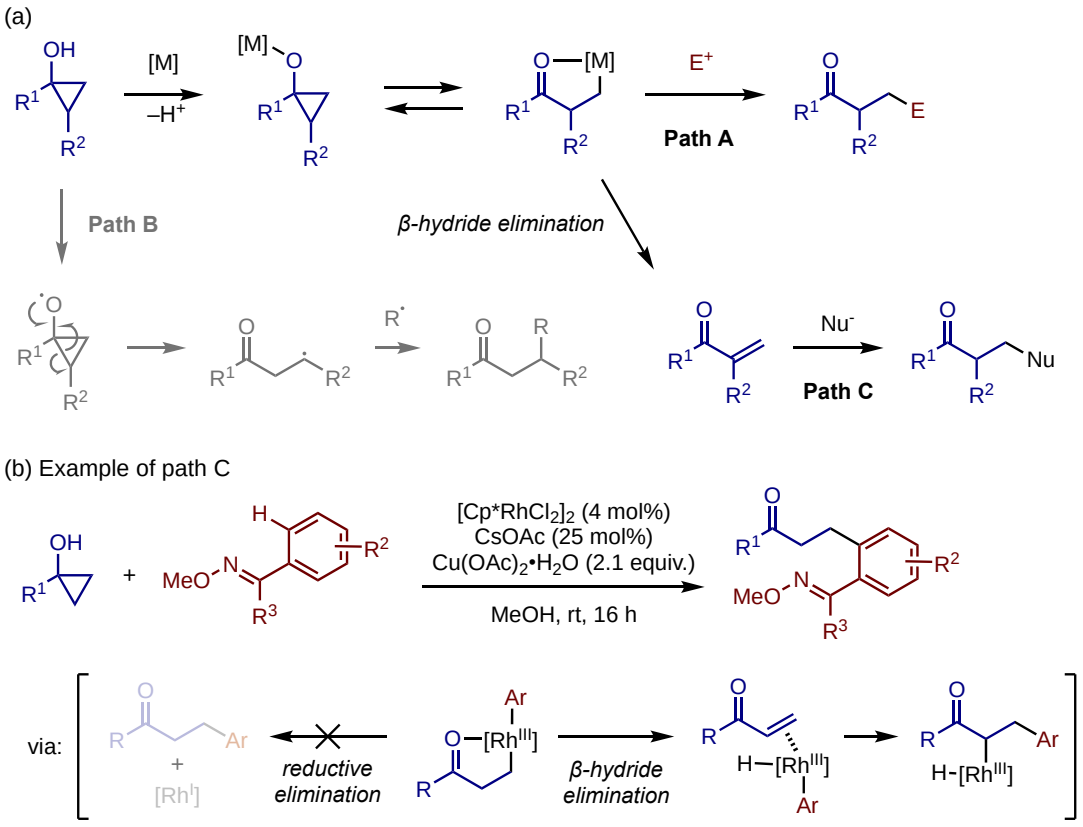

Since the report of the palladium-catalyzed arylation by Orellana in 2013 (it should be noted that Orellana's report on the palladium-catalyzed arylation of 1-alkyl/aryl-1-siloxycyclopropane in Scheme 1.11 demonstrated one example of using a cyclopropanol as the substrate[13]), more than 30 examples of transition metal-catalyzed transformations of cyclopropanols via homoenolate have been reported in the last ten years. Scheme 1.18 summarizes these intermolecular coupling reactions based on the transition metal catalyst used. A variety of transition metals, such as Pd,[29] Cu,[30] Co,[31] Ni[32] and Rh,[28, 33] have been used as catalysts with a variety of electrophiles.

Scheme 1.18. Transition Metal-Catalyzed Ring-Opening Intermolecular *β*-Functionalization of Cyclopropanols

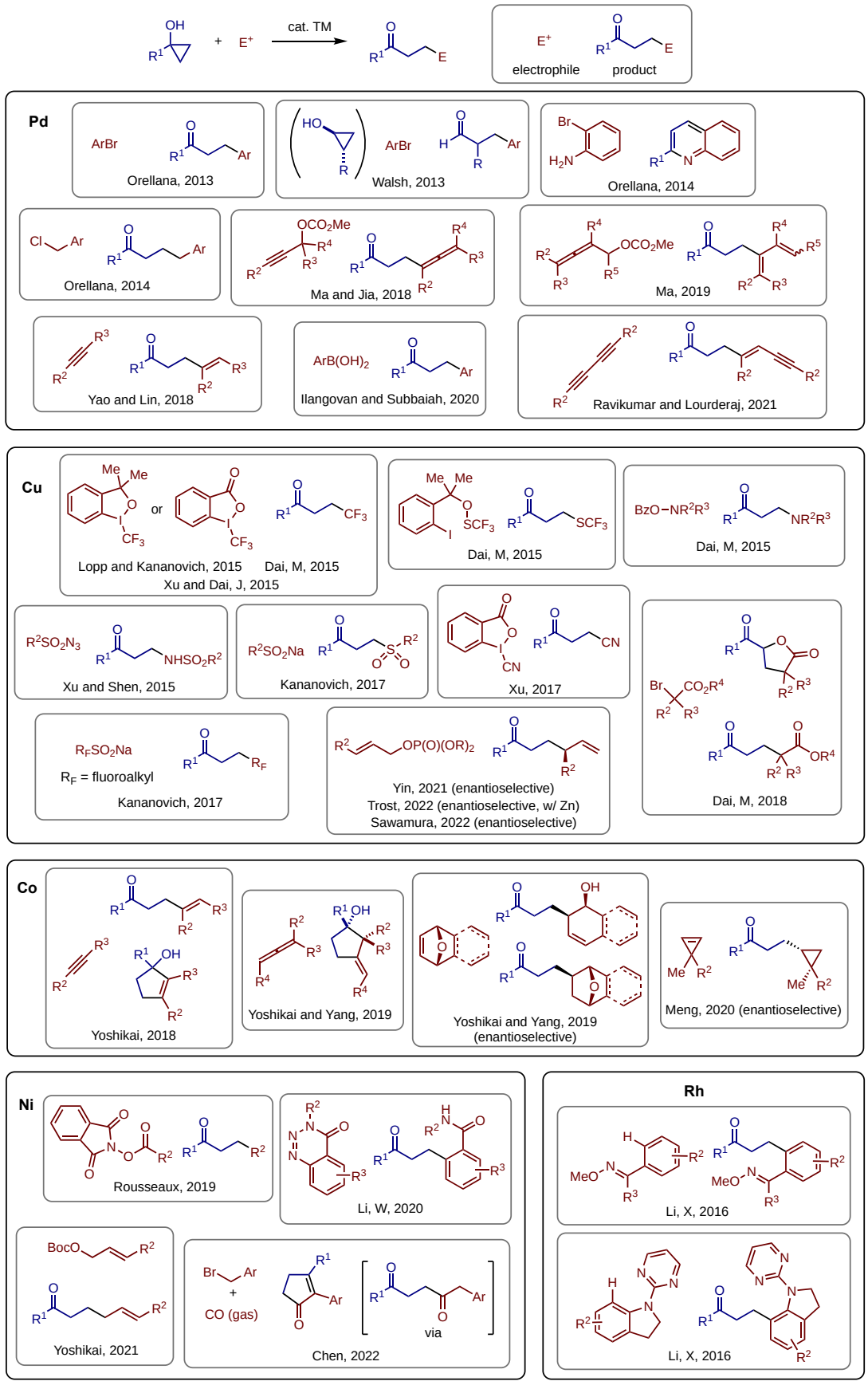

As shown in Scheme 1.18, recently, our group developed a series of cobalt-catalyzed ring-opening cross-couplings between cyclopropanols and unsaturated hydrocarbons via homoenolates.[31a-c] The first example was an alkenylation reaction with an internal alkyne in the presence of catalytic systems comprised of Co(II) salt, dppe, zinc dust and DABCO, which afforded either a β-alkenyl ketone in DMSO or a cyclopentenol in MeCN (Scheme 1.19).[31a] The mechanistic study suggested the formation of an alkenylcobalt species generated via insertion of the alkyne into a Co(I) homoenolate. While protodemetalation of this species is predominant in DMSO to afford the ketone product, intramolecular addition of the alkenyl−Co bond to the carbonyl group becomes favorable in MeCN to give the cyclopentenol. This solvent-controlled chemodivergence was explained by 1) the stronger acidity of the proton source in more polar DMSO to lead to the β-alkenyl ketone and 2) the less Lewis basic property of MeCN assisting coordination of the carbonyl oxygen to the cobalt center, which facilitated the intramolecular carbonyl addition to afford the cyclopentenol.

Scheme 1.19. Co-Catalyzed Chemodivergent Ring-Opening Coupling Between Cyclopropanols and Alkynes

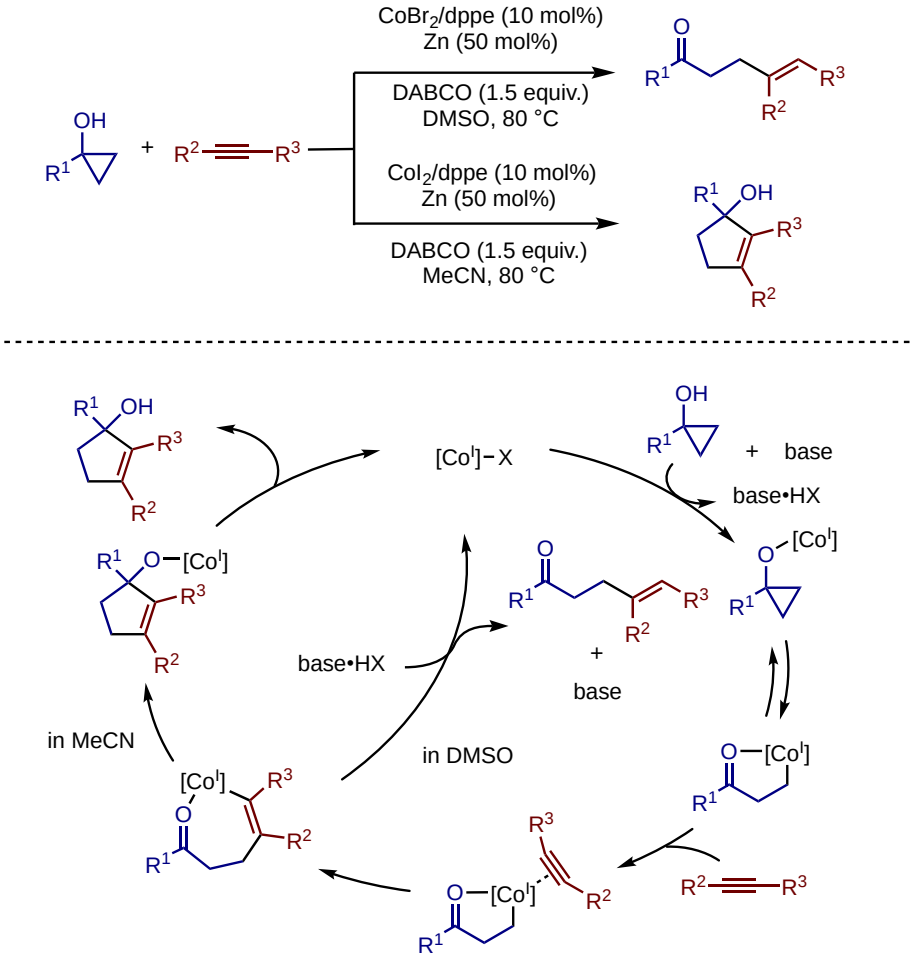

Cobalt catalysts were also found to promote ring-opening coupling of cyclopropanols with oxabicyclic alkenes in an enantioselective manner (Scheme 1.20).[31c] With a $CoCl_2$/(*R*,*R*)-bdpp catalyst, ring-opening alkylation with the cobalt homoenolate proceeded to afford 1,2-dihydronaphthalen-1-ol derivatives in high enantioselectivity. On the other hand, a $Co(OAc)_2$/(*R*,*R*)-bdpp catalyst, in the presence of MeOH, gave the hydroalkylation products without ring-opening of the oxabicyclic structure in high enantioselectivity.

Scheme 1.20. Co-Catalyzed Enantioselective Chemodivergent Ring-Opening Addition of Cyclopropanols and Oxabicyclic Alkenes

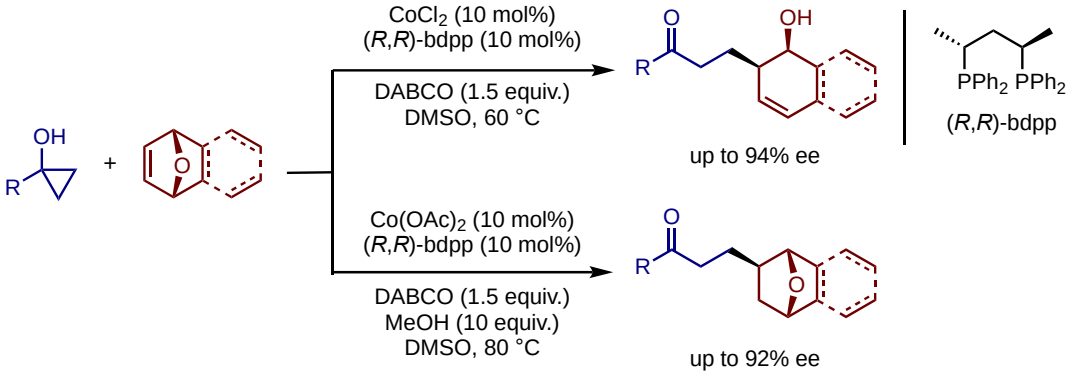

Since the above report, several additional examples of enantioselective transformations of cyclopropanols via homoenolate have been reported. In 2021, Meng reported an enantioselective insertion of cyclopropenes to homoenolate using a cobalt/chiral diphosphine-based catalytic system analogous to the one developed by our group (Scheme 1.21).[31d] (*R*,*R*)-Et-DuPhos was the best ligand to give the *β*-cyclopropyl ketones in high enantioselectivity.

Scheme 1.21. Co-Catalyzed Enantioselective Ring-Opening Addition of Cyclopropanols and Cyclopropenes

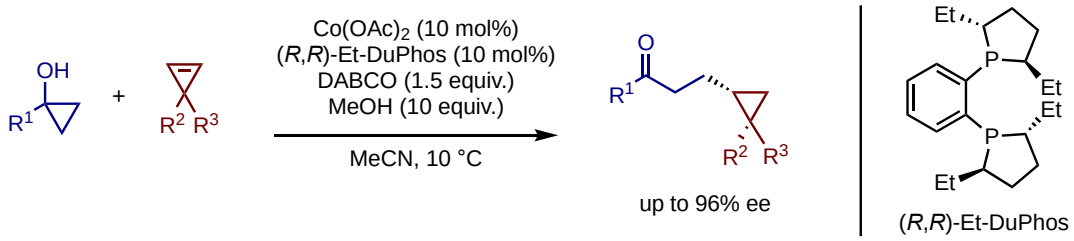

Very recently, the groups of Yin and Sawamura independently reported enantioselective copper-catalyzed ring-opening allylation using chiral NHC ligands containing a phenolic hydroxy group (Scheme 1.22).[30k, 30l] In the presence of a Cu(I)–chiral NHC catalyst and *t*BuOLi as a base, the *β*-allylation with allylic phosphates proceeded enantioselectively in an S_N2' manner.

Scheme 1.22. Cu-Catalyzed Enantioselective Ring-Opening *β*-Allylation of Cyclopropanols with Allylic Phosphates

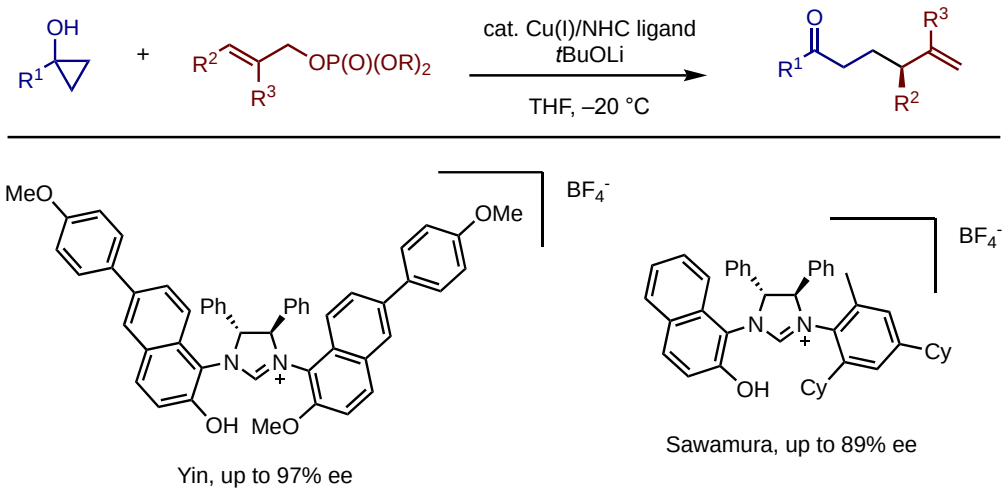

1.2 Cyclopropanol as Enolized Homoenolate Precursor

As shown in Section 1.1, metal homoenolates generated from cyclopropanol derivatives have been widely used as *β*-carbonyl nucleophiles to afford *β*-substituted esters and ketones. Given the intrinsic acidity of the *α*-CH of a carbonyl group, the homoenolate could be enolized to form the enolate of homoenolate, which we call "enolized homoenolate" (Scheme 1.23). The bis-nucleophilic feature of this species would potentially enable its sequential reaction with electrophiles to afford an *α*,*β*-disubstituted ketone. As shown later in the reported examples (see Scheme 1.25), it usually reacts with electrophiles first at the *β*-position and then at the *α*-position.

Scheme 1.23. Formation of Enolized Homoenolate from Homoenolate and Its Reactivity

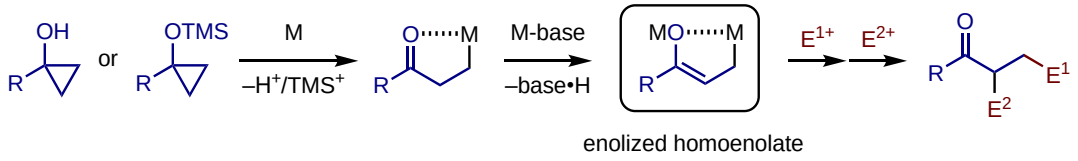

In the 1990s, Ryu and Sonoda reported the preparation of enolized homoenolate from 1-alkyl-1-siloxycyclopropane and demonstrated its unique reactivity in several reactions (Scheme 1.24).[34] Firstly, dichlorobutyltin homoenolate was prepared by the reaction of 1-alkyl-1-siloxycyclopropane and *n*BuSnCl$_3$.[35] This keto-homoenolate is stable enough to be isolated in the form of homoenolate, which means that the *β*C−Sn

bond is not nucleophilic enough to react with the carbonyl group. By treating this tin homoenolate with four equivalents of *n*BuLi, the lithium enolized homoenolate was generated *in situ* regio- and stereoselectively as only the *Z* isomer, as confirmed by its trapping with TMSCl.[34b, 34e] Interestingly, the formation of the lithium enolized homoenolate and its perfect *E*/*Z* selectivity were attributed to the chelating structure of the tin homoenolate. Thus, the chelate-free tributyltin homoenolate, which was prepared by treating dichlorobutyltin homoenolates with *n*BuMgBr, was found to react with *n*BuLi at the carbonyl group to afford a tertiary alkoxide.

Scheme 1.24. Generation of Lithium Enolized Homoenolates from Sn-Homoenolates

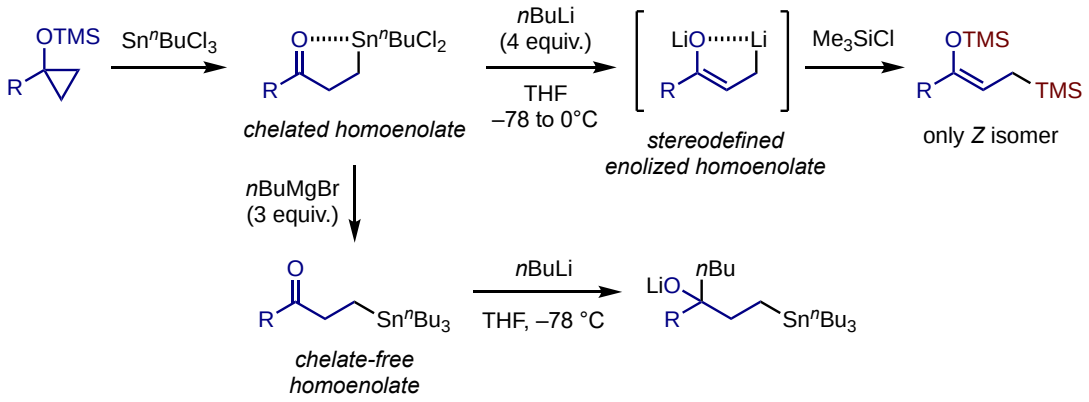

The authors next examined several sequential nucleophilic additions of the stereodefined lithium enolized homoenolate as a bis-nucleophilic intermediate to electrophiles (Scheme 1.25). In all the cases, the reaction with the first electrophile took place preferentially at the β-position to afford a lithium enolate. For example, the reaction with an aldehyde and subsequent quenching with water gave a homoaldol-type product.[34e] Interestingly, a small amount of vicinal diol was observed, which was generated by γ-allylation of the lithium enolized homoenolate. The carbolithiation to an alkene also proceeded at the β-position to afford an α,δ-dianion species. The reaction of this species with an alkyl bromide preferentially took place at the δ-position, followed by trapping of the resultant enolate with allyl bromide to afford an α,β-disubstituted ketone.[34f]

Scheme 1.25. Reactivity of Lithium Enolized Homoenolates

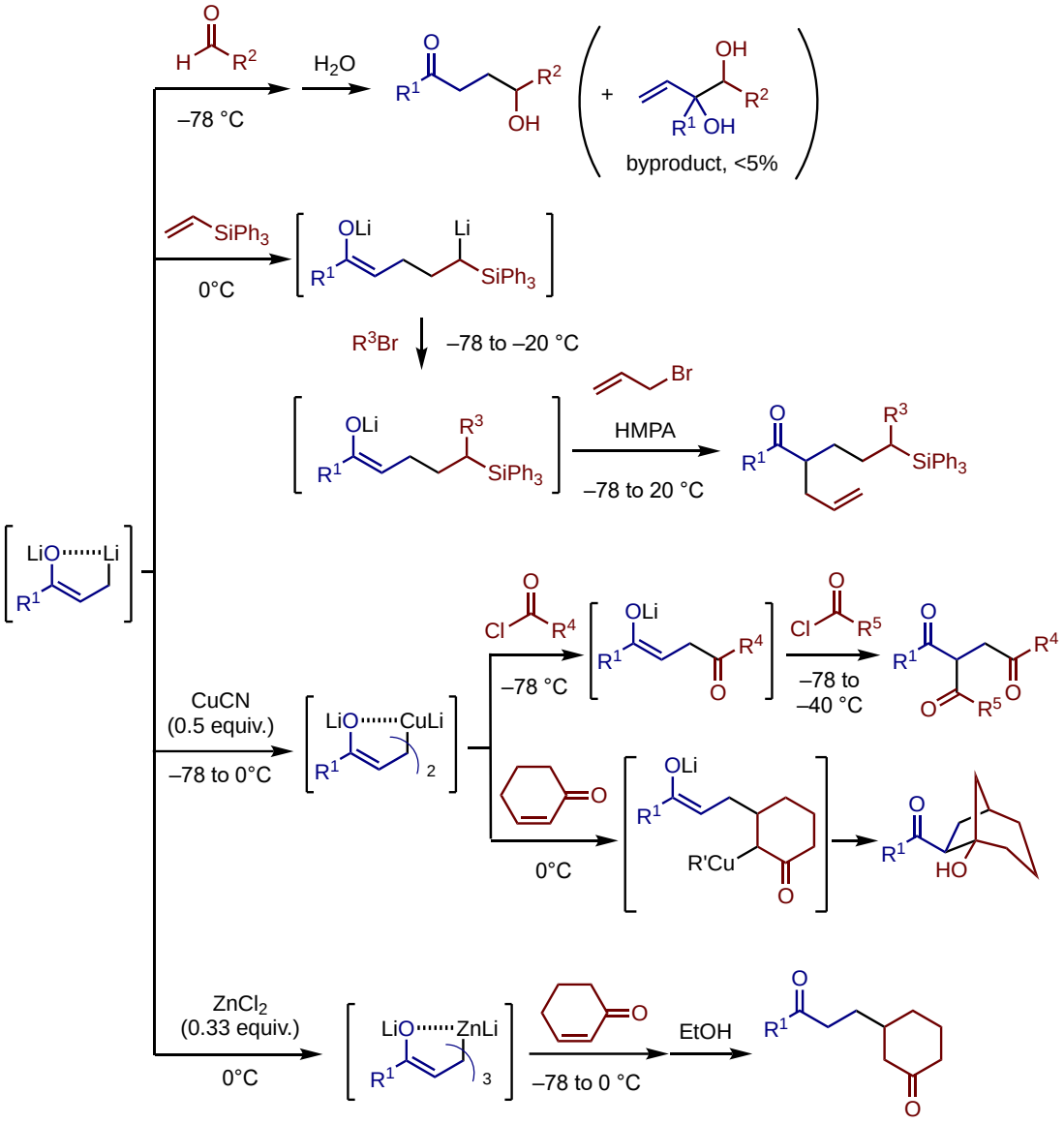

The lithium enolized homoenolate could be transformed into a cuprate-type enolized homoenolate by treating with CuCN. An acid chloride reacted with this cuprate species at the Cu−C bond to afford a lithium enolate intermediate, which reacted with another acid chloride to afford a triketone compound.[34d] The cuprate also underwent 1,4-addition to cyclohexenone, followed by intramolecular aldol reaction of the lithium enolate moiety to the ketone to form a *β*-hydroxy ketone bearing a bicyclo[3.2.1]octane structure.[34c] On the other hand, a zincate-type enolized homoenolate, which was derived from the lithium enolized homoenolate and 0.33 equivalent of $ZnCl_2$, underwent conjugate addition to cyclohexenone without the following intramolecular aldol reaction to afford a 1,6-diketone.[34b]

In 2009, Matsubara reported zincate-mediated rearrangement of a 2-(1-hydroxyalkyl)cyclopropanol to a vicinal-diol (Scheme 1.26).[36] The dilithium alkoxide, which could be generated by double deprotonation of 2-(1-hydroxyalkyl)cyclopropanol with *n*BuLi, would form a zincate via ligand exchange with *t*Bu$_3$ZnLi. The zincate would then undergo retro-aldol reaction to form a zinc complex of an aldehyde and an α-alkoxide allylic anion, which represents one of the resonance structures of enolized homoenolate. This intermediate was supposed to undergo allylation of the carbonyl group, thus affording a vicinal dialkoxide zincate.

Scheme 1.26. Zincate-Mediated Rearrangement of 2-(1-Hydroxyalkyl)cyclopropanols to Vicinal-Diols

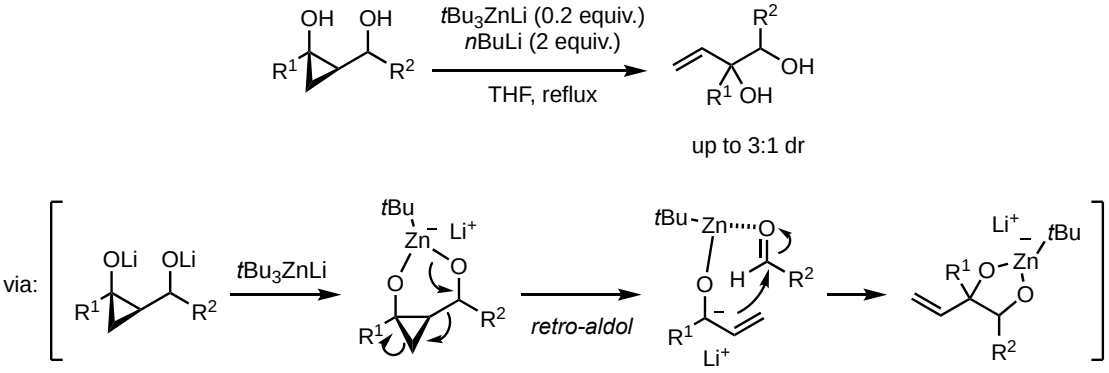

1.3 Design and Summary of Thesis Research

As discussed above, transition metal catalysts, cobalt catalysts in particular, have been demonstrated to promote ring-opening addition of cyclopropanols to strained and nonpolar unsaturated hydrocarbons such as alkynes,[31a] allenes,[31b] oxabicyclic alkenes,[31c] and cyclopropenes[31d] via homoenolate, with enantioselectivity in some cases. Given this and the well-established copper-catalyzed conjugate addition of preformed zinc ester homoenolate (Scheme 1.27a),[6c, 6h, 11] it appeared somewhat strange that conjugate addition of cyclopropanol-derived homoenolate, either stoichiometric or catalytic, remained elusive. In pursuit of such transformation, my attention was attracted to Cha's pioneering work on the Zn/Cu-mediated allylation of cyclopropanols with allylic halides or phosphates (Scheme 1.27b).[20] This reaction required a stoichiometric quantity of Et_2Zn, which appeared natural considering the nature of the transformation, i.e., substitution reaction between an anionic nucleophile and an electrophile having stable anionic leaving group. Meanwhile, I reasoned that the

situation could be different in the case of conjugate addition to an *α,β*-unsaturated carbonyl compound. Thus, if the conjugate addition of the homoenolate was feasible, the resulting enolate could be protonated by the cyclopropanol to give the product and regenerate the cyclopropoxide, thus achieving catalytic turnover. Furthermore, the enantioselectivity in the conjugate addition step could be controlled by a chiral ligand on the metal. Chapter 2 describes the successful implementation of this hypothesis without copper, that is, enantioselective conjugate addition of catalytically generated chiral zinc homoenolate to *α,β*-unsaturated ketones (Scheme 1.27c).[37] The catalytically generated chiral zinc homoenolate undergoes conjugate addition to *α,β*-unsaturated ketones to afford 1,6-diketones first, which are then cyclized via intramolecular aldol condensation to furnish cyclopentene derivatives in good to high enantioselectivities.

Scheme 1.27. Enantioselective Conjugate Addition of Catalytically Generated Zn-Homoenolate

(a) Cu-catalyzed conjugate addition of Zn ester-homoenolate

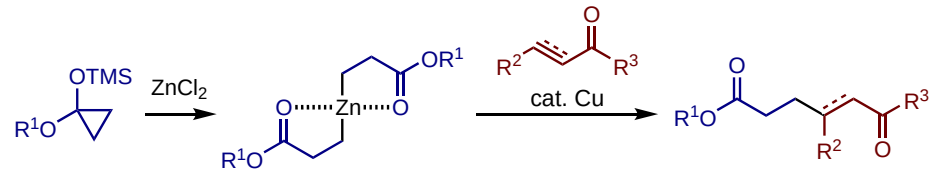

(b) Stoichiometric Zn/Cu keto-homoenolate substitution and proposed catalytic conjugate addition

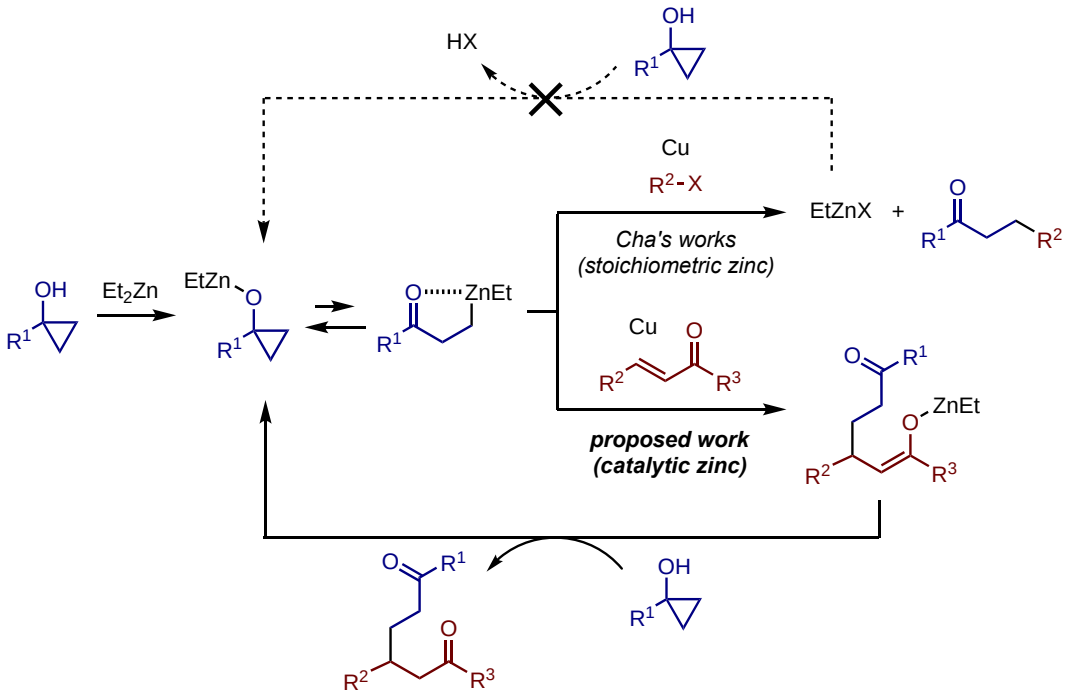

(c) Chapter 2: Enantioselective conjugate addition of catalytically generated Zn homoenolate

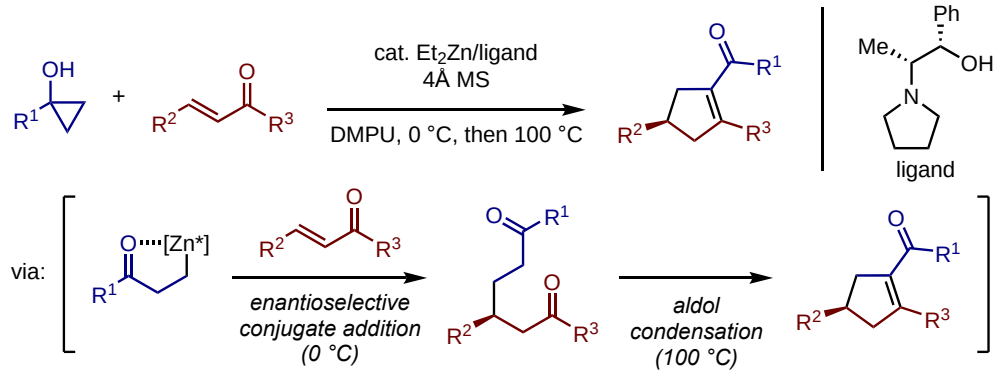

Having developed the above conjugate addition, I became interested in the reactivity of the zinc homoenolate toward other types of electrophiles. In this connection, and in light of the chemistry of enolized homoenolate (Chapter 1.2), I wondered whether an enolized homoenolate could be generated in equilibrium with the zinc homoenolate and then engaged in reaction with the electrophile. I reasoned that enolization of the zinc keto-homoenolate would be more facile than that of analogous

ketone because the acidity of the α-CH of the carbonyl group would be increased by the internal chelation. Thus, an equilibrium between the cyclopropoxide, the homoenolate, and the enolized homoenolate might be possible, where the cyclopropoxide itself might serve as a base to promote the enolization process (Scheme 1.28a). Then I hypothesized that electrophilic interception of the enolized homoenolate might be possible when the electrophile was not reactive enough to immediately react with the homoenolate. Chapter 3 describes the search for such reactivity of the putative enolized homoenolate, which culminated in the discovery of a zinc-catalyzed β-allylation reaction of cyclopropanols with allylic carbonates of Morita–Baylis–Hillman (MBH) reaction products (Scheme 1.28b).[38] In this reaction, the catalytically generated zinc enolized homoenolate preferentially reacts with a MBH carbonate at the α-position to afford an α-allylated Zn homoenolate, which then undergoes ring-closing and intermolecular transesterification to afford the cyclopropyl-fused δ-valerolactone derivative. Since the lack of reactivity of the MBH carbonate toward the homoenolate (β-position) allows the equilibrium formation of the enolized homoenolate, it seems reasonable that the MBH carbonate preferentially reacts at the α-position (enolate moiety) rather than the β-position of the enolized homoenolate. This is the first example of utilization of a catalytically generated enolized homoenolate, and its unprecedented reaction mode as enolized homoenolate (see the previous examples in Scheme 1.25) enables a formal C−H activation of β-position of cyclopropanol, which have not yet been reported.[39]

Scheme 1.28. *β*-Fuctionalization of Cyclopropanols via Catalytically Generated Zn-Enolized Homoenolate

(a) Proposed mechanism for generation of zinc enolized homoenolate

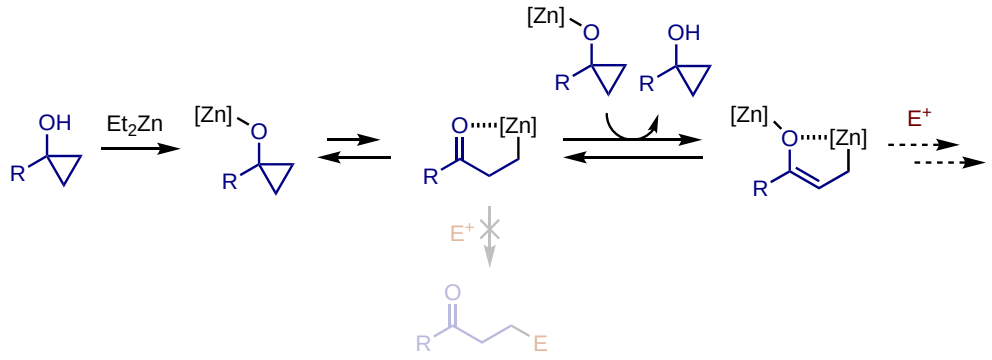

(b) Chapter 3: Zinc-catalyzed *β*-functionalization of cyclopropanols via enolized homoenolate

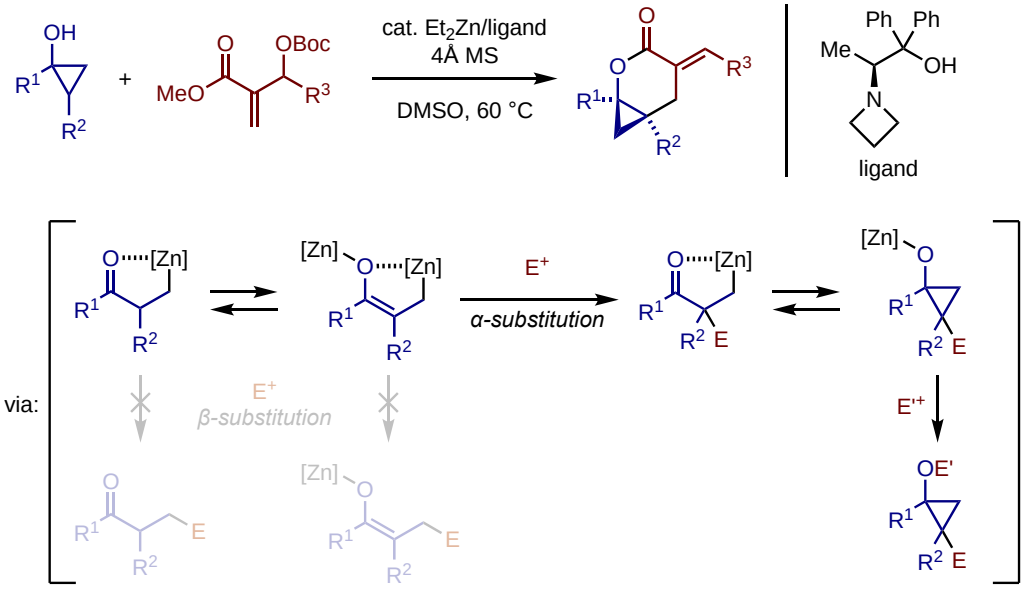

While the above reaction features the enolate mode of reactivity of the enolized homoenolate, I hypothesized that this reactive species would also have potential to serve as allylzinc nucleophile depending on the electrophilic reaction partner. In this respect, my attention was attracted to aldehydes as electrophiles, as carbonyl allylation with allylmetal reagents, including allylzincs, represents one of the most extensively developed C–C bond-forming reactions (Scheme 1.29a).[40] Chapter 4 describes the realization of this proposed reactivity, that is, a zinc-mediated diastereoselective hydroxyallylation of aldehydes with cyclopropanols via enolized homoenolate (Scheme 1.29b).[41] The reaction is promoted by a superstoichiometic quantity of Et_2Zn in the presence of bipyridine, affording vicinal *anti-sec,tert*-diols with high diastereoselectivity under mild conditions. The high diastereoselectivity of the reaction

was ascribed to the stereodefined enolized homoenolate derived from sequential deprotonations of a cyclopropanol and the resulting homoenolate.

Scheme 1.29. Zn-Mediated Hydroalkylation of Aldehydes with Cyclopropanols via Zn-Enolized Homoenolate

(a) Addition of allylmetals to aldehydes

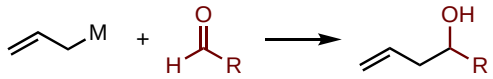

M = Li, Mg, Al, Si, Ti, Zn, Sn

(b) Chapter 4: Zinc-mediated hydroxyallylation of aldehydes with cyclopropanols to afford vicinal diols

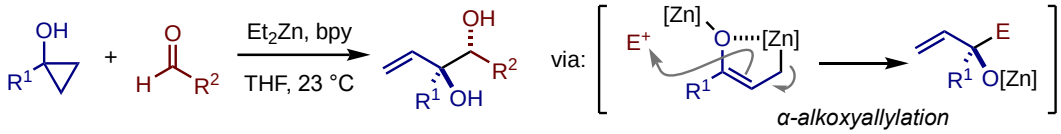

Overall, this thesis research has yielded new advances in the synthetic chemistry of metal homoenolate and enolized homoenolate. The enantioselective conjugate addition (Chapter 2) is the first example to make the reaction of cyclopropanol-derived zinc homoenolate catalytic and enantioselective. In a broader context, this transformation is also notable as a rare example of enantioselective C–C bond formation of catalytically generated carbanions other than enolates and acetylides. The *β*-functionalization of cyclopropanols (Chapter 3) and the hydroxyallylation of aldehydes (Chapter 4) not only represent unique and attractive synthetic transformations themselves but also have opened a new dimension in the reaction chemistry of zinc homoenolate, that is, zinc enolized homoenolate functioning as enolate or *γ*-allylmetal species. Such reaction patterns are also unique in comparison with the known reaction patterns of preformed enolized homoenolates. Given the accessibility of cyclopropanols and the ever-improving methods for their synthesis,[42] the multifaceted reactivity of zinc homoenolate revealed by the present thesis research will inspire further development of synthetically attractive transformations of cyclopropanols via homoenolates as well as mechanistic investigation to provide better understanding and prediction of the electrophile-dependent reaction modes.

1.4 References

1. (a) Kuwajima, I.; Nakamura, E., Metal Homoenolates from Siloxycyclopropanes. *Top. Curr. Chem.* **1990,** *155*, 1-39; (b) Kulinkovich, O. G., The Chemistry of Cyclopropanols. *Chem. Rev.* **2003,** *103*, 2597-2632; (c) Kimura, M., Metal Homoenolates. In *Comprehensive Organic Synthesis II*, Knochel, P., Ed. Elsevier: 2014; Vol. 2; (d) Nikolaev, A.; Orellana, A., Transition-Metal-Catalyzed C–C and C–X Bond-Forming Reactions Using Cyclopropanols. *Synthesis* **2016,** *48*, 1741-1768; (e) Mills, L. R.; Rousseaux, S. A. L., Modern Developments in the Chemistry of Homoenolates. *Eur. J. Org. Chem.* **2019,** *2019*, 8-26; (f) Sekiguchi, Y.; Yoshikai, N., Metal-Catalyzed Transformations of Cyclopropanols via Homoenolates. *Bull. Chem. Soc. Jpn.* **2021,** *94*, 265-280; (g) McDonald, T. R.; Mills, L. R.; West, M. S.; Rousseaux, S. A. L., Selective Carbon–Carbon Bond Cleavage of Cyclopropanols. *Chem. Rev.* **2021,** *121*, 3-79.

2. Rühlmann, K., Die Umsetzung von Carbonsäureestern mit Natrium in Gegenwart von Trimethylchlorsilan. *Synthesis* **1971,** *1971*, 236-253.

3. Rousseau, G.; Slougui, N., An Improved Synthesis of Substituted Cyclopropanone Acetals and Hemiacetals. *Tetrahedron Lett.* **1983,** *24*, 1251-1254.

4. Rubottom, G. M.; Lopez, M. I., Reaction of Trimethysilyl Enol Ethers with Simmons-Smith Reagent. Facile Synthesis of Trimethylsilyl Cyclopropyl Ethers and Cyclopropanols. *J. Org. Chem.* **1973,** *38*, 2097-2099.

5. Kulinkovich, O.; Sviridov, S.; Vasilevskii, D.; Prityts kaya, T., Reaction of Ethylmagnesium Bromide with Esters of Carboxylic-Acids in the Presence of Tetraisopropoxytitanium. *Zh. Org. Khim.* **1989,** *25*, 2244-2245.

6. (a) Nakamura, E.; Kuwajima, I., Homoenolate Anion Precursor. Reaction of Ester Homoenol Silyl Ether with Carbonyl Compounds. *J. Am. Chem. Soc.* **1977,** *99*, 7360-7362; (b) Nakamura, E.; Kuwajima, I., Metal Homoenolate Chemistry. Isolation and Reactions of Titanium Homoenolates of Esters. *J. Am. Chem. Soc.* **1983,** *105*, 651-652; (c) Nakamura, E.; Kuwajima, I., Copper-Catalyzed Acylation and Conjugate Addition of Zinc Homoenolate. Synthesis of 4- and 5-Oxo Esters. *J. Am. Chem. Soc.* **1984,** *106*, 3368-3370; (d) Nakamura, E.; Shimada, J.; Kuwajima, I., A Ring-Opening Reaction of 1-Siloxy-1-alkoxycyclopropanes. Preparation of Main-Group Metal Homoenolates of Alkyl Propionate. *Organometallics* **1985,** *4*, 641-646; (e) Oshino, H.; Nakamura, E.; Kuwajima, I., Catalytic Homo-Reformatskii Reaction. Ambident Chemical Reactivities of the Zinc Homoenolate of Propionate. *J. Org. Chem.* **1985,** *50*,

2802-2804; (f) Nakamura, E.; Kuwajima, I., Palladium Catalyzed Reactions of Propionate Homoemolate. Arylation, Vinylation, and Acylation. *Tetrahedron Lett.* **1986,** *27*, 83-86; (g) Nakamura, E.; Oshino, H.; Kuwajima, I., Trichlorotitanium and Alkoxytitanium Homoenolates. Preparation, Characterization, and Utilization for Organic Synthesis. *J. Am. Chem. Soc.* **1986,** *108*, 3745-3755; (h) Nakamura, E.; Aoki, S.; Sekiya, K.; Oshino, H.; Kuwajima, I., Carbon-Carbon Bond-Forming Reactions of Zinc Homoenolate of Esters. A Novel Three-Carbon Nucleophile with General Synthetic Utility. *J. Am. Chem. Soc.* **1987,** *109*, 8056-8066; (i) Nakamura, E.; Sekiya, K.; Kuwajima, I., Chiral Zinc Homoenolate of Methyl Isobutyrate. A New Building Block for the Synthesis of Chiral *α*-Methylesters. *Tetrahedron Lett.* **1987,** *28*, 337-340; (j) Aoki, S.; Fujimura, T.; Nakamura, E.; Kuwajima, I., Palladium-Catalyzed Arylation of Siloxycyclopropanes with Aryl Triflates. Carbon Chain Elongation via Catalytic Carbon-Carbon Bond Cleavage. *J. Am. Chem. Soc.* **1988,** *110*, 3296-3298; (k) Aoki, S.; Nakamura, E.; Kuwajima, I., Synthesis of 4-Keto Pimelates by Palladium-Catalyzed Carbonylativesymmetrical Coupling of Siloxycyclopropanes. *Tetrahedron Lett.* **1988,** *29*, 1541-1542; (l) Aoki, S.; Nakamura, E., Synthesis of 1,4-Dicarbonyl Compounds by Palladium-Catalyzed Carbonylative Arylation of Siloxycyclopropanes. *Synlett* **1990,** *1990*, 741-742; (m) Aoki, S.; Nakamura, E., Synthesis of 1,4-Dicarbonyl Compounds and 4-Keto Pimelates by Palladium-Catalyzed Carbonylation of Siloxycyclopropanes. *Tetrahedron* **1991,** *47*, 3935-3946; (n) Fujimura, T.; Aoki, S.; Nakamura, E., Synthesis of 1,4-Keto Esters and 1,4-Diketones via Palladium-Catalyzed Acylation of Siloxycyclopropanes. Synthetic and Mechanistic Studies. *J. Org. Chem.* **1991,** *56*, 2809-2821.

7. Burke, E. D.; Lim, N. K.; Gleason, J. L., Catalytic Enantioselective Homoaldol Reactions Using BINOL Titanium(IV) Fluoride Catalysts. *Synlett* **2003,** 390-392.

8. (a) Nakamura, E.; Kuwajima, I., Stereocontrolled Construction of Oxygenated Steroidal Side Chains. Synthesis and Stereochemistry of Depresosterol. *J. Am. Chem. Soc.* **1985,** *107*, 2138-2141; (b) Horiguchi, Y.; Nakamura, E.; Kuwajima, I., Total Synthesis of (±)-Cortisone. Double Hydroxylation Reaction for the Construction of Corticoid Side Chain. *J. Org. Chem.* **1986,** *51*, 4323-4325; (c) Crimmins, M. T.; Wang, Z.; McKerlie, L. A., Rearrangement of Cyclobutyl Carbinyl Radicals: Total Synthesis of the Spirovetivane Phytoalexin (±)-Lubiminol. *Tetrahedron Lett.* **1996,** *37*, 8703-8706; (d) Crimmins, M. T.; Wang, Z.; McKerlie, L. A., Double Diastereoselection in Intramolecular Photocycloadditions: A Radical Rearrangement Approach to the Total

Synthesis of the Spirovetivane Phytoalexin (±)-Lubiminol. *J. Am. Chem. Soc.* **1998,** *120*, 1747-1756; (e) Barrett, A. G. M.; Damiani, F., A Formal Synthesis of Pumiliotoxin 251D, via a Highly Diastereoselective Addition of a Titanium Homoenolate to an L-Proline Derivative. *J. Org. Chem.* **1999,** *64*, 1410-1411; (f) Crimmins, M. T.; Pace, J. M.; Nantermet, P. G.; Kim-Meade, A. S.; Thomas, J. B.; Watterson, S. H.; Wagman, A. S., Total Synthesis of (±)-Ginkgolide B. *J. Am. Chem. Soc.* **1999,** *121*, 10249-10250; (g) Crimmins, M. T.; Pace, J. M.; Nantermet, P. G.; Kim-Meade, A. S.; Thomas, J. B.; Watterson, S. H.; Wagman, A. S., The Total Synthesis of (±)-Ginkgolide B. *J. Am. Chem. Soc.* **2000,** *122*, 8453-8463; (h) Evans, D. A.; Kværnø, L.; Dunn, T. B.; Beauchemin, A.; Raymer, B.; Mulder, J. A.; Olhava, E. J.; Juhl, M.; Kagechika, K.; Favor, D. A., Total Synthesis of (+)-Azaspiracid-1. An Exhibition of the Intricacies of Complex Molecule Synthesis. *J. Am. Chem. Soc.* **2008,** *130*, 16295-16309.

9. Yoshikai, N.; Nakamura, E., Mechanisms of Nucleophilic Organocopper(I) Reactions. *Chem. Rev.* **2012,** *112*, 2339-2372.

10. (a) Yamamoto, Y.; Yamamoto, S.; Yatagai, H.; Ishihara, Y.; Maruyama, K., Lewis Acid Mediated Reactions of Organocopper Reagents. Entrainment in the Conjugate Addition to *α,β*-Unsaturated Ketones, Esters, and Acids via the $RCu{\cdot}BF_3$ System. *J. Org. Chem.* **1982,** *47*, 119-126; (b) Nakamura, E.; Yamanaka, M.; Mori, S., Complexation of Lewis Acid with Trialkylcopper(III): On the Origin of BF_3-Acceleration of Cuprate Conjugate Addition. *J. Am. Chem. Soc.* **2000,** *122*, 1826-1827.

11. (a) Crimmins, M. T.; Nantermet, P. G., Addition of Zinc Homoenolates to Acetylenic Esters: A Formal [3+2] Cycloaddition. *J. Org. Chem.* **1990,** *55*, 4235-4237; (b) Crimmins, M. T.; Nantermet, P. G.; Trotter, B. W.; Vallin, I. M.; Watson, P. S.; McKerlie, L. A.; Reinhold, T. L.; Cheung, A. W. H.; Stetson, K. A.; Dedopoulou, D.; Gray, J. L., Addition of Zinc Homoenolates to Acetylenic Esters and Amides: A Formal [3 + 2] Cycloaddition. *J. Org. Chem.* **1993,** *58*, 1038-1047.

12. Cheng, B.-Q.; Zhang, S.-X.; Cui, Y.-Y.; Chu, X.-Q.; Rao, W.; Xu, H.; Han, G.-Z.; Shen, Z.-L., Copper(II)-Mediated Ring Opening/Alkynylation of Tertiary Cyclopropanols by Using Nonmodified Terminal Alkynes. *Org. Lett.* **2020,** *22*, 5456-5461.

13. Rosa, D.; Orellana, A., Palladium-Catalyzed Cross-Coupling of Cyclopropanols with Aryl Halides under Mild Conditions. *Org. Lett.* **2011,** *13*, 110-113.

14. Ryu, I.; Matsumoto, K.; Ando, M.; Murai, S.; Sonoda, N., Synthesis of *β*-Mercuri Ketones by the Reaction of Siloxycyclopropanes with Mercuric Acetate and

Their Conversion to α-Methylene Ketones and γ-Ketoesters. *Tetrahedron Lett.* **1980,** *21*, 4283-4286.

15. Nakahira, H.; Ryu, I.; Ikebe, M.; Oku, Y.; Ogawa, A.; Kambe, N.; Sonoda, N.; Murai, S., β-Trichlorostannyl Ketones and Aldehydes. Preparation and Facile Amine-Induced Dehydrostannation Leading to α-Methylene Ketones and Aldehydes. *J. Org. Chem.* **1992,** *57*, 17-28.

16. Nakahira, H.; Ryu, I.; Han, L.; Kambe, N.; Sonoda, N., β-Trichlorotelluro Ketones. Preparation and Extremely Facile Dehydrotelluration Leading to α-Methylene Ketones. *Tetrahedron Lett.* **1991,** *32*, 229-232.

17. Ikura, K.; Ryu, I.; Ogawa, A.; Sonoda, N.; Harada, S.; Kasai, N., Synthesis, Characterization, and Properties of Ethylene-Coordinated Complexes of β-Platinum(II) Ketones. *Organometallics* **1991,** *10*, 528-529.

18. Ryu, I.; Ando, M.; Ogawa, A.; Murai, S.; Sonoda, N., A β-Metal Ketone Strategy. Reactions of Siloxycyclopropanes with Silver(I) Tetrafluoroborate and Copper(II) Tetrafluoroborate Leading to 1,6-Diketones. *J. Am. Chem. Soc.* **1983,** *105*, 7192-7194.

19. Ryu, I.; Matsumoto, K.; Kameyama, Y.; Ando, M.; Kusumoto, N.; Ogawa, A.; Kambe, N.; Murai, S.; Sonoda, N., β-Copper(II) Ketones. Generation, Coupling, and Highly Stereoselective Trapping by Electron-Deficient Acetylenes. *J. Am. Chem. Soc.* **1993,** *115*, 12330-12339.

20. (a) Das, P. P.; Belmore, K.; Cha, J. K., S_N2' Alkylation of Cyclopropanols via Homoenolates. *Angew. Chem. Int. Ed.* **2012,** *51*, 9517-9520; (b) Murali, R. V. N. S.; Rao, N. N.; Cha, J. K., C-Alkynylation of Cyclopropanols. *Org. Lett.* **2015,** *17*, 3854-3856.

21. Parida, B. B.; Das, P. P.; Niocel, M.; Cha, J. K., C-Acylation of Cyclopropanols: Preparation of Functionalized 1,4-Diketones. *Org. Lett.* **2013,** *15*, 1780-1783.

22. Rao, N. N.; Cha, J. K., Concise Synthesis of Alkaloid (−)-205B. *J. Am. Chem. Soc.* **2015,** *137*, 2243-2246.

23. Trost, B. M.; Zhang, G.; Xu, M.; Qi, X., ProPhenol Derived Ligands to Simultaneously Coordinate a Main-Group Metal and a Transition Metal: Application to a Zn−Cu Catalyzed Reaction. *Chem. Eur. J.* **2022,** *28*, e202104268.

24. Trost, B. M.; Bartlett, M. J., ProPhenol-Catalyzed Asymmetric Additions by Spontaneously Assembled Dinuclear Main Group Metal Complexes. *Acc. Chem. Res.* **2015,** *48*, 688-701.

25. Mills, L. R.; Barrera Arbelaez, L. M.; Rousseaux, S. A. L., Electrophilic Zinc Homoenolates: Synthesis of Cyclopropylamines from Cyclopropanols and Amines. *J. Am. Chem. Soc.* **2017,** *139*, 11357-11360.

26. Murakami, M.; Ishida, N., *β*-Scission of Alkoxy Radicals in Synthetic Transformations. *Chem. Lett.* **2017,** *46*, 1692-1700.

27. Park, S.-B.; Cha, J. K., Palladium-Mediated Ring Opening of Hydroxycyclopropanes. *Org. Lett.* **2000,** *2*, 147-149.

28. Zhou, X.; Yu, S.; Qi, Z.; Kong, L.; Li, X., Rhodium(III)-Catalyzed Mild Alkylation of (Hetero)Arenes with Cyclopropanols via C–H Activation and Ring Opening. *J. Org. Chem.* **2016,** *81*, 4869-4875.

29. (a) Rosa, D.; Orellana, A., Palladium-Catalyzed Cross-Coupling of Cyclopropanol-Derived Ketone Homoenolates with Aryl Bromides. *Chem. Commun.* **2013,** *49*, 5420-5422; (b) Cheng, K.; Walsh, P. J., Arylation of Aldehyde Homoenolates with Aryl Bromides. *Org. Lett.* **2013,** *15*, 2298-2301; (c) Nikolaev, A.; Nithiy, N.; Orellana, A., One-Step Synthesis of Quinolines via Palladium-Catalyzed Cross-Coupling of Cyclopropanols with Unprotected *ortho*-Bromoanilines. *Synlett* **2014,** *25*, 2301-2305; (d) Nithiy, N.; Orellana, A., Palladium-Catalyzed Cross-Coupling of Benzyl Chlorides with Cyclopropanol-Derived Ketone Homoenolates. *Org. Lett.* **2014,** *16*, 5854-5857; (e) Liu, H.; Fu, Z.; Gao, S.; Huang, Y.; Lin, A.; Yao, H., Palladium-Catalyzed Hydroalkylation of Alkynes with Cyclopropanols: Access to *γ,δ*-Unsaturated Ketones. *Adv. Synth. Catal.* **2018,** *360*, 3171-3175; (f) Wu, P.; Jia, M.; Lin, W.; Ma, S., Matched Coupling of Propargylic Carbonates with Cyclopropanols. *Org. Lett.* **2018,** *20*, 554-557; (g) Lin, J.; Zhu, T.; Jia, M.; Ma, S., A Pd-Catalyzed Ring Opening Coupling Reaction of 2,3-Allenylic Carbonates with Cyclopropanols. *Chem. Commun.* **2019,** *55*, 4523-4526; (h) Ramar, T.; Subbaiah, M. A. M.; Ilangovan, A., Utility of Organoboron Reagents in Arylation of Cyclopropanols via Chelated Pd(II) Catalysis: Chemoselective Access to *β*-Aryl Ketones. *J. Org. Chem.* **2020,** *85*, 7711-7727; (i) Pati, B. V.; Ghosh, A.; Yadav, K.; Banjare, S. K.; Pandey, S.; Lourderaj, U.; Ravikumar, P. C., Palladium-Catalyzed Selective C–C Bond Cleavage and Stereoselective Alkenylation between

Cyclopropanol and 1,3-Diyne: One-Step Synthesis of Diverse Conjugated Enynes. *Chem. Sci.* **2022,** *13*, 2692-2700.

30. (a) He, X.-P.; Shu, Y.-J.; Dai, J.-J.; Zhang, W.-M.; Feng, Y.-S.; Xu, H.-J., Copper-Catalysed Ring-Opening Trifluoromethylation of Cyclopropanols. *Org. Biomol. Chem.* **2015,** *13*, 7159-7163; (b) Kananovich, D. G.; Konik, Y. A.; Zubrytski, D. M.; Järving, I.; Lopp, M., Simple Access to *β*-Trifluoromethyl-Substituted Ketones via Copper-Catalyzed Ring-Opening Trifluoromethylation of Substituted Cyclopropanols. *Chem. Commun.* **2015,** *51*, 8349-8352; (c) Li, Y.; Ye, Z.; Bellman, T. M.; Chi, T.; Dai, M., Efficient Synthesis of *β*-CF_3/SCF_3-Substituted Carbonyls via Copper-Catalyzed Electrophilic Ring-Opening Cross-Coupling of Cyclopropanols. *Org. Lett.* **2015,** *17*, 2186-2189; (d) Shen, M.-H.; Lu, X.-L.; Xu, H.-D., Copper(II) Acetate Catalysed Ring-Opening Cross-Coupling of Cyclopropanols with Sulfonyl Azides. *Rsc Adv.* **2015,** *5*, 98757-98761; (e) Ye, Z.; Dai, M., An Umpolung Strategy for the Synthesis of *β*-Aminoketones via Copper-Catalyzed Electrophilic Amination of Cyclopropanols. *Org. Lett.* **2015,** *17*, 2190-2193; (f) Ye, Z.; Gettys, K. E.; Shen, X.; Dai, M., Copper-Catalyzed Cyclopropanol Ring Opening C_{sp3}–C_{sp3} Cross-Couplings with (Fluoro)Alkyl Halides. *Org. Lett.* **2015,** *17*, 6074-6077; (g) Feng, Y.-S.; Shu, Y.-J.; Cao, P.; Xu, T.; Xu, H.-J., Copper(I)-Catalyzed Ring-Opening Cyanation of Cyclopropanols. *Org. Biomol. Chem.* **2017,** *15*, 3590-3593; (h) Konik, Y. A.; Elek, G. Z.; Kaabel, S.; Järving, I.; Lopp, M.; Kananovich, D. G., Synthesis of *γ*-Keto Sulfones by Copper-Catalyzed Oxidative Sulfonylation of Tertiary Cyclopropanols. *Org. Biomol. Chem.* **2017,** *15*, 8334-8340; (i) Konik, Y. A.; Kudrjashova, M.; Konrad, N.; Kaabel, S.; Järving, I.; Lopp, M.; Kananovich, D. G., Two-Step Conversion of Carboxylic Esters into Distally Fluorinated Ketones via Ring Cleavage of Cyclopropanol Intermediates: Application of Sulfinate Salts as Fluoroalkylating Reagents. *Org. Biomol. Chem.* **2017,** *15*, 4635-4643; (j) Ye, Z.; Cai, X.; Li, J.; Dai, M., Catalytic Cyclopropanol Ring Opening for Divergent Syntheses of *γ*-Butyrolactones and *δ*-Ketoesters Containing All-Carbon Quaternary Centers. *ACS Catal.* **2018,** *8*, 5907-5914; (k) Zhang, Q.; Zhou, S.-W.; Shi, C.-Y.; Yin, L., Catalytic Asymmetric Allylic Substitution with Copper(I) Homoenolates Generated from Cyclopropanols. *Angew. Chem. Int. Ed.* **2021,** *60*, 26351-26356; (l) Kitabayashi, A.; Mizushima, S.; Higashida, K.; Yasuda, Y.; Shimizu, Y.; Sawamura, M., Insights into the Mechanism of Enantioselective Copper-Catalyzed Ring-Opening Allylic Alkylation of Cyclopropanols. *Adv. Synth. Catal.* **2022,** *364*, 1855-1862;

31. (a) Yang, J.; Shen, Y.; Lim, Y. J.; Yoshikai, N., Divergent Ring-Opening Coupling between Cyclopropanols and Alkynes under Cobalt Catalysis. *Chem. Sci.* **2018,** *9*, 6928-6934; (b) Yang, J.; Sun, Q.; Yoshikai, N., Cobalt-Catalyzed Regio-and Diastereoselective Formal [3+2] Cycloaddition between Cyclopropanols and Allenes. *ACS Catal.* **2019,** *9*, 1973-1978; (c) Yang, J.; Sekiguchi, Y.; Yoshikai, N., Cobalt-Catalyzed Enantioselective and Chemodivergent Addition of Cyclopropanols to Oxabicyclic Alkenes. *ACS Catal.* **2019,** *9*, 5638-5644; (d) Huang, W.; Meng, F., Cobalt-Catalyzed Diastereo- and Enantioselective Hydroalkylation of Cyclopropenes with Cobalt Homoenolates. *Angew. Chem. Int. Ed.* **2021,** *60*, 2694-2698.

32. (a) Mills, L. R.; Zhou, C.; Fung, E.; Rousseaux, S. A. L., Ni-Catalyzed *β*-Alkylation of Cyclopropanol-Derived Homoenolates. *Org. Lett.* **2019,** *21*, 8805-8809; (b) Li, J.; Zheng, Y.; Huang, M.; Li, W., Ni-Catalyzed Denitrogenative Cross-Coupling of Benzotriazinones and Cyclopropanols: An Easy Access to Functionalized *β*-Aryl Ketones. *Org. Lett.* **2020,** *22*, 5020-5024; (c) Sekiguchi, Y.; Lee, Y. Y.; Yoshikai, N., Nickel-Catalyzed Ring-Opening Allylation of Cyclopropanols via Homoenolate. *Org. Lett.* **2021,** *23*, 5993-5997; (d) Hou, L.; Huang, W.; Wu, X.; Qu, J.; Chen, Y., Nickel-Catalyzed Carbonylation of Cyclopropanol with Benzyl Bromide for Multisubstituted Cyclopentenone Synthesis. *Org. Lett.* **2022,** *24*, 2699-2704.

33. Zhou, X.; Yu, S.; Kong, L.; Li, X., Rhodium(III)-Catalyzed Coupling of Arenes with Cyclopropanols via C–H Activation and Ring Opening. *ACS Catal.* **2016,** *6*, 647-651.

34. (a) Nakahira, H.; Ryu, I.; Ikrbe, M.; Kambe, N.; Sonoda, N., *β*-Lithio Ketone Enolates: Generation and Reactions with Electrophiles. *Angew. Chem. Int. Ed.* **1991,** *30*, 177-179; (b) Ryu, I.; Ikebe, M.; Sonoda, N.; Yamato, S.-y.; Yamamura, G.-h.; Komatsu, M., Conjugate Addition of Zincates Derived from Ketone *α,β*-Dianions to Enones. An Access to Unsymmetrical 1,6-Diketones. *Tetrahedron Lett.* **2000,** *41*, 5689-5692; (c) Ryu, I.; Nakahira, H.; Ikebe, M.; Sonoda, N.; Yamato, S.-y.; Komatsu, M., Chelation-Aided Generation of Ketone *α,β*-Dianions and Their Use as Copper Ate Complexes. Unprecedented Enolate Intervention in the Conjugate Addition to Enones. *J. Am. Chem. Soc.* **2000,** *122*, 1219-1220; (d) Ryu, I.; Ikebe, M.; Sonoda, N.; Yamato, S.-y.; Yamamura, G.-h.; Komatsu, M., Chemistry of Ketone *α,β*-Dianions. Acylation Reactions of Dianion Cuprates by Acid Chlorides. *Tetrahedron Lett.* **2002,** *43*, 1257-1259; (e) Nakahira, H.; Ikebe, M.; Oku, Y.; Sonoda, N.; Fukuyama, T.; Ryu, I., Generation of Ketone Dilithio *α,β*-Dianions and Their Reactions with Electrophiles.

Tetrahedron **2005,** *61*, 3383-3392; (f) Yamato, S.-y.; Yamamura, G.-h.; Komatsu, M.; Arai, M.; Fukuyama, T.; Ryu, I., An Anionic Strategy for Three- and Four-Component Coupling Reactions Leading to Ketone Frameworks Based on Vinylogous Conversion of Dilithio Ketone *α,β*-Dianions. *Org. Lett.* **2005,** *7*, 2489-2491.

35. Nakahira, H.; Ryu, I.; Ikebe, M.; Oku, Y.; Ogawa, A.; Kambe, N.; Sonoda, N.; Murai, S., *β*-Trichlorostannyl Ketones and Aldehydes. Preparation and Facile Amine-Induced Dehydrostannation Leading to *α*-Methylene Ketones and Aldehydes. *J. Org. Chem.* **1992,** *57*, 17-28.

36. (a) Nomura, K.; Matsubara, S., Zincate-Mediated Rearrangement Reaction of 2-(1-Hydroxyalkyl)-1-alkylcyclopropanol. *Chem. Commun.* **2009**, 2212-2213; (b) Nomura, K.; Matsubara, S., A New Zincate-Mediated Rearrangement Reaction of 2-(1-Hydroxyalkyl)-1-alkylcyclopropanol. *Chem. Eur. J.* **2010,** *16*, 703-708.

37. Sekiguchi, Y.; Yoshikai, N., Enantioselective Conjugate Addition of Catalytically Generated Zinc Homoenolate. *J. Am. Chem. Soc.* **2021,** *143*, 4775-4781.

38. Sekiguchi, Y.; Yoshikai, N., Zinc-Catalyzed *β*-Functionalization of Cyclopropanols via Enolized Homoenolate. *J. Am. Chem. Soc.* **2021,** *143*, 18400-18405.

39. Sustac Roman, D.; Charette, A. B., Catalytic C–H Bond Functionalization of Cyclopropane Derivatives. In *C-H Bond Activation and Catalytic Functionalization II*, Dixneuf, P. H.; Doucet, H., Eds. Springer International Publishing: Cham, 2016; pp 91-113.

40. Altenbach, H. J., 4.5 - Functional Group Transformations via Allyl Rearrangement. In *Comprehensive Organic Synthesis*, Trost, B. M.; Fleming, I., Eds. Pergamon: Oxford, 1991; pp 829-871.

41. Sekiguchi, Y.; Yoshikai, N., Zinc-Mediated Hydroxyallylation of Aldehydes with Cyclopropanols: Direct Access to Vicinal *anti-sec,tert*-Diols via Enolized Homoenolates. *Org. Lett.* **2022,** *24*, 960-965.

42. Ni, J.; Xia, X.; Zheng, W.-F.; Wang, Z., Ti-Catalyzed Diastereoselective Cyclopropanation of Carboxylic Derivatives with Terminal Olefins. *J. Am. Chem. Soc.* **2022,** *144*, 7889-7900.

Chapter 2. Enantioselective Conjugate Addition of Catalytically Generated Zinc Homoenolate to Enone

2.1 Introduction

Metal homoenolates represent useful organometallic nucleophiles that allow for umpolung functionalization of the *β*-position of a carbonyl group.[1] Pioneering studies by Nakamura and Kuwajima established 1-alkoxy-1-siloxycyclopropanes as precursors to various main group and transition-metal ester-homoenolates, among which zinc homoenolate proved to be a particularly versatile nucleophile for fundamental C−C bond-forming reactions including 1,2/1,4-addition, allylic substitution, and cross-coupling (Scheme 2.1a).[2] Nevertheless, an enantioselective variant of such transformations remains elusive. This is in sharp contrast to the fact that the catalytic enantioselective 1,2/1,4-addition and allylic substitution reactions of simple dialkylzincs have been developed and matured to the level that they now serve as benchmarks for the evaluation of new chiral ligands and catalysts.[3] For example, more than 800 and 100 articles can be found for the enantioselective addition of Et_2Zn to benzaldehyde and cyclohexenone, respectively, while no analogous asymmetric reaction involving a preformed zinc homoenolate has been reported.[4]

Recently, cyclopropanols have emerged as viable precursors for the *in situ* generation of keto-homoenolates.[1c-f] One of seminal studies in this context is Cha's work on allylic and propargylic substitutions mediated by stoichiometric Et_2Zn in combination with Cu(I) salt, where equilibrium generation of zinc homoenolate from the corresponding cyclopropoxide and its transmetalation to Cu(I) are likely involved (Scheme 2.1b).[5] However, such *in situ* generated zinc homoenolate has also not been exploited for an enantioselective C−C bond formation.[6,7]

This chapter describes the development of an enantioselective conjugate addition (ECA) of a catalytically generated chiral zinc homoenolate to *α*,*β*-unsaturated ketones (Scheme 2.1c).[8,9] A catalyst generated from Et_2Zn and a chiral *β*-amino alcohol promotes ring-opening addition of cyclopropanols to chalcone and related enones, which displays the feature of ligand-accelerated catalysis and represents a rare example of transition-metal-free ECA of organozinc reagents.[10] Upon heating, the 1,6-diketone products undergo facile intramolecular aldol condensation to afford multisubstituted cyclopentene derivatives with high enantioselectivity. The obtained chiral

cyclopentenes have the potential to serve as valuable building blocks for highly substituted cyclopentanes, which are often found structures in the natural products.[11]

Scheme 2.1. Generation and C−C Bond-Forming Reactions of Zinc Homoenolate

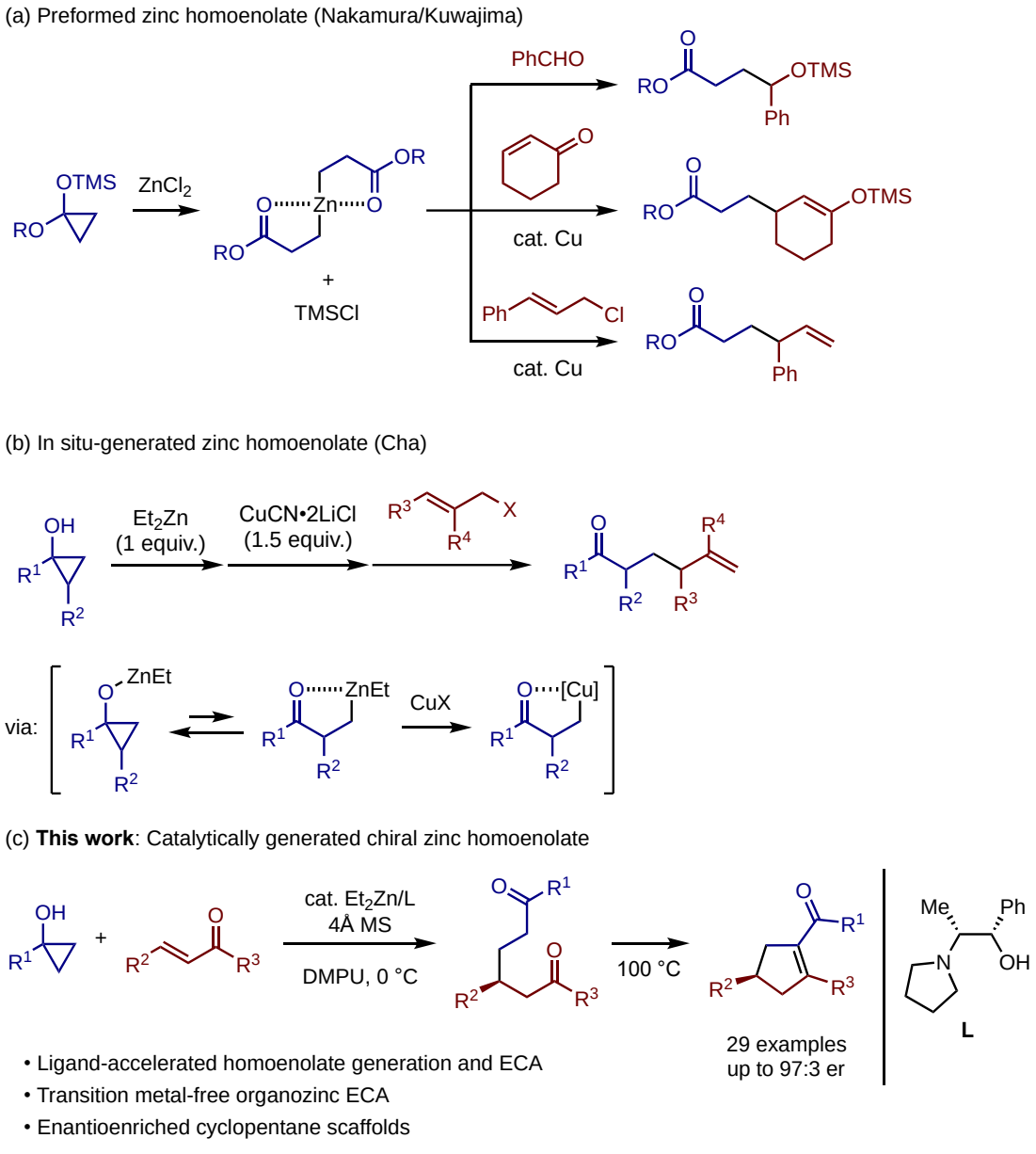

2.2 Results and Discussions

In light of Cha's seminal work on the equilibrium generation of zinc homoenolate from zinc cyclopropoxide,[5] the first question was whether it is possible to exploit such a process for C−C bond formation *catalytic* in zinc. Thus, the reaction between 1-phenylcyclopropanol (**1a**) and chalcone (**2a**) was initially examined. Upon brief screening, a catalytic system composed of Et_2Zn (10 mol%) and DABCO (10

mol%) was found to promote the desired ring-opening conjugate addition in DMSO at 80 °C, affording 1,6-diketone **3aa** in 47% yield along with a small amount of cyclopentene derivative **4aa** as a result of intramolecular aldol condensation of **3aa** (Scheme 2.2). By adding molecular sieves 4 Å, the reaction gave **4aa** as the dominant product.

Scheme 2.2. Racemic Reaction of Zinc-Catalyzed Addition of 1-Phenylcyclopropanol (**1a**) to Chalcone (**2a**)

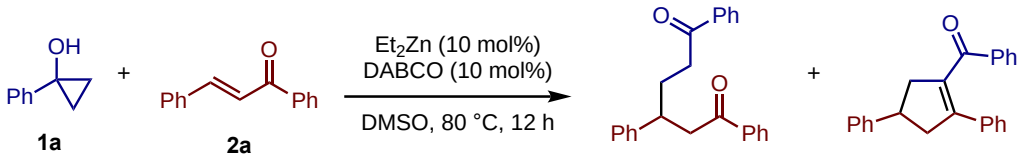

	3aa	**4aa**
without 4Å MS	47%	7%
with 4Å MS	5%	57%

Given the feasibility of zinc-catalyzed generation and conjugate addition of homoenolate from cyclopropanol, I next attempted to render the reaction enantioselective. In this respect, I explored a host of chiral *β*-amino alcohols as ligands, which have found extensive use in the enantioselective addition of dialkylzincs[3a] as well as preformed or *in situ*-generated zinc acetylides.[12] In view of the relevance of five-membered ring scaffolds in bioactive compounds,[11] I decided to focus on the formation of the cyclopentene product rather than the 1,6-diketone. Upon screening of ligands, solvents, and other reaction conditions, a few amino alcohols (**L1**, **L3**, and **L5**−**L7**) emerged as promising ligands (Table 2.1, entries 1−7). For example, the reaction of **1a** and **2a** in the presence of Et_2Zn and the norephedrine derivative **L6** (10 mol% each) and 4 Å MS in DMSO was performed at 30 °C for 24 h, followed by heating at 100 °C for 6 h, to afford the cyclopentene **4aa** in 73% yield with 87:13 er (entry 6). The use of DMPU as the solvent improved the enantioselectivity to 93:7 er (entry 8). It should be noted that other less coordinating solvents, such as THF, gave **4aa** in lower yields (see also Figure 2.1g). By performing the ECA step at 0 °C for 48 h with an increased catalyst loading (15 mol%), an additional improvement in the yield (89%) and the enantioselectivity (95:5 er) was achieved (entry 9).

Table 2.1. Zinc-Catalyzed Addition of 1-Phenylcyclopropanol (**1a**) to Chalcone (**2a**)[a]

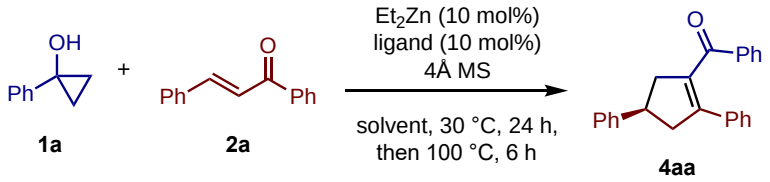

entry	ligand	solvent	yield[b] (%)	er[c]
1	**L1**	DMSO	88	82:18
2	**L2**	DMSO	65	47:54
3	**L3**	DMSO	69	79:21
4	**L4**	DMSO	63	52:48
5	**L5**	DMSO	71	77:23
6	**L6**	DMSO	73	87:13
7	**L7**	DMSO	50	82:18
8	**L6**	DMPU	79	93:7
9[d]	**L6**	DMPU	89	95:5

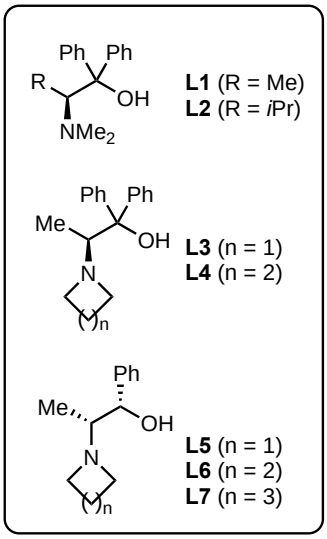

[a]The reaction was performed using 0.15 mmol of **1a** and 0.1 mmol of **2a** in 0.3 mL of solvent (0.33 M). [b]Determined by GC using mesitylene as an internal standard. [c]Determined by chiral HPLC. [d]15 mol% each of Et_2Zn and **L6** was used. The reaction was performed at 0 °C for 48 h and then at 100 °C for 6 h.

With the optimized catalytic system (Table 2.1, entry 9) in hand, the scope of the present homoenolate ECA was explored. First, a variety of cyclopropanols were subjected to the reaction with chalcone (**2a**) (Scheme 2.3). Various 1-arylcyclopropanols participated in the ring-opening conjugate addition/intramolecular aldol cascade, thus affording cyclopentenes **4aa**–**4ha** in moderate to high yields and enantioselectivities with tolerance to methoxy, bromo, iodo, and trifluoromethyl groups. A modest trend of decreasing enantioselectivity with electron-withdrawing aryl group was observed, as manifested in the case of the *p*-trifluoromethyl group (see **4ea**). The absolute configuration of the Br-substituted product **4da** was determined to be *R* by X-ray crystallographic analysis. The reaction of **1a** could be performed on a 3 mmol scale without a decrease in the enantioselectivity. Importantly, the reaction of **1a** and **2a**, when quenched before the aldol step, gave the 1,6-diketone product **3aa** in good yield with enantioselectivity (95:5 er) identical to that of **4aa**. This underlines that the enantiomeric ratio of **4aa** solely reflects the ECA step. 1-(2-Thienyl)cyclopropanol and 1-(1-cyclohexenyl)cyclopropanol also smoothly took part in the reaction to furnish the desired products **4ia** and **4ja**, respectively, with 96:4 er. The reactions of 1-(*sec*-alkyl)cyclopropanols were somewhat sluggish and required higher temperatures.

Nonetheless, the corresponding cyclopentene products (**4ka** and **4la**) were obtained with excellent enantioselectivity (97:3 er). In contrast, the reaction of 1-pentylcyclopropanol produced a mixture of inseparable products, as indicated by GC analysis prior to aldol condensation. The formation of the desired ECA product along with other bimolecular reaction products (e.g., enolate Michael adduct) was suggested but not unambiguously confirmed.

Scheme 2.3. Asymmetric Ring-Opening Addition of Various Cyclopropanols to **2a**[a]

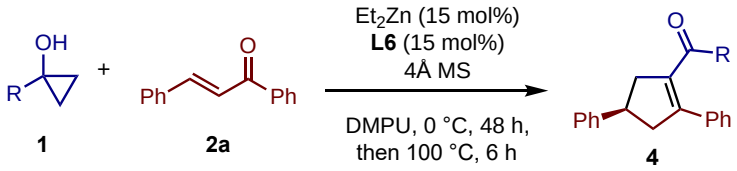

1 2a 4

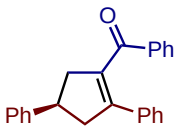

4aa, 80%, 95:5 er (70%, 95:5 er)[b]

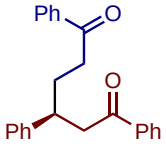

3aa, 86%, 95:5 er[c]

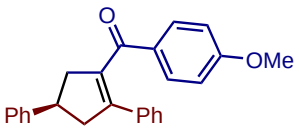

4ba, 67%, 95:5 er

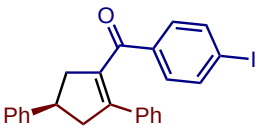

4ca, 85%, 93:7 er

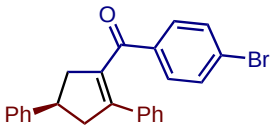

4da, 91%, 93:7 er[d] CCDC 2056575

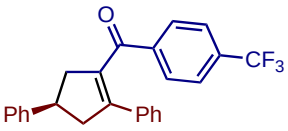

4ea, 85%, 87:13 er[e]

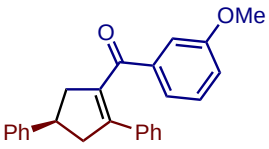

4fa, 77%, 94:6 er[d]

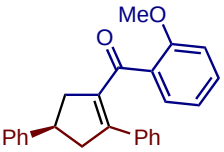

4ga, 69%, 91:9 er[f]

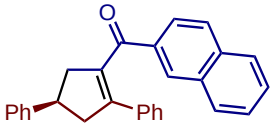

4ha, 93%, 95:5 er[d]

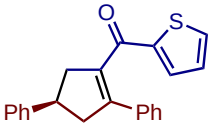

4ia, 82%, 96:4 er

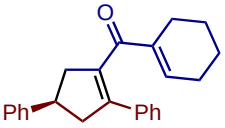

4ja, 54%, 96:4 er

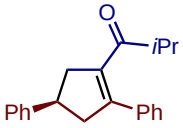

4ka, 48%, 97:3 er[f]

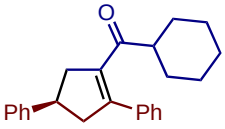

4la, 74%, 97:3 er[f]

[a]The reaction was performed on a 0.3 mmol scale under the conditions in Table 2.1, entry 9. [b]3 mmol scale reaction. [c]The reaction was quenched without aldol condensation step. [d]The ECA step was performed at 0 °C for 72 h. [e]The ECA step was performed at 30 °C for 12 h. [f]The ECA step was performed at 30 °C for 48 h.

A racemic bicyclic cyclopropanol **1m** (2 equiv.) underwent selective cleavage of the less substituted C−C bond and afforded the desired conjugate adduct **3ma** as a diastereomeric mixture (78:22 dr) in 96% yield, with 98:2 and 90:10 ers for the major

and minor diastereomers, respectively (Scheme 2.4; note that the absolute configurations were not determined, and those shown in the scheme are only provisional). Meanwhile, the unreacted **1m** was isolated in the form of benzoyl ester **1m'** in 24% yield (based on **1m**) with 96:4 er. This outcome can be rationalized by highly selective kinetic resolution in the ring-opening step and moderately diastereoselective conjugate addition of each diastereomeric zinc homoenolate. Thus, if (*R*,*S*)-**3ma** was provisionally assigned as a major enantiomer of the major diastereomer (73% yield), the yield of (*R*,*R*)-**3ma**, which is one of the enantiomers of the minor diastereomer, would be either 20% or 1%. Since the kinetic resolution step was highly selective (**1m** was recovered in 96:4 er as **1m'**), the yield of (*R*,*R*)-**3ma** should be 20%.

Scheme 2.4. Addition of Bicyclic Cyclopropanol (**1m**) to **2a**

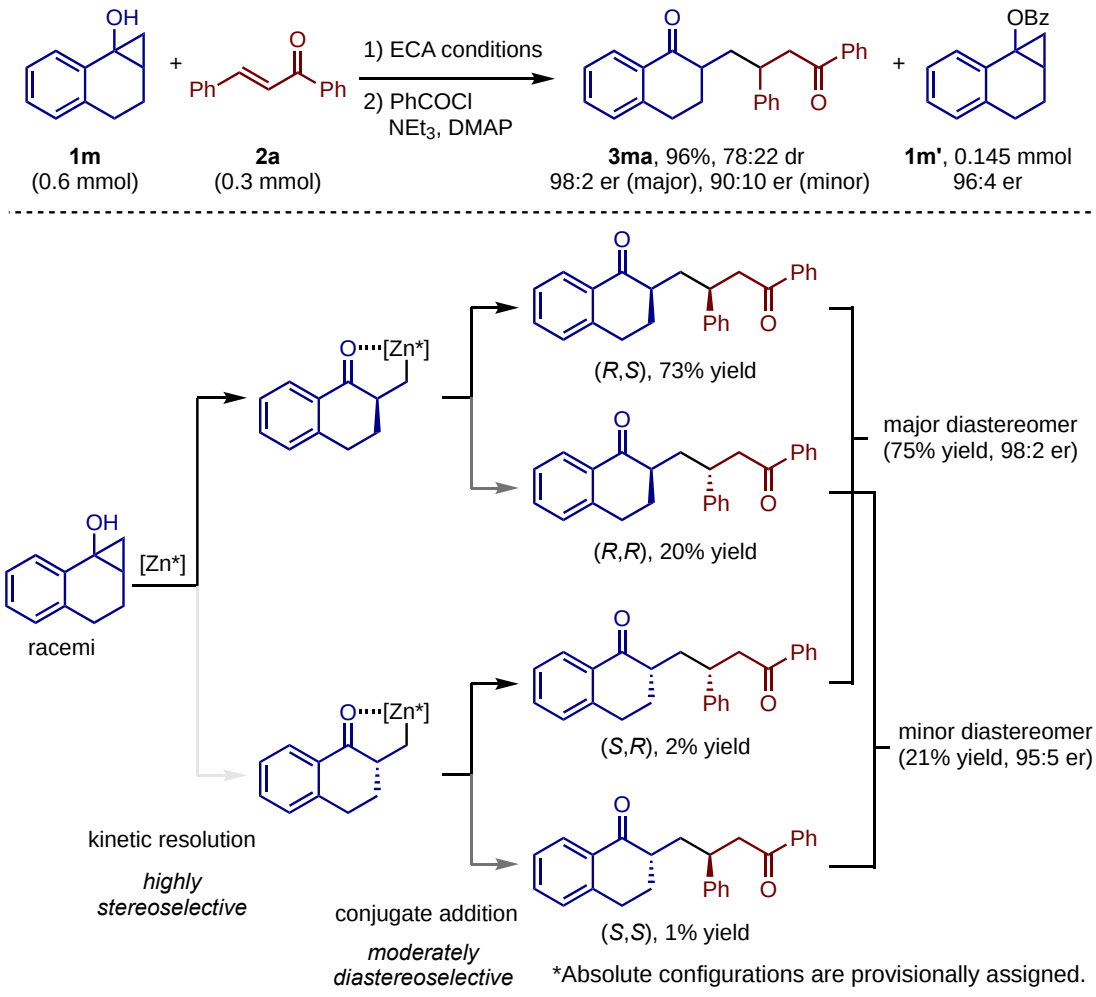

Next, the addition of **1a** to various *α*,*β*-unsaturated ketones was explored (Scheme 2.5). Chalcone-type di(hetero)-aryl-substituted enones proved to be excellent substrates, affording the corresponding cyclopentenes **4ab**−**4aj** in moderate to high yields with 92:8 to 97:3 er. A variety of functionalized aryl and heteroaryl groups could be tolerated on both ends of the enone skeleton. An *α*,*β*,*γ*,*δ*-unsaturated ketone underwent selective 1,4-addition of the homoenolate to give the alkenyl-substituted cyclopentene **4ak** with 97:3 er. Dibenzylideneacetone selectively afforded the monoconjugate addition product, which cyclized into the cyclopentene **4al** with equally high enantioselectivity (96:4 er). Unlike these examples, enones bearing an alkyl substituent at either the *β*-position or the acyl position failed to participate in the reaction under the standard conditions. Using **L3** as the ligand, such substrates afforded the desired products **4am** and **4an** with moderate enantioselectivities (ca. 80:20 er). *β*-Trifluoromethyl enone also took part in the reaction, albeit in modest yield and enantioselectivity (see **4ao**). GC analysis of the reaction mixture prior to aldol condensation indicated the formation of other bimolecular products. Cinnamaldehyde was also found to undergo the homoenolate conjugate addition, affording the disubstituted cyclopentene **4ap** in diminished yield and enantioselectivity.

Scheme 2.5. Asymmetric Ring-Opening Addition of **1a** to Various Enones[a]

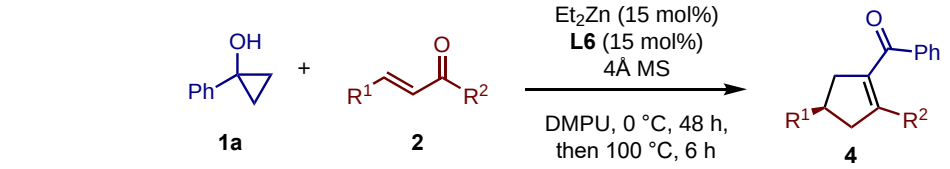

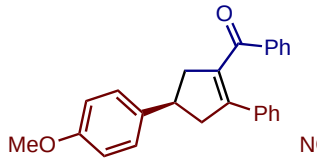

4ab, 68%, 96:4 er

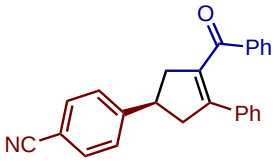

4ac, 70%, 92:8 er

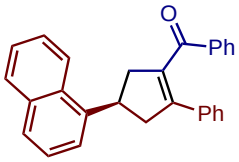

4ad, 80%, 96:4 er[b]

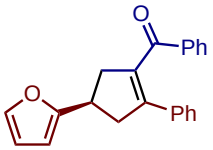

4ae, 77%, 97:3 er

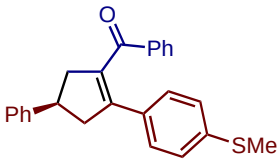

4af, 81%, 97:3 er

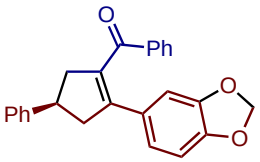

4ag, 84%, 95:5 er

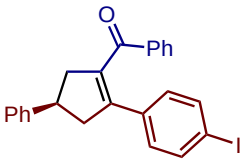

4ah, 85%, 96:4 er

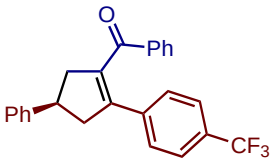

4ai, 93%, 93:7 er[b]

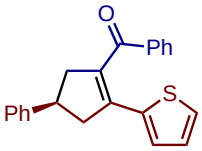

4aj, 83%, 95:5 er

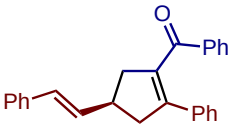

4ak, 75%, 97:3 er

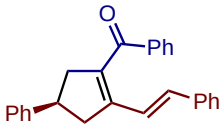

4al, 60%, 96:4 er

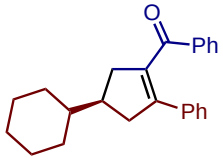

4am, 83%, 78:22 er[c,d]

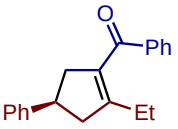

4an, 58%, 79:21 er[c,e]

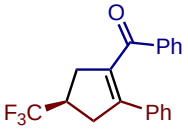

4ao, 39%, 77:23 er[c,f]

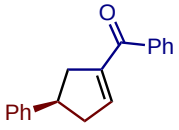

4ap, 34%, 62:38 er[g]

[a]The reaction was performed on a 0.3 mmol scale under the conditions in Table 2.1, entry 9. [b]The aldol condensation step was performed at 50 °C for 16 h. [c]**L3** was used instead of **L6**. [d]The reaction was performed in DMSO at 40 °C for 48 h and then 100 °C for 6 h. [e]The ECA step was performed at 30 °C for 48 h. [f]The ECA step was performed at 30 °C for 24 h. [g]The ECA and aldol condensation steps were performed at 60 °C for 12 h.

The reaction of (*E*)-2-benzylidenecyclohexan-1-one (**2q**) furnished, after 3 h of the aldol condensation step, a bicyclic product **4aq** as a mixture of diastereomers (80:20 dr) with ers of 84:16 (major) and 70:30 (minor) (Scheme 2.6). The relative stereochemistry of the major diastereomer of **4aq** was confirmed by X-ray crystallographic analysis of its anilide derivative **5aq**. Notably, extension of the condensation step for this product resulted in transposition of the C=C bond to the bicyclic juncture to give a tetrasubstituted olefin isomer **4aq'** (66% yield, 50:50 dr and 80:20 er for both diastereomers), presumably via a zinc dienolate intermediate. Note that other types of Michael acceptors such as cyclohexenone, methyl cinnamate, and *β*-

nitrostyrene failed to undergo homoenolate conjugate addition under the achiral reaction conditions (see Scheme 2.2). As such, the feasibility of their homoenolate ECA was not explored at this time.

Scheme 2.6. Addition of **1a** to (*E*)-2-Benzylidenecyclohexan-1-one (**2q**)

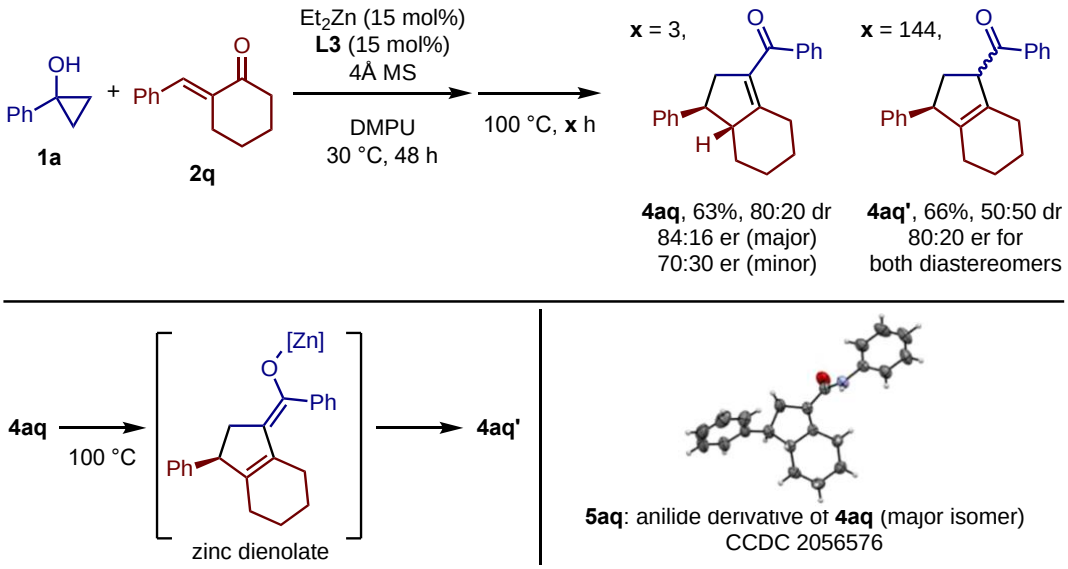

To gain insight into the ligand effect and the zinc species involved in the present homoenolate ECA, a series of mechanistic experiments were performed. The model reaction of **1a** and **2a** (performed at 30 °C to facilitate the reaction at low catalyst loadings and/or with low-ee catalysts) was found to display concentration-dependent nonlinear effects (NLEs; Figure 2.1a).[13] Thus, a clear positive NLE was observed with 20 mol% catalyst loading (67 mM [Zn]), while NLE became rather weak upon reducing the catalyst loading down to 10 mol% (33 mM [Zn]). Furthermore, the reaction procedure was found to have a slight but non-negligible influence on NLE. Thus, while the above NLE experiments were set up according to the general procedure, which involves sequential addition (without a break longer than 15s) of Et_2Zn, **2a**, and **1a** to a mixture of **L6** and 4 Å MS in DMPU, aging of a mixture of **L6** and Et_2Zn for 10 min at room temperature prior to the addition of **1a** and **2a** slightly enhanced the NLE (Figure 2.1b). On the other hand, the reaction temperature (30 °C vs 0 °C) and the solvent composition (DMPU vs DMPU/THF) had only a minor impact on NLE (Figure 2.1c and d). The ee of **L6** was also found to significantly influence the reaction rate. Thus, the initial rate of the reaction using enantiopure **L6** was found to be more than four times faster than that using racemic **L6** (Figure 2.1e). Note that the reaction

mixtures appeared clear and homogeneous regardless of using enantiopure or racemic **L6**. Apart from these observations under the actual reaction conditions in DMPU, mixing racemic **L6** and Et_2Zn in Et_2O immediately generated a white precipitate, which was a signature of the formation of insoluble heterochiral aggregates,[14] while a mixture of enantiopure **L6** and Et_2Zn in Et_2O formed a homogeneous solution. These observations may suggest that, in highly polar and Lewis basic DMPU, both homochiral and heterochiral Zn aminoalkoxide dimers form as soluble species and that the latter is reluctant to dissociate into catalytically relevant monomeric Zn species (*vide infra*).[13b]

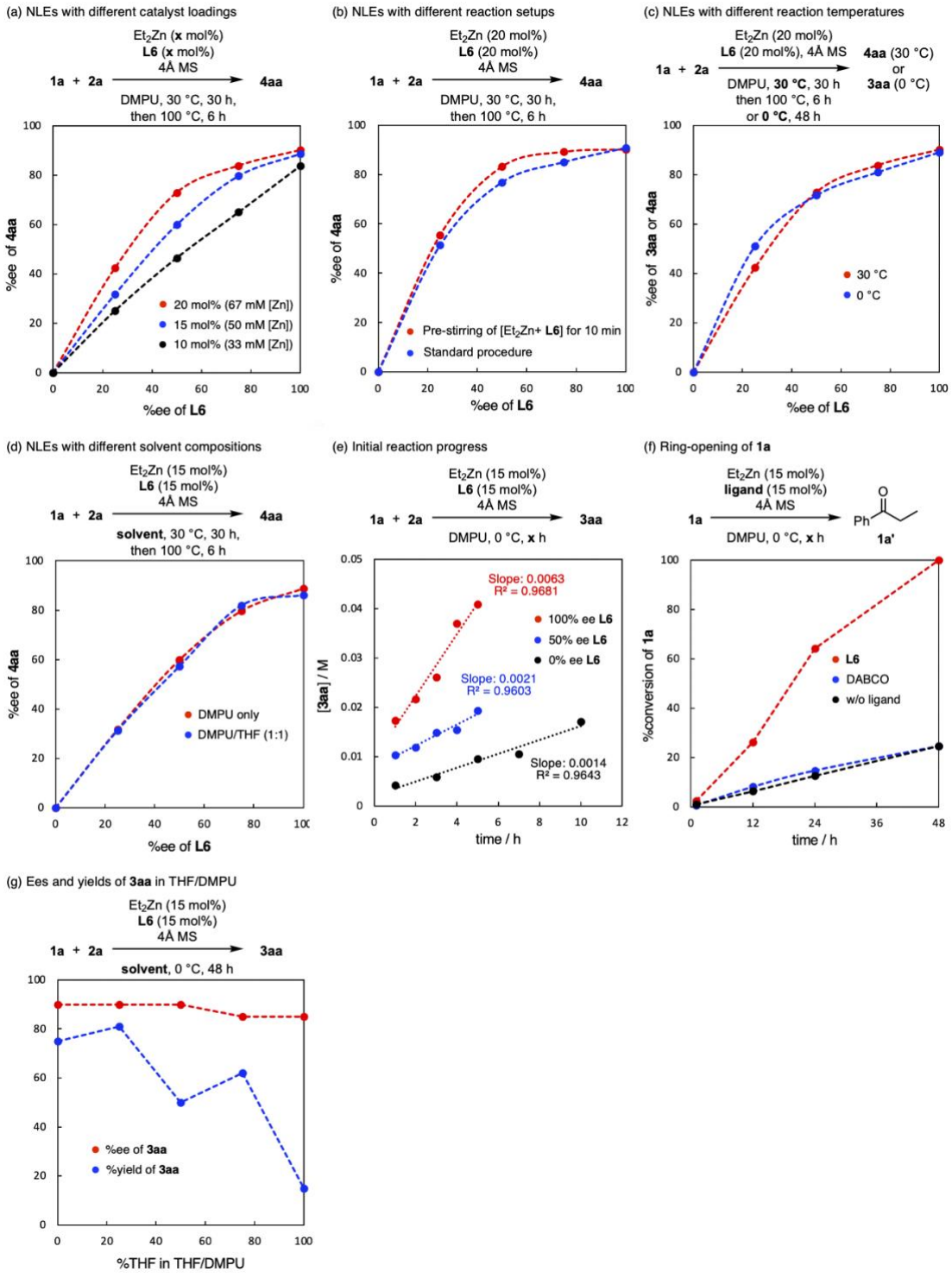

Figure 2.1. Mechanistic Experiments

The ability of the amino alcohol to accelerate the whole reaction process as well as the ring-opening step alone was clearly demonstrated by control experiments. Thus, no reaction took place between **1a** and **2a** by omitting **L6** from or replacing **L6** with DABCO under the standard conditions. The reaction of **1a** alone under the standard

conditions quantitatively produced propiophenone **1a'** after 48 h, while the ring opening was rather sluggish by omitting **L6** or using DABCO (Figure 2.1f). The solvent effect (DMPU, THF, and their mixed solvents) on the model reaction was also probed (Figure 2.1g). The enantioselectivity proved rather insensitive to the solvent composition. By contrast, the product yield dropped significantly in pure THF (15%) owing to competitive Michael addition of propiophenone enolate to **2a**, while the yield, albeit with some fluctuation, remained substantial (≥50%) in the mixed solvents (%THF up to 75%).

It is well established that a 1:1 mixture of Et_2Zn and chiral *β*-amino alcohol gives rise to homochiral and heterochiral ethylzinc aminoalkoxide dimers, depending on the enantiomeric composition of the ligand.[13b] The heterochiral dimer is often much more stable and reluctant to dissociate into monomers, which is responsible for NLE in Et_2Zn addition to aldehyde. A question relevant to the present reaction system is what happens to such ethylzinc aminoalkoxide dimers upon exposure to cyclopropanol. In attempts to address this question, I measured ^{1}H NMR spectra of zinc species formed by mixing **L6** and Et_2Zn in a 1:1 ratio followed by another alcohol (1 equiv.; *t*BuOH, *i*PrOH, or MeOH) as a model of the cyclopropanol substrate. Except for the case using MeOH, the ^{1}H NMR spectra showed clearly resolved quartet (~0.6 ppm) and triplet (~1.6 ppm) signals that could be assigned to an ethyl group on Zn. This observation indicates that ethylzinc aminoalkoxide [(**L6**-H)ZnEt] (**L6**-H represents the deprotonated **L6**) resists protonation of the remaining ethyl group by a bulky alcohol such as *t*BuOH and *i*PrOH, which should also be the case for the tertiary cyclopropanol substrates used in the present reaction (Scheme 2.7a). Similar observations have been made for the reluctance of [**L**ZnEt] species toward protonation of the Zn−Et bond by alcohol.[15] Note also that, a sample prepared by mixing Et_2Zn and *t*BuOH first, followed by **L6**, gave rise to a ^{1}H NMR spectrum close to that of the above-mentioned experiment (Scheme 2.7b). This suggests that the initially formed (*t*BuO)ZnEt underwent deprotonation of **L6** with *t*BuO rather than Et, thus generating [(**L6**-H)ZnEt] and *t*BuOH.

Scheme 2.7. Stoichiometric Reaction of Et_2Zn, Ligand and Bulky Alcohols

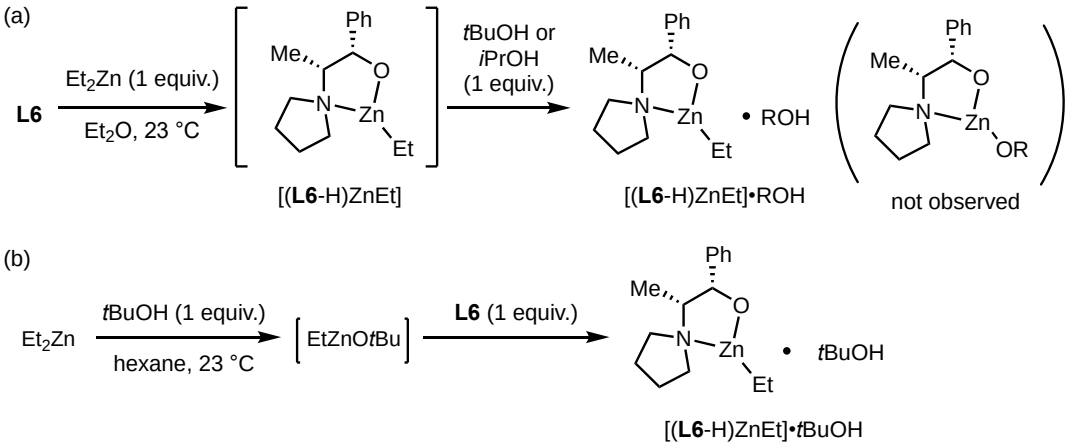

Given the reluctance of bulky alcohols to protonate the Zn−Et bond of [(**L6**-H)ZnEt], the formation of a mixed zinc bisalkoxide species such as [(**L6**-H)(**1**-H)Zn] in the present reaction system is less likely and that a zinc cyclopropoxide species would form as a transient rather than resting species via reversible protonation of the aminoalkoxide ligand. With this conjecture, and on the basis of the above NLE and other experiments as well as the literature knowledge on chiral amino alcohol-catalyzed organozinc addition,[3a, 13b] a tentative catalytic cycle illustrated in Scheme 2.8 is suggested. Coordination of the cyclopropanol **1** would break down the homochiral ethylzinc aminoalkoxide dimer $[\mathbf{A}]_2$ into a monomeric species [**A**·**1**]. Deprotonation of the cyclopropyl OH with the internal aminoalkoxide base would reversibly generate a cyclopropoxide species **B**, which would further undergo ring-opening to generate the corresponding homoenolate **C**. Association of the homoenolate **C** with the aminoalkoxide **A** and the enone **2** would generate a bimetallic species **D**,[16] followed by delivery of the homoenolate to give an enolate species **E**.[17] Proton transfer from the amino alcohol to the enolate would furnish the conjugate adduct **3** while regenerating the aminoalkoxide dimer $[\mathbf{A}]_2$. The heterochiral dimer [**A**·*ent*-**A**], preferentially formed when using racemic ligand, would be reluctant to dissociate into the monomer [**A**·**1**]. When there is no enone or ECA is sluggish, the homoenolate **C** could be protonated, possibly via internal proton transfer from the amino alcohol, to give the corresponding ketone **1'**, which could further participate in enolate Michael addition under zinc catalysis. On the basis of the solvent effect (Figure 2.1g), the ability of DMPU as a Lewis base to Zn, rather than its bulk polarity as a solvent, appears to be critical for the preferential CA of the homoenolate over its protonation. Thus, I speculate that

coordination of DMPU to zinc would assist in dissociation of the dimeric species and/or increasing the nucleophilicity of the homoenolate.

Scheme 2.8. Possible Catalytic Cycle

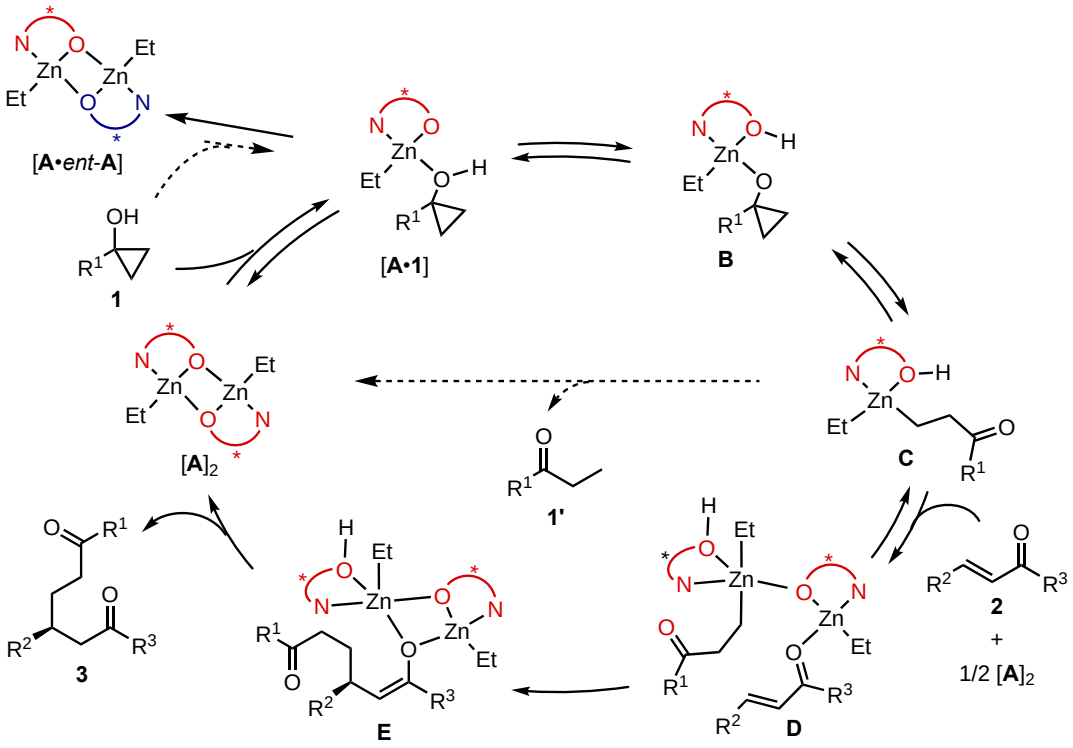

Selected transformations of the enantioenriched cyclopentene product **4aa** are shown in Scheme 2.9. Conversion of the benzoyl group to an anilide moiety via Beckmann rearrangement was achieved through oxime formation and subsequent treatment with Tf_2O, affording the product **5** in good yield. Epoxidation with *m*CPBA provided the tetrasubstituted epoxide **6** in a diastereoselective manner, albeit in a modest yield. Generation of a dienolate species from **4aa** and LiHMDS was followed by trapping with benzyl bromide, which took place regioselectively at the α-position to generate a quaternary stereocenter in the product **7** in a diastereoselective manner.

Scheme 2.9. Product Transformations

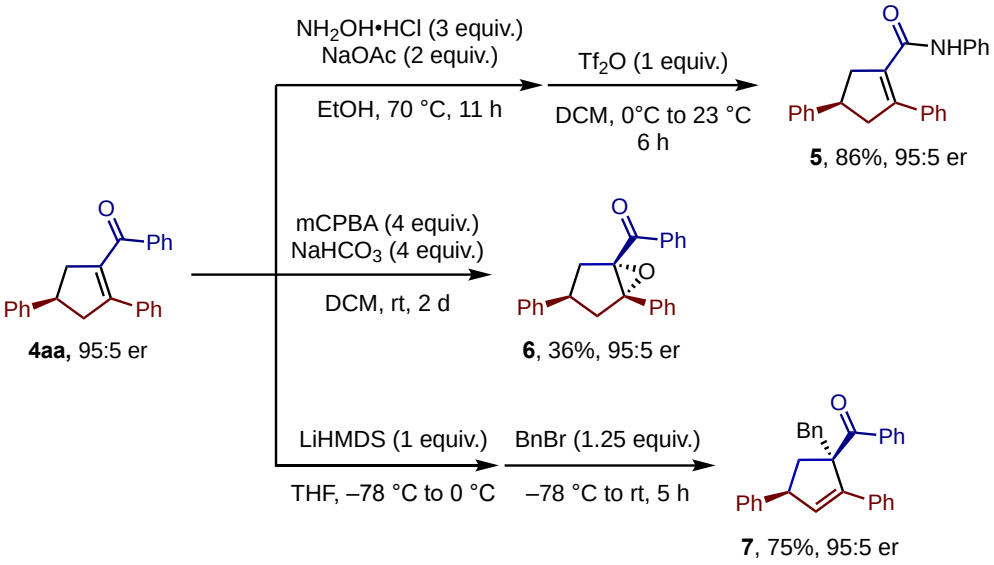

2.3 Conclusion

In summary, I have developed an enantioselective ring-opening conjugate addition of cyclopropanols to *α*,*β*-unsaturated ketones via catalytic generation of zinc homoenolate. A chiral *β*-amino alkoxide ligand on zinc accelerates the ring-opening of a cyclopropanol and aids in enantioselective addition of the resulting homoenolate to chalcones and related enones without assistance of a transition-metal catalyst. The ensuing intramolecular aldol condensation of the 1,6-diketone products allows for facile preparation of multisubstituted cyclopentene derivatives with good to high enantioselectivity. The reaction represents the first example of enantioselective transformation of zinc homoenolate and also a rare example of asymmetric transformations of metal homoenolates in general.

2.4 Experimental Section

General procedure: In an argon-filled glove box, a 4-mL vial equipped with a magnetic stir bar was charged sequentially with **L6** (9.2 mg, 0.045 mmol), molecular sieves 4 Å (300 mg), and DMPU (0.9 mL, stored in –20 °C fridge). To this mixture was added Et_2Zn (1 M in hexane, 45 μL, 0.045 mmol), enone **2** (0.30 mmol), and cyclopropanol **1** (0.45 mmol) sequentially, without a particular break (longer than 15 seconds) between additions. The vial was closed and removed from the glove box, and the mixture was stirred at 0 °C for 48 h. After confirmation of the full conversation of **2** by TLC or GC, the mixture was stirred at 100 °C for 6 h. Upon cooling to room

temperature, the reaction mixture was diluted with CH_2Cl_2 (3 mL) and filtered through a pad of silica gel with additional CH_2Cl_2 (10 mL) as an eluent. The organic solution was concentrated under reduced pressure, and the residue was purified by flash chromatography on silica gel or preparative TLC on silica gel to afford the desired product.

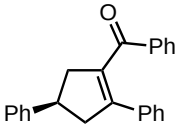

(*R*)-(2,4-Diphenylcyclopent-1-en-1-yl)(phenyl)methanone (4aa): Pale yellow solid (78.3 mg, 80%); R_f 0.31 (hexane/EtOAc = 19/1); m.p. 79-80 °C; **^{1}H NMR** (400 MHz, $CDCl_3$) δ 7.79-7.76 (m, 2H), 7.40-7.32 (m, 5H), 7.27-7.21 (m, 3H), 7.19-7.16 (m, 2H), 7.12-7.08 (m, 3H), 3.79 (quint, *J* = 8.3 Hz, 1H), 3.49-3.33 (m, 2H), 3.23-3.08 (m, 2H); **^{13}C{^{1}H} NMR** (100 MHz, $CDCl_3$) δ 197.6, 145.3, 145.0, 136.5, 136.3, 135.6, 132.8, 129.3, 128.6, 128.2, 128.0, 127.9, 127.9, 126.9, 126.3, 45.7, 45.2, 42.4; **HRMS** (ESI) Calcd for $C_{24}H_{21}O$ $[M + H]^+$ 325.1592, found 325.1592; $[\alpha]^{25}_D$ = +14.4 (*c* = 1.31 in $CHCl_3$, 95:5 er sample).

HPLC analysis: Daicel CHIRALPAK AS-H; hexane:*i*-PrOH = 95:5; detection wavelength = 254 nm; flow rate = 1.0 mL/min. t_R = 6.8 min (minor) and 7.6 min (major), 95:5 er.

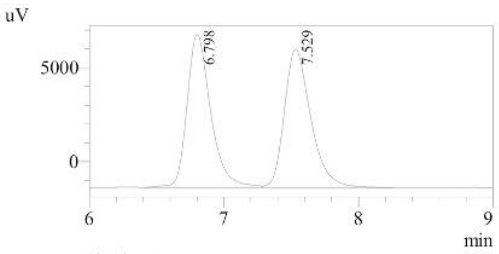

PeakTable
Detector A Ch1 254nm

Peak#	Ret. Time	Area %
1	6.798	49.818
2	7.529	50.182
Total		100.000

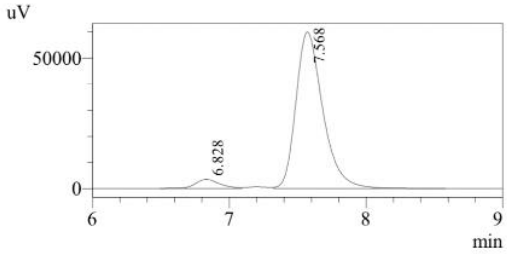

PeakTable
Detector A Ch1 254nm

Peak#	Ret. Time	Area %
1	6.828	4.949
2	7.568	95.051
Total		100.000

3 mmol-scale reaction: In an argon-filled glove box, a 50-mL Schlenk tube (pre-cooled in –20 °C fridge) equipped with a magnetic stir bar was charged sequentially with **L6** (92.4 mg, 0. 45 mmol), molecular sieves 4 Å (3.0 g), and DMPU (9 mL, stored in –20 °C fridge). To the mixture was added Et_2Zn (1 M in hexane, 450 μL, 0.45 mmol),

2a (625 mg, 3.0 mmol), and **1a** (604 mg, 4.5 mmol) sequentially. After stirring for 30 seconds, the Schlenk tube was closed and removed from the glove box, and the mixture was stirred at 0 °C for 48 h and then at 100 °C for 6 h. Upon cooling to room temperature, CH_2Cl_2 (30 mL) and H_2O (30 mL) were added to the reaction mixture. The aqueous layer was extracted with CH_2Cl_2 (2 × 30 mL) and the combined organic layers were dried over Na_2SO_4, filtered, and concentrated under reduced pressure. The residue was purified by flash chromatography on silica gel to afford the product as a pale yellow solid (683 mg, 70%, 95:5 er).

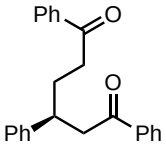

(*S*)-1,3,6-Triphenylhexane-1,6-dione (3aa): The reaction was performed at 0 °C for 48 h. White solid (88.1 mg, 86%); R_f 0.32 (hexane/EtOAc = 9/1); m.p. 146-148 °C; **^{1}H NMR** (400 MHz, $CDCl_3$) δ 7.90-7.88 (m, 2H), 7.83-7.81 (m, 2H), 7.55-7.48 (m, 2H), 7.44-7.37 (m, 4H), 7.32-7.25 (m, 4H), 7.22-7.18 (m, 1H), 3.48-3.41 (m, 1H), 3.39-3.28 (m, 2H), 2.93 (ddd, *J* = 17.1, 10.2, 5.9 Hz, 1H), 2.75 (ddd, *J* = 17.1, 10.1, 4.9 Hz, 1H), 2.27-2.19 (m, 1H), 2.12-2.02 (m, 1H); **^{13}C{^{1}H} NMR** (100 MHz, $CDCl_3$) δ 199.9, 198.6, 143.8, 137.1, 136.8, 133.0, 132.9, 128.7, 128.5, 128.5, 128.0, 127.9, 127.6, 126.6, 46.0, 40.7, 36.7, 30.5; **HRMS** (ESI) Calcd for $C_{24}H_{23}O_2$ $[M + H]^+$ 343.1698, found 343.1695; $[\alpha]^{25}_D$ = –11.7 (*c* = 2.30 in $CHCl_3$, 95:5 er sample).

HPLC analysis: Daicel CHIRALPAK ID; hexane:*i*-PrOH = 90:10; detection wavelength = 254 nm; flow rate = 1.0 mL/min. t_R = 20.5 min (minor) and 22.0 min (major), 95:5 er.

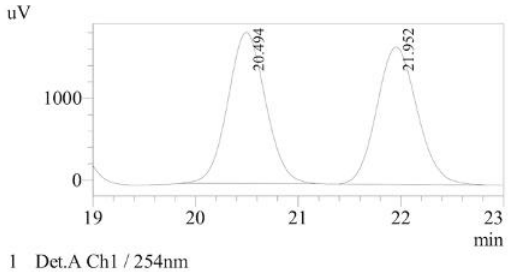

PeakTable
Detector A Ch1 254nm

Peak#	Ret. Time	Area %
1	20.494	50.482
2	21.952	49.518
Total		100.000

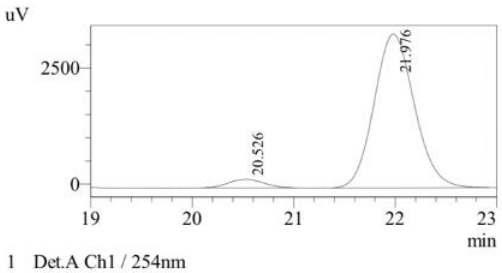

PeakTable
Detector A Ch1 254nm

Peak#	Ret. Time	Area %
1	20.526	4.687
2	21.976	95.313
Total		100.000

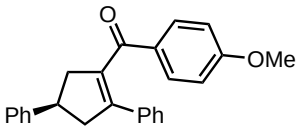

(*R*)-(2,4-Diphenylcyclopent-1-en-1-yl)(4-methoxyphenyl)methanone (4ba): Pale yellow oil (71.1 mg, 67%); R_f 0.21 (hexane/EtOAc = 19/1); **^{1}H NMR** (400 MHz, $CDCl_3$) δ 7.82-7.78 (m, 2H), 7.39-7.31 (m, 4H), 7.25-7.21 (m, 3H), 7.15-7.08 (m, 3H), 6.78-6.74 (m, 2H), 3.82-3.74 (m, 4H), 3.47-3.30 (m, 2H), 3.21-3.05 (m, 2H); **^{13}C{^{1}H} NMR** (100 MHz, $CDCl_3$) δ 196.5, 163.5, 145.4, 142.7, 136.6, 135.6, 131.7, 129.3, 128.5, 128.1, 127.8, 127.7, 126.9, 126.3, 113.6, 55.3, 45.5, 45.3, 42.4; **HRMS** (ESI) Calcd for $C_{25}H_{23}O_2$ $[M + H]^+$ 355.1698, found 355.1699; $[\alpha]^{25}_D$ = +13.1 (*c* = 1.12 in $CHCl_3$, 95:5 er sample).

HPLC analysis: Daicel CHIRALPAK ID; hexane:*i*-PrOH = 90:10; detection wavelength = 254 nm; flow rate = 1.0 mL/min. t_R = 12.3 min (minor) and 16.2 min (major), 95:5 er.

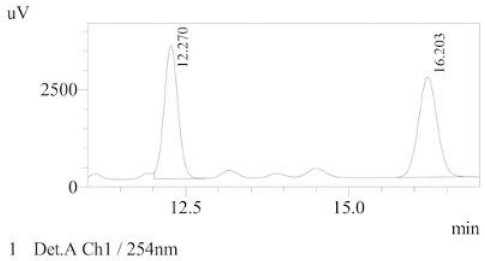

PeakTable
Detector A Ch1 254nm

Peak#	Ret. Time	Area %
1	12.270	50.097
2	16.203	49.903
Total		100.000

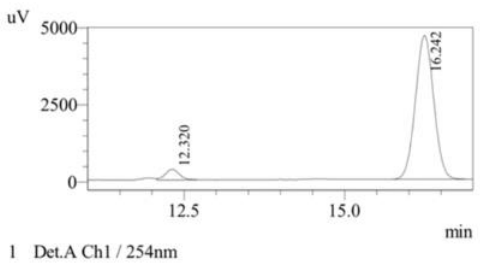

PeakTable
Detector A Ch1 254nm

Peak#	Ret. Time	Area %
1	12.320	5.265
2	16.242	94.735
Total		100.000

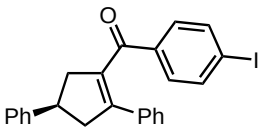

(*R*)-(2,4-Diphenylcyclopent-1-en-1-yl)(4-iodophenyl)methanone (4ca): White solid (115.4 mg, 85%); R_f 0.40 (hexane/EtOAc = 19/1); m.p. 131-133 °C; **^{1}H NMR** (400 MHz, $CDCl_3$) δ 7.61-7.58 (m, 2H), 7.46-7.43 (m, 2H), 7.38-7.32 (m, 4H), 7.26-7.22 (m, 1H), 7.16-7.11 (m, 5H), 3.78 (quint, *J* = 8.2 Hz, 1H), 3.49-3.42 (m, 1H), 3.38-3.32 (m, 1H), 3.21-3.06 (m, 2H); **^{13}C{^{1}H} NMR** (100 MHz, $CDCl_3$) δ 196.7, 146.0, 145.2, 137.5, 135.9, 135.8, 135.4, 130.7, 128.6, 128.2, 128.2, 127.9, 126.9, 126.4, 100.7, 45.8, 45.0, 42.3; **HRMS** (ESI) Calcd for $C_{24}H_{20}OI$ $[M + H]^+$ 451.0559, found 451.0558; $[\alpha]^{25}_D$ = +14.5 (*c* = 1.84 in $CHCl_3$, 93:7 er sample).

HPLC analysis: Daicel CHIRALPAK AS-H; hexane:*i*-PrOH = 98:2; detection wavelength = 254 nm; flow rate = 1.0 mL/min. t_R = 8.1 min (minor) and 9.1 min (major), 93:7 er.

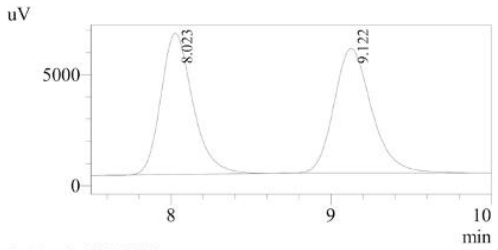

PeakTable
Detector A Ch1 254nm

Peak#	Ret. Time	Area %
1	8.023	49.028
2	9.122	50.972
Total		100.000

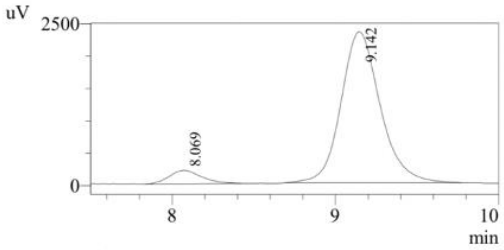

PeakTable
Detector A Ch1 254nm

Peak#	Ret. Time	Area %
1	8.069	6.837
2	9.142	93.163
Total		100.000

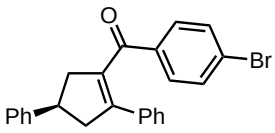

(*R*)-(4-Bromophenyl)(2,4-diphenylcyclopent-1-en-1-yl)methanone (4da): The reaction was performed at 0 °C for 72 h, followed by further heating at 100 °C for 6 h. White solid (109.6 mg, 91%); R_f 0.42 (hexane/EtOAc = 19/1); m.p. 99-101 °C; **^{1}H NMR** (400 MHz, $CDCl_3$) δ 7.61-7.58 (m, 2H), 7.38-7.32 (m, 6H), 7.26-7.23 (m, 1H), 7.16-7.11 (m, 5H), 3.79 (quint, *J* = 8.2 Hz, 1H), 3.49-3.43 (m, 1H), 3.39-3.32 (m, 1H), 3.22-3.07 (m, 2H); **^{13}C{^{1}H} NMR** (100 MHz, $CDCl_3$) δ 196.4, 146.1, 145.2, 135.8, 135.4, 135.4, 131.5, 130.8, 128.6, 128.2, 128.2, 127.9, 127.8, 126.9, 126.4, 45.8, 45.0, 42.3; **HRMS** (ESI) Calcd for $C_{24}H_{20}OBr$ $[M + H]^+$ 403.0696, found 403.0698; $[\alpha]^{25}_D$ = +16.2 (*c* = 1.25 in $CHCl_3$, 93:7 er sample).

HPLC analysis: Daicel CHIRALPAK ID; hexane:*i*-PrOH = 90:10; detection wavelength = 254 nm; flow rate = 1.0 mL/min. t_R = 13.0 min (minor) and 15.5 min (major), 93:7 er.

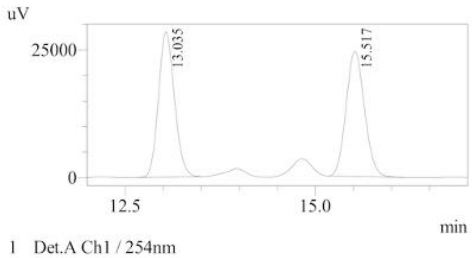

PeakTable

Detector A Ch1 254nm

Peak#	Ret. Time	Area %
1	13.035	50.218
2	15.517	49.782
Total		100.000

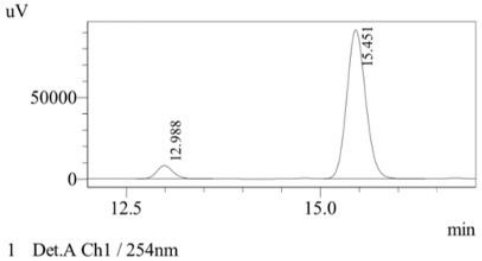

PeakTable

Detector A Ch1 254nm

Peak#	Ret. Time	Area %
1	12.988	7.159
2	15.451	92.841
Total		100.000

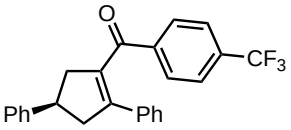

(*R*)-(2,4-Diphenylcyclopent-1-en-1-yl)(4-(trifluoromethyl)phenyl)methanone (4ea): The reaction was performed at 30 °C for 12 h and then at 100 °C for 6 h. White solid (100.2 mg, 85%); R_f 0.43 (hexane/EtOAc = 19/1); m.p. 128-129 °C; **^{1}H NMR** (400 MHz, $CDCl_3$) δ 7.78-7.76 (m, 2H), 7.46-7.44 (m, 2H), 7.39-7.33 (m, 4H), 7.26-7.22 (m, 1H), 7.12-7.06 (m, 5H), 3.79 (quint, J = 8.2 Hz, 1H), 3.51-3.36 (m, 2H), 3.23-3.10 (m, 2H); **^{13}C{^{1}H} NMR** (100 MHz, $CDCl_3$) δ 196.0, 148.2, 145.1, 139.7, 135.8, 135.4, 133.5 (q, $^2J_{C-F}$ = 32.5 Hz), 129.5, 128.6, 128.4, 128.1, 128.0, 126.9, 126.4, 125.0 (q, $^3J_{C-F}$ = 3.7 Hz), 123.5 (q, $^1J_{C-F}$ = 272.6 Hz), 46.2, 44.7, 42.2; **^{19}F NMR** (376 MHz, $CDCl_3$) δ –63.1; **HRMS** (ESI) Calcd for $C_{25}H_{20}OF_3$ $[M + H]^+$ 393.1466, found 393.1463; $[\alpha]^{25}_D$ = +15.7 (*c* = 1.52 in $CHCl_3$, 87:13 er sample).

HPLC analysis: Daicel CHIRALPAK ID; hexane:*i*-PrOH = 90:10; detection wavelength = 254 nm; flow rate = 1.0 mL/min. t_R = 5.4 min (minor) and 6.2 min (major), 87:13 er.

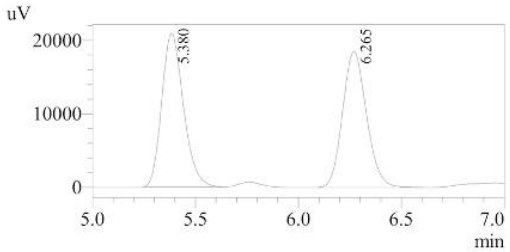

PeakTable

Detector A Ch1 254nm

Peak#	Ret. Time	Area %
1	5.380	50.478
2	6.265	49.522
Total		100.000

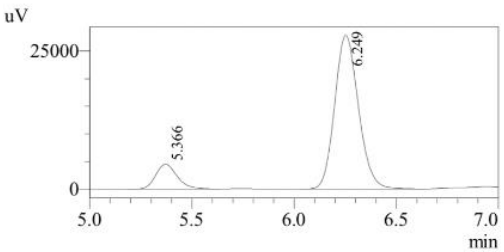

PeakTable

Detector A Ch1 254nm

Peak#	Ret. Time	Area %
1	5.366	12.745
2	6.249	87.255
Total		100.000

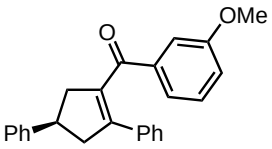

(*R*)-(2,4-Diphenylcyclopent-1-en-1-yl)(3-methoxyphenyl)methanone (4fa): The reaction was performed at 0 °C for 72 h and then at 100 °C for 6 h. Pale yellow oil (82.0 mg, 77%); R_f 0.26 (hexane/EtOAc = 19/1); **^{1}H NMR** (400 MHz, $CDCl_3$) δ 7.38-7.31 (m, 6H), 7.25-7.11 (m, 7H), 6.95-6.92 (m, 1H), 3.83-3.72 (m, 4H), 3.48-3.33 (m, 2H), 3.22-3.07 (m, 2H); **^{13}C{^{1}H} NMR** (100 MHz, $CDCl_3$) δ 197.4, 159.5, 145.3, 144.7, 137.8, 136.3, 135.6, 129.2, 128.6, 128.0, 127.9, 127.8, 126.9, 126.3, 122.3, 119.7, 113.1, 55.3, 45.6, 45.3, 42.3; **HRMS** (ESI) Calcd for $C_{25}H_{23}O_2$ $[M + H]^+$ 355.1698, found 355.1695; $[\alpha]^{25}_D$ = +6.8 (*c* = 0.38 in $CHCl_3$, 94:6 er sample).

HPLC analysis: Daicel CHIRALPAK AS-H; hexane:*i*-PrOH = 95:5; detection wavelength = 254 nm; flow rate = 0.5 mL/min. t_R = 17.1 min (minor) and 20.1 min (major), 94:6 er.

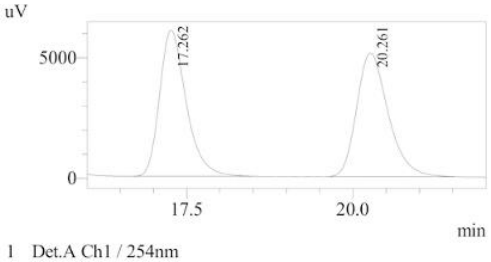

PeakTable
Detector A Ch1 254nm

Peak#	Ret. Time	Area %
1	17.262	49.959
2	20.261	50.041
Total		100.000

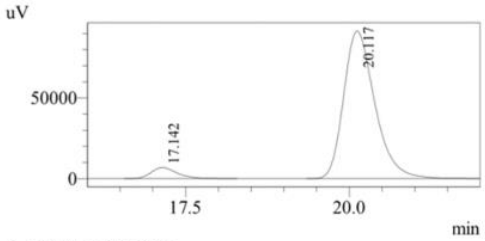

PeakTable
Detector A Ch1 254nm

Peak#	Ret. Time	Area %
1	17.142	5.822
2	20.117	94.178
Total		100.000

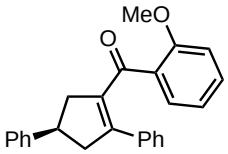

(*R*)-(2,4-Diphenylcyclopent-1-en-1-yl)(2-methoxyphenyl)methanone (4ga): The reaction was performed at 30 °C for 48 h and then at 100 °C for 6 h. Pale yellow oil (73.7 mg, 69%); R_f 0.15 (hexane/EtOAc = 19/1); **^{1}H NMR** (400 MHz, $CDCl_3$) δ 7.38-7.31 (m, 5H), 7.24-7.20 (m, 1H), 7.18-7.14 (m, 1H), 7.10-7.07 (m, 2H), 7.06-7.02 (m, 3H), 6.78-6.75 (m, 1H), 6.58-6.55 (m, 1H), 3.72-3.64 (m, 4H), 3.42-3.31 (m, 2H), 3.12-3.04 (m, 2H); **^{13}C{^{1}H} NMR** (100 MHz, $CDCl_3$) δ 195.6, 157.4, 149.0, 145.9, 138.1, 136.1, 132.2, 130.1, 129.3, 128.5, 127.8, 127.6, 127.4, 126.8, 126.2, 120.0, 110.7, 55.4,

47.6, 43.5, 41.7; **HRMS** (ESI) Calcd for $C_{25}H_{23}O_2$ $[M + H]^+$ 355.1698, found 355.1697; $[\alpha]^{25}_D$ = –4.3 (*c* = 0.35 in $CHCl_3$, 91:9 er sample).

HPLC analysis: Daicel CHIRALPAK ID; hexane:*i*-PrOH = 80:20; detection wavelength = 254 nm; flow rate = 1.0 mL/min. t_R = 9.6 min (minor) and 14.7 min (major), 91:9 er.

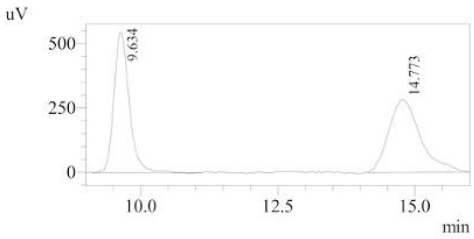

PeakTable

Detector A Ch1 254nm

Peak#	Ret. Time	Area %
1	9.634	48.120
2	14.773	51.880
Total		100.000

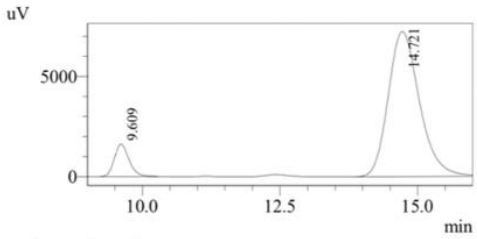

PeakTable

Detector A Ch1 254nm

Peak#	Ret. Time	Area %
1	9.609	9.459
2	14.721	90.541
Total		100.000

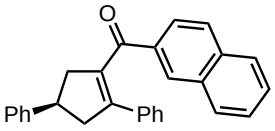

(*R*)-(2,4-Diphenylcyclopent-1-en-1-yl)(naphthalen-2-yl)methanone (4ha): The reaction was performed at 0 °C for 72 h and then at 100 °C for 6 h. Colorless oil (105.0 mg, 93%); R_f 0.31 (hexane/EtOAc = 19/1); **^{1}H NMR** (400 MHz, $CDCl_3$) δ 8.26 (s, 1H), 7.93-7.90 (m, 1H), 7.75-7.70 (m, 3H), 7.50-7.46 (m, 1H), 7.43-7.33 (m, 5H), 7.27-7.22 (m, 3H), 7.06-6.96 (m, 3H), 3.82 (quint, *J* = 8.0 Hz, 1H), 3.52-3.38 (m, 2H), 3.26-3.12 (m, 2H); **^{13}C{^{1}H} NMR** (100 MHz, $CDCl_3$) δ 197.6, 145.3, 144.5, 136.5, 135.5, 135.4, 133.7, 132.3, 131.6, 129.4, 128.6, 128.2, 128.2, 128.0, 127.8, 127.7, 127.6, 126.9, 126.4, 126.3, 124.5, 45.5, 45.4, 42.4; **HRMS** (ESI) Calcd for $C_{28}H_{23}O$ $[M + H]^+$ 375.1749, found 375.1747; $[\alpha]^{25}_D$ = +18.7 (*c* = 3.00 in $CHCl_3$, 95:5 er sample).

HPLC analysis: Daicel CHIRALPAK AD-H; hexane:*i*-PrOH = 90:10; detection wavelength = 254 nm; flow rate = 1.0 mL/min. t_R = 13.5 min (minor) and 14.9 min (major), 95:5 er.

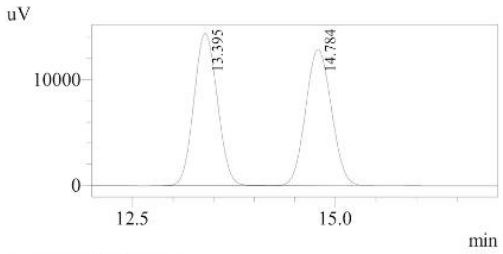

PeakTable

Detector A Ch1 254nm

Peak#	Ret. Time	Area %
1	13.395	50.403
2	14.784	49.597
Total		100.000

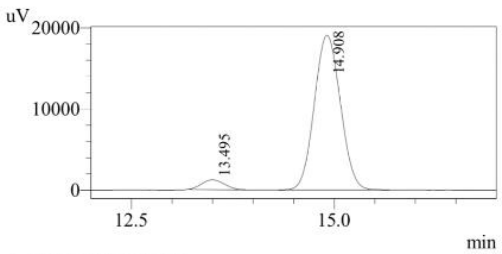

PeakTable

Detector A Ch1 254nm

Peak#	Ret. Time	Area %
1	13.495	5.295
2	14.908	94.705
Total		100.000

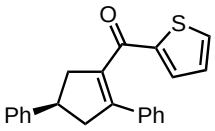

(*R*)-(2,4-Diphenylcyclopent-1-en-1-yl)(thiophen-2-yl)methanone (4ia): Pale yellow oil (81.2 mg, 82%); R_f 0.28 (hexane/EtOAc = 19/1); **^{1}H NMR** (400 MHz, $CDCl_3$) δ 7.50-7.49 (m, 1H), 7.41-7.32 (m, 5H), 7.29-7.13 (m, 6H), 6.88-6.86 (m, 1H), 3.77 (quint, *J* = 8.1 Hz, 1H), 3.47-3.35 (m, 2H), 3.20-3.08 (m, 2H); **^{13}C{^{1}H} NMR** (100 MHz, $CDCl_3$) δ 189.6, 145.3, 144.1, 143.6, 136.3, 135.6, 134.1, 134.0, 128.6, 128.2, 128.0, 127.9, 127.8, 126.9, 126.3 45.5, 45.3, 42.3; **HRMS** (ESI) Calcd for $C_{22}H_{19}OS$ $[M + H]^+$ 331.1157, found 331.1155; $[\alpha]^{25}_D$ = +9.23 (*c* = 2.15 in $CHCl_3$, 96:4 er sample).

HPLC analysis: Daicel CHIRALPAK ID; hexane:*i*-PrOH = 80:20; detection wavelength = 254 nm; flow rate = 1.0 mL/min. t_R = 10.7 min (minor) and 11.5 min (major), 96:4 er.

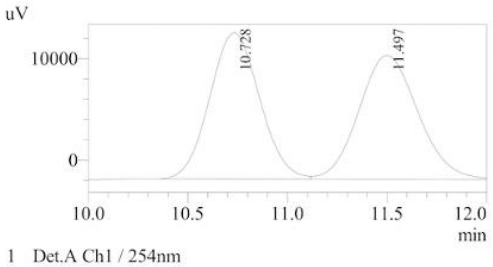

PeakTable

Detector A Ch1 254nm

Peak#	Ret. Time	Area %
1	10.728	49.918
2	11.497	50.082
Total		100.000

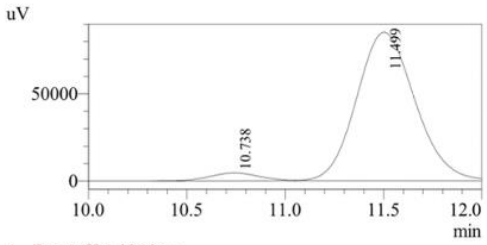

PeakTable

Detector A Ch1 254nm

Peak#	Ret. Time	Area %
1	10.738	4.270
2	11.499	95.730
Total		100.000

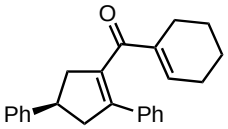

(*R*)-Cyclohex-1-en-1-yl(2,4-diphenylcyclopent-1-en-1-yl)methanone (4ja): White solid (53.4 mg, 54%); R_f 0.31 (hexane/EtOAc = 19/1); m.p. 73-75 °C; **^{1}H NMR** (400 MHz, $CDCl_3$) δ 7.35-7.17 (m, 10H), 6.65-6.63 (m, 1H), 3.71 (quint, *J* = 8.2 Hz, 1H), 3.38-3.32 (m, 1H), 3.27-3.21 (m, 1H), 3.12-3.05 (m, 1H), 3.01-2.94 (m, 1H), 2.24-2.21 (m, 2H), 1.94-1.91 (m, 2H), 1.54-1.48 (m, 2H), 1.44-1.38 (m, 2H); **^{13}C{^{1}H} NMR** (100 MHz, $CDCl_3$) δ 199.5, 145.5, 143.8, 142.8, 138.4, 136.9, 136.4, 128.5, 128.1, 127.6, 127.5, 126.9, 126.2, 45.3, 45.2, 42.3, 26.0, 23.0, 21.7, 21.4; **HRMS** (ESI) Calcd for $C_{24}H_{25}O$ $[M + H]^+$ 329.1903, found 329.1905; $[\alpha]^{25}_D$ = +10.12 (*c* = 2.10 in $CHCl_3$, 96:4 er sample).

HPLC analysis: Daicel CHIRALPAK OJ-H; hexane:*i*-PrOH = 95:5; detection wavelength = 254 nm; flow rate = 0.5 mL/min. t_R = 15.2 min (major) and 16.2 min (minor), 96:4 er.

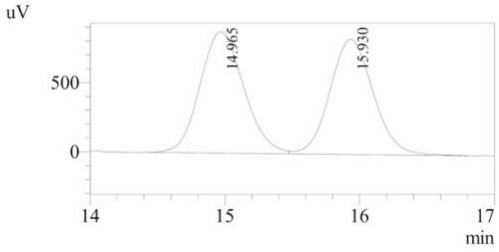

PeakTable

Detector A Ch1 254nm

Peak#	Ret. Time	Area %
1	14.965	51.573
2	15.930	48.427
Total		100.000

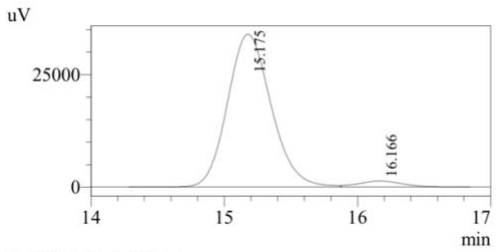

1 Det.A Ch1 / 254nm

PeakTable

Detector A Ch1 254nm

Peak#	Ret. Time	Area %
1	15.175	96.277
2	16.166	3.723
Total		100.000

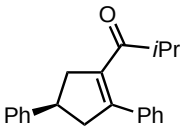

(*R*)-1-(2,4-Diphenylcyclopent-1-en-1-yl)-2-methylpropan-1-one (4ka): The reaction was performed at 30 °C for 48 h and then at 100 °C for 6 h. Pale yellow oil (41.8 mg, 48%); R_f 0.41 (hexane/EtOAc = 39/1); **^{1}H NMR** (400 MHz, $CDCl_3$) δ 7.38-7.21 (m, 10H), 3.65 (quint, *J* = 8.2 Hz, 1H), 3.35-3.23 (m, 2H), 3.09-2.94 (m, 2H), 2.63 (sept, *J* = 6.9 Hz, 1H), 0.98-0.96 (m, 6H); **^{13}C{^{1}H} NMR** (100 MHz, $CDCl_3$) δ 208.5, 147.1, 145.5, 137.7, 136.9, 128.6, 128.3, 128.3, 127.6, 126.8, 126.3, 47.3, 44.2, 41.9, 38.9,

18.6, 18.3; **HRMS** (ESI) Calcd for $C_{21}H_{23}O$ $[M + H]^+$ 291.1749, found 291.1743; $[\alpha]^{25}_D$ = –9.59 (*c* = 0.61 in $CHCl_3$, 97:3 er sample).

HPLC analysis: Daicel CHIRALPAK AD-H; hexane:*i*-PrOH = 99:1; detection wavelength = 254 nm; flow rate = 1.0 mL/min. t_R = 7.4 min (minor) and 8.0 min (major), 97:3 er.

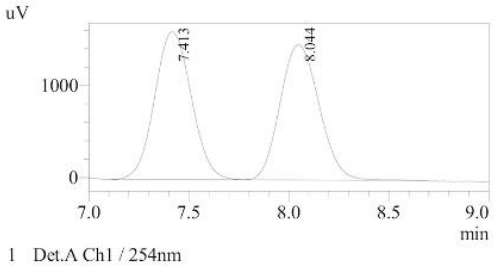

PeakTable

Detector A Ch1 254nm

Peak#	Ret. Time	Area %
1	7.413	50.667
2	8.044	49.333
Total		100.000

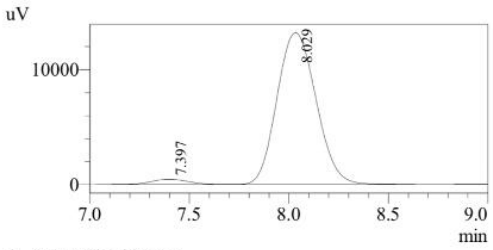

PeakTable

Detector A Ch1 254nm

Peak#	Ret. Time	Area %
1	7.397	3.140
2	8.029	96.860
Total		100.000

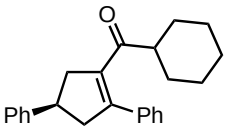

(*R*)-Cyclohexyl(2,4-diphenylcyclopent-1-en-1-yl)methanone (4la): The reaction was performed at 30 °C for 48 h and then at 100 °C for 6 h. Colorless oil (73.3 mg, 74%); R_f 0.19 (hexane/EtOAc = 39/1); **^{1}H NMR** (400 MHz, $CDCl_3$) δ 7.38-7.19 (m, 10H), 3.63 (quint, *J* = 8.2 Hz, 1H), 3.33-3.21 (m, 2H), 3.08-2.92 (m, 2H), 2.31 (tt, *J* = 11.5, 3.2 Hz, 1H), 1.70-1.61 (m, 4H), 1.54-1.50 (m, 1H), 1.35-1.22 (m, 2H), 1.15-1.04 (m, 1H), 0.97-0.84 (m, 2H); **^{13}C{^{1}H} NMR** (100 MHz, $CDCl_3$) δ 207.2, 147.5, 145.4, 137.8, 137.0, 128.5, 128.3, 128.1, 127.5, 126.8, 126.2, 48.8, 47.7, 43.8, 41.9, 28.9, 28.6, 25.7, 25.6, 25.5; **HRMS** (ESI) Calcd for $C_{24}H_{27}O$ $[M + H]^+$ 331.2062, found 331.2065; $[\alpha]^{25}_D$ = –5.28 (*c* = 2.35 in $CHCl_3$, 97:3 er sample).

HPLC analysis: Daicel CHIRALPAK AS-H; hexane:*i*-PrOH = 99:1; detection wavelength = 254 nm; flow rate = 1.0 mL/min. t_R = 6.4 min (minor) and 7.0 min (major), 97:3 er.

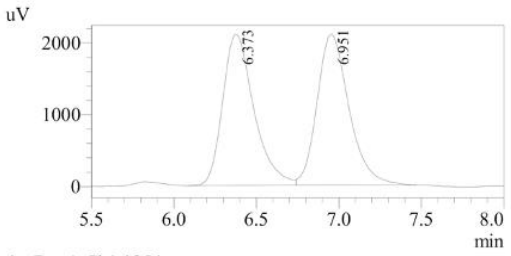

PeakTable

Detector A Ch1 254nm

Peak#	Ret. Time	Area %
1	6.373	49.574
2	6.951	50.426
Total		100.000

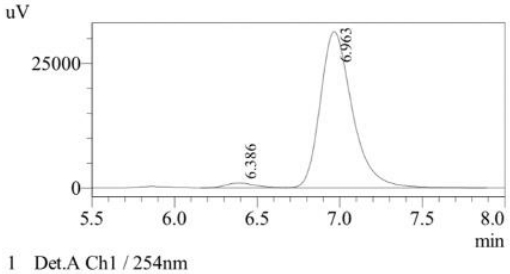

PeakTable

Detector A Ch1 254nm

Peak#	Ret. Time	Area %
1	6.386	2.766
2	6.963	97.234
Total		100.000

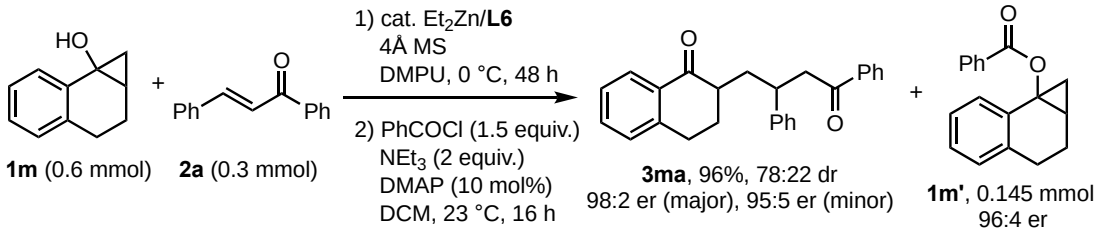

1m (0.6 mmol) **2a** (0.3 mmol)

3ma, 96%, 78:22 dr
98:2 er (major), 95:5 er (minor)

1m', 0.145 mmol
96:4 er

2-(4-Oxo-2,4-diphenylbutyl)-3,4-dihydronaphthalen-1(2*H*)-one (3ma): The reaction was conducted using 2 equiv. of **1m** at 0 °C for 48 h. A mixture of the unreacted cyclopropanol (**1m**) and the product (**3ma**) was obtained by silica gel chromatography. For the separation of these compounds and detection of **1m** by the UV detector in HPLC, the unreacted **1m** was transformed to the corresponding benzoyl derivative (**1m**') by the following procedure: To a solution of a mixture of **1m** and **3ma** in CH_2Cl_2 (0.5 mL) was added benzoyl chloride (63.3 mg, 0.45 mmol) and triethylamine (84 μL, 0.6 mmol), and DMAP (3.7 mg, 0.03 mmol). The reaction mixture was stirred at 23 °C for 16 h. The reaction was quenched with sat. aq. NH_4Cl and extracted with CH_2Cl_2 (3 times), and the combined organic extracts were dried over $MgSO_4$ and concentrated under reduced pressure. The residue was purified with silica gel chromatography to afford the title compound as a white solid (105.9 mg, 96%, 78:22 dr) along with **1m**' (38.4 mg, 0.145 mmol, 24%). Pure samples of both the diastereomers of **3ma** could be obtained by partial separation of the diastereomer mixture on silica gel using toluene as an eluent; R_f 0.31 (single spot, hexane/EtOAc = 19/1), 0.26 (major diastereomer, toluene), 0.18 (minor diastereomer, toluene); m.p. 152-153 °C (major diastereomer); **^{1}H NMR** (400 MHz, $CDCl_3$) major diastereomer: δ 7.97-7.96 (m, 1H), 7.89-7.87 (m, 2H), 7.54-7.50 (m, 1H), 7.43-7.38 (m, 3H), 7.34-7.14 (m, 7H), 3.61-3.54 (m, 1H), 3.32 (d, *J* = 6.8 Hz, 2H), 3.00 (dt, *J* = 16.8, 4.4 Hz, 1H), 2.87-3.79 (m, 1H), 2.60-2.53 (m, 1H), 2.42-2.35

(m, 1H), 2.21-2.13 (m, 1H), 1.93-1.83 (m, 1H), 1.80-1.73 (m, 1H); minor diastereomer: 8.00-7.98 (m, 1H), 7.89-7.87 (m, 2H), 7.54-7.49 (m, 1H), 7.44-7.38 (m, 3H), 7.30-7.24 (m, 5H), 7.18-7.14 (m, 2H), 3.75-3.67 (m, 1H), 3.38 (dd, *J* = 16.5, 7.7 Hz, 1H), 3.27 (dd, *J* = 16.5, 6.2 Hz, 1H), 2.91-2.87 (m, 2H), 2.52-2.46 (m, 1H), 2.43-2.35 (m, 1H), 2.13-2.06 (m, 1H), 1.88-1.78 (m, 1H), 1.72-1.65 (m, 1H); **^{13}C{^{1}H} NMR** (100 MHz, $CDCl_3$) major diastereomer: δ 200.1, 198.7, 143.9, 143.4, 137.1, 133.1, 133.0, 132.3, 128.7, 128.6, 128.5, 127.9, 127.7, 127.3, 126.6, 126.4, 46.6, 45.1, 37.8, 34.7, 28.4, 27.4; minor diastereomer: δ 200.1, 198.8, 144.8, 143.7, 137.1, 133.1, 132.9, 132.5, 128.6, 128.5, 128.5, 128.1, 127.7, 127.4, 126.5, 126.4, 46.0, 45.6, 39.4, 37.2, 29.6, 28.4; **HRMS** (ESI) Calcd for $C_{26}H_{25}O_2$ $[M + H]^+$ 369.1855, found 369.1852 (major diastereomer), 369.1857 (minor diastereomer); $[\alpha]^{25}_D$ = +7.48 (*c* = 0.99 in $CHCl_3$, 78:22 dr, 98:2 er (major), 90:10 er (minor) sample of **3ma**); $[\alpha]^{25}_D$ = –151 (*c* = 1.79 in $CHCl_3$, 96:4 er sample of **1m**').

HPLC analysis (major diastereomer of **3ma**): Daicel CHIRALPAK AS-H; hexane:*i*-PrOH = 70:30; detection wavelength = 254 nm; flow rate = 0.5 mL/min. t_R = 10.9 min (major) and 16.2 min (minor), 98:2 er.

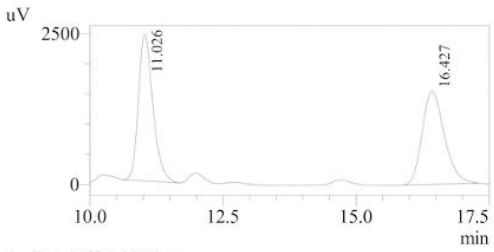

PeakTable

Detector A Ch1 254nm

Peak#	Ret. Time	Area %
1	11.026	50.849
2	16.427	49.151
Total		100.000

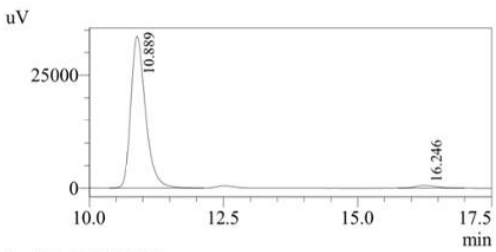

PeakTable

Detector A Ch1 254nm

Peak#	Ret. Time	Area %
1	10.889	97.534
2	16.246	2.466
Total		100.000

HPLC analysis (minor diastereomer of **3ma**): Daicel CHIRALPAK OD; hexane:*i*-PrOH = 98:2; detection wavelength = 254 nm; flow rate = 1.0 mL/min. t_R = 12.7 min (major) and 15.9 min (minor), 90:10 er.

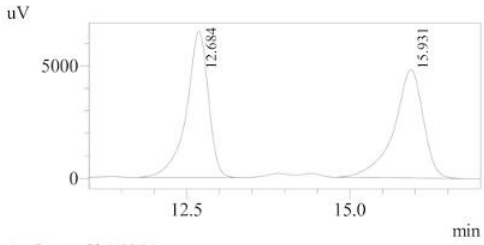

1 Det.A Ch1 / 254nm

PeakTable

Detector A Ch1 254nm

Peak#	Ret. Time	Area %
1	12.684	50.243
2	15.931	49.757
Total		100.000

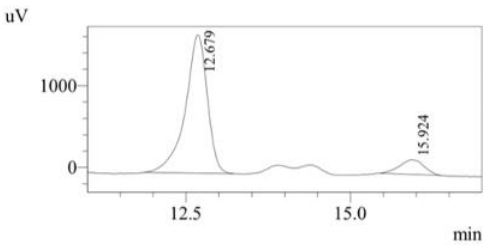

1 Det.A Ch1 / 254nm

PeakTable

Detector A Ch1 254nm

Peak#	Ret. Time	Area %
1	12.679	89.563
2	15.924	10.437
Total		100.000

HPLC analysis (**1m'**): Daicel CHIRALPAK ID; hexane:*i*-PrOH = 95:5; detection wavelength = 254 nm; flow rate = 1.0 mL/min. t_R = 5.1 min (minor) and 5.4 min (major), 96:4 er.

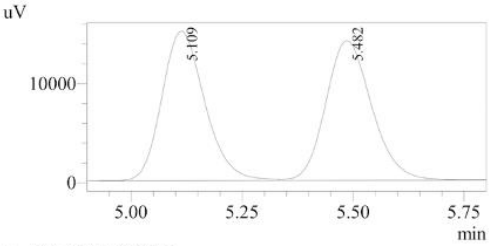

1 Det.A Ch1 / 254nm

PeakTable

Detector A Ch1 254nm

Peak#	Ret. Time	Area %
1	5.109	49.918
2	5.482	50.082
Total		100.000

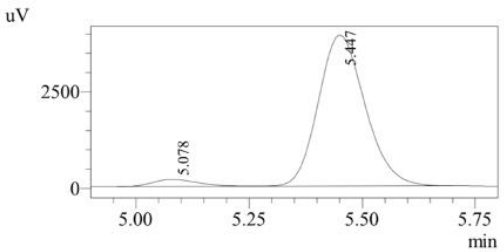

1 Det.A Ch1 / 254nm

PeakTable

Detector A Ch1 254nm

Peak#	Ret. Time	Area %
1	5.078	4.333
2	5.447	95.667
Total		100.000

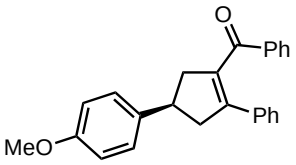

(*R*)-(4-(4-Methoxyphenyl)-2-phenylcyclopent-1-en-1-yl)(phenyl)methanone (4ab): White solid (72.7 mg, 68%); R_f 0.24 (hexane/EtOAc = 19/1); m.p. 119-120 °C; **^{1}H NMR** (400 MHz, $CDCl_3$) δ 7.78-7.75 (m, 2H), 7.40-7.35 (m, 1H), 7.31-7.23 (m, 4H), 7.19-7.15 (m, 2H), 7.11-7.08 (m, 3H), 6.90-6.87 (m, 2H), 3.79-7.70 (m, 4H), 3.46-3.29 (m, 2H), 3.17-3.03 (m, 2H); **^{13}C{^{1}H} NMR** (100 MHz, $CDCl_3$) δ 197.7, 158.1, 145.0, 137.4, 136.5, 136.4, 135.6, 132.8, 129.3, 128.2, 128.0, 127.9, 127.8, 113.9, 55.3, 45.9, 45.4, 41.7; **HRMS** (ESI) Calcd for $C_{25}H_{23}O_2$ $[M + H]^+$ 355.1698, found 355.1693; $[\alpha]^{25}_D$ = +12.3 (*c* = 1.11 in $CHCl_3$, 96:4 er sample).

HPLC analysis: Daicel CHIRALPAK ID; hexane:*i*-PrOH = 90:10; detection wavelength = 254 nm; flow rate = 1.0 mL/min. t_R = 10.6 min (minor) and 12.6 min (major), 96:4 er.

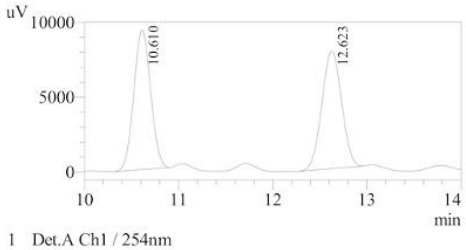

1 Det.A Ch1 / 254nm

PeakTable

Detector A Ch1 254nm

Peak#	Ret. Time	Area %
1	10.610	50.267
2	12.623	49.733
Total		100.000

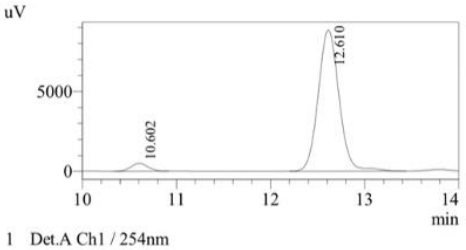

1 Det.A Ch1 / 254nm

PeakTable

Detector A Ch1 254nm

Peak#	Ret. Time	Area %
1	10.602	4.340
2	12.610	95.660
Total		100.000

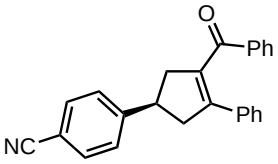

(*R*)-4-(3-Benzoyl-4-phenylcyclopent-3-en-1-yl)benzonitrile (4ac): Pale yellow oil (73.2 mg, 70%); R_f 0.12 (hexane/EtOAc = 19/1); **^{1}H NMR** (400 MHz, $CDCl_3$) δ 7.76-7.73 (m, 2H), 7.65-7.62 (m, 2H), 7.49-7.47 (m, 2H), 7.42-7.37 (m, 1H), 7.28-7.24 (m, 2H), 7.18-7.11 (m, 5H), 3.87-3.79 (m, 1H), 3.56-3.48 (m, 1H), 3.44-3.37 (m, 1H), 3.18-3.06 (m, 2H); **^{13}C{^{1}H} NMR** (100 MHz, $CDCl_3$) δ 197.2, 151.0, 144.7, 136.3, 135.9, 135.1, 133.0, 132.5, 129.3, 128.3, 128.2, 128.1, 127.9, 127.8, 118.9, 110.3, 45.4, 44.8, 42.3; **HRMS** (ESI) Calcd for $C_{25}H_{20}NO$ $[M + H]^+$ 350.1545, found 350.1545; $[\alpha]^{25}_D$ = +6.4 (*c* = 0.64 in $CHCl_3$, 92:8 er sample).

HPLC analysis: Daicel CHIRALPAK ID; hexane:*i*-PrOH = 70:30; detection wavelength = 254 nm; flow rate = 1.0 mL/min. t_R = 11.9 min (minor) and 13.2 min (major), 92:8 er.

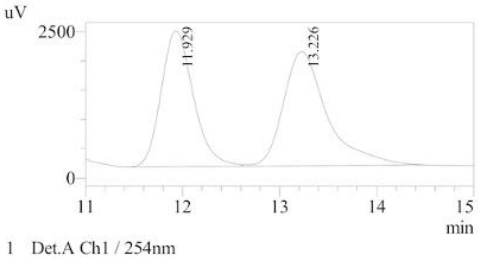

1 Det.A Ch1 / 254nm

PeakTable

Detector A Ch1 254nm

Peak#	Ret. Time	Area %
1	11.929	46.770
2	13.226	53.230
Total		100.000

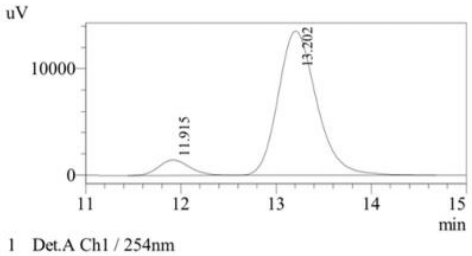

1 Det.A Ch1 / 254nm

PeakTable

Detector A Ch1 254nm

Peak#	Ret. Time	Area %
1	11.915	8.021
2	13.202	91.979
Total		100.000

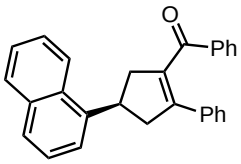

(*R*)-(4-(Naphthalen-1-yl)-2-phenylcyclopent-1-en-1-yl)(phenyl)methanone (4ad): The reaction was performed at 0 °C for 48 h and then at 50 °C for 16 h. Pale yellow oil (89.7 mg, 80%); R_f 0.29 (hexane/EtOAc = 19/1); **^{1}H NMR** (400 MHz, $CDCl_3$) δ 8.17-8.15 (m, 1H), 7.87-7.85 (m, 1H), 7.79-7.73 (m, 3H), 7.59-7.42 (m, 4H), 7.37-7.32 (m, 1H), 7.24-7.17 (m, 4H), 7.11-7.06 (m, 3H), 4.54-4.46 (m, 1H), 3.63-3.49 (m, 2H), 3.34-3.21 (m, 2H); **^{13}C{^{1}H} NMR** (100 MHz, $CDCl_3$) δ 197.6, 145.0, 140.8, 136.5, 136.4, 135.5, 134.1, 132.8, 131.5, 129.3, 129.0, 128.2, 128.0, 127.9, 127.9, 127.0, 125.9, 125.5, 125.5, 123.4, 122.8, 45.0, 44.4, 37.8; **HRMS** (ESI) Calcd for $C_{28}H_{23}O$ $[M + H]^+$ 375.1749, found 375.1751; $[\alpha]^{25}_D$ = –16.7 (*c* = 1.50 in $CHCl_3$, 96:4 er sample).

HPLC analysis: Daicel CHIRALPAK AS-H; hexane:*i*-PrOH = 95:5; detection wavelength = 254 nm; flow rate = 1.0 mL/min. t_R = 15.0 min (minor) and 19.8 min (major), 96:4 er.

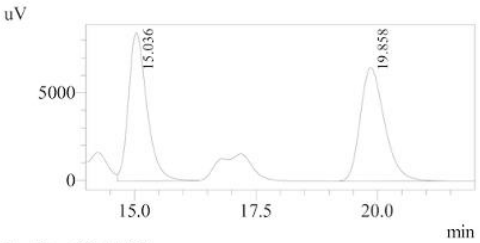

1 Det.A Ch1 / 254nm

PeakTable

Detector A Ch1 254nm

Peak#	Ret. Time	Area %
1	15.036	49.805
2	19.858	50.195
Total		100.000

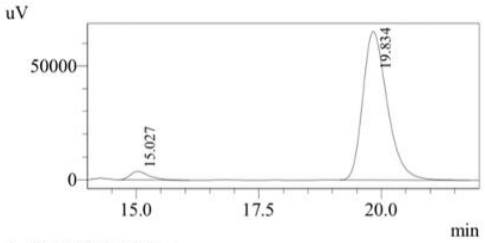

1 Det.A Ch1 / 254nm

PeakTable

Detector A Ch1 254nm

Peak#	Ret. Time	Area %
1	15.027	4.154
2	19.834	95.846
Total		100.000

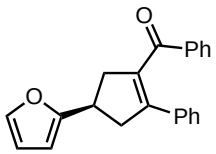

(*R*)-(4-(Furan-2-yl)-2-phenylcyclopent-1-en-1-yl)(phenyl)methanone (4ae): Colorless oil (72.4 mg, 77%); R_f 0.31 (hexane/EtOAc = 19/1); **^{1}H NMR** (400 MHz, $CDCl_3$) δ 7.75-7.73 (m, 2H), 7.38-7.34 (m, 2H), 7.25-7.21 (m, 2H), 7.17-7.13 (m, 2H), 7.10-7.07 (m, 3H), 6.33-6.31 (m, 1H), 6.14-6.14 (m, 1H), 3.81 (quint, *J* = 7.9 Hz, 1H), 3.39-3.21 (m, 3H), 3.17-3.11 (m, 1H); **^{13}C{^{1}H} NMR** (100 MHz, $CDCl_3$) δ 197.5, 158.0, 144.7, 141.3, 136.5, 136.0, 135.4, 132.8, 129.3, 128.2, 128.0, 127.9, 127.9, 110.1, 104.2, 43.0, 42.5, 35.7; **HRMS** (ESI) Calcd for $C_{22}H_{19}O_2$ $[M + H]^+$ 315.1385, found 315.1383; $[\alpha]^{25}_D$ = +23.3 (*c* = 2.63 in $CHCl_3$, 97:3 er).

HPLC analysis: Daicel CHIRALPAK ID; hexane:*i*-PrOH = 98:2; detection wavelength = 254 nm; flow rate = 1.0 mL/min. t_R = 10.1 min (minor) and 12.7 min (major), 97:3 er.

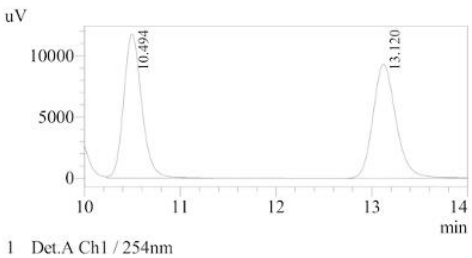

PeakTable

Detector A Ch1 254nm

Peak#	Ret. Time	Area %
1	10.494	49.742
2	13.120	50.258
Total		100.000

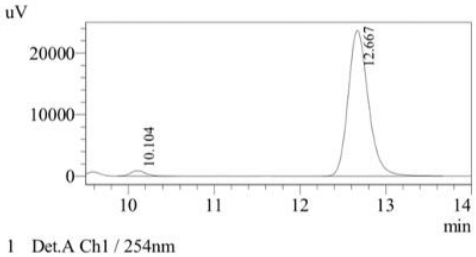

PeakTable

Detector A Ch1 254nm

Peak#	Ret. Time	Area %
1	10.104	2.740
2	12.667	97.260
Total		100.000

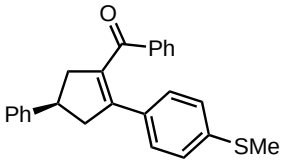

(*R*)-(2-(4-(Methylthio)phenyl)-4-phenylcyclopent-1-en-1-yl)(phenyl)methanone (4af): Pale yellow oil (89.5 mg, 81%); R_f 0.26 (hexane/EtOAc = 19/1); **^{1}H NMR** (400 MHz, $CDCl_3$) δ 7.79-7.77 (m, 2H), 7.44-7.22 (m, 8H), 7.12-7.10 (m, 2H), 7.00-6.98 (m, 2H), 3.78 (quint, *J* = 8.2 Hz, 1H), 3.46-3.31 (m, 2H), 3.19-3.06 (m, 2H), 2.38 (s, 3H); **^{13}C{^{1}H} NMR** (100 MHz, $CDCl_3$) δ 197.8, 145.3, 144.0, 138.6, 136.5, 136.0, 132.9, 132.2, 129.3, 128.6, 128.4, 128.3, 126.9, 126.4, 125.8, 45.5, 45.3, 42.4, 15.4; **HRMS**

(ESI) Calcd for $C_{25}H_{23}OS$ $[M + H]^+$ 371.1470, found 371.1465; $[\alpha]^{25}_D$ = +21.5 (*c* = 0.60 in $CHCl_3$, 97:3 er sample).

HPLC analysis: Daicel CHIRALPAK ID; hexane:*i*-PrOH = 95:5; detection wavelength = 254 nm; flow rate = 1.0 mL/min. t_R = 14.4 min (minor) and 15.8 min (major), 97:3 er.

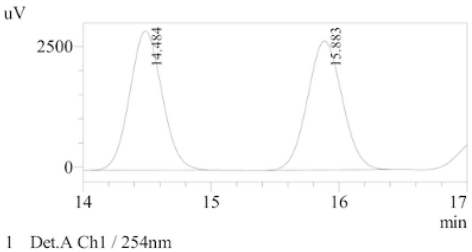

1 Det.A Ch1 / 254nm

PeakTable

Detector A Ch1 254nm

Peak#	Ret. Time	Area %
1	14.484	50.114
2	15.883	49.886
Total		100.000

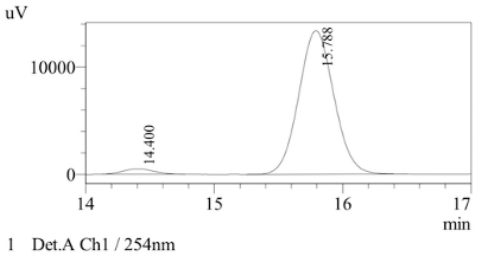

1 Det.A Ch1 / 254nm

PeakTable

Detector A Ch1 254nm

Peak#	Ret. Time	Area %
1	14.400	3.207
2	15.788	96.793
Total		100.000

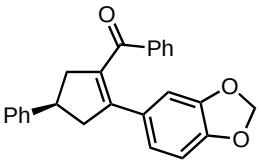

(*R*)-(2-(Benzo[*d*][1,3]dioxol-5-yl)-4-phenylcyclopent-1-en-1-yl)(phenyl)methanone (4ag): Pale yellow oil (92.7 mg, 84%); R_f 0.33 (hexane/EtOAc = 9/1); **^{1}H NMR** (400 MHz, $CDCl_3$) δ 7.79-7.77 (m, 2H), 7.43-7.21 (m, 8H), 6.69-6.67 (m, 2H), 6.55-6.53 (m, 1H), 5.82 (s, 2H), 3.75 (quint, *J* = 8.2 Hz, 1H), 3.42-3.29 (m, 2H), 3.15-3.04 (m, 2H); **^{13}C{^{1}H} NMR** (100 MHz, $CDCl_3$) δ 197.7, 147.3, 147.3, 145.3, 144.5, 136.6, 135.4, 132.8, 129.7, 129.3, 128.6, 128.3, 126.9, 126.3, 122.1, 108.1, 107.9, 101.0, 45.8, 45.1, 42.3; **HRMS** (ESI) Calcd for $C_{25}H_{21}O_3$ $[M + H]^+$ 369.1491, found 369.1493; $[\alpha]^{25}_D$ = +7.18 (*c* = 3.39 in $CHCl_3$, 95:5 er sample).

HPLC analysis: Daicel CHIRALPAK AS-H; hexane:*i*-PrOH = 98:2; detection wavelength = 254 nm; flow rate = 0.5 mL/min. t_R = 32.7 min (minor) and 36.3 min (major), 95:5 er.

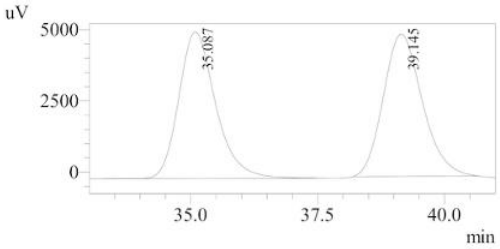

1 Det.A Ch1 / 254nm

PeakTable

Detector A Ch1 254nm

Peak#	Ret. Time	Area %
1	35.087	49.416
2	39.145	50.584
Total		100.000

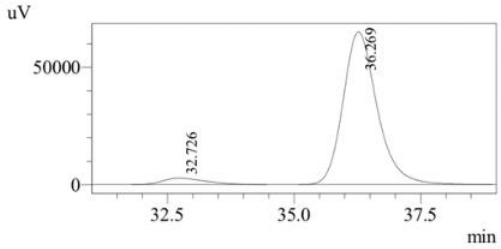

1 Det.A Ch1 / 254nm

PeakTable

Detector A Ch1 254nm

Peak#	Ret. Time	Area %
1	32.726	5.092
2	36.269	94.908
Total		100.000

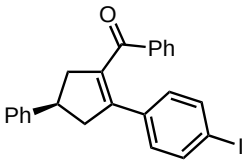

(*R*)-(2-(4-Iodophenyl)-4-phenylcyclopent-1-en-1-yl)(phenyl)methanone (4ah): Pale yellow oil (114.5 mg, 85%); R_f 0.29 (hexane/EtOAc = 19/1); **^{1}H NMR** (400 MHz, $CDCl_3$) δ 7.78-7.76 (m, 2H), 7.47-7.43 (m, 3H), 7.37-7.23 (m, 7H), 6.94-6.91 (m, 2H), 3.79 (quint, *J* = 8.2 Hz, 1H), 3.44-3.30 (m, 2H), 3.19-3.05 (m, 2H); **^{13}C{^{1}H} NMR** (100 MHz, $CDCl_3$) δ 197.5, 145.1, 143.2, 137.4, 137.2, 136.2, 135.0, 133.2, 129.5, 129.3, 128.6, 128.5, 126.9, 126.4, 93.7, 45.4, 42.4; **HRMS** (ESI) Calcd for $C_{24}H_{20}OI$ $[M + H]^+$ 451.0559, found 451.0557; $[\alpha]^{25}_D$ = +7.0 (*c* = 0.46 in $CHCl_3$, 96:4 er sample).

HPLC analysis: Daicel CHIRALPAK OD; hexane:*i*-PrOH = 99:1; detection wavelength = 254 nm; flow rate = 1.0 mL/min. t_R = 30.0 min (minor) and 32.4 min (major), 96:4 er.

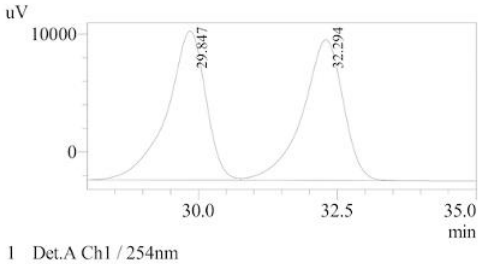

1 Det.A Ch1 / 254nm

PeakTable

Detector A Ch1 254nm

Peak#	Ret. Time	Area %
1	29.847	50.257
2	32.294	49.743
Total		100.000

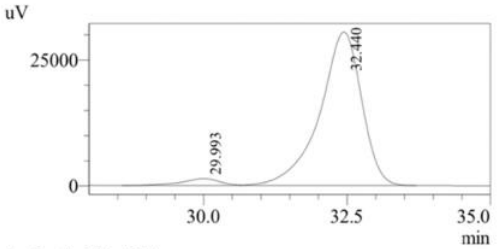

1 Det.A Ch1 / 254nm

PeakTable

Detector A Ch1 254nm

Peak#	Ret. Time	Area %
1	29.993	4.081
2	32.440	95.919
Total		100.000

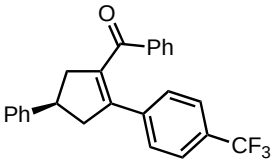

(*R*)-Phenyl(4-phenyl-2-(4-(trifluoromethyl)phenyl)cyclopent-1-en-1-yl)methanone (4ai): The reaction was performed at 0 °C for 48 h and then at 50 °C for 16 h. White solid (109.8 mg, 93%); R_f 0.35 (hexane/toluene = 1/1); m.p. 82-84 °C; **^{1}H NMR** (400 MHz, $CDCl_3$) δ 7.78-7.76 (m, 2H), 7.46-7.42 (m, 1H), 7.39-7.23 (m, 11H), 3.83 (quint, *J* = 8.2 Hz, 1H), 3.49-3.35 (m, 2H), 3.24-3.10 (m, 2H); **^{13}C{^{1}H} NMR** (100 MHz, $CDCl_3$) δ 197.3, 144.9, 142.8, 139.1, 138.8, 136.2, 133.3, 129.7 (q, $^2J_{C\text{-}F}$ = 32.7 Hz), 129.2, 128.7, 128.5, 128.0, 126.9, 126.5, 125.1 (q, $^3J_{C\text{-}F}$ = 3.8 Hz), 123.9 (q, $^1J_{C\text{-}F}$ = 271.9 Hz), 45.5, 45.4, 42.5; **^{19}F NMR** (376 MHz, $CDCl_3$) δ –63.2; **HRMS** (ESI) Calcd for $C_{25}H_{20}OF_3$ $[M + H]^+$ 393.1466, found 393.1461; $[\alpha]^{25}_D$ = +13 (*c* = 0.29 in $CHCl_3$, 93:7 er sample).

HPLC analysis: Daicel CHIRALPAK OD; hexane:*i*-PrOH = 99:1; detection wavelength = 254 nm; flow rate = 0.5 mL/min. t_R = 25.7 min (minor) and 27.4 min (major), 93:7 er.

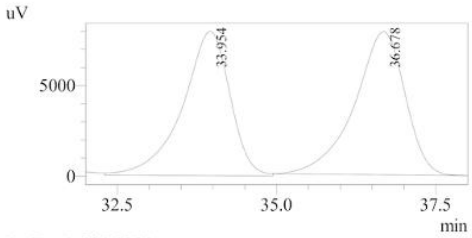

PeakTable
Detector A Ch1 254nm

Peak#	Ret. Time	Area %
1	33.954	48.674
2	36.678	51.326
Total		100.000

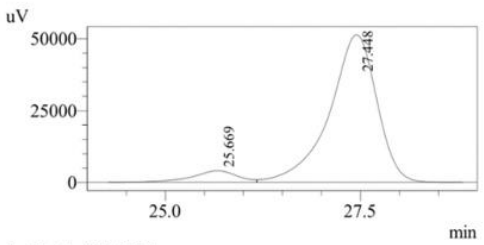

PeakTable
Detector A Ch1 254nm

Peak#	Ret. Time	Area %
1	25.669	6.963
2	27.448	93.037
Total		100.000

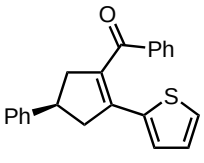

(*S*)-Phenyl(4-phenyl-2-(thiophen-2-yl)cyclopent-1-en-1-yl)methanone (4aj): Pale yellow oil (82.2 mg, 83%); R_f 0.49 (hexane/EtOAc = 9/1); **^{1}H NMR** (400 MHz, $CDCl_3$) δ 7.88-7.86 (m, 2H), 7.50-7.45 (m, 1H), 7.37-7.31 (m, 6H), 7.25-7.20 (m, 1H), 7.16-7.15 (m, 1H), 7.06-7.04 (m, 1H), 6.90-6.88 (m, 1H), 3.76 (quint, *J* = 8.2 Hz, 1H), 3.46-

3.39 (m, 1H), 3.33-3.27 (m, 1H), 3.18-3.02 (m, 2H); **^{13}C{^{1}H} NMR** (100 MHz, $CDCl_3$) δ 197.9, 145.3, 138.1, 136.4, 136.4, 135.1, 133.2, 129.3, 128.6, 128.5, 127.2, 126.9, 126.3, 125.4, 124.1, 45.4, 45.3, 42.3; **HRMS** (ESI) Calcd for $C_{22}H_{19}OS$ $[M + H]^+$ 331.1157, found 331.1159; $[\alpha]^{25}_D$ = +14 (*c* = 0.61 in $CHCl_3$, 95:5 er sample).

HPLC analysis: Daicel CHIRALPAK ID; hexane:*i*-PrOH = 90:10; detection wavelength = 254 nm; flow rate = 1.0 mL/min. t_R = 18.1 min (minor) and 21.3 min (major), 95:5 er.

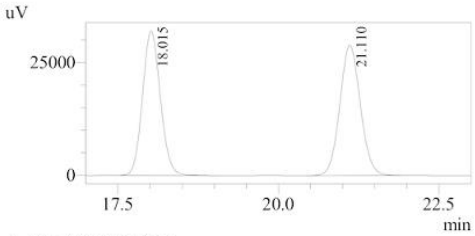

PeakTable
Detector A Ch1 254nm

Peak#	Ret. Time	Area %
1	18.015	49.026
2	21.110	50.974
Total		100.000

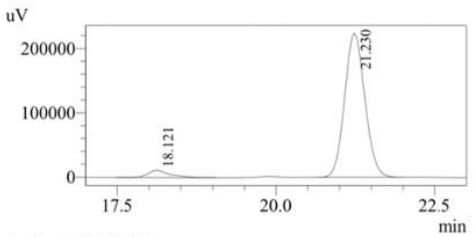

PeakTable
Detector A Ch1 254nm

Peak#	Ret. Time	Area %
1	18.121	4.941
2	21.230	95.059
Total		100.000

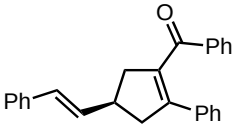

(*R*,*E*)-Phenyl(2-phenyl-4-styrylcyclopent-1-en-1-yl)methanone (4ak): Yellow oil (79.0 mg, 75%); R_f 0.32 (hexane/EtOAc = 19/1); **^{1}H NMR** (400 MHz, $CDCl_3$) δ 7.77-7.75 (m, 2H), 7.39-7.07 (m, 13H), 6.52-6.38 (m, 2H), 3.41-3.31 (m, 1H), 3.27-3.12 (m, 2H), 3.01-2.87 (m, 2H); **^{13}C{^{1}H} NMR** (100 MHz, $CDCl_3$) δ 197.6, 145.0, 137.3, 136.5, 136.3, 135.6, 133.3, 132.7, 129.4, 129.3, 128.5, 128.2, 128.0, 127.8, 127.8, 127.1, 126.0, 44.1, 43.7, 40.7; **HRMS** (ESI) Calcd for $C_{26}H_{23}O$ $[M + H]^+$ 351.1749, found 351.1744; $[\alpha]^{25}_D$ = +14.7 (*c* = 0.985 in $CHCl_3$, 97:3 er sample).

HPLC analysis: Daicel CHIRALPAK ID; hexane:*i*-PrOH = 95:5; detection wavelength = 254 nm; flow rate = 1.0 mL/min. t_R = 14.3 min (major) and 17.0 min (minor), 97:3 er.

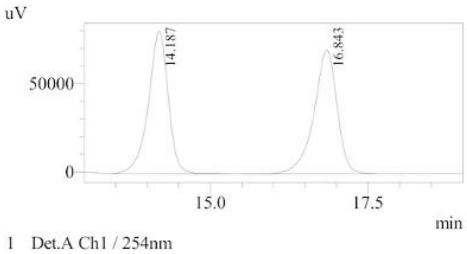

PeakTable

Detector A Ch1 254nm

Peak#	Ret. Time	Area %
1	14.187	49.548
2	16.843	50.452
Total		100.000

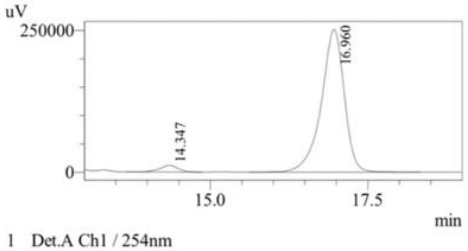

PeakTable

Detector A Ch1 254nm

Peak#	Ret. Time	Area %
1	14.347	3.486
2	16.960	96.514
Total		100.000

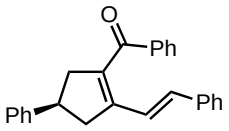

(*R*,*E*)-Phenyl(4-phenyl-2-styrylcyclopent-1-en-1-yl)methanone (4al): Pale yellow oil (63.1 mg, 60%); R_f 0.28 (hexane/EtOAc = 19/1); **^{1}H NMR** (400 MHz, $CDCl_3$) δ 7.83-7.81 (m, 2H), 7.57-7.54 (m, 1H), 7.47-7.44 (m, 2H), 7.34-7.33 (m, 4H), 7.25-7.18 (m, 6H), 7.02 (d, *J* = 16.1 Hz, 1H), 6.66 (d, *J* = 16.1 Hz, 1H), 3.65 (quint, *J* = 8.2 Hz, 1H), 3.38-3.23 (m, 2H), 3.11-2.96 (m, 2H); **^{13}C{^{1}H} NMR** (100 MHz, $CDCl_3$) δ 195.9, 147.3, 145.3, 139.3, 138.1, 136.7, 134.1, 132.6, 129.1, 128.7, 128.7, 128.6, 128.4, 127.0, 126.9, 126.4, 123.3, 44.3, 42.1, 42.0; **HRMS** (ESI) Calcd for $C_{26}H_{23}O$ $[M + H]^+$ 351.1749, found 351.1748; $[\alpha]^{25}_D$ = +79.9 (*c* = 2.10 in $CHCl_3$, 96:4 er sample).

HPLC analysis: Daicel CHIRALPAK IA; hexane:*i*-PrOH = 95:5; detection wavelength = 254 nm; flow rate = 1.0 mL/min. t_R = 13.5 min (minor) and 14.3 min (major), 96:4 er.

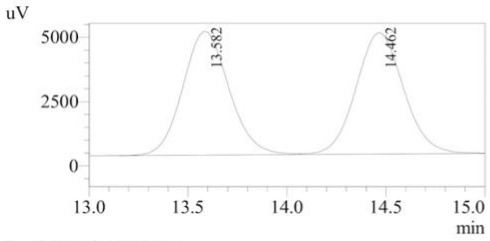

PeakTable

Detector A Ch1 254nm

Peak#	Ret. Time	Area %
1	13.582	49.718
2	14.462	50.282
Total		100.000

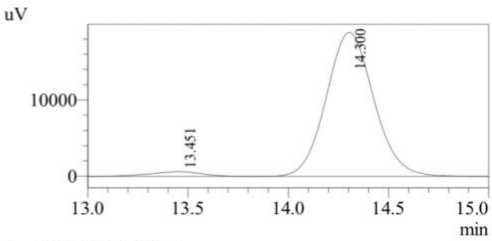

PeakTable

Detector A Ch1 254nm

Peak#	Ret. Time	Area %
1	13.451	3.734
2	14.300	96.266
Total		100.000

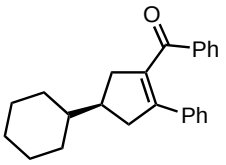

(*R*)-(4-Cyclohexyl-2-phenylcyclopent-1-en-1-yl)(phenyl)methanone (4am): The reaction was performed using **L3** as the ligand in DMSO at 40 °C for 48 h and then at 100 °C for 6 h. Colorless oil (82.4 mg, 83%); R_f 0.39 (hexane/EtOAc = 19/1); **^{1}H NMR** (400 MHz, $CDCl_3$) δ 7.73-7.71 (m, 2H), 7.37-7.33 (m, 1H), 7.24-7.20 (m, 2H), 7.14-7.05 (m, 5H), 3.07-2.91 (m, 2H), 2.79-2.65 (m, 2H), 2.29 (sext, *J* = 8.7 Hz, 1H), 1.84-1.66 (m, 5H), 1.41-1.13 (m, 4H), 1.07-0.96 (m, 2H); **^{13}C{^{1}H} NMR** (100 MHz, $CDCl_3$) δ 198.1, 145.7, 136.9, 136.6, 136.1, 132.6, 129.3, 128.1, 127.9, 127.8, 127.6, 43.6, 43.2, 42.0, 41.6, 31.5, 31.3, 26.5, 26.3, 26.2; **HRMS** (ESI) Calcd for $C_{24}H_{27}O$ $[M + H]^+$ 331.2062, found 331.2066; $[\alpha]^{25}_D$ = +13.2 (*c* = 2.17 in $CHCl_3$, 78:22 er sample). The absolute configuration was deduced as (*R*) based on the result that **L3** gave (*R*)-**4aa** as the major enantiomer in the reaction between **1a** and **2a**.

HPLC analysis: Daicel CHIRALPAK IA; hexane:*i*-PrOH = 99:1; detection wavelength = 254 nm; flow rate = 1.0 mL/min. t_R = 14.6 min (major) and 16.8 min (minor), 78:22 er.

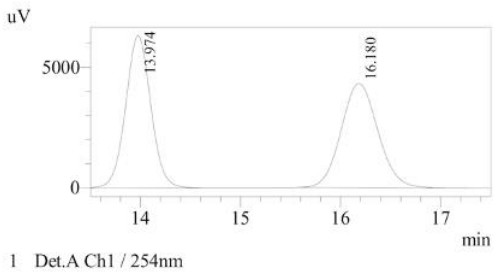

PeakTable

Detector A Ch1 254nm

Peak#	Ret. Time	Area %
1	13.974	50.111
2	16.180	49.889
Total		100.000

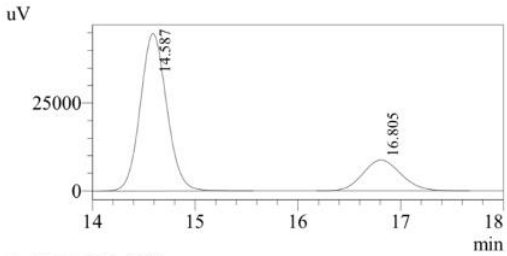

PeakTable

Detector A Ch1 254nm

Peak#	Ret. Time	Area %
1	14.587	77.924
2	16.805	22.076
Total		100.000

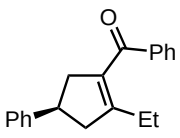

(*R*)-(2-Ethyl-4-phenylcyclopent-1-en-1-yl)(phenyl)methanone (4an): The reaction was performed using **L3** as the ligand at 30 °C for 48 h and then at 100 °C for 6 h. Colorless oil (47.9 mg, 58%); R_f 0.40 (hexane/EtOAc = 19/1); **^{1}H NMR** (400 MHz, $CDCl_3$) δ 7.82-7.79 (m, 2H), 7.56-7.52 (m, 1H), 7.46-7.43 (m, 2H), 7.35-7.29 (m, 4H),

7.24-7.19 (m, 1H), 3.58 (quint, J = 8.2 Hz, 1H), 3.19-3.13 (m, 1H), 3.04-2.91 (m, 2H), 2.76-2.69 (m, 1H), 2.15 (q, J = 7.5 Hz, 2H), 0.99 (t, J = 7.6 Hz, 3H); **^{13}C{^{1}H} NMR** (100 MHz, $CDCl_3$) δ 196.8, 153.3, 145.6, 139.0, 134.5, 132.5, 128.8, 128.5, 128.4, 126.9, 126.2, 44.6, 43.6, 42.2, 23.5, 12.4; **HRMS** (ESI) Calcd for $C_{20}H_{21}O$ $[M + H]^+$ 277.1592, found 277.1590; $[\alpha]^{25}_D$ = –7.17 (c = 0.600 in $CHCl_3$, 79:21 er sample).

HPLC analysis: Daicel CHIRALPAK AS-H; hexane:*i*-PrOH = 99:1; detection wavelength = 254 nm; flow rate = 1.0 mL/min. t_R = 6.6 min (minor) and 7.6 min (major), 79:21 er.

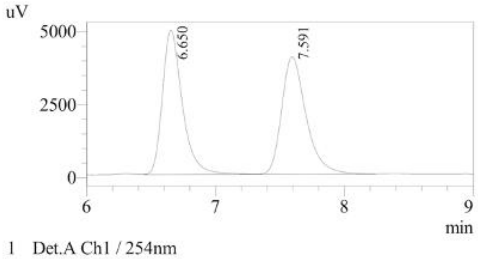

PeakTable
Detector A Ch1 254nm

Peak#	Ret. Time	Area %
1	6.650	50.079
2	7.591	49.921
Total		100.000

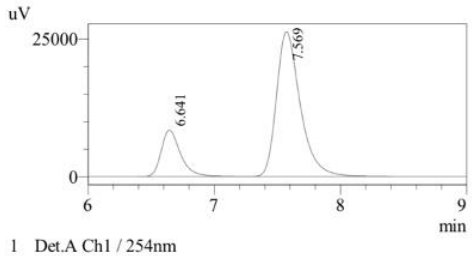

PeakTable
Detector A Ch1 254nm

Peak#	Ret. Time	Area %
1	6.641	20.669
2	7.569	79.331
Total		100.000

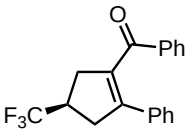

(*R*)-Phenyl(2-phenyl-4-(trifluoromethyl)cyclopent-1-en-1-yl)methanone (4ao): The reaction was performed using **L3** as the ligand at 30 °C for 24 h and then at 100 °C for 6 h. Pale yellow oil (36.8 mg, 39%); R_f 0.27 (hexane/EtOAc = 19/1); **^{1}H NMR** (400 MHz, $CDCl_3$) δ 7.72-7.70 (m, 2H), 7.40-7.37 (m, 1H), 7.27-7.23 (m, 2H), 7.14-7.09 (m, 5H), 3.28-3.08 (m, 5H); **^{13}C{^{1}H} NMR** (100 MHz, $CDCl_3$) δ 196.6, 143.7, 136.1, 134.8, 134.6, 133.0, 129.3, 128.4, 128.3, 128.1, 127.9 (q, $^{1}J_{C\text{-}F}$ = 277.1 Hz), 127.9, 39.5 (q, $^{2}J_{C\text{-}F}$ = 28.3 Hz), 37.7 (q, $^{3}J_{C\text{-}F}$ = 2.7 Hz), 37.1 (q, $^{3}J_{C\text{-}F}$ = 2.6 Hz); **^{19}F NMR** (376 MHz, $CDCl_3$) δ –73.2; **HRMS** (ESI) Calcd for $C_{19}H_{16}OF_3$ $[M + H]^+$ 317.1153, found 317.1154; $[\alpha]^{25}_D$ = +2.2 (c = 0.49 in $CHCl_3$, 77:23 er sample).

HPLC analysis: Daicel CHIRALPAK AS-H; hexane:*i*-PrOH = 95:5; detection wavelength = 254 nm; flow rate = 1.0 mL/min. t_R = 5.4 min (minor) and 8.0 min (major), 77:23 er.

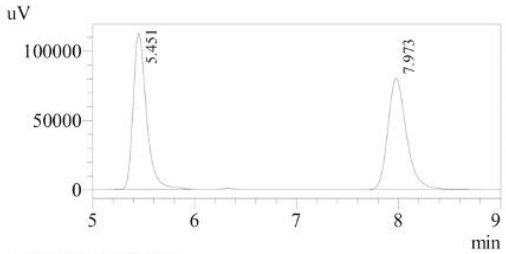

PeakTable

Detector A Ch1 254nm

Peak#	Ret. Time	Area %
1	5.451	50.299
2	7.973	49.701
Total		100.000

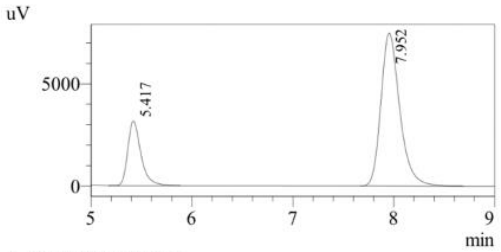

PeakTable

Detector A Ch1 254nm

Peak#	Ret. Time	Area %
1	5.417	22.781
2	7.952	77.219
Total		100.000

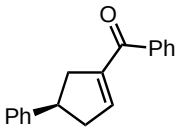

(*R*)-Phenyl(4-phenylcyclopent-1-en-1-yl)methanone (4ap): The reaction was performed at 60 °C for 12 h. Pale yellow oil (25.5 mg, 34%); R_f 0.16 (hexane/EtOAc = 19/1); **^{1}H NMR** (400 MHz, $CDCl_3$) δ 7.79-7.76 (m, 2H), 7.56-7.52 (m, 1H), 7.47-7.43 (m, 2H), 7.34-7.28 (m, 4H), 7.25-7.20 (m, 1H), 6.58-6.56 (m, 1H), 3.66 (quint, *J* = 8.3 Hz, 1H), 3.27-3.20 (m, 1H), 3.15-3.07 (m, 1H), 2.96-2.88 (m, 1H), 2.78-2.70 (m, 1H); **^{13}C{^{1}H} NMR** (100 MHz, $CDCl_3$) δ 193.8, 145.5, 145.1, 143.5 138.7, 131.9, 128.9, 128.5, 128.2, 126.9, 126.2, 42.9, 42.5, 39.8; **HRMS** (ESI) Calcd for $C_{18}H_{17}O$ $[M + H]^+$ 249.1279, found 249.1278; $[\alpha]^{25}_D$ = –3.07 (*c* = 1.76 in $CHCl_3$, 62:38 er sample).

HPLC analysis: Daicel CHIRALPAK OJ-H; hexane:*i*-PrOH = 95:5; detection wavelength = 254 nm; flow rate = 1.0 mL/min. t_R = 12.1 min (major) and 12.8 min (minor), 62:38 er.

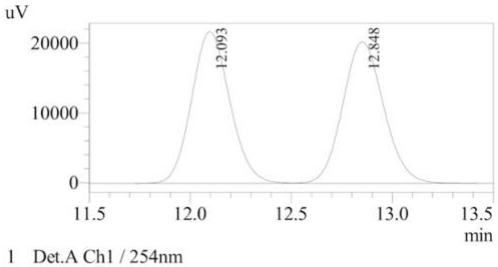

PeakTable

Detector A Ch1 254nm

Peak#	Ret. Time	Area %
1	12.093	50.056
2	12.848	49.944
Total		100.000

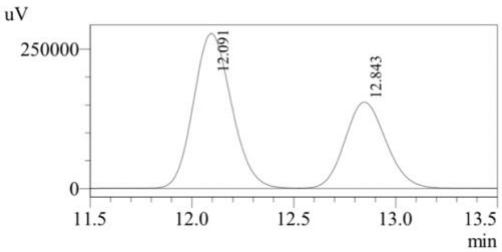

PeakTable

Detector A Ch1 254nm

Peak#	Ret. Time	Area %
1	12.091	62.305
2	12.843	37.695
Total		100.000

The reaction between 1a and 2q

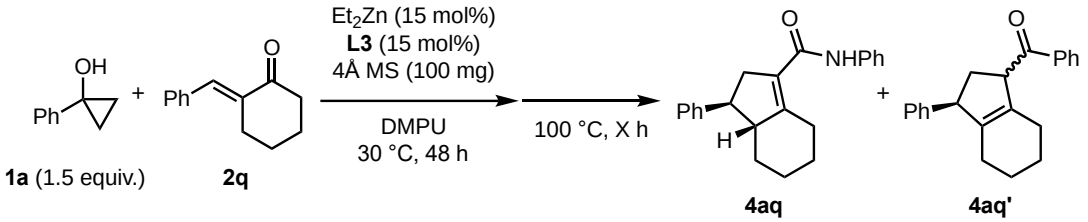

The reaction was performed using **L3** as the ligand at 30 °C for 48 h and then at 100 °C. The time profile of the aldol condensation step showed that **4aq** gradually transformed to **4aq'**, presumably via zinc dienolate intermediate (see Scheme 2.6). As the minor diastereomer of **4aq** had a higher rate of conversion than the major diastereomer, the de of **4aq** increased as the reaction proceeded. When the reaction was quenched after 3 h at 100 °C, **4aq** was obtained as a colorless oil (57.0 mg, 63%, 80:20 dr; The relative stereochemistry of the major diastereomer was determined by X-ray crystallographic analysis of its anilide derivative **5aq**). When the reaction was quenched after 6 h at 100 °C, **4aq** was obtained in 51% yield (46.6 mg, as a single diastereomer). When the reaction was quenched after 144 h at 100 °C, **4aq'** was obtained as a colorless oil (0.6 mmol scale, 120.5 mg, 66%, 50:50 dr).

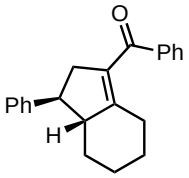

Phenyl((1*S*,7a*R*)-1-phenyl-2,4,5,6,7,7a-hexahydro-1*H*-inden-3-yl)methanone (4aq): R_f 0.34 (hexane/EtOAc = 19/1); **^{1}H NMR** (major diastereomer, 500 MHz, $CDCl_3$) δ 7.83-7.81 (m, 2H), 7.55-7.52 (m, 1H), 7.47-7.44 (m, 2H), 7.34-7.29 (m, 4H), 7.24-7.20 (m, 1H), 3.17-3.12 (m, 1H), 3.07 (q, *J* = 8.4 Hz, 1H), 2.99-2.93 (m, 1H), 2.73-2.68 (m, 1H), 2.47-2.44 (m, 1H), 2.13-2.10 (m, 1H), 1.84-1.77 (m, 2H), 1.72-1.69 (m, 1H), 1.36-1.19 (m, 3H); **^{13}C{^{1}H} NMR** (major diastereomer, 126 MHz, $CDCl_3$) δ 196.5, 153.5, 144.7, 139.2, 132.4, 131.8, 128.8, 128.5, 128.4, 127.3, 126.2, 56.3, 50.6, 42.6, 34.4, 28.6, 26.1, 25.2; **HRMS** (ESI) Calcd for $C_{22}H_{23}O$ $[M + H]^+$ 303.1749, found 303.1746; $[\alpha]^{25}_D$ = –14.0 (*c* = 2.36 in $CHCl_3$, 80:20 dr, 84:16 er (major), 70:30 er (minor) sample).

HPLC analysis (the sample obtained after 3 h at 100 °C, 80:20 dr): Daicel CHIRALPAK ID; hexane:*i*-PrOH = 80:20; detection wavelength = 254 nm; flow rate

= 0.2 mL/min. Major diastereomer t_R = 25.6 min (minor) and 27.7 min (major), 84:16 er. Minor diastereomer t_R = 29.0 min (minor) and 30.8 min (major), 70:30 er.

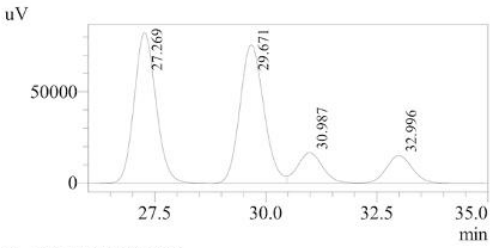

1 Det.A Ch1 / 254nm

PeakTable

Detector A Ch1 254nm

Peak#	Ret. Time	Area %
1	27.269	40.587
2	29.671	40.811
3	30.987	9.573
4	32.996	9.029
Total		100.000

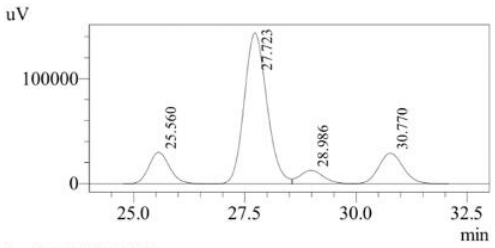

1 Det.A Ch1 / 254nm

PeakTable

Detector A Ch1 254nm

Peak#	Ret. Time	Area %
1	25.560	12.588
2	27.723	66.789
3	28.986	6.131
4	30.770	14.492
Total		100.000

HPLC analysis (the sample obtained after 6 h at 100 °C, single diastereomer): Daicel CHIRALPAK ID; hexane:*i*-PrOH = 80:20; detection wavelength = 254 nm; flow rate = 0.2 mL/min. t_R = 27.3 min (minor) and 29.7 min (major), 82:18 er.

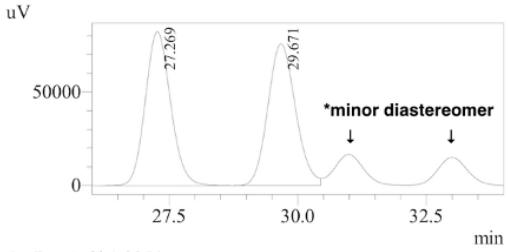

1 Det.A Ch1 / 254nm

PeakTable

Detector A Ch1 254nm

Peak#	Ret. Time	Area %
1	27.269	50.000
2	29.671	50.000
Total		100.000

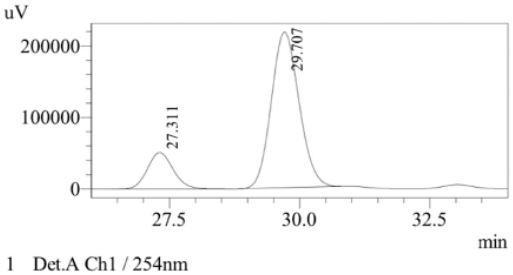

1 Det.A Ch1 / 254nm

PeakTable

Detector A Ch1 254nm

Peak#	Ret. Time	Area %
1	27.311	17.733
2	29.707	82.267
Total		100.000

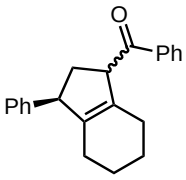

Phenyl(3-phenyl-2,3,4,5,6,7-hexahydro-1*H*-inden-1-yl)methanone (4aq'): Colorless oil (120.5 mg, 66%, 50:50 dr); R_f 0.49, 0.44 (hexane/EtOAc = 19/1); **^{1}H NMR** (400 MHz, $CDCl_3$) the diastereomer of R_f 0.49: δ 8.02-8.00 (m, 2H), 7.57-7.52 (m, 1H), 7.48-7.44 (m, 2H), 7.30-7.22 (m, 4H), 7.19-7.14 (m, 1H), 4.51-4.47 (m, 1H), 3.76 (brs, 1H), 2.80 (dt, *J* = 13.4, 9.2 Hz, 1H), 2.17-2.13 (m, 1H), 1.98 (dt, *J* = 13.6, 6.8 Hz, 1H), 1.89-1.85 (m, 1H), 1.75 (brs, 2H), 1.72-1.54 (m, 4H); the diastereomer of R_f

0.44: δ 8.02-7.99 (m, 2H), 7.58-7.54 (m, 1H), 7.48-7.44 (m, 2H), 7.33-7.29 (m, 2H), 7.23-7.19 (m, 1H), 7.17-7.15 (m, 2H), 4.61-4.58 (m, 1H), 3.89 (brs, 1H), 2.60 (ddd, *J* = 13.3, 8.8, 5.1 Hz, 1H), 2.15 (ddd, *J* = 13.3, 9.2, 5.3 Hz, 1H), 2.00 (brs, 2H), 1.89-1.85 (m, 1H), 1.77-1.55 (m, 5H); **^{13}C{^{1}H} NMR** (100 MHz, $CDCl_3$) the diastereomer of R_f 0.49: δ 202.3, 145.0, 140.7, 137.3, 134.9, 132.9, 128.5, 128.5, 128.4, 128.0, 126.1, 55.0, 54.3, 38.0, 25.2, 24.5, 22.8, 22.6; the diastereomer of R_f 0.44: δ 202.5, 145.3, 141.2, 137.3, 135.0, 132.9, 128.6, 128.5, 127.6, 126.2, 55.1, 53.9, 38.5, 25.4, 24.5, 22.9, 22.6; **HRMS** (ESI) Calcd for $C_{22}H_{23}O$ $[M + H]^+$ 303.1749, found 303.1739; $[\alpha]^{25}_D$ = –56.9 (*c* = 1.80 in $CHCl_3$, 80:20 er sample of the diastereomer of R_f 0.49), –111 (*c* = 1.52 in $CHCl_3$, 80:20 er sample of the diastereomer of R_f 0.44).

HPLC analysis (the diastereomer of R_f 0.49): Daicel CHIRALPAK IA; hexane:*i*-PrOH = 90:10; detection wavelength = 254 nm; flow rate = 1.0 mL/min. t_R = 5.0 min (minor) and 6.1 min (major), 80:20 er.

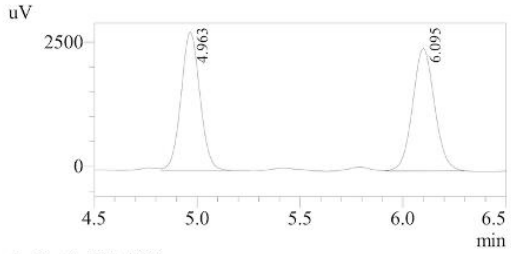

PeakTable
Detector A Ch1 254nm

Peak#	Ret. Time	Area %
1	4.963	49.289
2	6.095	50.711
Total		100.000

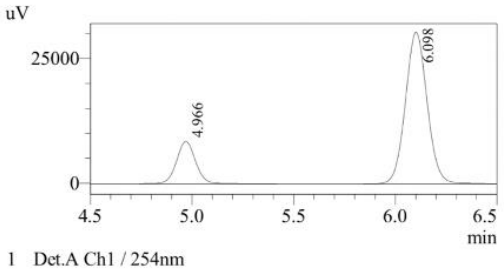

PeakTable
Detector A Ch1 254nm

Peak#	Ret. Time	Area %
1	4.966	19.560
2	6.098	80.440
Total		100.000

HPLC analysis (the diastereomer of R_f 0.44): Daicel CHIRALPAK ID; hexane:*i*-PrOH = 90:10; detection wavelength = 254 nm; flow rate = 1.0 mL/min. t_R = 5.0 min (minor) and 5.3 min (major), 80:20 er.

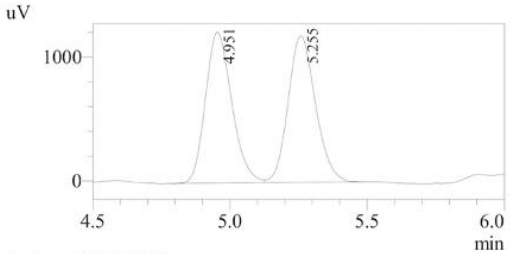

PeakTable
Detector A Ch1 254nm

Peak#	Ret. Time	Area %
1	4.951	49.777
2	5.255	50.223
Total		100.000

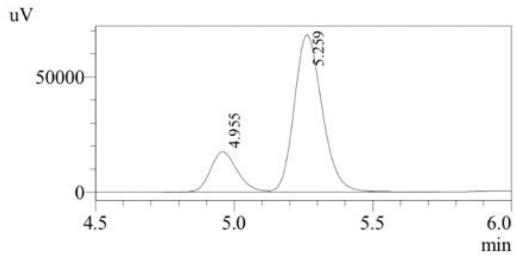

PeakTable
Detector A Ch1 254nm

Peak#	Ret. Time	Area %
1	4.955	19.626
2	5.259	80.374
Total		100.000

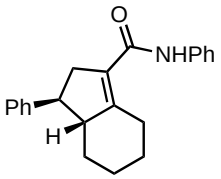

(1*S*,7a*R*)-*N*,1-Diphenyl-2,4,5,6,7,7a-hexahydro-1*H*-indene-3-carboxamide (5aq): Prepared according to the synthetic procedure for **5** (*vide infra*). Pale yellow solid (59.2 mg, 62%); R_f 0.18 (hexane/EtOAc = 19/1); m.p. 148-150 °C; **^{1}H NMR** (400 MHz, $CDCl_3$) δ 7.56-7.54 (m, 2H), 7.33-7.20 (m, 8H), 7.10-7.06 (m, 1H), 3.63-3.60 (m, 1H), 3.09-2.97 (m, 2H), 2.83-2.76 (m, 1H), 2.67-2.61 (m, 1H), 2.07-1.97 (m, 2H), 1.88-1.76 (m, 2H), 1.38-1.13 (m, 3H); **^{13}C{^{1}H} NMR** (100 MHz, $CDCl_3$) δ 164.6, 155.5, 144.5, 137.9, 128.9, 128.5, 127.3, 126.3, 125.5, 124.1, 120.0, 55.9, 50.4, 41.3, 34.1, 27.6, 26.0, 25.2; **HRMS** (ESI) Calcd for $C_{22}H_{24}NO$ $[M + H]^+$ 318.1858, found 318.1857; $[\alpha]^{25}_D$ = –20.8 (*c* = 2.86 in $CHCl_3$, 84:16 er sample).

HPLC analysis: Daicel CHIRALPAK ID; hexane:*i*-PrOH = 80:20; detection wavelength = 254 nm; flow rate = 1.0 mL/min. t_R = 14.8 min (minor) and 17.2min (major), 84:16 er.

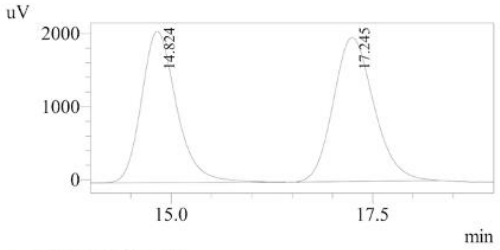

PeakTable
Detector A Ch1 254nm

Peak#	Ret. Time	Area %
1	14.824	47.583
2	17.245	52.417
Total		100.000

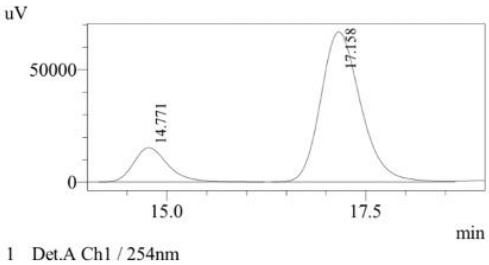

PeakTable
Detector A Ch1 254nm

Peak#	Ret. Time	Area %
1	14.771	16.495
2	17.158	83.505
Total		100.000

Product Transformations

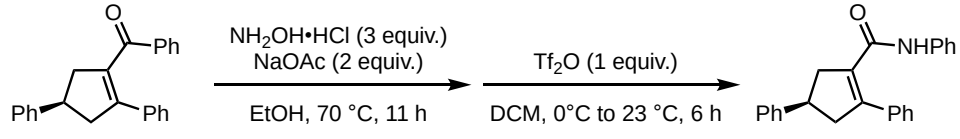

4aa
0.3 mmol, 95:5 er

5
86%, 95:5 er

(*R*)-*N*,2,4-Triphenylcyclopent-1-ene-1-carboxamide (5): A 4-mL vial equipped with a magnetic stir bar was charged with **4aa** (97.3 mg, 0.30 mmol, 95:5 er), hydroxylammonium chloride (62.6 mg, 0.90 mmol, 3 equiv.) and sodium acetate (49.2 mg, 0.6 mmol, 2 equiv.), followed by the addition of ethanol (0.9 mL). The mixture

was stirred at 70 °C for 11 h. After the reaction mixture was concentrated under the reduced pressure, the residue was diluted with H_2O (1.5 mL) and CH_2Cl_2 (2 mL). The layers were separated, and the aqueous layer was extracted with CH_2Cl_2 (3 × 2 mL). The combined organic layers were dried Na_2SO_4, filtered, and concentrated to give the crude oxime intermediate as a colorless oil. The crude oxime product was dissolved in anhydrous CH_2Cl_2 (4 mL) and the solution was stirred at 0 °C. To the mixture was added triflic anhydride solution (84.3 mg in CH_2Cl_2 (2 mL)) dropwise over 15 min, and the resulting mixture was stirred and allowed to warm to room temperature. After 6 h, the reaction mixture was washed with sat. $NaHCO_3$ aq (2 mL) and the organic layers were dried over Na_2SO_4, filtered, and concentrated. The crude product was purified by flash column chromatography to afford the product as a pale yellow solid (88.0 mg, 86%); R_f 0.23 (hexane/EtOAc = 9/1); m.p. 126-127 °C; **^{1}H NMR** (400 MHz, $CDCl_3$) δ 7.41-7.32 (m, 9H), 7.24-7.15 (m, 6H), 7.04-7.00 (m, 1H), 3.66 (quint, J = 8.2 Hz, 1H), 3.43-3.28 (m, 2H), 3.12-3.02 (m, 2H); **^{13}C{^{1}H} NMR** (100 MHz, $CDCl_3$) δ 164.3, 145.3, 145.2, 137.7, 135.9, 133.3, 128.9, 128.8, 128.6, 128.5, 127.8, 126.8, 126.3, 124.0, 119.4, 47.8, 43.0, 41.6; **HRMS** (ESI) Calcd for $C_{24}H_{22}NO$ $[M + H]^+$ 340.1701, found 340.1703; $[\alpha]^{25}_D$ = +8.18 (c = 2.29 in $CHCl_3$, 95:5 er sample).

HPLC analysis: Daicel CHIRALPAK ID; hexane:*i*-PrOH = 90:10; detection wavelength = 254 nm; flow rate = 1.0 mL/min. t_R = 19.3 min (minor) and 21.0 min (major), 95:5 er.

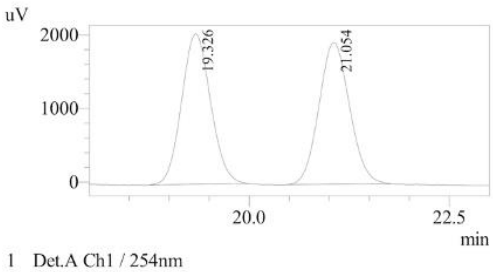

1 Det.A Ch1 / 254nm

PeakTable

Detector A Ch1 254nm

Peak#	Ret. Time	Area %
1	19.326	50.037
2	21.054	49.963
Total		100.000

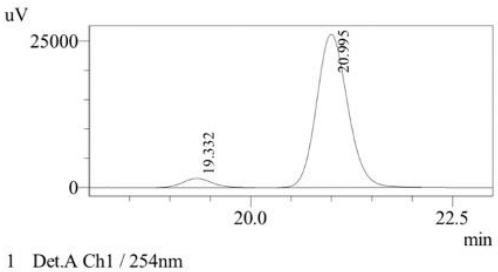

1 Det.A Ch1 / 254nm

PeakTable

Detector A Ch1 254nm

Peak#	Ret. Time	Area %
1	19.332	5.248
2	20.995	94.752
Total		100.000

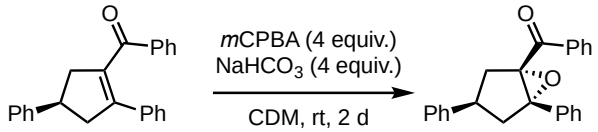

4aa
0.3 mmol, 95:5 er

6
36%, 95:5 er

((1*S*,3*R*,5*S*)-3,5-Diphenyl-6-oxabicyclo[3.1.0]hexan-1-yl)(phenyl)methanone (6): A 25 mL round bottom flask equipped with a magnetic stir bar was charged with **4aa** (97.3 mg, 0.30 mmol, 95:5 er), *m*-chloroperoxybenzoic acid (50-55 wt%, 414 mg, ca. 1.2 mmol, 4 equiv.) and sodium bicarbonate (100.8 mg, 1.20 mmol, 4 equiv.), followed by the addition of CH_2Cl_2 (9 mL). The mixture was stirred at rt for 48 h. The reaction progress was monitored by GC-MS as R_f of the product was very close to that of the starting material. The reaction mixture was diluted with CH_2Cl_2 (15 mL) and washed with sat. $NaHCO_3$ aq (2 × 10 mL) and brine (10 mL). The organic layers were dried over Na_2SO_4, filtered, and concentrated. The crude product was purified by flash column chromatography to afford the product as a colorless oil (36.9 mg, 36%); R_f 0.31 (hexane/EtOAc = 19/1); **^{1}H NMR** (400 MHz, $CDCl_3$) δ 7.86-7.84 (m, 2H), 7.53-7.49 (m, 1H), 7.41-7.31 (m, 8H), 7.27-7.17 (m, 4H), 3.41-3.32 (m, 1H), 2.80-2.64 (m, 4H); **^{13}C{^{1}H} NMR** (100 MHz, $CDCl_3$) δ 195.8, 142.2, 135.8, 134.5, 133.3, 129.0, 128.6, 128.4, 128.2, 128.1, 127.4, 126.7, 126.0, 75.9, 72.5, 39.5, 38.9, 38.7; **HRMS** (ESI) Calcd for $C_{24}H_{21}O_2$ $[M + H]^+$ 341.1542, found 341.1544; $[\alpha]^{25}_D$ = –7.80 (*c* = 1.30 in $CHCl_3$, 95:5 er sample).

HPLC analysis: Daicel CHIRALPAK ID; hexane:*i*-PrOH = 98:2; detection wavelength = 254 nm; flow rate = 1.0 mL/min. t_R = 9.9 min (minor) and 12.0 min (major), 95:5 er.

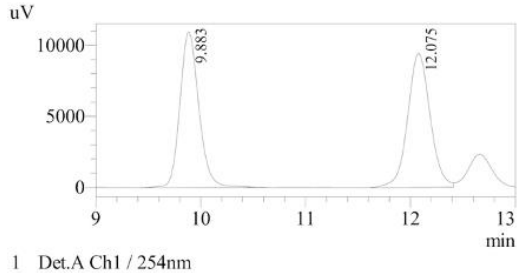

PeakTable
Detector A Ch1 254nm

Peak#	Ret. Time	Area %
1	9.883	49.464
2	12.075	50.536
Total		100.000

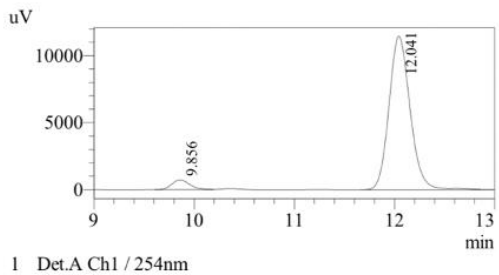

PeakTable
Detector A Ch1 254nm

Peak#	Ret. Time	Area %
1	9.856	5.122
2	12.041	94.878
Total		100.000

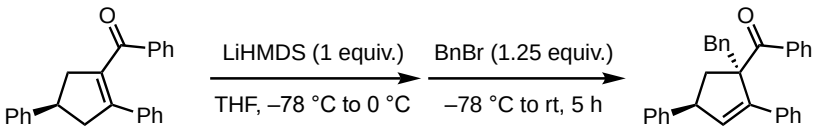

4aa
0.3 mmol, 95:5 er

7
75%, 95:5 er

((1*S*,4*S*)-1-Benzyl-2,4-diphenylcyclopent-2-en-1-yl)(phenyl)methanone (7): A 10 mL Schlenk flask equipped with a magnetic stir bar was charged with **4aa** (97.3 mg, 0.30 mmol, 95:5 er) and anhydrous THF (3 mL) under nitrogen atmosphere. The mixture was cooled to –78 °C, and lithium bis(trimethylsilyl)amide (1.3 M in THF, 0.23 mL, 0.30 mmol) was added slowly. The resulting pale yellow mixture was stirred at 0 °C for 1 h. The mixture was cooled again to –78 °C, followed by dropwise addition of benzyl bromide (1.25 equiv., 64.4 mg, 0.375 mmol). The reaction mixture was gradually warmed to room temperature. After 5 h, the reaction mixture was concentrated in vacuo. The crude product was purified by flash column chromatography to afford the product as a colorless oil (93.5 mg, 75%); R_f 0.15 (hexane/EtOAc = 5/1); **^{1}H NMR** (400 MHz, $CDCl_3$) δ 8.08-8.06 (m, 2H), 7.53-7.51 (m, 2H), 7.42-7.38 (m, 1H), 7.33-7.28 (m, 4H), 7.27-7.10 (m, 9H), 6.97-6.95 (m, 2H), 6.44 (d, *J* = 2.2 Hz, 1H), 3.56 (d, *J* = 13.8 Hz, 1H), 3.38 (d, *J* = 13.8 Hz, 1H), 2.89-2.84 (m, 1H), 2.64 (dd, *J* = 13.5, 8.2 Hz, 1H), 2.48 (ddd, *J* = 13.5, 9.5, 0.9 Hz, 1H); **^{13}C{^{1}H} NMR** (100 MHz, $CDCl_3$; peaks showing positive and negative DEPT 135 signals are indicated with + and –, respectively) δ 204.2, 145.0, 144.2, 138.0, 137.5, 135.2 (+), 134.6, 131.9 (+), 131.0 (+), 129.5 (+), 128.9 (+), 128.5 (+), 128.1 (+), 127.8 (+), 127.6 (+), 127.2 (+), 126.7 (+), 126.4 (+), 126.4 (+), 66.7, 49.9 (+), 45.2 (–), 40.7 (–); **HRMS** (ESI) Calcd for $C_{31}H_{27}O$ $[M + H]^+$ 415.2062, found 415.2067; $[\alpha]^{25}_D$ = –62.7 (*c* = 1.10 in $CHCl_3$, 95:5 er sample).

HPLC analysis: Daicel CHIRALPAK IA; hexane:*i*-PrOH = 98:2; detection wavelength = 254 nm; flow rate = 1.0 mL/min. t_R = 8.2 min (minor) and 11.4 min (major), 95:5 er.

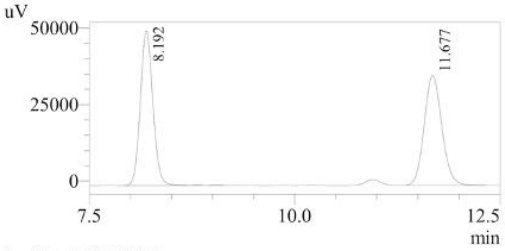

PeakTable

Detector A Ch1 254nm

Peak#	Ret. Time	Area %
1	8.192	50.007
2	11.677	49.993
Total		100.000

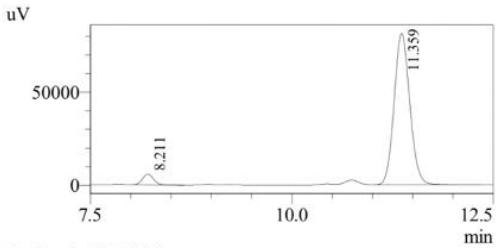

PeakTable

Detector A Ch1 254nm

Peak#	Ret. Time	Area %
1	8.211	4.874
2	11.359	95.126
Total		100.000

2.5 References

1. (a) Kuwajima, I.; Nakamura, E., Metal Homoenolates from Siloxycyclopropanes. *Top. Curr. Chem.* **1990,** *155*, 1-39; (b) Kimura, M., Metal Homoenolates. In *Comprehensive Organic Synthesis II*, Knochel, P., Ed. Elsevier: 2014; Vol. 2; (c) Mills, L. R.; Rousseaux, S. A. L., Modern Developments in the Chemistry of Homoenolates. *Eur. J. Org. Chem.* **2019,** *2019*, 8-26; (d) Nikolaev, A.; Orellana, A., Transition-Metal-Catalyzed C–C and C–X Bond-Forming Reactions Using Cyclopropanols. *Synthesis* **2016,** *48*, 1741-1768; (e) McDonald, T. R.; Mills, L. R.; West, M. S.; Rousseaux, S. A. L., Selective Carbon–Carbon Bond Cleavage of Cyclopropanols. *Chem. Rev.* **2021,** *121*, 3-79; (f) Sekiguchi, Y.; Yoshikai, N., Metal-Catalyzed Transformations of Cyclopropanols via Homoenolates. *Bull. Chem. Soc. Jpn.* **2021,** *94*, 265-280.

2. (a) Nakamura, E.; Kuwajima, I., Copper-Catalyzed Acylation and Conjugate Addition of Zinc Homoenolate. Synthesis of 4- and 5-Oxo Esters. *J. Am. Chem. Soc.* **1984,** *106*, 3368-3370; (b) Nakamura, E.; Aoki, S.; Sekiya, K.; Oshino, H.; Kuwajima, I., Carbon–Carbon Bond-Forming Reactions of Zinc Homoenolate of Esters. A Novel Three-Carbon Nucleophile with General Synthetic Utility. *J. Am. Chem. Soc.* **1987,** *109*, 8056-8066.

3. (a) Soai, K.; Niwa, S., Enantioselective Addition of Organozinc Reagents to Aldehydes. *Chem. Rev.* **1992,** *92*, 833-856; (b) Yamada, K.-i.; Tomioka, K., Copper-Catalyzed Asymmetric Alkylation of Imines with Dialkylzinc and Related Reactions. *Chem. Rev.* **2008,** *108*, 2874-2886; (c) Kobayashi, S.; Mori, Y.; Fossey, J. S.; Salter, M. M., Catalytic Enantioselective Formation of C−C Bonds by Addition to Imines and Hydrazones: A Ten-Year Update. *Chem. Rev.* **2011,** *111*, 2626-2704; (d) Alexakis, A.;

Bäckvall, J. E.; Krause, N.; Pàmies, O.; Diéguez, M., Enantioselective Copper-Catalyzed Conjugate Addition and Allylic Substitution Reactions. *Chem. Rev.* **2008,** *108*, 2796-2823; (e) Jerphagnon, T.; Pizzuti, M. G.; Minnaard, A. J.; Feringa, B. L., Recent Advances in Enantioselective Copper-Catalyzed 1,4-Addition. *Chem. Soc. Rev.* **2009,** *38*, 1039-1075.

4. *Reaxys*. https://www.reaxys.com (accessed 2021-01-15).

5. Das, P. P.; Belmore, K.; Cha, J. K., S_N2' Alkylation of Cyclopropanols via Homoenolates. *Angew. Chem. Int. Ed.* **2012,** *51*, 9517-9520.

6. (a) Parida, B. B.; Das, P. P.; Niocel, M.; Cha, J. K., C-Acylation of Cyclopropanols: Preparation of Functionalized 1,4-Diketones. *Org. Lett.* **2013,** *15*, 1780-1783; (b) Murali, R. V. N. S.; Rao, N. N.; Cha, J. K., C-Alkynylation of Cyclopropanols. *Org. Lett.* **2015,** *17*, 3854-3856; (c) Mills, L. R.; Barrera Arbelaez, L. M.; Rousseaux, S. A. L., Electrophilic Zinc Homoenolates: Synthesis of Cyclopropylamines from Cyclopropanols and Amines. *J. Am. Chem. Soc.* **2017,** *139*, 11357-11360.

7. (a) Nomura, K.; Matsubara, S., Preparation of Zinc–Homoenolate from *α*-Sulfonyloxy Ketone and Bis(iodozincio)methane. *Chem. Lett.* **2006,** *36*, 164-165; (b) Nomura, K.; Matsubara, S., Stereospecific Construction of Chiral Tertiary and Quaternary Carbon by Nucleophilic Cyclopropanation with Bis(iodozincio)methane. *Chem. Asian J.* **2010,** *5*, 147-152.

8. In fact, examples of enantioselective transformation of catalytically generated metal homoenolates remain very rare. See the following references and ref 9: (a) Yang, J.; Shen, Y.; Lim, Y. J.; Yoshikai, N., Divergent Ring-Opening Coupling Between Cyclopropanols and Alkynes under Cobalt Catalysis. *Chem. Sci.* **2018,** *9*, 6928-6934; (b) Yang, J.; Sekiguchi, Y.; Yoshikai, N., Cobalt-Catalyzed Enantioselective and Chemodivergent Addition of Cyclopropanols to Oxabicyclic Alkenes. *ACS Catal.* **2019,** *9*, 5638-5644; (c) Huang, W.; Meng, F., Cobalt-Catalyzed Diastereo- and Enantioselective Hydroalkylation of Cyclopropenes with Cobalt Homoenolates. *Angew. Chem. Int. Ed.* **2021,** *60*, 2694-2698.

9. Burke, E. D.; Lim, N. K.; Gleason, J. L., Catalytic Enantioselective Homoaldol Reactions Using BINOL Titanium (IV) Fluoride Catalysts. *Synlett* **2003**, 390-392.

10. (a) Soai, K.; Okudo, M.; Okamoto, M., Enantioselective Conjugate Addition of Diethylzinc to Enones Using Chiral *β*-Aminoalcohol as Chiral Catalyst or Ligand. *Tetrahedron Lett.* **1991,** *32*, 95-96; (b) Bräse, S.; Höfener, S., Asymmetric Conjugate

Addition of Organozinc Compounds to *α,β*-Unsaturated Aldehydes and Ketones with [2.2]Paracyclophaneketimine Ligands without Added Copper Salts. *Angew. Chem. Int. Ed.* **2005,** *44*, 7879-7881.

11. For the importance of cyclopentanes in bioactive natural products and pharmacetutical drugs, see: (a) Hudlicky, T.; Price, J. D., Anionic Approaches to the Construction of Cyclopentanoids. *Chem. Rev.* **1989,** *89*, 1467-1486; (b) Das, S.; Chandrasekhar, S.; Yadav, J. S.; Grée, R., Recent Developments in the Synthesis of Prostaglandins and Analogues. *Chem. Rev.* **2007,** *107*, 3286-3337; (c) Liu, G.; Shirley, M. E.; Van, K. N.; McFarlin, R. L.; Romo, D., Rapid Assembly of Complex Cyclopentanes Employing Chiral, *α,β*-Unsaturated Acylammonium Intermediates. *Nat. Chem.* **2013,** *5*, 1049-1057; (d) Heasley, B., Recent Developments in the Stereocontrolled Synthesis of Highly Substituted Cyclopentane Core Structures: From Drug Discovery Research to Natural Product Synthesis. *Curr. Org. Chem.* **2014,** *18*, 641-686.

12. (a) Frantz, D. E.; Fässler, R.; Tomooka, C. S.; Carreira, E. M., The Discovery of Novel Reactivity in the Development of C−C Bond-Forming Reactions: In Situ Generation of Zinc Acetylides with Zn(II)/R_3N. *Acc. Chem. Res.* **2000,** *33*, 373-381; (b) Trost, B. M.; Weiss, A. H., The Enantioselective Addition of Alkyne Nucleophiles to Carbonyl Groups. *Adv. Synth. Catal.* **2009,** *351*, 963-983.

13. (a) Satyanarayana, T.; Abraham, S.; Kagan, H. B., Nonlinear Effects in Asymmetric Catalysis. *Angew. Chem. Int. Ed.* **2009,** *48*, 456-494; (b) Noyori, R.; Suga, S.; Oka, H.; Kitamura, M., Self and Nonself Recognition of Chiral Catalysts: The Origin of Nonlinear Effects in the Amino-Alcohol Catalyzed Asymmetric Addition of Diorganozincs to Aldehydes. *Chem. Rec.* **2001,** *1*, 85-100; (c) Girard, C.; Kagan, H. B., Nonlinear Effects in Asymmetric Synthesis and Stereoselective Reactions: Ten Years of Investigation. *Angew. Chem. Int. Ed.* **1998,** *37*, 2922-2959; (d) Noyori, R.; Kitamura, M., Enantioselective Addition of Organometallic Reagents to Carbonyl Compounds: Chirality Transfer, Multiplication, and Amplification. *Angew. Chem. Int. Ed.* **1991,** *30*, 49-69.

14. Geiger, Y.; Achard, T.; Maisse-François, A.; Bellemin-Laponnaz, S., Hyperpositive Nonlinear Effects in Asymmetric Catalysis. *Nat. Catal.* **2020,** *3*, 422-426.

15. For example, see: (a) Labourdette, G.; Lee, D. J.; Patrick, B. O.; Ezhova, M. B.; Mehrkhodavandi, P., Unusually Stable Chiral Ethyl Zinc Complexes: Reactivity and Polymerization of Lactide. *Organometallics* **2009,** *28*, 1309-1319; (b) Wang, H.; Yang,

Y.; Ma, H., Exploring Steric Effects in Diastereoselective Synthesis of Chiral Aminophenolate Zinc Complexes and Stereoselective Ring-Opening Polymerization of *rac*-Lactide. *Inorg. Chem.* **2016,** *55*, 7356-7372.

16. Alternatively, the aminoalkoxide oxygen of **A** may form a hydrogen bond with the amino alcohol OH of the homoenolate **C** to give a different association complex. For such a complex, one may conceive a mechanism involving concerted proton transfer from **C** to along with the nucleophile delivery. In any case, the bimetallic mechanism for the conjugate addition remains speculative and warrants further investigation.

17. Note that the model reaction between **1a** and **2a** under the standard conditions did not give any trace of a byproduct arising from conjugate addition of the ethyl group to **2a**.

Chapter 3. Zinc-Catalyzed *β*-Functionalization of Cyclopropanols via Enolized Homoenolate

3.1 Introduction

The cyclopropane ring has attracted the attention of synthetic chemists over decades for its high strain-driven reactivity as well as for its presence in many biologically active substances.[1] Among all cyclopropanes, cyclopropanols represent unique three-carbon synthons in synthetic methodology development and total synthesis.[2] They have been extensively explored as precursors to homoenolates and *β*-keto radicals, formed through two distinct ring-opening pathways, which serve as intermediates of orthogonal reactivity for the synthesis of *β*-functionalized ketones (Scheme 3.1a). Because of the high propensity of cyclopropanols toward these and other ring-opening modes, it is difficult to install a new functional group into existing cyclopropanols without rupture of the three-membered ring. This marks a sharp contrast with the extensive development of C−H activation of other types of cyclopropanes containing directing groups.[3]

While metal homoenolate has been predominantly used as a precursor to *β*-functionalized ketones, it is an intrinsically amphoteric species that has a nucleophilic *β*-carbon and an electrophilic carbonyl group (Scheme 3.1a). This amphoteric nature has recently been exploited in several reactions.[4] A particularly notable example in this context is the zinc-mediated conversion of cyclopropanol to cyclopropylamine by Rousseaux, which elegantly utilized the electrophilicity of the aldehyde allowing the condensation with secondary amine and the nucleophilicity of the carbon−zinc bond allowing the ring closure (Scheme 3.1b).[5] Inspired by this and other precedents on zinc homoenolate[6] and prompted by my own work on catalytic generation of zinc homoenolate (Chapter 2),[7] I wondered if it would be possible to enolize the zinc homoenolate, thus rendering the *α*-carbon nucleophilic (see Scheme 3.1a). Electrophilic trapping of the resulting bis-nucleophilic, enolized homoenolate at the *α*-position, followed by ring closure of the homoenolate, would furnish *α*,*β*-functionalized cyclopropanol. Along with this hypothesis, I have discovered a zinc-catalyzed *β*-allylation of a cyclopropanol with a Morita−Baylis−Hillman (MBH) carbonate with retention of the cyclopropyl ring, which is described in detail in this chapter (Scheme 3.1c). A catalyst generated from Et_2Zn and a *β*-amino alcohol promotes allylation of

the β-position and subsequent lactonization to afford cyclopropyl-fused α-alkylidene-δ-valerolactones in moderate to good yields,[8] which overall represents the first example of direct C−H functionalization of a cyclopropanol. Mechanistic experiments have proved consistent with the proposed reaction pathway involving α-functionalization of the enolized homoenolate. Besides MBH carbonates, alkylidene malononitriles are also engaged in the reaction with the enolized homoenolate, affording bicyclic cyclopropane derivatives in a diastereoselective fashion.

Scheme 3.1. Cyclopropanol as Three-Carbon Synthons

(a) Cyclopropanol as precursor to homoenolate and β-keto radical

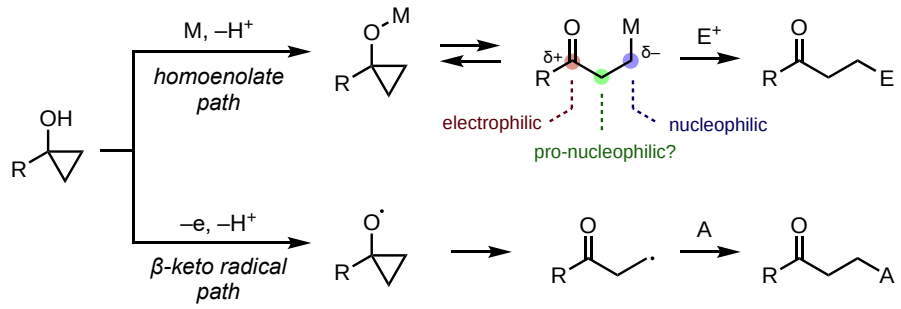

(b) Homoenolate as amphoteric species (Rousseaux)

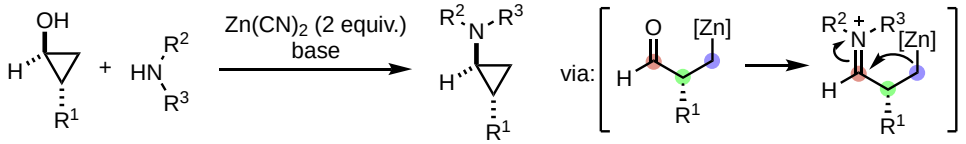

(c) **This work**: Homoenolate as latent α,β-bisnucleophile

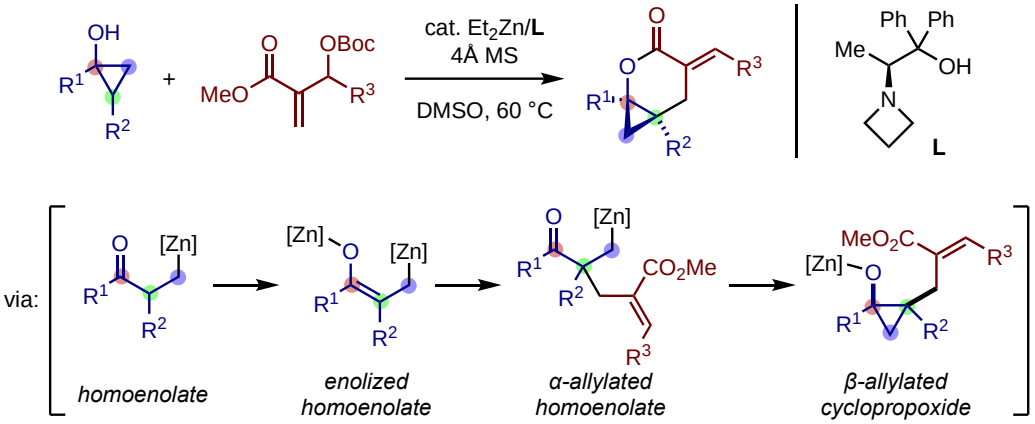

3.2 Results and Discussions

To realize the aforementioned hypothesis on ring-opening/α-functionalization/ring-closure functionalization of cyclopropanol in a catalytic manner,

two major requirements, among others, should be satisfied. First, the electrophile should not be directly intercepted by the initially generated zinc homoenolate, but has to wait for it to enolize for the desired α-functionalization. Second, even if the α-functionalization and subsequent ring closure were feasible, the thus-formed cyclopropanol product should not take part in the homoenolate chemistry again, which might lead to multiple substitution or ring-opening decomposition. Retrospectively, MBH carbonate appears to meet these requirements for its lack of reactivity toward organozinc reagents and its ester moiety allowing irreversible lactonization.

Table 3.1 shows the optimization of the reaction between 1-phenylcyclopropanol (**1a**) and MBH carbonate (**2a**) derived from methyl acrylate and benzaldehyde. A catalytic system comprised of Et_2Zn (20 mol%), alanine-derived amino alcohol **L1** (20 mol%), and 4 Å molecular sieves (MS) promoted the reaction in DMSO at 60 °C to afford [4.1.0]-bicyclic lactone **3aa** in 49% yield with 17% ee along with propiophenone (**1'**) and its α-allylated product (**4**), both in 8% yields (entry 1). The reaction became sluggish in less polar and less coordinating solvents such as THF and toluene (entries 2 and 3). Omission of either 4 Å MS or **L1** led to a diminished yield of **3aa** (entries 4 and 5). Amino alcohols other than **L1** and dinitrogen bidentate-type chial ligands were ineffective in terms of the yield, except that **L3** and **L6** displayed comparable yields (entries 6−19). The ee values also remained low to moderate, thus the maximum ee was 18% with **L9** (entry 13). Finally, the yield of **3aa** could be improved to 74% with excess **1a** (1.5 equiv.), reduced catalyst loadings (10 mol% Et_2Zn and 15 mol% **L1**), and prolonged reaction time (24 h; entries 20 and 21).

Table 3.1. Zinc-Catalyzed Reaction between 1-Phenylcyclopropanol (**1a**) to MBH Carbonate (**2a**)[a]

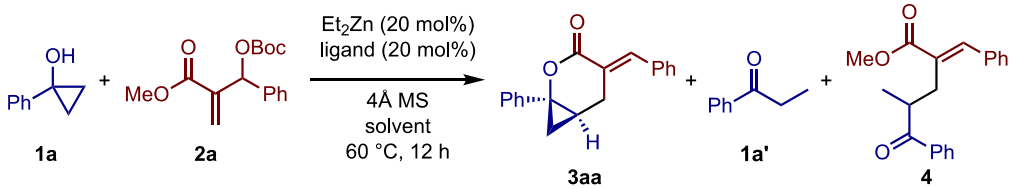

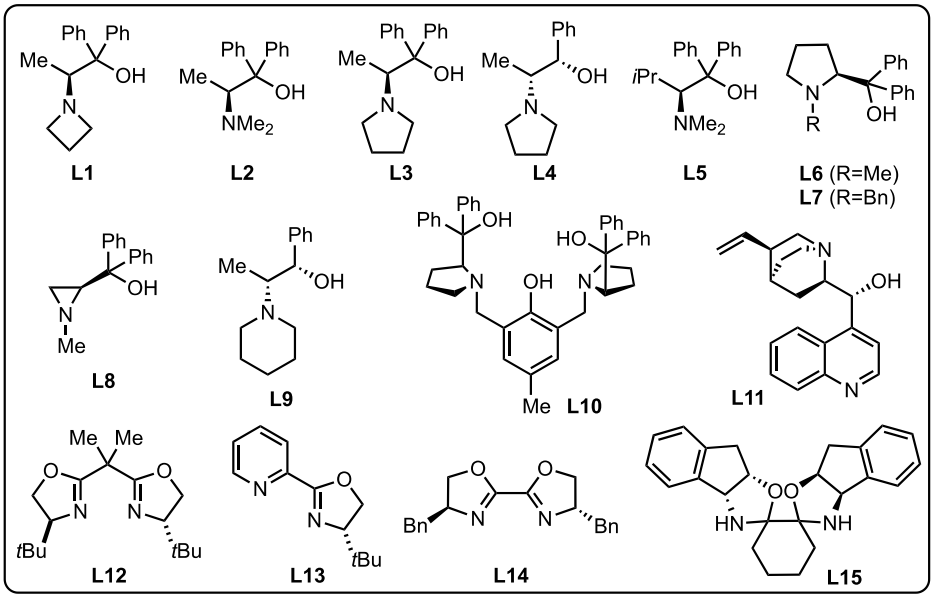

entry	ligand	solvent	**3aa** (%)[b]	ee of **3aa** (%)[c]	**1a'** (%)[b]	**4** (%)[b]
1	**L1**	DMSO	49	17	8	8
2	**L1**	THF	12	-	12	5
3	**L1**	Toluene	9	-	60	6
4[d]	**L1**	DMSO	13	-	41	8
5	-	DMSO	22	-	26	12
6	**L2**	DMSO	32	1	23	19
7	**L3**	DMSO	44	17	34	11
8	**L4**	DMSO	20	12	37	13
9	**L5**	DMSO	24	0	41	15
10	**L6**	DMSO	49	3	21	8
11	**L7**	DMSO	26	2	32	13
12	**L8**	DMSO	41	8	20	17
13	**L9**	DMSO	26	18	25	11
14[e]	**L10**	DMSO	5	-	49	38
15	**L11**	DMSO	20	6	33	7
16	**L12**	DMSO	22	0	33	14
17	**L13**	DMSO	21	3	28	13
18	**L14**	DMSO	26	1	49	23
19	**L15**	DMSO	23	4	29	12
20[f]	**L1**	DMSO	63	-	35	11
21[f,g]	**L1**	DMSO	74	-	13	10

[a]The reaction was performed using 0.1 mmol of **1a** and **2a** in solvent (0.11 M). [b]Determined by GC using mesitylene as an internal standard.[c]Determined by chiral HPLC. [d]4Å MS was omitted. [e]10 mol% of **L10** was used. [f]0.15 mmol of **1a** and 0.1 mmol of **2a** were used. [g]10 mol% of Et_2Zn and 15 mol% of **L1** was used. The reaction was performed for 24 h.

With the optimized catalytic system (Table 3.1, entry 21) in hand, the scope of the present allylation was explored. First, a variety of cyclopropanols were subjected to the reaction with **2a** (Scheme 3.2). A series of 1-arylcyclopropanols participated in the allylation to afford the corresponding lactones **3aa**−**3ja** in moderate to good yields, with tolerance to methyl, iodo, bromo, chloro, and trifluoromethyl groups. Methoxy groups on the *meta* (**3ga**) and the *ortho* (**3ha**) positions were also tolerated. The reaction of **1a** could be performed on a 5 mmol scale, albeit in a moderate yield (45%). The reactions of 1-(2-naphthyl)- and 1-(2-thienyl)cyclopropanols also afforded the desired products **3ia** and **3ja**, respectively. The molecular structure of the former was unambiguously confirmed by X-ray crystallographic analysis. The latter was difficult to purify by flash chromatography and thus was obtained by recrystallization in moderate yield (32%). 1-Alkylcyclopropanols bearing secondary alkyl groups also reacted with **2a** to afford the corresponding products **3ka** and **3la** in moderate yields, while the reaction of 1-pentylcyclopropanol was complex and failed to give the desired product. Interestingly, bicyclic cyclopropanols **1m** and **1n** underwent allylation with MBH carbonate **2m** at the more hindered *β*-position to afford methano-bridged polycyclic lactones **3mm** and **3nm**, respectively, in moderate yields. The structure of the latter was confirmed by X-ray crystallographic analysis. Given these results, it appeared less likely that the present reaction proceeded through direct cleavage of the *β*-C−H bond (*vide infra*).

Scheme 3.2. *β*-Allylation of Various Cyclopropanols with MBH Carbonate (**2a**)[a]

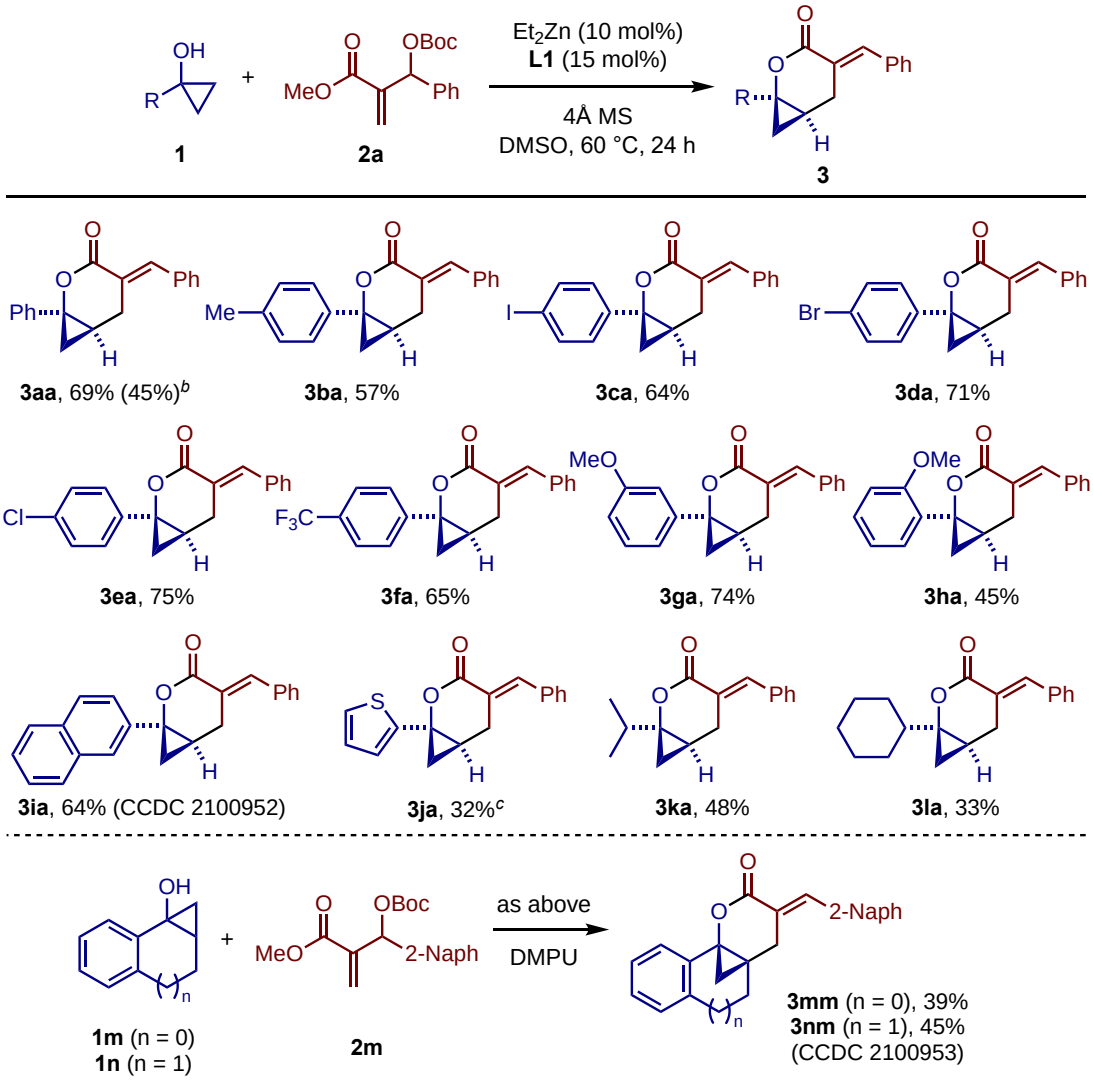

[a]The reaction was performed on a 0.3 mmol scale. [b]The yield of a 5 mmol scale reaction is shown in the parentheses. [c]The product was isolated by recrystallization.

Next, the addition of **1a** to various MBH carbonates was explored (Scheme 3.3). A series of MBH carbonates derived from (hetero)aryl aldehydes proved to be good substrates, affording the corresponding bicyclic lactones **3ab**–**3ag** in moderate to good yields. Those derived from aliphatic aldehydes were also tolerated to furnish the products **3ah**–**3ak**, albeit in somewhat lower yields. The formaldehyde-derived MBH carbonate **2l** also took part in the reaction to give the desired product **3al**. Note that change of the methyl ester moiety of the MBH carbonate to cyclohexyl or *tert*-butyl ester led to diminished yields.

Scheme 3.3. *β*-Allylation of Cyclopropanol (**1a**) with Various MBH Carbonates[a]

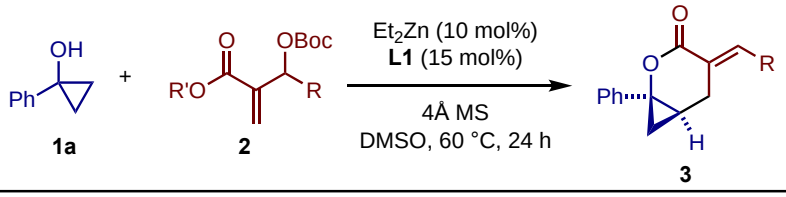

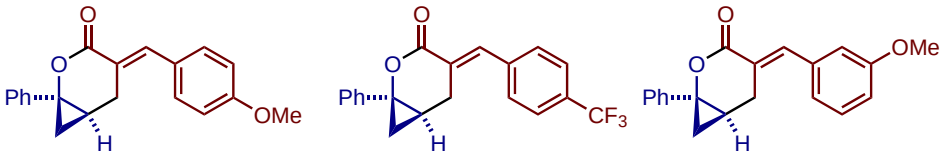

3ab, 74%

3ac, 26%[b]

3ad, 64%

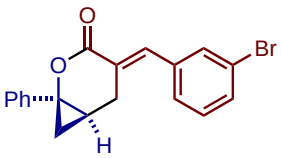

3ae, 69%

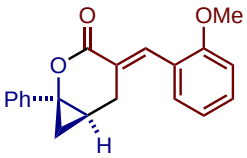

3af, 65%

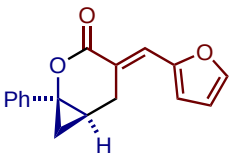

3ag, 57%

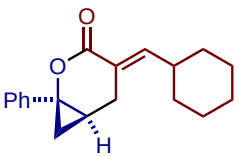

3ah, 32%

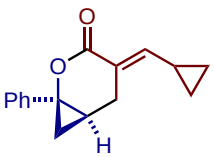

3ai, 57%

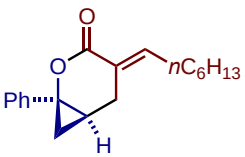

3aj, 37%

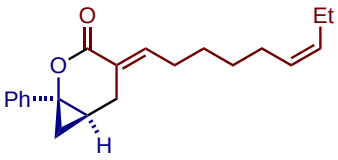

3ak, 39%

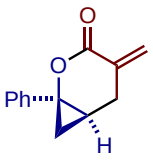

3al, 37%

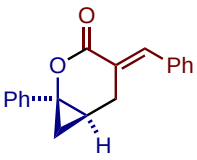

3aa
36% (R' = Cy)[c]
trace (R' = *t*Bu)[c]

[a]The reaction was performed on a 0.3 mmol scale. R' = Me unless otherwise noted. [b]The product was isolated by recrystallization. [c]The reaction was performed under the conditions in Table 3.1, entry 1.

To gain insight into the mechanism, a series of control experiments were performed. First, compounds **4**, **5**, and **6** were synthesized to probe their possible involvement as intermediates (Scheme 3.4a). The *α*-allylated propiophenone **4** is the byproduct in the reaction between **1a** and **2a** (*vide supra*). Another isomer **5** is the product of the ring-opening allylation of **1a** with **2a** via homoenolate.[9] The failure of **4** and **5** to give **3aa** excludes the possibility of their *β*-deprotonation and cyclization of the resulting homoenolate to cyclopropoxide, which was unsurprising in light of the

low acidity of the *β*-CH. Meanwhile, the lack of reactivity of cyclopropyl ester **6** ruled out a pathway involving ester-directed *β*-deprotonation of the cyclopropane ring.

Scheme 3.4. Control Experiments

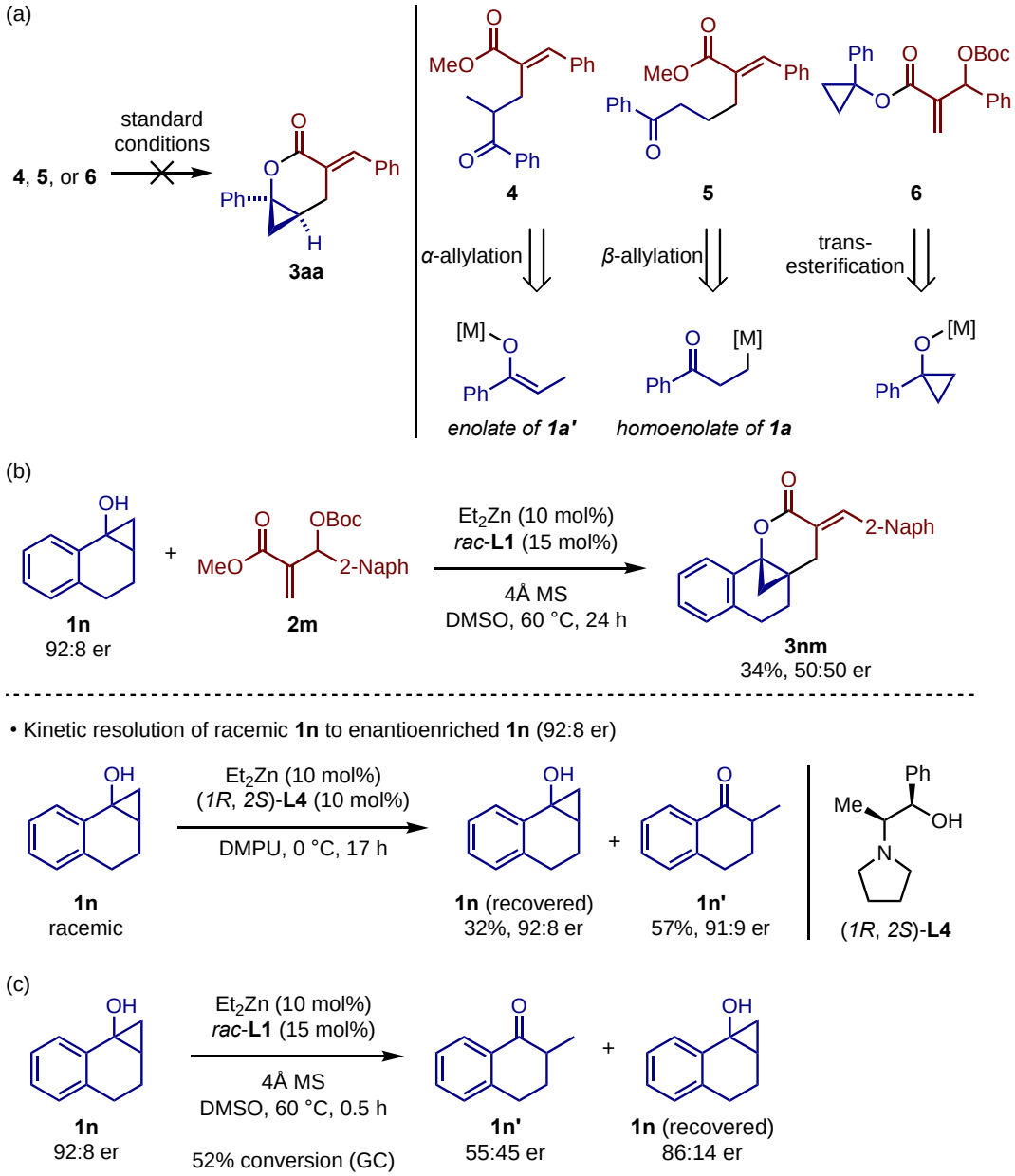

Next, an enantioenriched sample (92:8 er) of the cyclopropanol **1n**, which was prepared by kinetic resolution using the Et_2Zn/**L4** catalyst (see Scheme 2.4 in Chapter 2), was used to probe the stereochemical integrity during the reaction. The reaction of enantioenriched **1n** with **2m** using racemic **L1** afforded a racemic mixture of **3nm** in 34% yield (Scheme 3.4b). This excludes the possibility of direct *β*-allylation of **1n** and indicates that the stereochemical information on **1n** is lost through ring-opening

formation of zinc homoenolate and its enolization (*vide infra*). Exposure of **1n** to the reaction conditions in the absence of MBH carbonate resulted in conversion (52% in 0.5 h) into its ketone isomer **1n'** as a near racemic mixture (55:45 er) as well as recovery of **1n** with a partially decreased enantiomeric ratio (84:16 er; Scheme 3.4c). While the former observation may be attributable not only to the enolization of homoenolate but also to that of the ketone **1n'** itself, the latter appears to reflect the reversibility of the ring-opening and the homoenolate enolization.

On the basis of the above experiments and previous studies on organozinc/*β*-amino alcohol systems including ours,[7, 10] a catalytic cycle in Scheme 3.5 is proposed. Et_2Zn and **L1** would afford ethylzinc aminoalkoxide **A**, which would exist in equilibrium with the alkoxide-bridged dimer $[\mathbf{A}]_2$. Homoenolate **D**, formed through cyclopropanol coordination to **A**, deprotonation, and ring-opening, would be deprotonated by another molecule of **A** to generate the "enolized homoenolate" **E**.[11] Interception of **E** with MBH carbonate **2** would afford *α*-allylated homoenolate **F** along with *tert*-butoxide species **J**, which would regenerate **A** by releasing *t*BuOH. Reconstruction of the cyclopropane ring from **F** would be followed by intramolecular transesterification of the cyclopropoxide **G** to afford **3** and methoxide species **H**, which would release MeOH and regenerate **A**. The role of 4 Å MS would be to absorb MeOH, which would otherwise kill the activity of the zinc catalyst by protonation.

Scheme 3.5. Possible Catalytic Cycle

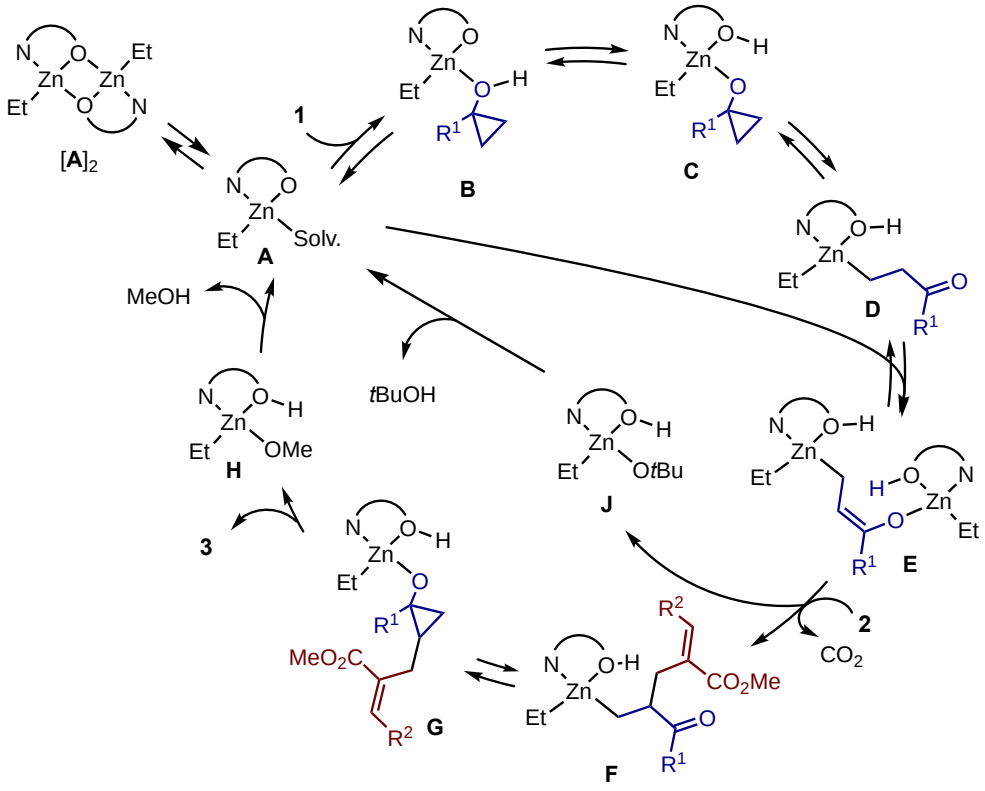

With the above proposed mechanism, I have found that the enolized homoenolate mode of reactivity also operates with benzylidenemalononitrile (**7a**) as an electrophile (Scheme 3.6). Thus, the reaction of **1a** and **7a** in the presence of Et_2Zn (10 mol%) and DABCO (20 mol%) afforded the annulated cyclopropane **8aa** in 61% yield with high diastereoselectivity. This was rather unexpected given the fact that the same catalytic system promoted the homoenolate addition when using α,β-unsaturated ketone as the Michael acceptor.[7] This transformation has also proved feasible with a bicyclic cyclopropanol (**8oa**) and an alkylmethylidenemalononitrile (**8ab**).

Scheme 3.6. Reaction with Alkylidenemalononitrile[a]

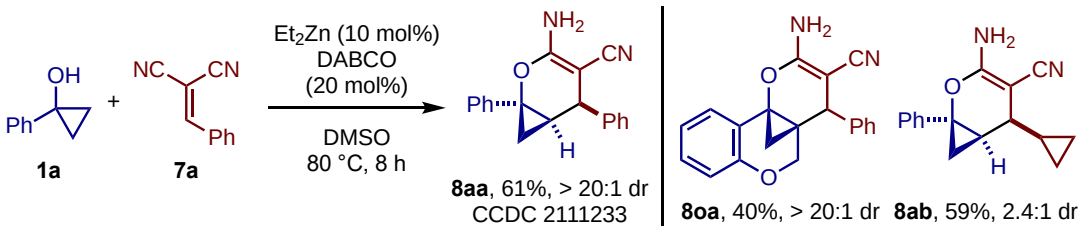

[a]The reaction was performed with 20 mol% Et_2Zn and 40 mol% DABCO for **8oa** and **8ab**.

Selected transformations of the product **3aa** are shown in Scheme 3.7a. 1,2-Disubstituted cyclopropanols **9**, **10**, and **11** were obtained by reduction with DIBAL, amidation with piperidine, and basic hydrolysis/methylation, respectively. The 1,4-reduction mediated by DIBAL and $Co(acac)_2$ afforded the lactone **12** as a mixture of separable diastereomers. The *β*-functionalized cyclopropanols obtained above could be further exploited as precursors to homoenolate or a *β*-keto radical. Thus, the nickel-catalyzed reaction of **11** with cinnamyl carbonate[9] afforded the *α*,*β*-difunctionalized ketone **13** in good yield (Scheme 3.7b). Meanwhile, treatment of **10** with catalytic $AgNO_3$ and ammonium persulfate[12] resulted in *β*-scission of the more substituted C−C bond and oxidative radical cyclization onto the nearby benzene ring to give the dihydronaphthalene derivative **14** (Scheme 3.7c).

Scheme 3.7. Product Transformation

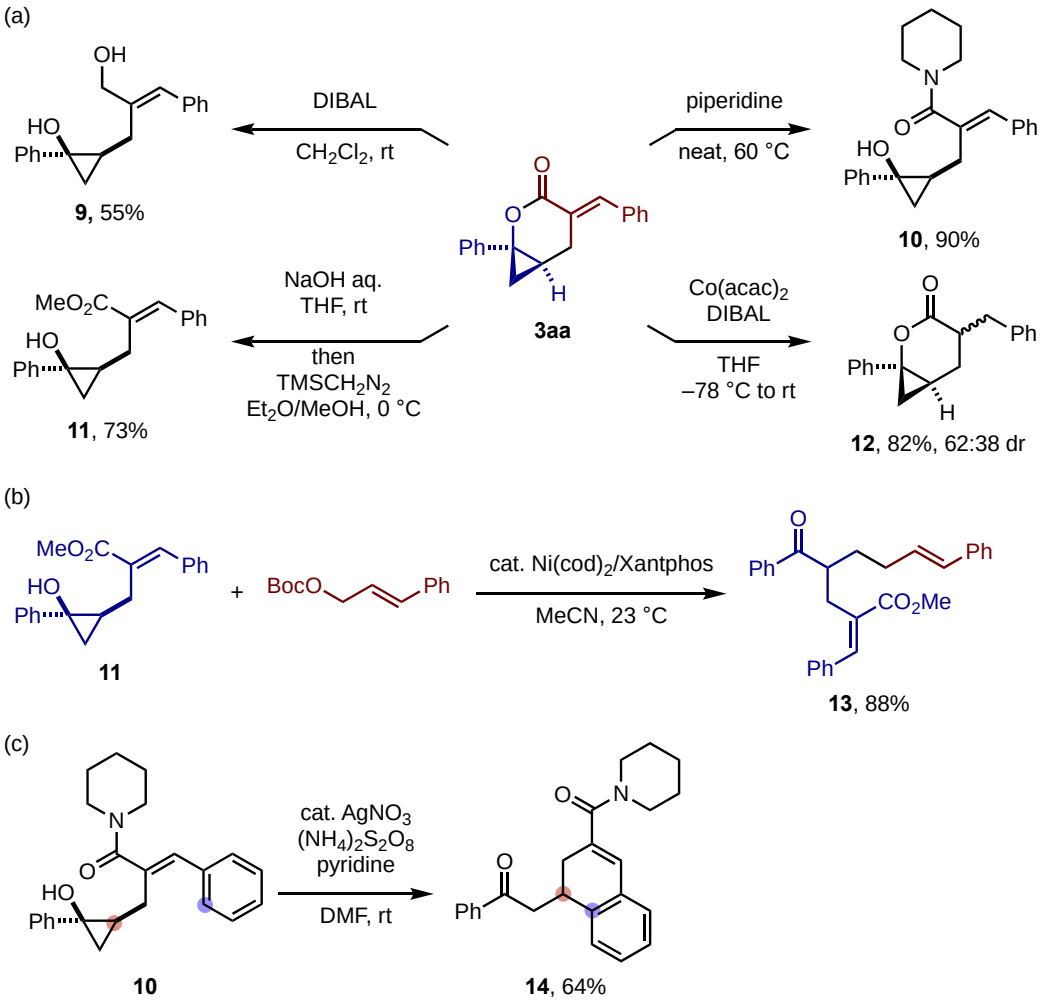

3.3 Conclusion

In summary, I have developed a zinc-catalyzed *β*-allylation of cyclopropanols with MBH carbonate without rupture of the cyclopropane ring. The reaction features a ring-opening/*α*-allylation/ring-closure mechanism involving enolized homoenolate as the key intermediate. The enolized homoenolate mode of reactivity also predominates in the reaction of alkylidenemalononitrile. The small but finite asymmetric induction observed in the present reaction holds promise for the development of an enantioselective variant. While interconversion between homoenolate and enolate is a common and important process in N-heterocyclic carbene catalysis,[13] the present reaction represents a rare example of a related process in the chemistry of metal homoenolates.

3.4 Experimental Section

Zinc-Catalyzed *β*-Allylation of Cyclopropanols with MBH Carbonates

General procedure: In an argon-filled glove box, an 8-mL vial equipped with a magnetic stir bar was charged sequentially with MBH carbonate **2** (0.30 mmol), molecular sieves 4 Å (1.2 g), **L1** (12.0 mg, 0.045 mmol), cyclopropanol **1** (0.45 mmol), DMSO (2.7 mL) and Et_2Zn (1 M in hexane, 30 μL, 0.030 mmol). The vial was closed and removed from the glove box, and the mixture was stirred at 60 °C for 24 h. Upon cooling to room temperature, the reaction mixture was diluted with CH_2Cl_2 (3 mL) and filtered through a pad of silica gel with additional CH_2Cl_2 (10 mL) as an eluent. The organic solution was concentrated under reduced pressure, and the residue was purified by automated flash chromatography on silica gel or preparative TLC on silica gel to afford the desired product.

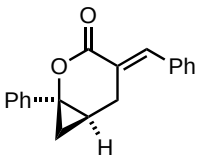

(*E*)-4-Benzylidene-1-phenyl-2-oxabicyclo[4.1.0]heptan-3-one (3aa): White solid (56.9 mg, 69%); R_f 0.28 (hexane/EtOAc = 9/1); m.p. 150-151 °C; **^{1}H NMR** (400 MHz, $CDCl_3$) δ 7.89 (br s, 1H), 7.45-7.34 (m, 9H), 7.30-7.27 (m, 1H), 3.26 (ddd, *J* = 16.2, 5.6, 2.3 Hz, 1H), 3.22-3.17 (m, 1H), 1.78-1.71 (m, 1H), 1.43 (dd, *J* = 9.6, 6.9 Hz, 1H), 1.30 (t, *J* = 7.0 Hz, 1H); **^{13}C{^{1}H} NMR** (100 MHz, $CDCl_3$) δ 166.0, 142.7, 139.7, 134.6,

129.9, 129.2, 128.5, 128.5, 127.3, 124.6, 123.7, 64.7, 24.9, 20.6, 19.6; **FTIR** (KBr, thin film, cm^{-1}): 3063, 3030, 2918, 2847, 1715, 1705, 1329, 1256, 1198, 1126, 1026, 955, 756, 696, 559, 515, 419; **HRMS** (ESI) Calcd for $C_{19}H_{17}O_2$ $[M + H]^+$ 277.1229, found 277.1225. $[\alpha]^{25}_D$ = 20.5 (*c* = 1.09 in $CHCl_3$, 59:41 er sample).

HPLC analysis: Daicel CHIRALPAK ID; hexane:*i*-PrOH = 90:10; detection wavelength = 254 nm; flow rate = 1.0 mL/min. t_R = 17.9 min (minor) and 19.3 min (major), 59:41 er.

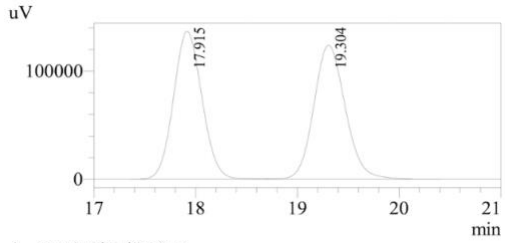

PeakTable

Detector A Ch1 254nm

Peak#	Ret. Time	Area %
1	17.915	49.922
2	19.304	50.078
Total		100.000

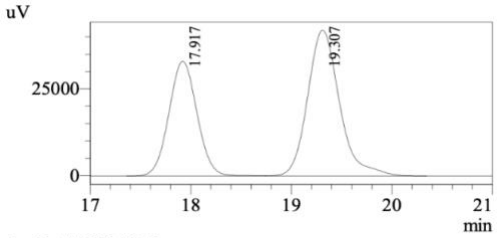

PeakTable

Detector A Ch1 254nm

Peak#	Ret. Time	Area %
1	17.917	40.965
2	19.307	59.035
Total		100.000

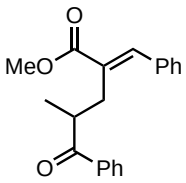

Methyl (*E*)-2-benzylidene-4-methyl-5-oxo-5-phenylpentanoate (4): This compound is the byproduct of the reaction between **1a** and **2a**. Pale yellow oil (11.2 mg, 12%); R_f 0.33 (hexane/EtOAc = 9/1); **^{1}H NMR** (400 MHz, $CDCl_3$) δ 7.96-7.94 (m, 2H), 7.79 (m, 1H), 7.56-7.52 (m, 1H), 7.46-7.31 (m, 7H), 3.87-3.82 (m, 4H), 2.98-2.93 (m, 1H), 2.81 (dd, *J* = 13.8, 9.2 Hz, 1H), 1.07 (d, *J* = 6.9 Hz, 3H); **^{13}C{^{1}H} NMR** (100 MHz, $CDCl_3$) δ 203.6, 168.6, 141.5, 136.3, 135.5, 132.9, 130.8, 129.0, 128.6 (overlap), 128.4, 128.4, 52.0, 39.6, 30.8, 16.2; **FTIR** (KBr, thin film, cm^{-1}): 3059, 3024, 2972, 2949, 2934, 1713, 1682, 1597, 1447, 1435, 1260, 1234, 1202, 1126, 972, 760, 702, 501; **HRMS** (ESI) Calcd for $C_{20}H_{21}O_3$ $[M + H]^+$ 309.1491, found 309.1483.

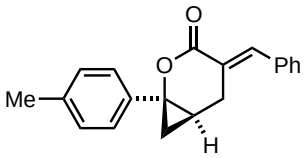

(*E*)-4-Benzylidene-1-(*p*-tolyl)-2-oxabicyclo[4.1.0]heptan-3-one (3ba): Pale yellow solid (49.8 mg, 57%); R_f 0.37 (hexane/EtOAc = 9/1); m.p. 113-114 °C; **^{1}H NMR** (500 MHz, $CDCl_3$) δ 7.87 (br s, 1H), 7.44-7.36 (m, 5H), 7.25-7.24 (m, 2H), 7.17-7.16 (m, 2H), 3.23 (ddd, *J* = 16.2, 5.6, 2.2 Hz, 1H), 3.20-3.16 (m, 1H), 2.34 (s, 3H), 1.72-1.67 (m, 1H), 1.38 (dd, *J* = 9.6, 6.9 Hz, 1H), 1.24 (t, *J* = 7.0 Hz, 1H); **^{13}C{^{1}H} NMR** (126 MHz, $CDCl_3$) δ 166.0, 142.4, 137.1, 136.7, 134.6, 129.9, 129.1, 128.5, 124.7, 123.7, 64.7, 24.8, 21.0, 20.2, 19.2; **FTIR** (KBr, $CHCl_3$, cm^{-1}): 3059, 3013 1707, 1622, 1518, 1491, 1447, 1325, 1292, 1258, 1221, 1198, 1188, 1124, 1022, 1007, 957, 812, 696, 667, 559, 513; **HRMS** (ESI) Calcd for $C_{20}H_{19}O_2$ $[M + H]^+$ 291.1385, found 291.1384.

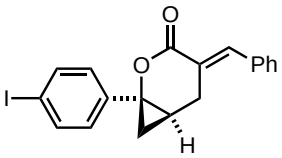

(*E*)-4-Benzylidene-1-(4-iodophenyl)-2-oxabicyclo[4.1.0]heptan-3-one (3ca): Pale yellow oil (77.2 mg, 64%); R_f 0.27 (hexane/EtOAc = 9/1); **^{1}H NMR** (500 MHz, $CDCl_3$) δ 7.88 (br s, 1H), 7.67-7.66 (m, 2H), 7.44-7.35 (m, 5H), 7.08-7.07 (m, 2H), 3.27-3.17 (m, 2H), 1.73-1.68 (m, 1H), 1.38 (dd, *J* = 9.6, 7.1 Hz, 1H), 1.29 (t, *J* = 7.1 Hz, 1H); **^{13}C{^{1}H} NMR** (126 MHz, $CDCl_3$) δ 165.6, 142.9, 139.6, 137.4, 134.3, 129.9, 129.2, 128.5, 126.3, 123.2, 92.5, 64.1, 24.7, 20.7, 19.7; **FTIR** (KBr, thin film, cm^{-1}): 3055, 3024, 2972, 2918, 2849, 1715, 1622, 1489, 1323, 1252, 1196, 1121, 1001, 818, 766, 694, 557, 517; **HRMS** (ESI) Calcd for $C_{19}H_{16}O_2I$ $[M + H]^+$ 403.0195, found 403.0193.

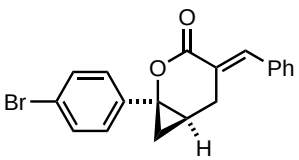

(*E*)-4-Benzylidene-1-(4-bromophenyl)-2-oxabicyclo[4.1.0]heptan-3-one (3da): Pale yellow oil (75.4 mg, 71%); R_f 0.28 (hexane/EtOAc = 9/1); **^{1}H NMR** (400 MHz, $CDCl_3$) δ 7.88 (br s, 1H), 7.48-7.35 (m, 7H), 7.22-7.20 (m, 2H), 3.28-3.17 (m, 2H), 1.74-1.68 (m, 1H), 1.38 (dd, *J* = 9.5, 7.1 Hz, 1H), 1.29 (t, *J* = 7.1 Hz, 1H); **^{13}C{^{1}H} NMR** (100 MHz, $CDCl_3$) δ 165.6, 142.9, 138.9, 134.4, 131.5, 129.9, 129.2, 128.5,

126.2, 123.2, 121.1, 64.2, 24.7, 20.6, 19.6; **FTIR** (KBr, thin film, cm^{-1}): 3057, 3026, 2953, 2926, 2851, 1715, 1622, 1491, 1447,1396, 1325, 1281,1254, 1213, 1196, 1126, 1074, 1007, 908, 826, 768, 733, 696, 557, 519; **HRMS** (ESI) Calcd for $C_{19}H_{16}O_2Br$ $[M + H]^+$ 355.0334, found 355.0332.

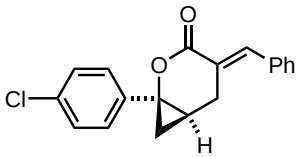

(*E*)-4-Benzylidene-1-(4-chlorophenyl)-2-oxabicyclo[4.1.0]heptan-3-one (3ea): Pale yellow solid (70.3 mg, 75%); R_f 0.33 (hexane/EtOAc = 9/1); m.p. 117-118 °C; **^{1}H NMR** (400 MHz, $CDCl_3$) δ 7.88 (br s, 1H), 7.45-7.35 (m, 5H), 7.33-7.25 (m, 4H), 3.28-3.17 (m, 2H), 1.74-1.68 (m, 1H), 1.38 (dd, *J* = 9.6, 7.0 Hz, 1H), 1.28 (t, *J* = 7.1 Hz, 1H); **^{13}C{^{1}H} NMR** (100 MHz, $CDCl_3$) δ 165.6, 142.9, 138.3, 134.4, 133.0, 129.9, 129.2, 128.5, 128.5, 125.9, 123.2, 64.1, 24.6, 20.5, 19.5; **FTIR** (KBr, thin film, cm^{-1}): 3055, 2994, 2901, 2845, 1715, 1622, 1493, 1447, 1398, 1323, 1254, 1194, 1182, 1121, 1094, 1009, 955, 936, 827, 766, 723, 696, 557, 519; **HRMS** (ESI) Calcd for $C_{19}H_{16}O_2Cl$ $[M + H]^+$ 311.0839 found 311.0838.

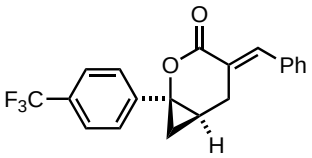

(*E*)-4-Benzylidene-1-(4-(trifluoromethyl)phenyl)-2-oxabicyclo[4.1.0]heptan-3-one (3fa): Pale yellow solid (67.2 mg, 65%); R_f 0.25 (hexane/EtOAc = 9/1); m.p. 108-109 °C; **^{1}H NMR** (400 MHz, $CDCl_3$) δ 7.91 (br s, 1H), 7.62-7.60 (m, 2H), 7.45-7.36 (m, 7H), 3.32-3.20 (m, 2H), 1.83-1.76 (m, 1H), 1.48 (dd, *J* = 9.6, 7.1 Hz, 1H), 1.39 (t, *J* = 7.2 Hz, 1H); **^{13}C{^{1}H} NMR** (100 MHz, $CDCl_3$) δ 165.5, 144.0, 143.2, 134.4, 129.9, 129.3, 129.3 (q, $^2J_{C\text{-}F}$ = 32.6 Hz), 128.6, 125.4 (q, $^3J_{C\text{-}F}$ = 3.7 Hz), 124.3, 124.0 (q, $^1J_{C\text{-}F}$ = 272.0 Hz, the second highest frequency peak in the quartet overlaps), 123.1, 64.0, 24.7, 21.5, 20.6; **^{19}F NMR** (376 MHz, $CDCl_3$): δ – 63.2; **FTIR** (KBr, $CHCl_3$, cm^{-1}): 3026, 3013, 1717, 1709, 1620, 1493, 1447, 1410, 1327, 1258, 1198, 1171, 1128, 1070, 1015, 957, 843, 696, 604, 519; **HRMS** (ESI) Calcd for $C_{20}H_{16}O_2F_3$ $[M + H]^+$ 345.1102, found 345.1102.

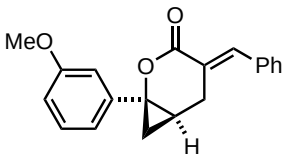

(*E*)-4-Benzylidene-1-(3-methoxyphenyl)-2-oxabicyclo[4.1.0]heptan-3-one (3ga): Pale yellow solid (68.3 mg, 74%); R_f 0.16 (hexane/EtOAc = 9/1); m.p. 136-137 °C; **^{1}H NMR** (500 MHz, $CDCl_3$) δ 7.88 (br s, 1H), 7.44-7.41 (m, 2H), 7.39-7.35 (m, 3H), 7.26 (t, *J* = 7.9 Hz, 1H), 6.95 (br t, *J* = 2.0 Hz, 1H), 6.87 (d, *J* = 7.7 Hz, 1H), 6.81 (dd, *J* = 8.2, 1.9 Hz, 1H), 3.81 (s, 3H), 3.24 (ddd, *J* = 16.2, 5.7, 2.2 Hz, 1H), 3.19-3.16 (m, 1H), 1.75-1.70 (m, 1H), 1.40 (dd, *J* = 9.6, 6.9 Hz, 1H), 1.37 (t, *J* = 7.0 Hz, 1H); **^{13}C{^{1}H} NMR** (126 MHz, $CDCl_3$) δ 165.8, 159.7, 142.5, 141.4, 134.5, 129.8, 129.5, 129.1, 128.5, 123.6, 116.5, 112.7, 110.5, 64.5, 55.2, 24.7, 20.7, 19.7; **FTIR** (KBr, thin film, cm^{-1}): 3080, 3026, 3001, 2938, 2835, 1717, 1609, 1489, 1456, 1325, 1292, 1258, 1194, 1121, 1038, 772, 694, 517; **HRMS** (ESI) Calcd for $C_{20}H_{19}O_3$ $[M + H]^+$ 307.1334, found 307.1328.

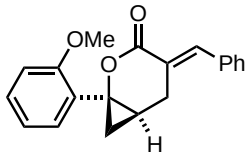

(*E*)-4-Benzylidene-1-(2-methoxyphenyl)-2-oxabicyclo[4.1.0]heptan-3-one (3ha): Pale yellow oil (41.4 mg, 45%); R_f 0.16 (hexane/EtOAc = 9/1); **^{1}H NMR** (500 MHz, $CDCl_3$) δ 7.84 (br s, 1H), 7.45-7.30 (m, 7H), 6.93-6.87 (m, 2H), 3.82 (s, 3H), 3.44 (ddd, *J* = 16.1, 6.7, 1.9 Hz, 1H), 3.05-3.01 (m, 1H), 1.53-1.48 (m, 1H), 1.42 (dd, *J* = 9.5, 6.6 Hz, 1H), 1.10 (t, *J* = 6.7 Hz, 1H); **^{13}C{^{1}H} NMR** (126 MHz, $CDCl_3$) δ 167.0, 158.9, 140.5, 135.1, 130.4, 130.2, 129.8, 128.8, 128.5, 126.4, 125.0, 120.1, 110.8, 63.0, 55.2, 25.6, 17.4, 16.7; **FTIR** (KBr, thin film, cm^{-1}): 3053, 3024, 3001, 2959, 2936, 2835, 1715, 1624, 1605, 1584, 1497, 1462, 1447, 1435, 1321, 1292, 1260, 1244, 1192, 1115, 1040, 1026, 1003, 955, 937, 897 837, 756, 696, 563, 546, 517; **HRMS** (ESI) Calcd for $C_{20}H_{19}O_3$ $[M + H]^+$ 307.1334, found 307.1339.

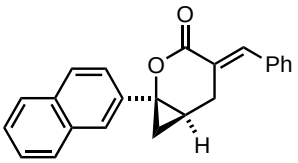

(*E*)-4-Benzylidene-1-(naphthalen-2-yl)-2-oxabicyclo[4.1.0]heptan-3-one (3ia): White solid (62.2 mg, 64%); R_f 0.25 (hexane/EtOAc = 9/1); m.p. 177-178 °C; **^{1}H NMR** (500 MHz, $CDCl_3$) δ 7.93 (br s, 2H), 7.83-7.81 (m, 3H), 7.50-7.43 (m, 4H), 7.40-7.38 (m, 3H), 7.32 (dd, *J* = 8.6, 1.8 Hz, 1H), 3.29 (ddd, *J* = 16.2, 5.5, 2.3 Hz, 1H), 3.27-3.23 (m, 1H), 1.88-1.83 (m, 1H), 1.54 (dd, *J* = 9.6, 7.0 Hz, 1H), 1.36 (t, *J* = 7.1 Hz, 1H); **^{13}C{^{1}H} NMR** (126 MHz, $CDCl_3$) δ 166.0, 142.8, 136.9, 134.6, 133.1, 132.5, 129.9, 129.2, 128.5, 128.4, 128.0, 127.5, 126.4, 126.0, 123.6 (overlap), 122.3, 64.9, 24.8, 20.5, 19.5; **FTIR** (KBr, $CHCl_3$, cm^{-1}): 3019, 2976, 1707, 1622, 1508, 1447, 1431, 1323, 1219, 1211, 1134, 1125, 932, 625, 529, 513, 478; **HRMS** (ESI) Calcd for $C_{23}H_{19}O_2$ $[M + H]^+$ 327.1385, found 327.1389.

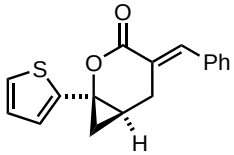

(*E*)-4-Benzylidene-1-(thiophen-2-yl)-2-oxabicyclo[4.1.0]heptan-3-one (3ja): Since the product was difficult to separate completely from the byproduct (α-allylated ketone analogous to **4**) by automated flash column, recrystallization was performed from THF/pentane to obtain the pure product as yellow crystals (26.8 mg, 32%, after recrystallization); R_f 0.53 (toluene); m.p. 151-152 °C; **^{1}H NMR** (500 MHz, $CDCl_3$) δ 7.89 (br s, 1H), 7.46-7.37 (m, 5H), 7.24 (dd, *J* = 5.1, 1.3 Hz, 1H), 7.00 (dd, *J* = 3.5, 1.3 Hz, 1H), 6.96 (dd, *J* = 5.0, 3.6 Hz, 1H), 3.26 (ddd, *J* = 16.2, 5.5, 2.4 Hz, 1H), 3.19 (ddd, *J* = 16.2, 2.8, 1.9 Hz, 1H), 1.82-1.77 (m, 1H), 1.42 (dd, *J* = 9.6, 6.9 Hz, 1H), 1.32 (t, *J* = 7.0 Hz, 1H); **^{13}C{^{1}H} NMR** (126 MHz, $CDCl_3$) δ 165.4, 143.6, 143.0, 134.5, 129.9, 129.2, 128.5, 126.8, 125.0, 123.9, 123.2, 62.1, 24.7, 21.1, 20.0; **FTIR** (KBr, $CHCl_3$, cm^{-1}): 3078, 3019, 1713, 1622, 1491, 1447, 1321, 1263, 1213, 1194, 1121, 1030, 993, 955, 930, 907, 853, 667, 515; **HRMS** (ESI) Calcd for $C_{17}H_{15}O_2S$ $[M + H]^+$ 283.0793, found 283.0790.

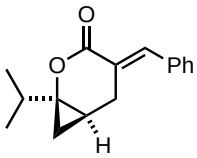

(*E*)-4-Benzylidene-1-isopropyl-2-oxabicyclo[4.1.0]heptan-3-one (3ka): White solid (35.0 mg, 48%); R_f 0.25 (hexane/cyclopentyl methyl ether = 9/1); m.p. 98-99 °C; **^{1}H NMR** (400 MHz, $CDCl_3$) δ 7.80 (br s, 1H), 7.44-7.34 (m, 5H), 3.14-3.03 (m, 2H), 1.53 (sept, *J* = 6.9 Hz, 1H), 1.27-1.21 (m, 1H), 1.12 (d, *J* = 6.8 Hz, 3H), 1.06 (d, *J* = 6.8 Hz, 3H), 0.82 (dd, *J* = 9.4, 6.7 Hz, 1H), 0.74 (t, *J* = 6.6 Hz, 1H); **^{13}C{^{1}H} NMR** (100 MHz, $CDCl_3$) δ 166.8, 141.8, 134.8, 129.9, 129.0, 128.4, 124.4, 68.9, 34.6, 24.8, 18.1, 17.9, 16.1, 14.6; **FTIR** (KBr, $CHCl_3$, cm^{-1}): 3019, 2968, 1701, 1622, 1319, 1271, 1159, 1126, 696; **HRMS** (ESI) Calcd for $C_{16}H_{19}O_2$ $[M + H]^+$ 243.1385, found 243.1384.

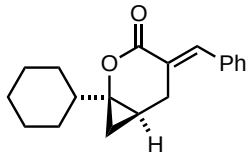

(*E*)-4-Benzylidene-1-cyclohexyl-2-oxabicyclo[4.1.0]heptan-3-one (3la): Colorless oil (28.2 mg, 33%); R_f 0.31 (hexane/cyclopentyl methyl ether = 9/1); **^{1}H NMR** (400 MHz, $CDCl_3$) δ 7.79 (br s, 1H), 7.44-7.33 (m, 5H), 3.11-3.02 (m, 2H), 1.83-1.67 (m, 5H), 1.48-1.39 (m, 1H), 1.33-1.15 (m, 6H), 0.83 (dd, *J* = 9.4, 6.7 Hz, 1H), 0.73 (t, *J* = 6.6 Hz, 1H); **^{13}C{^{1}H} NMR** (100 MHz, $CDCl_3$) δ 166.9, 141.7, 134.8, 129.9, 128.9, 128.4, 124.6, 68.4, 44.1, 28.5, 28.2, 26.2, 26.2, 26.1, 24.9, 15.8, 14.2; **FTIR** (KBr, thin film, cm^{-1}): 3057, 3011, 2922, 2849, 1707, 1633, 1447, 1327, 1269, 1254, 1215, 1200, 1121, 1028, 766, 696, 615, 513; **HRMS** (ESI) Calcd for $C_{19}H_{23}O_2$ $[M + H]^+$ 283.1698, found 283.1699.

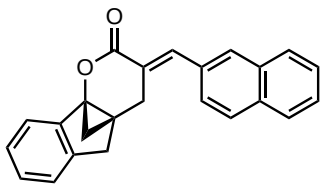

(*E*)-3-(Naphthalen-2-ylmethylene)-3,4-dihydro-2*H*,5*H*-4a,9b-methanoindeno[1,2-*b*]pyran-2-one (3mm): White solid (39.5 mg, 39%); R_f 0.28 (hexane/EtOAc = 9/1); m.p. 154-155 °C; **^{1}H NMR** (400 MHz, $CDCl_3$) δ 8.02 (br s, 1H), 7.90-7.83 (m, 4H), 7.62-7.60 (m, 1H), 7.56-7.53 (m, 2H), 7.47-7.45 (m, 1H), 7.29-7.20 (m, 2H), 7.17-7.15 (m, 1H), 3.65 (d, *J* = 15.9 Hz, 1H), 3.16 (d, *J* = 16.3 Hz, 2H), 3.02 (d, *J* = 16.9 Hz, 1H),

1.57 (d, *J* = 6.2 Hz, 1H), 0.85 (d, *J* = 6.2 Hz, 1H); **^{13}C{^{1}H} NMR** (100 MHz, $CDCl_3$) δ 165.7, 143.6, 142.1, 139.4, 133.2, 132.9, 132.0, 129.9, 128.4, 128.1, 127.7, 127.6, 127.2, 127.0, 126.8, 126.7, 125.3, 123.7, 122.9, 71.9, 40.6, 29.7, 26.7, 23.9; **FTIR** (KBr, $CHCl_3$, cm^{-1}): 2976, 1713, 1614, 1522, 1477, 1425, 1193, 1172, 1126, 1088, 1047, 1028, 928, 629, 478; **HRMS** (ESI) Calcd for $C_{24}H_{19}O_2$ $[M + H]^+$ 339.1385, found 339.1392.

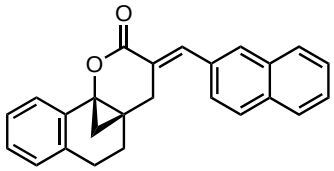

(*E*)-3-(Naphthalen-2-ylmethylene)-3,4,5,6-tetrahydro-2*H*-4a,10b-methanobenzo[*h*]chromen-2-one (3nm): White solid (47.1 mg, 45%); R_f 0.27 (hexane/EtOAc = 9/1); m.p. 171-172 °C; **^{1}H NMR** (400 MHz, $CDCl_3$) δ 8.00 (br s, 1H), 7.92-7.83 (m, 5H), 7.55-7.51 (m, 2H), 7.46 (dd, *J* = 8.5, 1.5 Hz, 1H), 7.30 (t, *J* = 7.6 Hz, 1H), 7.18 (td, *J* = 7.4, 1.2 Hz, 1H), 7.08 (d, *J* = 7.5 Hz, 1H), 3.45 (dd, *J* = 15.8, 0.9 Hz, 1H), 3.04 (dd, *J* = 15.7, 1.6 Hz, 1H), 2.72 (ddd, *J* = 16.4, 5.3, 1.5 Hz, 1H), 2.48-2.39 (m, 1H), 2.03 (ddd, *J* = 13.0, 6.2, 1.6 Hz, 1H), 1.71 (td, *J* = 13.4, 5.4 Hz, 1H), 1.38 (d, *J* = 7.0 Hz, 1H), 1.28 (d, *J* = 7.0 Hz, 1H); **^{13}C{^{1}H} NMR** (100 MHz, $CDCl_3$, +; positive DEPT 135 signal, –; negative DEPT 135 signal) δ 165.8, 142.4 (+), 135.5, 133.2, 132.9, 132.0, 131.9, 129.8 (+), 128.4 (+), 128.3 (+), 128.2 (+), 127.7 (+), 127.1 (+), 126.9 (+), 126.7 (+), 126.6 (+), 126.3 (+), 124.8, 124.5 (+), 62.7, 30.8 (–), 26.4 (–), 24.8 (–), 23.7, 19.7 (–); **FTIR** (KBr, $CHCl_3$, cm^{-1}): 2976, 2924, 2857, 1707, 1616, 1506, 1491, 1329, 1281, 1260, 1175, 1142, 1107, 1080, 1034, 961, 928, 860, 627, 478; **HRMS** (ESI) Calcd for $C_{25}H_{21}O_2$ $[M + H]^+$ 353.1542, found 353.1537.

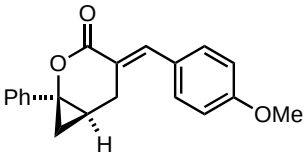

(*E*)-4-(4-Methoxybenzylidene)-1-phenyl-2-oxabicyclo[4.1.0]heptan-3-one (3ab): White solid (67.7 mg, 74%); R_f 0.19 (hexane/EtOAc = 9/1); m.p. 118-119 °C; **^{1}H NMR** (500 MHz, $CDCl_3$) δ 7.86 (br s, 1H), 7.36-7.35 (m, 6H), 7.28-7.25 (m, 1H), 6.96-6.94 (m, 2H), 3.84 (s, 3H), 3.28-3.20 (m, 2H), 1.76-1.71 (m, 1H), 1.41 (dd, *J* = 9.6, 6.9 Hz, 1H), 1.26 (t, *J* = 7.0 Hz, 1H); **^{13}C{^{1}H} NMR** (126 MHz, $CDCl_3$) δ 166.1, 160.4, 142.6, 139.8,, 131.9, 128.4, 127.2, 127.2, 124.5, 121.0, 114.0, 64.6, 55.3, 24.8, 20.4, 19.5;

FTIR (KBr, thin film, cm^{-1}): 3031, 2934, 2837, 1715, 1705, 1508, 1456, 1302, 1257, 1175, 1121, 1028, 831, 756, 698, 527; **HRMS** (ESI) Calcd for $C_{20}H_{19}O_3$ $[M + H]^+$ 307.1334, found 307.1326.

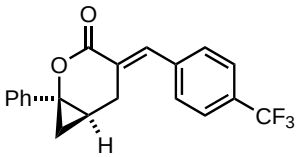

(*E*)-1-Phenyl-4-(4-(trifluoromethyl)benzylidene)-2-oxabicyclo[4.1.0]heptan-3-one (3ac): Since the product was difficult to separate completely from the byproduct (α-allylated ketone analogous to **4**) by automated flash column, recrystallization was conducted from THF/pentane to obtain the pure product. Colorless crystals (26.6 mg, 26%, after recrystallization); R_f 0.28 (hexane/EtOAc = 9/1); m.p. 108-109 °C; **^{1}H NMR** (400 MHz, $CDCl_3$) δ 7.87 (br s, 1H), 7.70-7.68 (m, 2H), 7.48-7.46 (m, 2H), 7.39-7.33 (m, 4H), 7.31-7.27 (m, 1H), 3.27 (ddd, J = 16.2, 5.8, 2.3 Hz, 1H), 3.17-3.11 (m, 1H), 1.79-1.73 (m, 1H), 1.46 (dd, J = 9.6, 7.0 Hz, 1H), 1.30 (t, J = 7.1 Hz, 1H); **^{13}C{^{1}H} NMR** (100 MHz, $CDCl_3$) δ 165.5, 140.6, 139.4, 138.0, 130.8 (q, $^2J_{C\text{-}F}$ = 32.7 Hz), 129.9, 128.5, 127.4, 126.1, 125.5 (q, $^3J_{C\text{-}F}$ = 3.7 Hz), 124.6, 123.8 (q, $^1J_{C\text{-}F}$ = 272.2 Hz), 64.8, 24.9, 20.7, 19.3; **^{19}F NMR** (376 MHz, $CDCl_3$): δ – 62.9; **FTIR** (KBr, $CHCl_3$, cm^{-1}): 3063, 3019, 1713, 1618, 1501, 1453, 1412, 1325, 1258, 1200, 1173, 1132, 1069, 1016, 957, 926, 853, 833, 696, 598, 517; **HRMS** (ESI) Calcd for $C_{20}H_{16}O_2F_3$ $[M + H]^+$ 345.1102, found 345.1109.

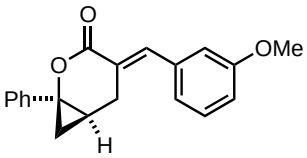

(*E*)-4-(3-Methoxybenzylidene)-1-phenyl-2-oxabicyclo[4.1.0]heptan-3-one (3ad): Pale yellow oil (59.1 mg, 64%); R_f 0.22 (hexane/EtOAc = 9/1); **^{1}H NMR** (400 MHz, $CDCl_3$) δ 7.84 (br s, 1H), 7.38-7.32 (m, 5H), 7.29-7.25 (m, 1H), 6.96-6.89 (m, 3H), 3.83 (s, 3H), 3.28-3.16 (m, 2H), 1.76-1.71 (m, 1H), 1.42 (dd, J = 9.6, 6.9 Hz, 1H), 1.28 (t, J = 7.1 Hz, 1H); **^{13}C{^{1}H} NMR** (100 MHz, $CDCl_3$) δ 165.9, 159.5, 142.4, 139.7, 135.8, 129.5, 128.4, 127.2, 124.5, 123.9, 122.2, 115.4, 114.6, 64.6, 55.3, 24.9, 20.5, 19.5; **FTIR** (KBr, thin film, cm^{-1}): 3061, 3030, 2957, 2938, 2835,1714, 1622, 1597, 1578, 1489, 1454, 1433, 1319, 1294, 1265, 1246, 1204, 1186, 1123, 1045, 955, 910,

785, 752, 733, 696, 592, 561; **HRMS** (ESI) Calcd for $C_{20}H_{19}O_3$ $[M + H]^+$ 307.1334, found 307.1331.

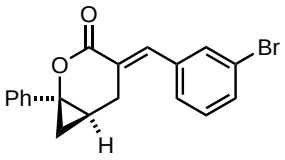

(*E*)-4-(3-Bromobenzylidene)-1-phenyl-2-oxabicyclo[4.1.0]heptan-3-one (3ae): Pale yellow solid (73.5 mg, 69%); R_f 0.28 (hexane/EtOAc = 9/1); m.p. 109-111 °C; **^{1}H NMR** (400 MHz, $CDCl_3$) δ 7.78 (br s, 1H), 7.52-7.49 (m, 2H), 7.38-7.32 (m, 4H), 7.30-7.25 (m, 3H), 3.24 (ddd, *J* = 16.2, 5.8, 2.3 Hz, 1H), 3.13 (ddd, *J* = 16.2, 2.8, 1.6 Hz, 1H), 1.78-1.71 (m, 1H), 1.44 (dd, *J* = 9.6, 7.0 Hz, 1H), 1.30 (t, *J* = 7.0 Hz, 1H); **^{13}C{^{1}H} NMR** (100 MHz, $CDCl_3$) δ 165.5, 140.6, 139.5, 136.5, 132.4, 132.0, 130.0, 128.5, 128.4, 127.3, 125.2, 124.5, 122.6, 64.7, 24.8, 20.6, 19.3; **FTIR** (KBr, thin film, cm^{-1}): 3055, 2986, 1715, 1634, 1624, 1558, 1474, 1327, 1265, 1196, 1126, 787, 739, 700, 592, 561; **HRMS** (ESI) Calcd for $C_{19}H_{16}O_2Br$ $[M + H]^+$ 355.0334, found 355.0336.

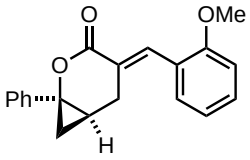

(*E*)-4-(2-Methoxybenzylidene)-1-phenyl-2-oxabicyclo[4.1.0]heptan-3-one (3af): Pale yellow oil (60.1 mg, 65%); R_f 0.25 (hexane/EtOAc = 9/1); **^{1}H NMR** (500 MHz, $CDCl_3$) δ 8.01 (br s, 1H), 7.38-7.35 (m, 5H), 7.28-7.25 (m, 1H), 7.22-7.21 (m, 1H), 6.98 (t, *J* = 7.5 Hz, 1H), 6.93 (d, *J* = 8.3 Hz, 1H), 3.84 (s, 3H), 3.18 (ddd, *J* = 16.0, 5.7, 2.3 Hz, 1H), 3.09-3.05 (m, 1H), 1.74-1.69 (m, 1H), 1.39 (dd, *J* = 9.5, 6.9 Hz, 1H), 1.32 (t, *J* = 7.0 Hz, 1H); **^{13}C{^{1}H} NMR** (126 MHz, $CDCl_3$) δ 166.1, 158.0, 139.9, 138.7, 130.7, 130.3, 128.4, 127.1, 124.5, 123.5, 123.4, 112.0, 110.7, 64.6, 55.4, 25.0, 20.4, 19.8; **FTIR** (KBr, thin film, cm^{-1}): 3063, 2938, 2837, 1715, 1622, 1616, 1599, 1456, 1290, 1246, 1192, 1113, 1026, 955, 754, 698; **HRMS** (ESI) Calcd for $C_{20}H_{19}O_3$ $[M + H]^+$ 307.1334, found 307.1331.

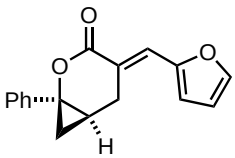

(*E*)-4-(Furan-2-ylmethylene)-1-phenyl-2-oxabicyclo[4.1.0]heptan-3-one (3ag): Pale brown solid (45.8 mg, 57%); R_f 0.22 (hexane/EtOAc = 9/1); m.p. 101-102 °C; **^{1}H NMR** (500 MHz, $CDCl_3$) δ 7.62 (br s, 1H), 7.58 (d, *J* = 1.2 Hz, 1H), 7.36-7.35 (m, 4H), 7.28-7.25 (m, 1H), 6.68 (d, *J* = 3.4 Hz, 1H), 6.53 (dd, *J* = 3.4, 1.8 Hz, 1H), 3.51-3.47 (m, 1H), 3.37 (ddd, *J* = 17.4, 6.0, 2.2 Hz, 1H), 1.80-1.75 (m, 1H), 1.46 (dd, *J* = 9.7, 6.9 Hz, 1H), 1.28 (t, *J* = 7.1 Hz, 1H); **^{13}C{^{1}H} NMR** (126 MHz, $CDCl_3$) δ 165.5, 151.3, 145.1, 139.8, 128.7, 128.4, 127.2, 124.5, 118.9, 117.1, 112.3, 65.1, 24.9, 20.8, 18.9; **FTIR** (KBr, thin film, cm^{-1}): 3142, 3123, 3063, 3030, 2920, 2849, 1715, 1703, 1616, 1325, 1256, 1196, 1123, 1020, 752, 698, 592, 567; **HRMS** (ESI) Calcd for $C_{17}H_{15}O_3$ $[M + H]^+$ 267.1021, found 267.1016.

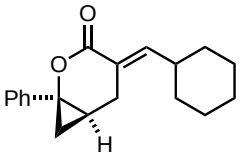

(*E*)-4-(Cyclohexylmethylene)-1-phenyl-2-oxabicyclo[4.1.0]heptan-3-one (3ah): Colorless oil (26.7 mg, 32%); R_f 0.23 (hexane/EtOAc = 19/1); **^{1}H NMR** (400 MHz, $CDCl_3$) δ 7.37-7.32 (m, 4H), 7.28-7.24 (m, 1H), 6.81 (br d, *J* = 9.8 Hz, 1H), 2.98-2.89 (m, 2H), 2.38-2.28 (m, 1H), 1.78-1.62 (m, 6H), 1.42-1.15 (m, 7H); **^{13}C{^{1}H} NMR** (100 MHz, $CDCl_3$) δ 165.9, 151.4, 139.9, 128.4, 127.2, 124.6, 121.4, 64.6, 37.3, 31.8, 31.6, 25.7, 25.4, 25.4, 23.5, 20.1, 19.7; **FTIR** (KBr, $CHCl_3$, cm^{-1}): 2930, 2853, 1713, 1639, 1503, 1450, 1323, 1300, 1256, 1198, 1161, 1101, 1028, 955, 932, 696, 667, 563; **HRMS** (ESI) Calcd for $C_{19}H_{23}O_2$ $[M + H]^+$ 283.1698, found 283.1690.

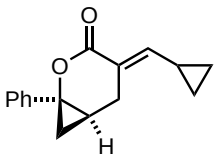

(*E*)-4-(Cyclopropylmethylene)-1-phenyl-2-oxabicyclo[4.1.0]heptan-3-one (3ai): Colorless oil (41.1 mg, 57%); R_f 0.24 (hexane/EtOAc = 9/1); **^{1}H NMR** (400 MHz, $CDCl_3$) δ7.37-7.32 (m, 4H), 7.27-7.24 (m, 1H), 6.36 (br d, *J* = 10.9 Hz, 1H), 3.11-3.00 (m, 2H), 1.80-1.74 (m, 1H), 1.66-1.57 (m, 1H), 1.43 (dd, *J* = 9.6, 6.9 Hz, 1H), 1.31 (t,

J = 7.0 Hz, 1H), 1.06-0.98 (m, 2H), 0.74-0.66 (m, 2H); **^{13}C{^{1}H} NMR** (100 MHz, $CDCl_3$) δ 165.5, 151.9, 140.0, 128.4, 127.1, 124.4, 119.8, 64.7, 23.5, 20.3, 19.6, 11.6, 9.0, 8.9; **FTIR** (KBr, thin film, cm^{-1}): 3061, 3028, 3007, 2926, 2849, 1714, 1632, 1501, 1452, 1321, 1252, 1215, 1198, 1179, 1111, 1053, 1026, 963, 951, 756, 733, 698, 598, 565, 503; **HRMS** (ESI) Calcd for $C_{16}H_{17}O_2$ $[M + H]^+$ 241.1229, found 241.1219.

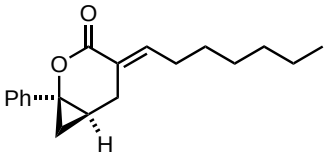

(*E*)-4-Heptylidene-1-phenyl-2-oxabicyclo[4.1.0]heptan-3-one (3aj): Colorless oil (31.7 mg, 37%); R_f 0.45 (hexane/EtOAc = 9/1); **^{1}H NMR** (500 MHz, $CDCl_3$) δ7.37-7.23 (m, 4H), 7.28-7.25 (m, 1H), 6.99 (br t, *J* = 7.6 Hz, 1H), 2.95-2.88 (m, 2H), 2.26-2.13 (m, 2H), 1.77-1.72 (m, 1H), 1.50-1.40 (m, 3H), 1.36-1.25 (m, 7H), 0.89 (t, *J* = 6.8 Hz, 3H); **^{13}C{^{1}H} NMR** (126 MHz, $CDCl_3$) δ 165.5, 146.9, 139.9, 128.4, 127.2, 124.5, 123.0, 64.6, 31.5, 29.0, 28.3, 28.2, 23.4, 22.5, 20.2, 19.6, 14.0; **FTIR** (KBr, thin film, cm^{-1}): 3063, 3030, 2955, 2928, 2857, 1722, 1645, 1456, 1319, 1254, 1200, 1184, 1151, 1107, 752, 731, 696, 600, 563; **HRMS** (ESI) Calcd for $C_{19}H_{25}O_2$ $[M + H]^+$ 285.1855, found 285.1853.

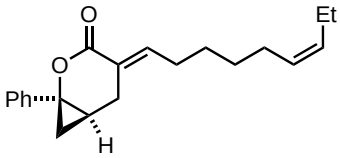

(*E*)-4-((*Z*)-Non-6-en-1-ylidene)-1-phenyl-2-oxabicyclo[4.1.0]heptan-3-one (3ak): Colorless oil (36.3 mg, 39%); R_f 0.30 (hexane/EtOAc = 9/1); **^{1}H NMR** (400 MHz, $CDCl_3$) δ7.37-7.32 (m, 4H), 7.28-7.24 (m, 1H), 5.41-5.26 (m, 2H), 6.97 (tt, *J* = 11.3, 1.7 Hz, 1H), 2.96-2.87 (m, 2H), 2.27-2.13 (m, 2H), 2.07-2.00 (m, 4H), 1.77-1.71 (m, 1H), 1.53-1.45 (m, 2H), 1.43-1.35 (m, 3H), 1.26 (t, *J* = 7.0 Hz, 1H), 0.96 (t, *J* = 7.5 Hz, 3H); **^{13}C{^{1}H} NMR** (100 MHz, $CDCl_3$) δ 165.5, 146.7, 139.9, 132.0, 128.5, 128.4, 127.2, 124.5, 123.1, 64.6, 29.3, 28.1, 27.9, 26.7, 23.4, 20.5, 20.2, 19.6, 14.3; **FTIR** (KBr, thin film, cm^{-1}): 3003, 2961, 2930, 2855, 1721, 1645, 1501, 1454, 1317, 1285, 1254, 1198, 1186, 1172, 1144, 111, 1078, 1028, 955, 924, 893, 754, 727, 696, 602, 563; **HRMS** (ESI) Calcd for $C_{21}H_{27}O_2$ $[M + H]^+$ 311.2011, found 311.2007.

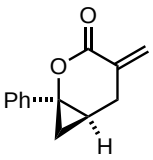

4-Methylene-1-phenyl-2-oxabicyclo[4.1.0]heptan-3-one (3al): Colorless oil (22.3 mg, 37%); R_f 0.28 (hexane/EtOAc = 9/1); **^{1}H NMR** (400 MHz, $CDCl_3$) δ7.38-7.26 (m, 5H), 6.29 (s, 1H), 5.58 (s, 1H), 3.14-3.09 (m, 1H), 2.88-2.83 (m, 1H), 1.79-1.73 (m, 1H), 1.44 (dd, *J* = 9.4, 7.1 Hz, 1H), 1.34 (t, *J* = 7.1 Hz, 1H); **^{13}C{^{1}H} NMR** (100 MHz, $CDCl_3$) δ 164.9, 139.6, 132.4, 128.5, 128.5, 127.3, 124.6, 65.4, 29.2, 20.3, 19.9; **FTIR** (KBr, thin film, cm^{-1}): 3030, 2926, 2851, 1732, 1638, 1605, 1452, 1402, 1301, 1269, 1157, 1026, 1011, 957, 804, 752, 698, 650, 590, 559; **HRMS** (ESI) Calcd for $C_{13}H_{13}O_2$ $[M + H]^+$ 201.0916, found 201.0911.

Zinc-Catalyzed β-Alkylation of Cyclopropanols with Alkylidenemalononitriles

General procedure: In an argon-filled glove box, an 8-mL vial equipped with a magnetic stir bar was charged sequentially with alkylidenemalononitrile **7** (0.30 mmol), cyclopropanol **1** (0.45 mmol), DABCO (0.06 mmol, 6.7 mg), DMSO (0.9 mL) and Et_2Zn (1 M in hexane, 30 μL, 0.03 mmol). The vial was closed and removed from the glove box, and the mixture was stirred at 80 °C for 8 h. Upon cooling to room temperature, the reaction mixture was diluted with Et_2O (3 mL) and sat. NH_4Cl aq. (2 mL) was added. The organic phase was separated and the aqueous phase was extracted with ethyl acetate/hexane (1:1) solution (3 mL) for 2 times. The combined organic solution was dried over Na_2SO_4, and concentrated under reduced pressure. The crude mixture was purified by automated flash chromatography on silica gel to afford the desired product.

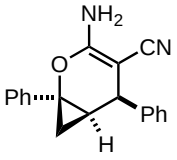

(1*R,5*R**,6*R**)-3-Amino-1,5-diphenyl-2-oxabicyclo[4.1.0]hept-3-ene-4-carbonitrile (8aa):** White solid (52.7 mg, 61%); R_f 0.17 (hexane/EtOAc = 4/1); m.p. 173-174 °C; **^{1}H NMR** (400 MHz, $CDCl_3$) δ 7.40-7.35 (m, 4H), 7.32-7.27 (m, 6H), 4.59 (s, 2H), 4.15 (d, *J* = 5.8 Hz, 1H), 1.88 (ddd, *J* = 10.1, 7.6, 5.8 Hz, 1H), 1.53 (t, *J* = 7.4 Hz, 1H), 1.24 (dd, *J* = 10.0, 7.0 Hz, 1H); **^{13}C{^{1}H} NMR** (100 MHz, $CDCl_3$, +; positive

DEPT 135 signal, –; negative DEPT 135 signal) δ 161.0, 141.4, 139.0, 128.8 (+), 128.6 (+), 127.7 (+), 127.6 (+), 127.3 (+), 124.8 (+), 120.8, 66.0, 56.2, 35.6 (+), 27.7 (+), 15.8 (–); **FTIR** (KBr, $CHCl_3$, cm^{-1}): 3445, 3406, 3321, 2188, 1637, 1632, 1623, 1589, 1580, 1455, 1404, 1380, 1351, 1306, 1122, 700; **HRMS** (ESI) Calcd for $C_{19}H_{17}N_2O$ $[M + H]^+$ 289.1341, found 289.1337.

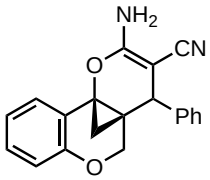

2-Amino-4-phenyl-4*H*,5*H*-4a,10b-methanopyrano[3,2-*c*]chromene-3-carbonitrile (8oa): The reaction was conducted with 20 mol% of Et_2Zn and 40 mol% of DABCO. After quenching the reaction, the product was extracted with $CHCl_3$. Due to its low solubility to organic solvents, it was difficult to conduct flash chromatography. Since the reaction was clean and **1o'** (ring-opening ketone of **1o**) was the only byproduct (the crude was analyzed by ^1H NMR, GC and TLC), the product could be isolated by the recrystallization of the crude from hot $CHCl_3$ to afford pale yellow crystals (38.2 mg, 40%); R_f 0.30 ($CHCl_3$); m.p. 237-238 °C; **^{1}H NMR** (400 MHz, $CDCl_3$) δ 7.58 (dd, *J* = 7.6, 1.6 Hz, 1H), 7.42-7.39 (m, 2H), 7.36-7.31 (m, 1H), 7.29-7.26 (m, 2H), 7.19 (td, *J* = 7.7, 1.7 Hz, 1H), 7.07 (td, *J* = 7.6, 1.6 Hz, 1H), 6.88 (dd, *J* = 8.1, 1.0 Hz, 1H), 4.65 (s, 2H), 4.13 (d, *J* = 10.4 Hz, 1H), 3.83 (s, 1H), 3.78 (d, *J* = 10.5 Hz, 1H), 1.78 (d, *J* = 6.7 Hz, 1H), 1.42 (d, *J* = 6.7 Hz, 1H); **^{13}C{^{1}H} NMR** (100 MHz, $CDCl_3$) δ 160.3, 150.9, 139.2, 128.9, 127.9, 127.9, 127.8, 124.4, 123.7, 122.1, 120.2, 117.5, 65.2, 60.6, 57.4, 37.3, 33.5, 17.5; **FTIR** (KBr, $CHCl_3$, cm^{-1}): 3471, 3409, 3352, 2193, 2178, 1634, 1589, 1493, 1454, 1407, 1276, 1265, 1164, 1140, 1111, 1033, 704; **HRMS** (ESI) Calcd for $C_{20}H_{17}N_2O_2$ $[M + H]^+$ 317.1290, found 317.1281.

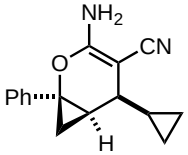

(1*R,5*S**,6*R**)-3-Amino-5-cyclopropyl-1-phenyl-2-oxabicyclo[4.1.0]hept-3-ene-4-carbonitrile (8ab):** The reaction was conducted with 20 mol% of Et_2Zn and 40 mol% of DABCO. Pale yellow solid (44.8 mg, 59%, 2.4:1 dr, After recrystallization from THF/pentane, 7.3:1 dr sample was obtained.); R_f 0.29 (hexane/EtOAc = 4/1); m.p. 150-

152 °C (sample of 7.3:1 dr); **^{1}H NMR** (400 MHz, $CDCl_3$) major diastereomer: δ 7.39-7.29 (m, 5H), 4.38 (s, 2H), 1.97 (dd, *J* = 9.6, 5.3 Hz, 1H), 1.75 (ddd, *J* = 10.0, 7.5, 5.3 Hz, 1H), 1.52 (t, *J* = 7.2 Hz, 1H), 1.34 (dd, *J* = 9.9, 7.0 Hz, 1H), 0.91-0.74 (m, 2H), 0.54-0.47 (m, 2H), 0.25-0.19 (m, 1H); **^{13}C{^{1}H} NMR** (100 MHz, $CDCl_3$) major diastereomer: δ 159.7, 139.3, 128.5, 127.6, 125.0, 121.2, 65.3, 57.6, 35.2, 25.2, 15.4, 14.8, 5.2, 2.0; **FTIR** (KBr, $CHCl_3$, cm^{-1}): 3016, 2188, 1637, 1632, 1587, 1580, 1404, 1380, 1126, 1030, 1022; **HRMS** (ESI) Calcd for $C_{16}H_{17}N_2O$ $[M + H]^+$ 253.1341, found 253.1338.

Product Transformations

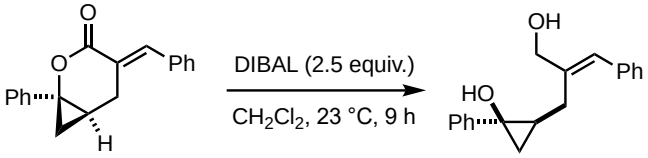

3aa **9**, 55%

(*E*)-2-(2-(Hydroxymethyl)-3-phenylallyl)-1-phenylcyclopropan-1-ol (9): A 5 mL J-Young Schlenk tube equipped with a magnetic stir bar was charged with **3aa** (55.3 mg, 0.20 mmol) and CH_2Cl_2 (2.5 mL). Diisobutylaluminium hydride (DIBAL, 1 M/THF, 0.5 mL, 0.50 mmol) was added at 0 °C. The mixture was stirred at room temperature for 9 h until complete consumption of the starting material (monitored by TLC). The reaction mixture was quenched with 1.5 N HCl aq. and filtered through a pad of Celite. The mixture was extracted with CH_2Cl_2, and the combined organic layer was washed with sat. $NaHCO_3$ aq., dried over Na_2SO_4, and concentrated under reduced pressure. The crude product was purified by flash column chromatography to afford the title compound as a colorless oil (31.1 mg, 55%); R_f 0.16 (hexane/EtOAc = 4/1); **^{1}H NMR** (400 MHz, $CDCl_3$) δ 7.37-7.17 (m, 10H), 6.45 (s, 1H), 4.80 (br s, 1H), 4.29 (d, *J* = 12.3 Hz, 1H), 4.09 (d, *J* = 12.4 Hz, 1H), 3.17 (dd, *J* = 15.2, 2.5 Hz, 1H), 2.94 (s, 1H), 2.34 (dd, *J* = 14.9, 11.1 Hz, 1H), 1.31 (dd, *J* = 9.6, 5.6 Hz, 1H), 1.14-1.07 (m, 1H), 0.96 (dd, *J* = 7.0, 5.7 Hz, 1H); **^{13}C{^{1}H} NMR** (100 MHz, $CDCl_3$) δ 145.3, 140.8, 137.0, 128.9, 128.3, 128.2, 127.9, 126.8, 126.0, 123.5, 68.6, 58.7, 29.0, 26.6, 22.7; **FTIR** (KBr, thin film, cm^{-1}): 3308, 3059, 2920, 2851, 1495, 1447, 1288, 1240, 11145, 1076, 1013, 918, 849, 750; **HRMS** (ESI) Calcd for $C_{19}H_{21}O_2$ $[M + H]^+$ 281.1542, found 281.1539.

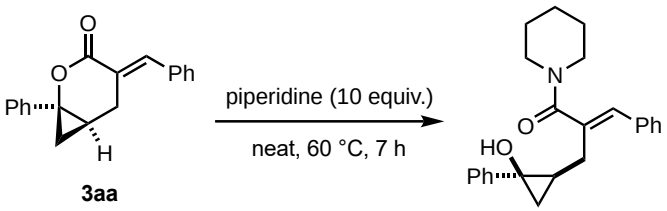

3aa **10**, 90%

(*E*)-2-((2-Hydroxy-2-phenylcyclopropyl)methyl)-3-phenyl-1-(piperidin-1-yl)prop-2-en-1-one (10): A 4 mL vial equipped with a magnetic stir bar was charged with **3aa** (55.3 mg, 0.20 mmol) and piperidine (170 mg, 2.0 mmol). The mixture was stirred at 60 °C for 7 h until complete consumption of the starting material (monitored by TLC). The crude mixture was directly purified by column chromatography to afford the title compound as a colorless oil (65.0 mg, 90%); R_f 0.30 (hexane/EtOAc = 4/1); **^{1}H NMR** (400 MHz, $CDCl_3$) δ 7.40-7.36 (m, 2H), 7.31-7.20 (m, 7H), 7.14-7.11 (m, 1H), 6.40 (d, *J* = 1.5 Hz, 1H), 5.11 (s, 1H), 3.46-3.18 (m, 5H), 2.70 (ddd, *J* = 15.9, 11.2, 2.4 Hz, 1H), 1.41-0.99 (m, 8H), 0.76 (br s, 1H); **^{13}C{^{1}H} NMR** (100 MHz, $CDCl_3$) δ 172.6, 146.1, 136.4, 135.6, 128.9, 128.9, 128.3, 127.9, 127.6, 125.4, 123.1, 57.0, 48.5, 42.7, 28.3, 27.8, 26.2, 24.6, 24.2, 23.8; **FTIR** (KBr, thin film, cm^{-1}): 3316, 3057, 3024, 2999, 2936, 2857, 1589, 1495, 1470, 1447, 1292, 1260, 1238, 1126, 1003, 853, 752, 698, 652, 552; **HRMS** (ESI) Calcd for $C_{24}H_{28}NO_2$ $[M + H]^+$ 362.2120, found 362.2124.

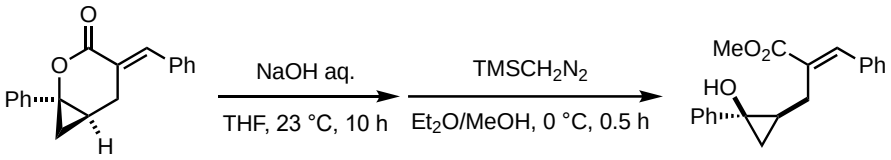

3aa **11**, 73%

Methyl (*E*)-2-((2-hydroxy-2-phenylcyclopropyl)methyl)-3-phenylacrylate (11): A 4 mL vial equipped with a magnetic stir bar was charged with **3aa** (55.3 mg, 0.20 mmol) and THF (0.3 mL), followed by the addition of NaOH aq. (20w/v%, 100 μL). The mixture was stirred at room temperature for 10 h until complete consumption of the starting material (monitored by TLC). The reaction mixture was quenched with sat. NH_4Cl aq. and diluted with CH_2Cl_2. The aqueous layer was neutralized with 1.5 N HCl aq. and extracted with CH_2Cl_2. The combined organic layer was dried over Na_2SO_4 and concentrated under reduced pressure. The crude product was dissolved in Et_2O/MeOH (4:1, 0.3 mL), and (trimethylsilyl)diazomethane (2 M/hexane, 0.2 mL, 0.4 mmol) was added at 0 °C. After stirring for 30 min, the reaction mixture was concentrated, and the crude product was purified by flash column chromatography to afford the title

compound as a white solid (44.8 mg, 73%); R_f 0.31 (hexane/THF = 8/1); m.p. 95-96 °C; **^{1}H NMR** (400 MHz, $CDCl_3$) δ 7.72 (br s, 1H), 7.44-7.43 (m, 4H), 7.41-7.36 (m, 1H), 7.32-7.27 (m, 4H), 7.19-7.15 (m, 1H), 5.37 (s, 1H, *Disappeared after D_2O exchange), 3.79 (s, 3H), 3.12 (dd, *J* = 14.6, 1.9 Hz, 1H), 2.59 (dd, *J* = 14.5, 10.2 Hz, 1H), 1.32 (dd, *J* = 9.6, 5.5 Hz, 1H), 1.22-1.15 (m, 1H), 1.01 (dd, *J* = 6.8, 5.7 Hz, 1H); **^{13}C{^{1}H} NMR** (100 MHz, $CDCl_3$) δ 170.0, 145.8, 140.7, 135.2, 132.1, 129.3, 128.8, 128.6, 128.1, 125.8, 124.0, 58.3, 52.5, 28.9, 25.5, 22.3; **FTIR** (KBr, $CHCl_3$, cm^{-1}): 3397, 3061, 3026, 3011, 2953, 1688, 1603, 1495, 1447, 1437, 1371, 1292, 1265, 1227, 1206, 1132, 1086, 1003, 934, 899, 698, 529, 501; **HRMS** (ESI) Calcd for $C_{20}H_{21}O_3$ $[M + H]^+$ 309.1491, found 309.1490.

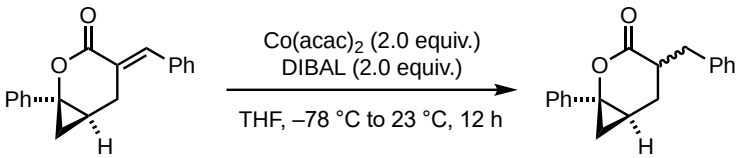

3aa **12**, 82%, 62:38 dr

4-Benzyl-1-phenyl-2-oxabicyclo[4.1.0]heptan-3-one (12): A 5 mL J-Young Schlenk tube equipped with a magnetic stir bar was charged with $Co(acac)_2$ (103 mg, 0.40 mmol) and THF (1.4 mL). The mixture was cooled to –78 °C and diisobutylaluminium hydride (DIBAL, 1 M/THF, 0.4 mL, 0.40 mmol) was added, followed by stirring for 10 min. To the mixture was added a THF solution of **3aa** (55.3 mg, 0.20 mmol, in 0.6 mL THF). The reaction mixture was stirred at 23 °C for 12 h, quenched with 1.5 N HCl aq. and filtered through a pad of Celite. The filtrate was extracted with Et_2O and the combined organic layer was washed with sat. $NaHCO_3$ aq., dried over Na_2SO_4, and concentrated under reduced pressure. The crude product was purified by flash column chromatography to afford both diastereomers of the title compound separately as colorless oils (major: 28.3 mg, minor: 17.4 mg, 82% overall yield, 62:38 dr); R_f 0.31 (minor diastereomer), 0.22 (major diastereomer) (hexane/EtOAc = 9/1); **^{1}H NMR** (400 MHz, $CDCl_3$) major diastereomer: δ 7.40-7.36 (m, 2H), 7.31-7.21 (m, 6H), 7.14-7.11 (m, 2H), 3.16 (dd, *J* = 12.2, 3.7 Hz, 1H), 2.74-2.63 (m, 2H), 2.27-2.20 (m, 1H), 1.90 (dt, *J* = 14.4, 4.9 Hz, 1H), 1.71-1.63 (m, 1H), 1.49 (dd, *J* = 9.6, 6.8 Hz, 1H), 1.41 (t, *J* = 7.0 Hz, 1H); minor diastereomer: δ 7.35-7.16 (m, 10H), 3.43 (dd, *J* = 13.8, 3.8 Hz, 1H), 2.66-2.58 (m, 1H), 2.55-2.48 (m, 2H), 1.69-1.61 (m, 1H), 1.50 (dd, *J* = 9.5, 6.4 Hz, 1H), 1.45-1.37 (m, 1H), 1.31 (t, *J* = 6.7 Hz, 1H); **^{13}C{^{1}H} NMR** (100 MHz, $CDCl_3$) major diastereomer: δ 172.7, 140.4, 138.0, 128.9. 128.6, 128.6, 127.0, 126.7, 123.5,

65.3, 40.1, 36.0, 26.1, 23.1, 19.1; minor diastereomer: δ 174.8, 140.6, 138.9, 129.1. 128.6, 128.5, 127.0, 126.5, 123.6, 64.0, 41.2, 35.9, 29.7, 25.8, 22.0; **FTIR** (KBr, thin film, cm^{-1}) major diastereomer: 3086, 3061, 3026, 2930, 2866, 1748, 1732, 1603, 1497, 1454, 1362, 1339, 1254, 1236, 1192, 1163, 1103, 1076, 1030, 1020, 957, 908, 891, 752, 698, 598, 573, 550, 507, 484; major diastereomer: 3061, 3026, 2955, 2926, 2870, 1753, 1746, 1603, 1497, 1452, 1385, 1360, 1290, 1184, 1159, 1099, 1078, 1030, 912, 752, 731, 698, 665, 548, 511; **HRMS** (ESI) Calcd for $C_{19}H_{19}O_2$ $[M + H]^+$ 279.1385, found 279.1387 (major diastereomer), 279.1384 (minor diastereomer).

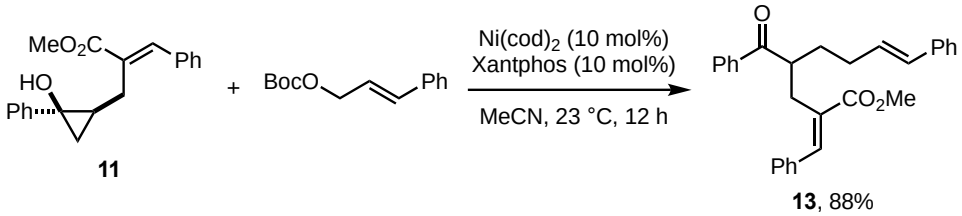

Methyl (*E*)-4-benzoyl-2-((*E*)-benzylidene)-8-phenyloct-7-enoate (13): The reaction was performed using **11** (61.7 mg, 0.2 mmol) and *tert*-butyl cinnamyl carbonate (56.2 mg, 0.24 mmol) according to the literature procedure.[9] Colorless oil (75.1 mg, 88%); R_f 0.34 (hexane/EtOAc = 9/1); **^{1}H NMR** (400 MHz, $CDCl_3$) δ 7.91-7.90 (m, 2H) 7.74 (br s, 1H), 7.55-7.51 (m, 1H), 7.24-7.31 (m, 7H), 7.27-7.15 (m, 5H), 6.15 (d, *J* = 15.9 Hz, 1H), 6.02 (dd, *J* = 15.7, 6.6 Hz, 1H), 3.93-3.85 (m, 1H), 3.75 (s, 3H), 2.93 (dd, *J* = 13.8, 6.1 Hz, 1H), 2.84 (dd, *J* = 13.8, 8.3 Hz, 1H), 2.14-1.90 (m, 3H), 1.65-1.56 (m, 1H); **^{13}C{^{1}H} NMR** (100 MHz, $CDCl_3$, +; positive DEPT 135 signal, –; negative DEPT 135 signal) δ 203.6, 168.4, 141.5 (+), 137.5, 137.2, 135.3, 133.0 (+), 130.6, 130.6 (+), 129.8 (+), 129.0 (+), 128.6 (+), 128.5 (+), 128.5 (+), 128.4 (+), 128.4 (+), 126.9 (+), 125.9 (+), 52.0 (+), 44.1 (+), 30.9 (–), 30.8 (–), 30.2 (–); **FTIR** (KBr, thin film, cm^{-1}): 3080, 3057, 3024, 2997, 2947, 2926, 2849, 1709, 1680, 1630, 1597, 1578, 1493, 1447, 1435, 1375, 1315, 1250, 1204, 1161, 1099, 968, 910, 835, 785, 733, 692, 648, 527, 503; **HRMS** (ESI) Calcd for $C_{29}H_{29}O_3$ $[M + H]^+$ 425.2117, found 425.2118.

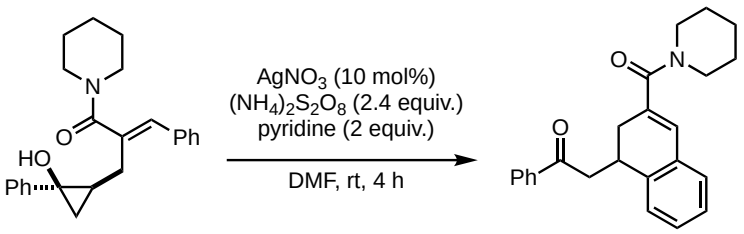

10 **14**, 64%

1-Phenyl-2-(3-(piperidine-1-carbonyl)-1,2-dihydronaphthalen-1-yl)ethan-1-one (14): In an argon-filled glove box, a 4 mL vial equipped with a magnetic stir bar was charged with **10** (108 mg, 0.30 mmol), $AgNO_3$ (5.1 mg, 0.03 mmol), $(NH_4)_2S_2O_8$ (164 mg, 0.72 mmol), pyridine (48 μL, 0.6 mmol) and DMF (2.6 mL). The vial was closed and removed from the glove box, and the mixture was stirred at room temperature (23 °C) for 4 h. The reaction mixture was filtered through a celite pad using Et_2O as an eluent. Sat. $NaHCO_3$ aq. was added to the filtrate, and the mixture were extracted with Et_2O. The combined organic layer was dried over Na_2SO_4 and concentrated under reduced pressure. The crude product was purified by flash column chromatography to afford the title compound as a colorless oil (68.7 mg, 64%); R_f 0.26 (hexane/EtOAc = 2/1); **^{1}H NMR** (500 MHz, $CDCl_3$) δ 7.90-7.89 (m, 2H), 7.53-7.50 (m, 1H), 7.42-7.39 (m, 2H), 7.21-7.16 (m, 3H), 7.12-7.11 (m, 1H), 6.58 (d, *J* = 2.3 Hz, 1H), 3.76-3.71 (m, 1H), 3.61-3.54 (m, 4H), 3.37 (dd, *J* = 17.1, 8.1 Hz, 1H), 3.15 (dd, *J* = 17.1, 5.6 Hz, 1H), 2.77 (ddd, *J* = 17.0, 6.7, 2.4 Hz, 1H), 2.52 (dd, *J* = 17.1, 3.8 Hz, 1H), 1.68-1.55 (m, 6H); **^{13}C{^{1}H} NMR** (126 MHz, $CDCl_3$) δ 198.7, 170.3, 138.1, 137.0, 133.0, 132.8, 132.0, 128.4, 128.3, 128.0, 127.3, 127.3, 127.0, 126.6, 47.8 (broad), 42.8, 42.8 (overlap, broad), 32.8, 30.3, 26.0 (broad), 24.6; **FTIR** (KBr, thin film, cm^{-1}): 3061, 2992, 2936, 2855, 1736, 1682, 1614, 1597, 1468, 1447, 1435, 1371, 1356, 1283, 1271, 1256, 1240, 1221, 1152, 1117, 1045, 1026, 1001, 953, 903, 853, 758, 692, 610, 554, 515; **HRMS** (ESI) Calcd for $C_{24}H_{26}NO_2$ $[M + H]^+$ 360.1964, found 360.1969.

3.5 References

1. (a) Dian, L.; Marek, I., Asymmetric Preparation of Polysubstituted Cyclopropanes Based on Direct Functionalization of Achiral Three-Membered Carbocycles. *Chem. Rev.* **2018,** *118*, 8415-8434; (b) Fumagalli, G.; Stanton, S.; Bower, J. F., Recent Methodologies That Exploit C–C Single-Bond Cleavage of Strained Ring Systems by Transition Metal Complexes. *Chem. Rev.* **2017,** *117*, 9404-9432; (c) Schneider, T. F.; Kaschel, J.; Werz, D. B., A New Golden Age for Donor–Acceptor

Cyclopropanes. *Angew. Chem. Int. Ed.* **2014,** *53*, 5504-5523; (d) Rubin, M.; Rubina, M.; Gevorgyan, V., Transition Metal Chemistry of Cyclopropenes and Cyclopropanes. *Chem. Rev.* **2007,** *107*, 3117-3179.

2. (a) McDonald, T. R.; Mills, L. R.; West, M. S.; Rousseaux, S. A. L., Selective Carbon–Carbon Bond Cleavage of Cyclopropanols. *Chem. Rev.* **2021,** *121*, 3-79; (b) Cai, X.; Liang, W.; Dai, M., Total Syntheses via Cyclopropanols. *Tetrahedron* **2019,** *75*, 193-208; (c) Nikolaev, A.; Orellana, A., Transition-Metal-Catalyzed C–C and C–X Bond-Forming Reactions Using Cyclopropanols. *Synthesis* **2016,** *48*, 1741-1768; (d) Sekiguchi, Y.; Yoshikai, N., Metal-Catalyzed Transformations of Cyclopropanols via Homoenolates. *Bull. Chem. Soc. Jpn.* **2021,** *94*, 265-280; (e) Murakami, M.; Ishida, N., *β*-Scission of Alkoxy Radicals in Synthetic Transformations. *Chem. Lett.* **2017**, *46*, 1692-1700.

3. Sustac Roman, D.; Charette, A. B., Catalytic C–H Bond Functionalization of Cyclopropane Derivatives. In *C-H Bond Activation and Catalytic Functionalization II*, Dixneuf, P. H.; Doucet, H., Eds. Springer International Publishing: Cham, 2016; pp 91-113.

4. (a) Yang, J.; Shen, Y.; Lim, Y. J.; Yoshikai, N., Divergent Ring-Opening Coupling between Cyclopropanols and Alkynes under Cobalt Catalysis. *Chem. Sci.* **2018,** *9*, 6928-6934; (b) Yang, J.; Sun, Q.; Yoshikai, N., Cobalt-Catalyzed Regio-and Diastereoselective Formal [3+2] Cycloaddition between Cyclopropanols and Allenes. *ACS Catal.* **2019,** *9*, 1973-1978; (c) Davis, D. C.; Walker, K. L.; Hu, C.; Zare, R. N.; Waymouth, R. M.; Dai, M., Catalytic Carbonylative Spirolactonization of Hydroxycyclopropanols. *J. Am. Chem. Soc.* **2016,** *138*, 10693-10699; (d) Cai, X.; Liang, W.; Liu, M.; Li, X.; Dai, M., Catalytic Hydroxycyclopropanol Ring-Opening Carbonylative Lactonization to Fused Bicyclic Lactones. *J. Am. Chem. Soc.* **2020,** *142*, 13677-13682.

5. (a) Mills, L. R.; Barrera Arbelaez, L. M.; Rousseaux, S. A. L., Electrophilic Zinc Homoenolates: Synthesis of Cyclopropylamines from Cyclopropanols and Amines. *J. Am. Chem. Soc.* **2017,** *139*, 11357-11360; (b) West, M. S.; Mills, L. R.; McDonald, T. R.; Lee, J. B.; Ensan, D.; Rousseaux, S. A. L., Synthesis of *trans*-2-Substituted Cyclopropylamines from *α*-Chloroaldehydes. *Org. Lett.* **2019,** *21*, 8409-8413.

6. (a) Das, P. P.; Belmore, K.; Cha, J. K., S_N2' Alkylation of Cyclopropanols via Homoenolates. *Angew. Chem. Int. Ed.* **2012,** *51*, 9517-9520; (b) Nakamura, E.; Aoki,

S.; Sekiya, K.; Oshino, H.; Kuwajima, I., Carbon-Carbon Bond-Forming Reactions of Zinc Homoenolate of Esters. A Novel Three-Carbon Nucleophile with General Synthetic Utility. *J. Am. Chem. Soc.* **1987,** *109*, 8056-8066.

7. Sekiguchi, Y.; Yoshikai, N., Enantioselective Conjugate Addition of Catalytically Generated Zinc Homoenolate. *J. Am. Chem. Soc.* **2021,** *143*, 4775-4781.

8. For the construction of related benzo-fused skeletons, see: (a) Xia, W.; Shao, Y.; Gui, W.; Yang, C., Efficient Synthesis of Polysubstituted Isochromanones via a Novel Photochemical Rearrangement. *Chem. Commun.* **2011,** *47*, 11098-11100; (b) Zhang, C.; Chen, S.; Ye, C.-X.; Harms, K.; Zhang, L.; Houk, K. N.; Meggers, E., Asymmetric Photocatalysis by Intramolecular Hydrogen-Atom Transfer in Photoexcited Catalyst–Substrate Complex. *Angew. Chem. Int. Ed.* **2019,** *58*, 14462-14466.

9. Sekiguchi, Y.; Lee, Y. Y.; Yoshikai, N., Nickel-Catalyzed Ring-Opening Allylation of Cyclopropanols via Homoenolate. *Org. Lett.* **2021,** *23*, 5993-5997.

10. (a) Noyori, R.; Suga, S.; Oka, H.; Kitamura, M., Self and Nonself Recognition of Chiral Catalysts: The Origin of Nonlinear Effects in the Amino-Alcohol Catalyzed Asymmetric Addition of Diorganozincs to Aldehydes. *Chem. Rec.* **2001,** *1*, 85-100; (b) Frantz, D. E.; Fässler, R.; Tomooka, C. S.; Carreira, E. M., The Discovery of Novel Reactivity in the Development of C−C Bond-Forming Reactions: In Situ Generation of Zinc Acetylides with Zn(II)/R_3N. *Acc. Chem. Res.* **2000,** *33*, 373-381.

11. Huang, W.; Meng, F., Cobalt-Catalyzed Diastereo- and Enantioselective Hydroalkylation of Cyclopropenes with Cobalt Homoenolates. *Angew. Chem. Int. Ed.* **2021,** *60*, 2694-2698.

12. Chiba, S.; Cao, Z.; El Bialy, S. A. A.; Narasaka, K., Generation of β-Keto Radicals from Cyclopropanols Catalyzed by $AgNO_3$. *Chem. Lett.* **2006,** *35*, 18-19.

13. (a) Enders, D.; Niemeier, O.; Henseler, A., Organocatalysis by N-Heterocyclic Carbenes. *Chem. Rev.* **2007,** *107*, 5606-5655; (b) Marion, N.; Díez-González, S.; Nolan, S. P., N-Heterocyclic Carbenes as Organocatalysts. *Angew. Chem. Int. Ed.* **2007,** *46*, 2988-3000; (c) Hopkinson, M. N.; Richter, C.; Schedler, M.; Glorius, F., An Overview of N-Heterocyclic Carbenes. *Nature* **2014,** *510*, 485-496; (d) Mahatthananchai, J.; Bode, J. W., On the Mechanism of N-Heterocyclic Carbene-Catalyzed Reactions Involving Acyl Azoliums. *Acc. Chem. Res.* **2014,** *47*, 696-707; (e) Flanigan, D. M.; Romanov-Michailidis, F.; White, N. A.; Rovis, T., Organocatalytic Reactions Enabled by N-Heterocyclic Carbenes. *Chem. Rev.* **2015,** *115*, 9307-9387.

Chapter 4. Zinc-Mediated Hydroxyallylation of Aldehydes with Cyclopropanols: Direct Access to Vicinal *anti-sec,tert*-Diols via Enolized Homoenolates

4.1 Introduction

The vicinal diol motif is prevalent in biologically active natural products and synthetically valuable intermediates, and hence its stereoselective construction represents a long-standing challenge in synthetic organic chemistry. Among various approaches to vicinal diols, the addition of γ-alkoxyallylmetal species to aldehydes (α-alkoxyallylation) has received considerable attention, as it provides diols bearing a synthetically versatile olefin moiety.[1] Despite the advancement in this reaction manifold with new approaches to the requisite alkoxyallylmetal nucleophile,[2] α-alkoxylallylation reactions that allow for the diastereocontrolled synthesis of sterically congested *sec,tert*-diols remain scarce.[3] Marek reported carbocupration/zinc homologation of ynol ethers as a means to generate (*E*)-configured α-alkoxyallylzinc species, which reacted with aldehydes to afford *syn-sec,tert*-diols (Scheme 4.1a).[4] Recently, Krische disclosed an enantioselective ruthenium-catalyzed reductive coupling of alkoxyallene and aldehyde via (*Z*)-configured α-alkoxyallyl ruthenium species, which also afforded *syn*-diol products (Scheme 4.1b).[5] Besides the need for deprotection of the alkoxy groups, a common limitation in these reactions concerns the scope of the α-substituent in the allylmetal species. Marek's approach was limited by the scope of organocopper reagents capable of carbocupration (R = primary alkyl), whereas Krische's method employed only α-methylalkoxyallene due to the difficulty in the preparation of differently substituted alkoxyallenes. In terms of direct access to unprotected diols, another notable approach is the pinacol-type reductive coupling between the enone and aldehyde. Following the seminal report by Takai on a Cr(II)/Me_3SiCl-mediated process,[6] Loh described a Zn/$InCl_3$-mediated coupling in an aqueous medium, which was supposed to involve α-oxyallylzinc species bearing indium(III) (Scheme 4.1c).[7] However, the reaction displayed varying and often moderate diastereoselectivity and was also limited in the scope of the α-substituent (Et or Me). Matsubara reported that zincate-mediated rearrangement of 2-(1-hydroxyalkyl)-1-alkylcyclopropanols[8] also afforded vicinal diols with low to moderate *anti*-selectivity via retro-aldol reaction (Scheme 4.1d, also see Scheme 1.26 in Chapter

1).[9] It should be noted that they proposed the intermediate as an α-alkoxide allylic anion rather than an enolized homoenolate, which is proposed in this work (*vide infra*).

This chapter describes a direct and diastereoselective synthesis of *anti-sec,tert*-diols via zinc-mediated hydroxylallylation of aldehydes with cyclopropanols (Scheme 4.1e). The reaction is promoted using the combination of Et_2Zn and 2,2′-bipyridine (bpy) at room temperature, engaging a variety of 1-substituted cyclopropanols and bicyclic cyclopropanols as well as aromatic and aliphatic aldehydes. The present reaction features the action of an enolized homoenolate,[10] formed through Et_2Zn-mediated ring opening of cyclopropanol and subsequent enolization of the resulting homoenolate, as a stereodefined α-oxyallylzinc nucleophile toward the aldehyde. The complementary *anti*-selectivity of the reaction, which is also complementary to the typical diastereoselectivity in diol synthesis via vinylation of α-hydroxyketones,[11] is ascribed to a bicyclic chairlike transition state of allylation, where the aldehyde substituent prefers to occupy the pseudoaxial position.

The present work was designed on the basis of previous studies, including those by myself, on the chemistry of zinc homoenolate. Since the seminal report of Cha and co-workers,[12] zinc homoenolate (**II**) generated by ring opening of zinc cyclopropoxide (**I**) has proved to serve as a β-carbonyl nucleophile in allylation,[12] acylation,[13] alkynylation,[14] and conjugate addition (Scheme 4.1e, mode 1; see Chapter 2).[15] Furthermore, I have found a zinc-catalyzed β-functionalization of cyclopropanols with Morita−Baylis−Hillman carbonates, which involves enolization of **II** into enolized homoenolate **III**, its reaction as an enolate toward the electrophile, and ring closure of the homoenolate to cyclopropoxide (mode 2; see Chapter 3).[10a] Following this finding, I became interested in the potential reactivity of **III** as an α-oxyallyl nucleophile (mode 3). Prompted by this conjecture and the aforementioned importance of vicinal diols, I decided to explore zinc-mediated reaction of cyclopropanols toward aldehydes.

Scheme 4.1. Aldehyde Allylation Approaches to Vicinal *sec,tert*-Diols

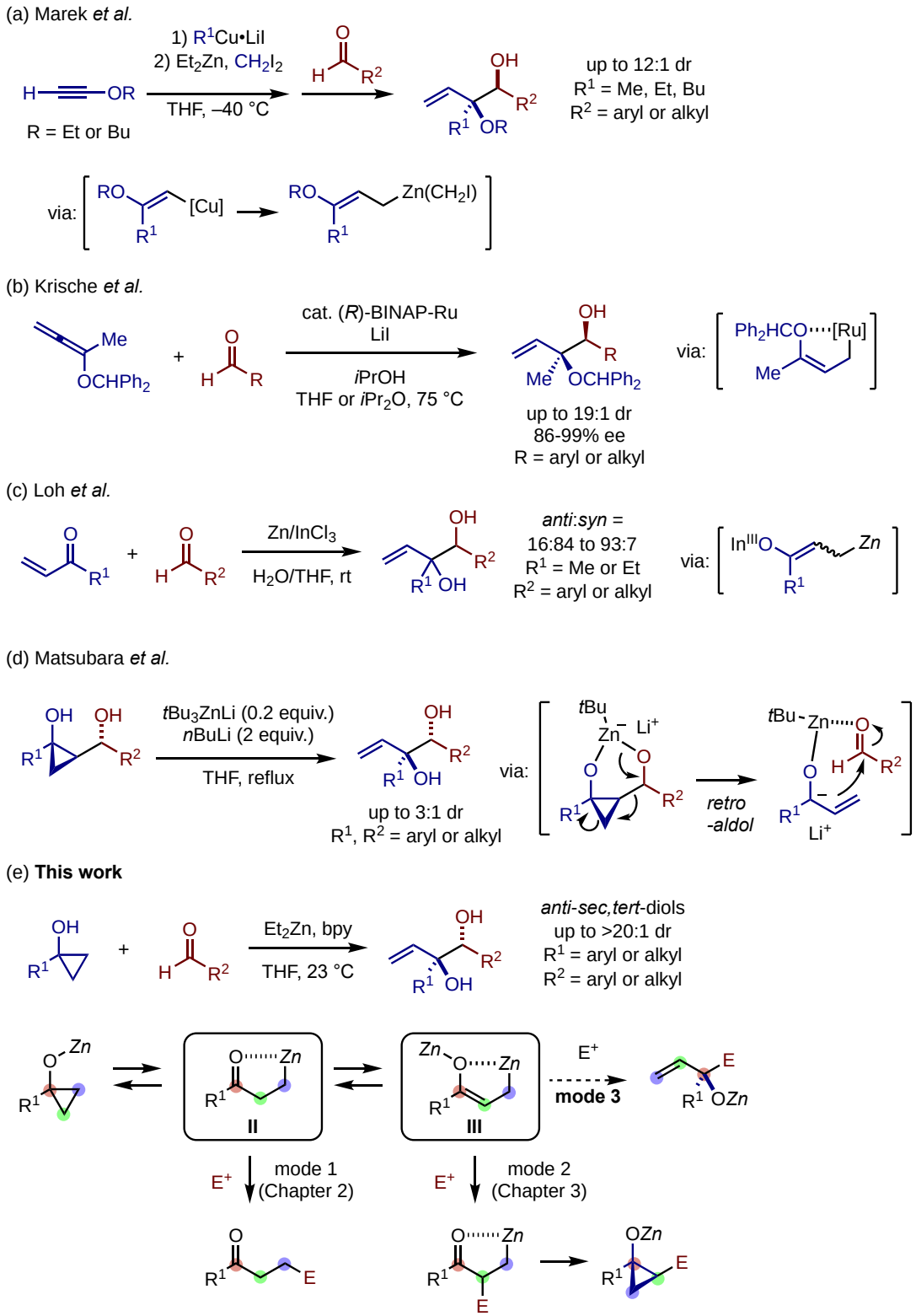

4.2 Results and Discussions

The reaction between 1-phenylcyclopropanol (**1a**) and benzaldehyde (**2a**) in the presence of Et_2Zn (2 equiv.) proceeded smoothly in DMSO at 80 °C in 1 h, affording

the *anti*-diol **3aa** in 73% yield with diastereoselectivity of 3:1 (Table 4.1, entry 1). Note that alternative coupling products arising from the mode 1 and mode 2 reactivities were not observed. The relative configuration of **3aa** was confirmed by comparison with the opposite diastereomer obtained by the addition of vinyl Grignard reagent to *α*-hydroxyketone.[11b] Unlike my previous studies on zinc homoenolate and enolized homoenolate reactions (Chapters 2 and 3),[10a, 15c] the reaction was also feasible in less coordinating THF, furnishing **3aa** with improved diastereoselectivity (entry 2), while noncoordinating toluene completely shut down the reaction (entry 3). Although the reaction in THF failed at 23 °C (entry 4), the addition of coordinating nitrogen additives (2 equiv.) was found to restore the reactivity, among which bpy gave the best results in terms of the yield and the diastereoselectivity (entries 5−8). The amount of bpy could be reduced to 1 equiv. without problem (entry 9), while further reduction led to a more sluggish reaction (entry 10). Lowering the amount of Et_2Zn resulted in a decrease in the diastereoselectivity (entry 11).

Table 4.1. Et_2Zn-Mediated Hydroxyallylation of Benzaldehyde (**2a**) with 1-Phenylcyclopropanol (**1a**)[a]

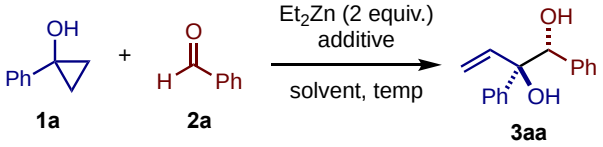

1a **2a** **3aa**

entry	additive (equiv)	solvent	temp (°C)	time (h)	yield (%)[b]	dr[c]
1	-	DMSO	80	1	73	3:1
2	-	THF	80	1	66	8:1
3	-	toluene	80	1	0	-
4	-	THF	23	12	0	-
5	bpy (2)	THF	23	12	73	11:1
6	byridine (2)	THF	23	12	17	7:1
7	TMEDA (2)	THF	23	12	64	7:1
8	DABCO (2)	THF	23	12	79	3:1
9	bpy (1)	THF	23	12	71	11:1
10	bpy (0.5)	THF	23	12	53	16:1
11[d]	bpy (1)	THF	23	12	64	4:1

[a]The reaction was performed using 0.05 mmol of **1a** and 0.075 mmol **2a** in solvent (0.33 M). [b]Determined by GC using mesitylene as an internal standard. [c]Determined by ^{1}H NMR of the crude mixture. [d]1 equiv. of Et_2Zn was used.

With the optimized conditions (Table 4.1, entry 9) in hand, the reaction of various cyclopropanols with **2a** was explored first (Scheme 4.2). A series of 1-

(hetero)arylcyclopropanols participated in the hydroxyallylation to afford the corresponding anti diols **3aa**–**3ha** in moderate to good yields. As a general trend, higher diastereoselectivities were observed with electron-rich aryl groups (>20:1, see **3ba** and **3ca**) than with electron deficient aryl groups (6:1, see **3da**–**3fa**). The model reaction could be performed on a 6 mmol scale, affording **3aa** in 64% yield with 12:1 dr. 1-Alkylcyclopropanols bearing a primary or secondary alkyl group also reacted with **2a** at an elevated temperature (80 °C) to afford the corresponding diols **3ia**–**3la** in moderate yields with good to high diastereoselectivities. Bicyclic cyclopropanols **1m** and **1n** also successfully participated in the reaction to afford the diols **3ma** and **3na**. The structure of the latter was confirmed by X-ray crystallographic analysis.

Scheme 4.2. Hydroxyallylation of Benzaldehyde (**2a**) with Various Cyclopropanols[a]

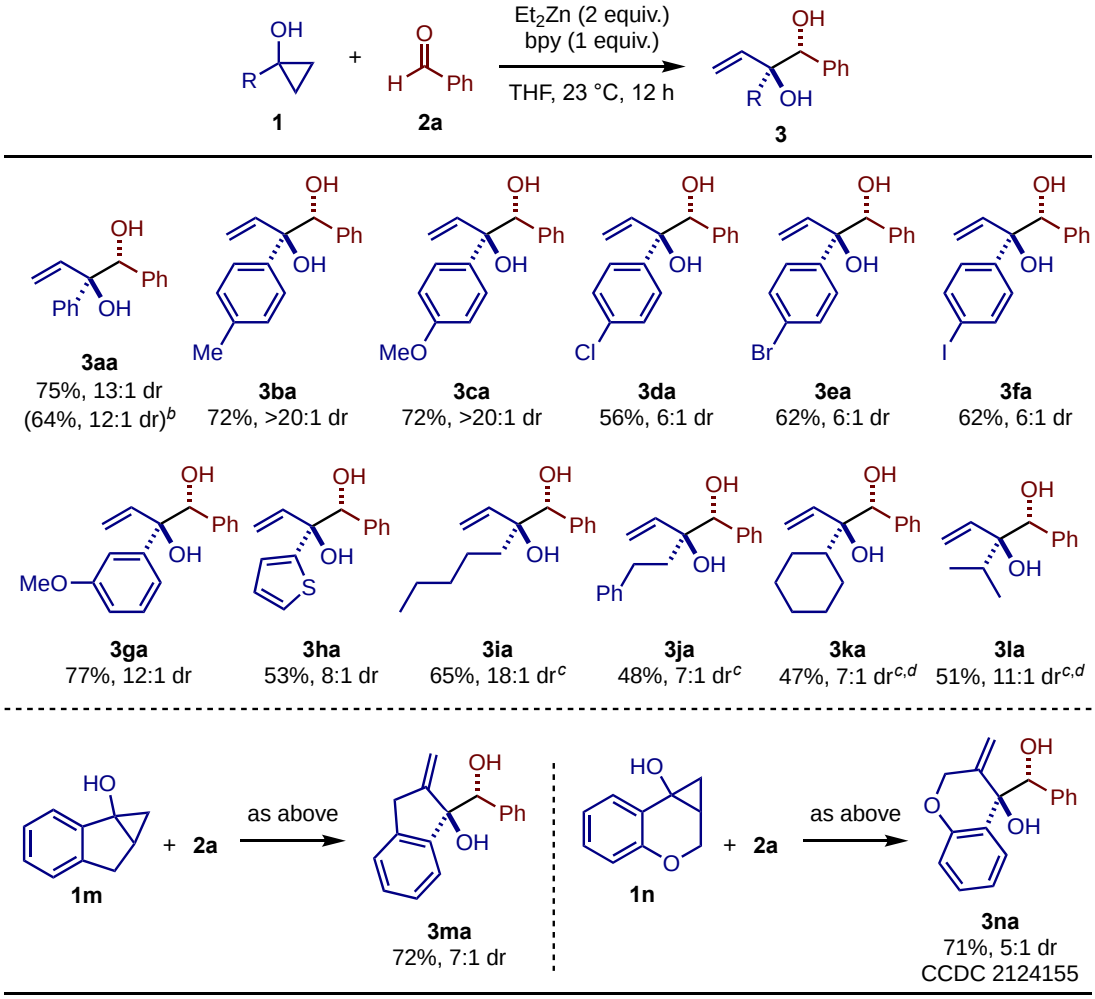

[a]The reaction was performed on a 0.3 mmol scale. [b]The yield of a 6 mmol scale reaction is shown in the parentheses. [c]The reaction was performed at 80 °C for 1 h. [d]The reaction was performed in DMSO in the absence of bpy.

I next explored the reaction of **1a** with various aldehydes (Scheme 4.3). A series of (hetero)aryl aldehydes proved to be good substrates, affording the corresponding products **3ab**−**3aj** in moderate to good yields with moderate to high diastereoselectivities. Electron-rich aldehydes reacted smoothly under the standard conditions with high diastereoselectivities (see **3ab**−**3ad**). On the other hand, the reactions of electron-deficient aldehydes had to be carried out at 0 °C to ensure good diastereoselectivity (see **3ae** and **3af**). The reaction of 3-methyl-2-butenal afforded the desired 1,2-addition product **3ak**. Primary alkyl aldehydes also participated in the reaction at 80 °C to give the diols **3al** and **3am** with good diastereoselectivity. Interestingly, the reactions of secondary alkyl aldehydes produced the desired vicinal diols **3an**−**3ap** as the major products with excellent diastereoselectivity, which were accompanied by 2-(1-hydroxyalkyl)-1-phenylcyclopropanols **4an**−**4ap**, as a result of *β*-functionalization of **1a** (i.e., mode 2 reactivity). Likewise, the reaction of nonracemic (−)-menthyl 3-carboxaldehyde afforded the adduct **3aq** as the dominant isomer in 50% yield,[16] while the corresponding cyclopropanol-type product was also obtained in 34% yield as a mixture of more than three isomers (data not shown). Pivalaldehyde afforded the cyclopropanol **4ar** as the exclusive product, the relative configuration of which was determined by X-ray crystallographic analysis.

Scheme 4.3. Hydroxyallylation of Various Aldehydes with 1-Phenylcyclopropanol (**1a**)[a]

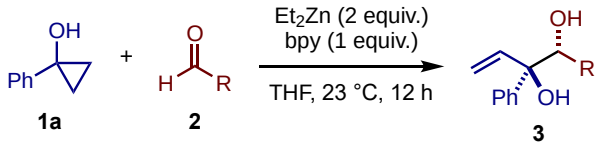

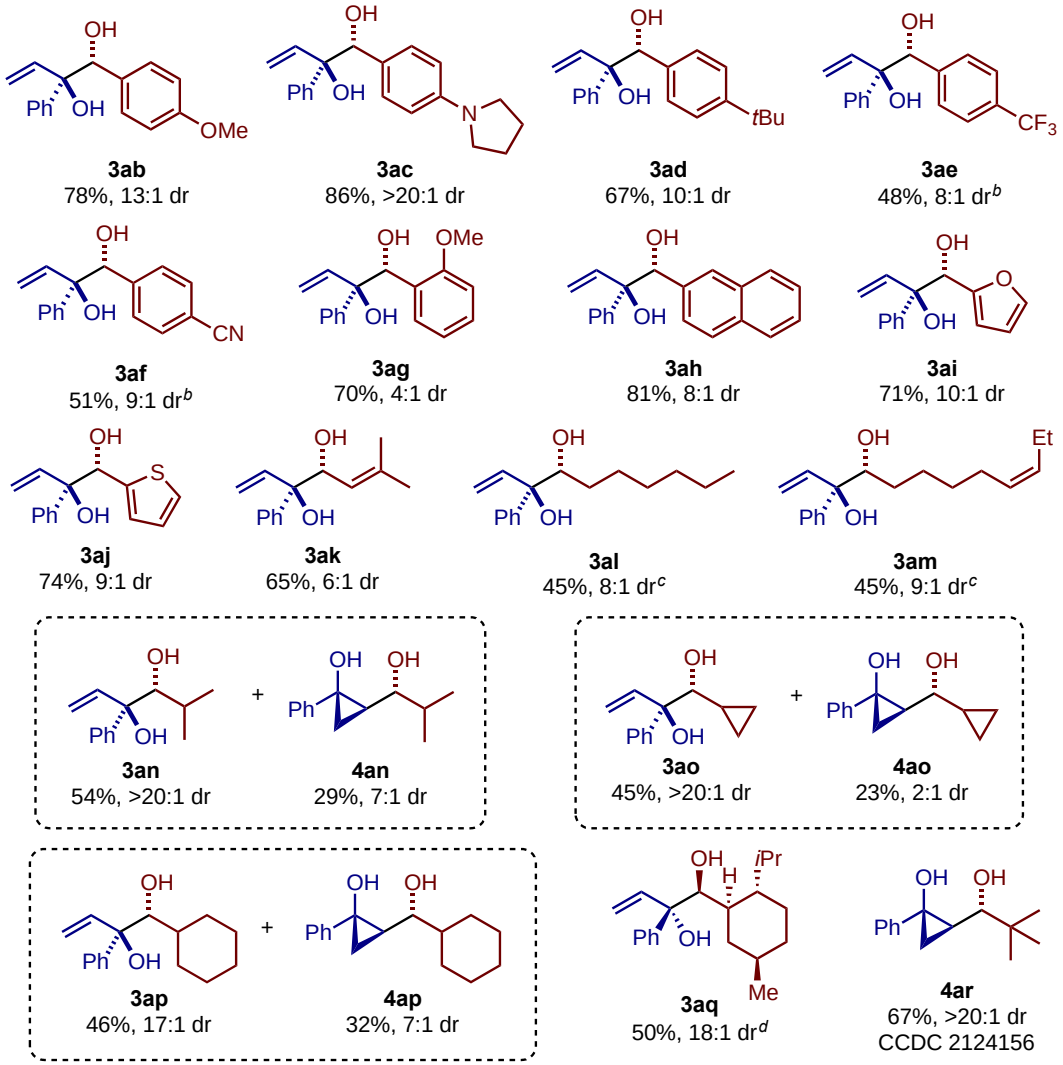

[a]The reaction was performed on a 0.3 mmol scale. [b]The reaction was performed at 0 °C for 24 h. [c]The reaction was performed at 80 °C using 0.1 equiv. of bpy. [d]The ratio of the major diastereomer and the rest indicated from ^{1}H NMR analysis of the crude product. The cyclopropanol-type product such as **4ap** was also obtained as a mixture of diastereomers (34% yield).

We performed a preliminary study on hydroxyallylation to a ketone electrophile as well as an enantioselective variant. The Et_2Zn-mediated reaction between **1a** and strained cyclobutanone (**2s**) proceeded in DMSO at 80 °C, affording the *tert*,*tert*-diol **3as** in 47% yield (Scheme 4.4a). Meanwhile, an attempted reaction of **1a** with cyclopentanone resulted in a complex mixture. We have also been able to observe

asymmetric induction in the model reaction between **1a** and **2a** in the presence of cinchonidine, albeit with moderate enantioselectivity of 84:16 er (Scheme 4.4b).

Scheme 4.4. (a) Addition to Cyclobutanone and (b) a Preliminary Enantioselective Variant

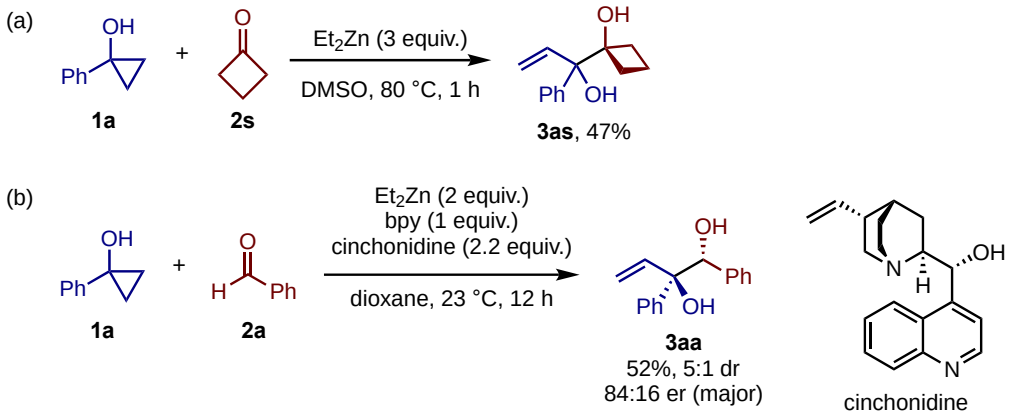

Showing consistently good *anti*-selectivity, the present reaction complements the previously reported *syn*-selective alkoxyallylations (Scheme 4.1a,b). To probe the origin of this diastereoselectivity, DFT calculations on model reactions between enolized homoenolates and aldehydes were performed (Figure 4.1a,b). First, (*Z*)-configured enolized homoenolate (*Z*)-**CP**, which is derived from **1a** and features chelation between the enolate oxygen and homoenolate zinc, was calculated to be far more stable ($\Delta\Delta G$ = 7.4 kcal mol^{-1}) than its (*E*)-counterpart ((*E*)-**CP**) (Figure 4.1a). Despite the strong chelation, boat-like transition states for the addition of (*Z*)-**CP** to **2a** were not located. Instead, it was found to form bicyclic chairlike transition states *anti*-**TS1** and *syn*-**TS1**, where the aldehyde oxygen was coordinated not only by the homoenolate zinc but also by the enolate zinc (Figure 4.1b).

With the aldehyde phenyl group at the pseudoaxial position, *anti*-**TS1** was lower in energy than *syn*-**TS1** by 1.0 kcal mol^{-1}, which was qualitatively in line with the observed selectivity toward *anti*-**3aa**. The same trend was also found with other TSs that modeled substrate combinations such as **1a**/acetaldehyde and 1-methylcyclopropanol/**2a**. Thus, unfavorable two gauche interactions encountered with psudoequatorial placement of the aldehyde substituent, as described by Marek,[17] would account for the *anti*-selectivity.

Besides the diastereoselectivity in hydroxyallylation, the origin of the diastereoselectivity in the formation of the 1,3-diol such as **4ar** was also probed (Figure

4.1c). Notably, in the aldol reaction step, the bulky *tert*-butyl group displayed preference for occupying the pseudoaxial position in the chairlike **TS** (*anti*-**TS2**) to avoid the gauche interaction with the zinciomethyl group in the alternative **TS** (*syn*-**TS2**). Following this aldol step, the subsequent ring closure would occur while avoiding the steric clash between the phenyl group and the alkoxide moiety, thus setting the relative configuration of the cyclopropane substituents. Compared with a related synthesis of 2-(1-hydroxyalkyl)-1-alkylcyclopropanol via Cr(II)-mediated coupling of enone and aldehyde by Takai,[18] which also involves aldol and cyclopropanation steps but with moderate diastereoselectivity with respect to the former, the high diastereoselectivity may be ascribed to the fixed (*Z*)-configuration of the enolized homoenolate.

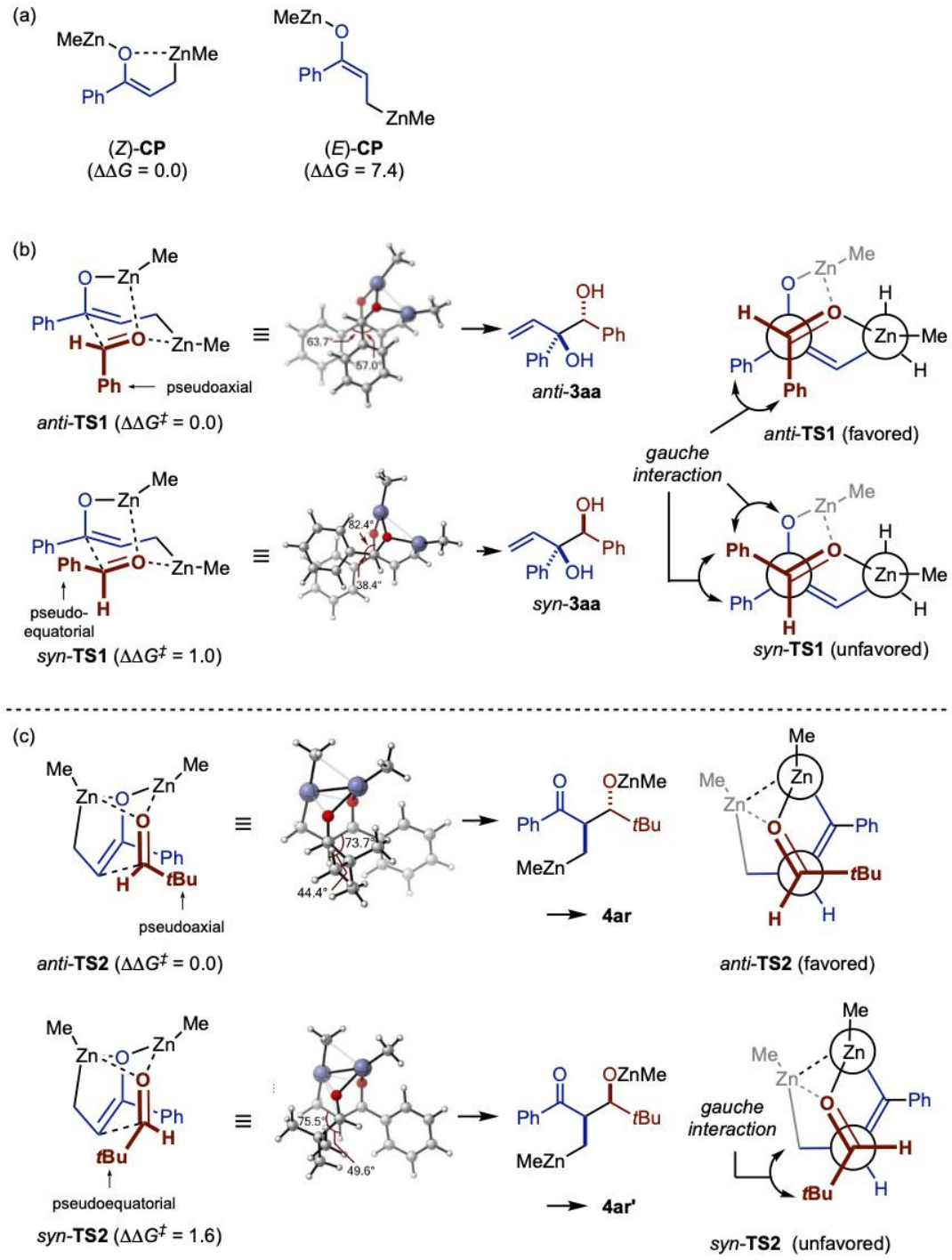

Figure 4.1. Results of DFT calculations (M062X-SMD(THF)/631+G(d,p)//M062X/6-31G(d)): (a) Comparison of (*Z*)- and (*E*)-configured enolized homoenolate (b) Transition states of hydroxyallylation leading to the major and minor diastereomers of **3aa**. (c) Transition states of aldol reaction leading to the major and minor diastereomers of **4ar**.

4.3 Conclusion

In summary, I have developed a zinc-mediated hydroxyallylation of aldehydes with cyclopropanols for the synthesis of vicinal *anti*-*sec*,*tert*-diols under operationally simple and mild conditions, which complements the existing alkoxyallylation reactions. It may be reemphasized that the addition of a vinyl Grignard reagent to α-hydroxyketones, an alternative approach to the present diol scaffold, has been reported to display *syn*-selectivity for relatively limited substitution patterns.[11] This, together with the ease of preparation of cyclopropanols,[19] would make this hydroxyallylation a uniquely useful approach to diastereodefined diols. Featuring the reaction mode of enolized homoenolate as a γ-oxyallyl nucleophile, the present hydroxyallylation further expands the utility of cyclopropanols beyond well-explored homoenolate and β-keto radical transformations.[15a, 15b, 15e]

4.4 Experimental Section

General procedure: In an argon-filled glove box, an 8-mL vial equipped with a magnetic stir bar was charged sequentially with 2,2'-bipyridine (46.9 mg, 0.30 mmol), cyclopropanol **1** (0.30 mmol), THF (1.8 mL), Et_2Zn (1 M in hexane, 0.60 mL, 0.60 mmol) and aldehyde **2** (0.45 mmol).The vial was closed and removed from the glove box, and the mixture was stirred at 23 °C (room temperature) for 12 h. The reaction mixture was diluted with Et_2O (3 mL), sat. NH_4Cl aq. (1 mL) and 1.5N HCl aq. (1 mL) were added dropwise. The white precipitate was removed by filtration and the aqueous phase was extracted with ethyl acetate (3 mL, 4 times). The combined organic phase was washed with brine, dried over Na_2SO_4, and concentrated under reduced pressure. The residue was analyzed by ^{1}H NMR to determine the diastereomer ratio (dr), and then purified by automated flash chromatography on silica gel or preparative TLC on silica gel to afford the desired product.

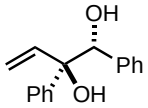

(1*R,2*R**)-1,2-Diphenylbut-3-ene-1,2-diol (3aa):** White solid (54.1 mg, 75%); R_f 0.23 (hexane/EtOAc = 4/1); 13:1 dr (determined by ^{1}H NMR of the crude mixture); m.p. 102-104 °C; **^{1}H NMR** (400 MHz, $CDCl_3$) δ 7.39-7.37 (m, 2H), 7.34-7.21 (m, 6H), 7.09-7.07 (m, 2H), 6.20 (dd, *J* = 17.2, 10.8 Hz, 1H), 5.26 (dd, *J* = 17.1, 1.1 Hz, 1H),

5.20 (dd, J = 10.8, 1.1 Hz, 1H), 4.94 (s, 1H), 2.79 (s, 1H), 2.63 (br s, 1H); **^{13}C{^{1}H} NMR** (100 MHz, $CDCl_3$) δ 142.6, 139.0, 138.5, 128.1, 127.8, 127.8, 127.6, 127.5, 126.5, 115.6, 80.2, 79.5; **FTIR** (KBr, $CHCl_3$, cm^{-1}): 344.7, 3090, 3067, 1491, 1449, 1051, 991; **HRMS** (ESI) Calcd for $C_{16}H_{17}O_2$ $[M + H]^+$ 241.1229, found 241.1227.

*The ^{1}H NMR spectrum of the minor diastereomer of the obtained **3aa** was identical to that of the reported (1*S*,2*R*)-**3aa**.[11b]

Enantioselective Reaction: In an argon-filled glove box, an 8-mL vial equipped with a magnetic stir bar was charged sequentially with 2,2'-bipyridine (46.9 mg, 0.30 mmol), cinchonidine (194 mg, 0.66 mmol), dioxane (1.8 mL) and Et_2Zn (1 M in hexane, 0.6 mL, 0.6 mmol). After stirring for 30 seconds, **1a** (40.3 mg, 0.30 mmol) and **2a** (47.8 mg, 0.45 mmol) were added. The vial was closed and removed from the glove box, and the mixture was stirred at 23 °C for 12 h. The reaction mixture was worked up as same as the general procedure to obtain **3aa** as a white solid (37.2 mg, 52%); 5:1 dr (determined by ^{1}H NMR of the crude mixture); $[\alpha]^{25}_D$ = –22.2 (c = 3.10 in $CHCl_3$, 5:1 dr, 84:16 er sample).

HPLC analysis: Daicel CHIRALPAK ID; hexane:*i*-PrOH = 95:5; detection wavelength = 210 nm; flow rate = 1.0 mL/min. t_R = 20.1 min (major) and 22.1 min (minor), 84:16 er.

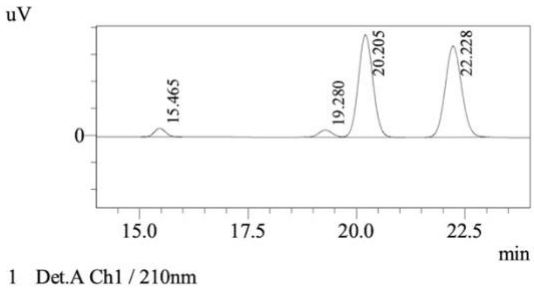

1 Det.A Ch1 / 210nm

PeakTable

Detector A Ch1 210nm

Peak#	Ret. Time	Area %
1	15.465	3.023
2	19.280	3.123
3	20.205	46.984
4	22.228	46.870
Total		100.000

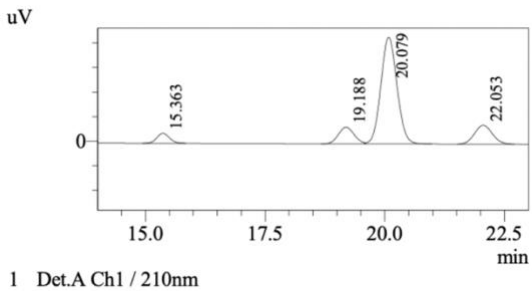

1 Det.A Ch1 / 210nm

PeakTable

Detector A Ch1 210nm

Peak#	Ret. Time	Area %
1	15.363	5.101
2	19.188	10.776
3	20.079	70.329
4	22.053	13.793
Total		100.000

*The left two peaks (15 and 19 min) are the minor diastereomer.

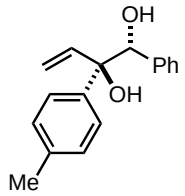

(1*R,2*R**)-1-Phenyl-2-(*p*-tolyl)but-3-ene-1,2-diol (3ba):** White solid (54.9 mg, 72%); R_f 0.30 (hexane/EtOAc = 4/1); >20:1 dr (determined by ^{1}H NMR of the crude mixture); m.p. 60-62 °C; **^{1}H NMR** (400 MHz, $CDCl_3$) δ 7.28-7.21 (m, 5H), 7.13-7.08 (m, 4H), 6.16 (dd, *J* = 17.2, 10.8 Hz, 1H), 5.24 (dd, *J* = 17.1, 1.2 Hz, 1H), 5.17 (dd, *J* = 10.8, 1.2 Hz, 1H), 4.92 (s, 1H), 2.73 (s, 1H), 2.62 (s, 1H), 2.33 (s, 3H); **^{13}C{^{1}H} NMR** (100 MHz, $CDCl_3$) δ 139.6, 139.2, 138.5, 137.1, 128.8, 127.8, 127.8, 127.5, 126.3, 115.4, 80.1, 79.4, 21.0; **FTIR** (KBr, $CHCl_3$, cm^{-1}): 3549, 3449, 3090, 3030, 2922, 1512, 1452, 1335, 1179, 928, 731; **HRMS** (ESI) Calcd for $C_{17}H_{19}O_2$ $[M + H]^+$ 255.1385, found 255.1380.

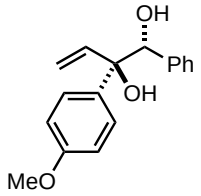

(1*R,2*R**)-2-(4-Methoxyphenyl)-1-phenylbut-3-ene-1,2-diol (3ca):** Colorless oil (58.7 mg, 72%); R_f 0.17 (hexane/EtOAc = 4/1); >20:1 dr (determined by ^{1}H NMR of the crude mixture); **^{1}H NMR** (400 MHz, $CDCl_3$) δ 7.29-7.25 (m, 2H), 7.24-7.20 (m, 3H), 7.07-7.05 (m, 2H), 6.85-6.81 (m, 2H), 6.17 (dd, *J* = 17.2, 10.8 Hz, 1H), 5.28 (dd, *J* = 17.2, 1.3 Hz, 1H), 5.20 (dd, *J* = 10.8, 1.2 Hz, 1H), 4.90 (s, 1H), 3.78 (s, 3H), 2.78 (s, 1H), 2.71 (br s, 1H); **^{13}C{^{1}H} NMR** (100 MHz, $CDCl_3$) δ 158.8, 139.0, 138.6, 124.6, 127.8, 127.7 (overlap), 127.5, 115.5, 113.4, 80.3, 79.2, 55.2; **FTIR** (KBr, thin film, cm^{-1}): 3456, 3061, 3030, 2957, 2934, 2837, 2247, 1728, 1609, 1510, 1454, 1298, 1250, 1032, 924, 829, 735, 702; **HRMS** (ESI) Calcd for $C_{17}H_{19}O_3$ $[M + H]^+$ 271.1334, found 271.1335.

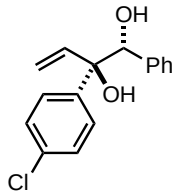

(1*R,2*R**)-2-(4-Chlorophenyl)-1-phenylbut-3-ene-1,2-diol (3da):** White solid (46.4 mg, 56%); R_f 0.24 (hexane/EtOAc = 4/1); 6:1 dr (determined by ^{1}H NMR of the crude mixture); m.p. 90-91 °C; **^{1}H NMR** (400 MHz, $CDCl_3$) δ 7.30-7.21 (m, 7H), 7.07-7.05 (m, 2H), 6.18 (dd, *J* = 17.2, 10.8 Hz, 1H), 5.27 (dd, *J* = 17.1, 1.0 Hz, 1H), 5.22 (dd, *J* = 10.8, 1.0 Hz, 1H), 4.86 (d, *J* = 3.4 Hz, 1H), 2.83 (s, 1H), 2.63 (d, *J* = 3.6 Hz, 1H); **^{13}C{^{1}H} NMR** (100 MHz, $CDCl_3$) δ 141.1, 138.6, 138.2, 133.3, 128.1, 128.1, 128.1, 127.7, 127.7, 116.1, 80.3, 79.2; **FTIR** (KBr, $CHCl_3$, cm^{-1}): 3462, 3090, 3065, 1491, 1094, 1015, 930; **HRMS** (ESI) Calcd for $C_{16}H_{16}O_2Cl$ $[M + H]^+$ 275.0839, found 275.0844.

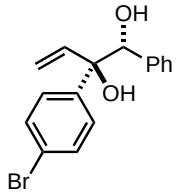

(1*R,2*R**)-2-(4-Bromophenyl)-1-phenylbut-3-ene-1,2-diol (3ea):** White solid (59.4 mg, 62%); R_f 0.22 (hexane/EtOAc = 4/1); 6:1 dr (determined by ^{1}H NMR of the crude mixture); m.p. 102-104 °C; **^{1}H NMR** (400 MHz, $CDCl_3$) δ 7.44-7.40 (m, 2H), 7.26-7.20 (m, 5H), 7.08-7.05 (m, 2H), 6.16 (dd, *J* = 17.2, 10.8 Hz, 1H), 5.26 (dd, *J* = 17.2, 1.1 Hz, 1H), 5.22 (dd, *J* = 10.8, 1.0 Hz, 1H), 4.85 (s, 1H), 2.84 (s, 1H), 2.66 (br s, 1H); **^{13}C{^{1}H} NMR** (100 MHz, $CDCl_3$) δ 141.6, 138.6, 138.2, 131.1, 128.4, 128.0, 127.7, 127.7, 121.5, 116.1, 80.2, 79.2; **FTIR** (KBr, $CHCl_3$, cm^{-1}): 3543, 3090, 3065, 1487, 1452, 1395, 1074, 1009, 932, 631; **HRMS** (ESI) Calcd for $C_{16}H_{16}O_2Br$ $[M + H]^+$ 319.0334, found 319.0333.

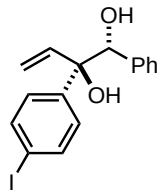

(1*R,2*R**)-2-(4-Iodophenyl)-1-phenylbut-3-ene-1,2-diol (3fa):** White solid (68.5 mg, 62%); R_f 0.22 (hexane/EtOAc = 4/1); 6:1 dr (determined by ^{1}H NMR of the crude mixture); m.p. 134-136 °C; **^{1}H NMR** (400 MHz, $CDCl_3$) δ 7.64-7.61 (m, 2H), 7.26-7.23 (m, 3H), 7.11-7.07 (m, 4H), 6.15 (dd, *J* = 17.2, 10.8 Hz, 1H), 5.26 (dd, *J* = 17.2, 1.0 Hz, 1H), 5.21 (dd, *J* = 10.8, 0.9 Hz, 1H), 4.86 (d, *J* = 2.4 Hz, 1H), 2.80 (s, 1H), 2.59 (d, *J* = 3.4 Hz, 1H); **^{13}C{^{1}H} NMR** (100 MHz, $CDCl_3$) δ 142.4, 138.6, 138.2, 137.1, 128.6, 128.1, 127.7, 127.7, 116.1, 93.3, 80.1, 79.3; **FTIR** (KBr, $CHCl_3$, cm^{-1}): 3478, 3333, 3028, 3011, 1483, 1450, 1412, 1389, 1150, 1067, 1001, 949, 932, 839, 737, 700, 629; **HRMS** (ESI) Calcd for $C_{16}H_{16}O_2I$ $[M + H]^+$ 367.0195, found 367.0189.

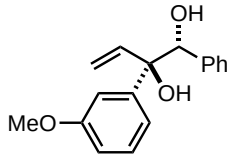

(1*R,2*R**)-2-(3-Methoxyphenyl)-1-phenylbut-3-ene-1,2-diol (3ga):** White solid (62.5 mg, 77%); R_f 0.17 (hexane/EtOAc = 4/1); 12:1 dr (determined by ^{1}H NMR of the crude mixture); m.p. 100-101 °C; **^{1}H NMR** (400 MHz, $CDCl_3$) δ 7.25-7.21 (m, 4H), 7.12-7.10 (m, 2H), 6.98-6.93 (m, 2H), 6.82-6.80 (m, 1H), 6.16 (dd, *J* = 17.2, 10.8 Hz, 1H), 5.24 (dd, *J* = 17.2, 1.2 Hz, 1H), 5.17 (dd, *J* = 10.8, 1.2 Hz, 1H), 4.92 (d, *J* = 3.4 Hz, 1H), 3.74 (s, 3H), 2.81 (d, *J* = 3.0 Hz, 1H), 2.65 (br s, 1H); **^{13}C{^{1}H} NMR** (100 MHz, $CDCl_3$) δ 159.4, 144.3, 139.0, 138.4, 129.1, 127.8, 127.8, 127.5, 118.7, 115.5, 112.9, 112.3, 80.1, 79.5, 55.2; **FTIR** (KBr, $CHCl_3$, cm^{-1}): 3443, 3352, 3084, 2940, 2835, 1601, 1489, 1464, 1425, 1341, 1096, 1038, 993, 943, 862, 818, 698; **HRMS** (ESI) Calcd for $C_{17}H_{19}O_3$ $[M + H]^+$ 271.1334, found 271.1324.

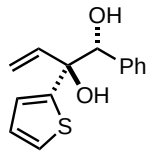

(1*R,2*S**)-1-Phenyl-2-(thiophen-2-yl)but-3-ene-1,2-diol (3ha):** Colorless oil (38.9 mg, 53%); R_f 0.22 (hexane/EtOAc = 4/1); 8:1 dr (determined by ^{1}H NMR of the crude

mixture); **^{1}H NMR** (400 MHz, $CDCl_3$) δ 7.29-7.24 (m, 4H), 7.15-7.12 (m, 2H), 6.96 (dd, *J* = 5.1, 3.6 Hz, 1H), 6.81 (dd, *J* = 3.6, 1.1 Hz, 1H), 6.09 (dd, *J* = 17.1, 10.7 Hz, 1H), 5.41 (dd, *J* = 17.1, 1.1 Hz, 1H), 5.28 (dd, *J* = 10.7, 1.0 Hz, 1H), 4.97 (d, *J* = 3.6 Hz, 1H), 3.01 (s, 1H), 2.67 (d, *J* = 3.7 Hz, 1H); **^{13}C{^{1}H} NMR** (100 MHz, $CDCl_3$) δ 147.2, 138.2, 138.1, 128.0, 127.6, 127.6, 126.7, 125.1, 125.0, 115.9, 80.8, 78.8; **FTIR** (KBr, $CHCl_3$, cm^{-1}): 3445, 3090, 3067, 1495, 1454, 1410, 1049, 934, 827, 792; **HRMS** (ESI) Calcd for $C_{14}H_{15}O_2S$ $[M + H]^+$ 247.0793, found 247.0788.

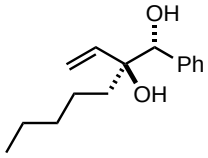

(1*R,2*S**)-1-Phenyl-2-vinylheptane-1,2-diol (3ia):** White solid (46.0 mg, 65%); R_f 0.26 (hexane/EtOAc = 4/1); 18:1 dr (determined by ^{1}H NMR of the crude mixture); m.p. 53-55 °C; **^{1}H NMR** (400 MHz, $CDCl_3$) δ 7.36-7.27 (m, 5H), 5.66 (dd, *J* = 17.4, 10.8 Hz, 1H), 5.24 (dd, *J* = 17.4, 1.4 Hz, 1H), 5.20 (dd, *J* = 10.8, 1.4 Hz, 1H), 4.58 (s, 1H), 2.67 (br s, 1H), 2.34 (br s, 1H), 1.64-1.58 (m, 1H), 1.47-1.18 (m, 7H), 10.86 (t, *J* = 6.9 Hz, 3H); **^{13}C{^{1}H} NMR** (100 MHz, $CDCl_3$) δ 139.8, 138.9, 127.8, 127.8, 127.6, 115.1, 79.9, 78.1, 36.8, 32.2, 22.7, 22.6, 14.0; **FTIR** (KBr, $CHCl_3$, cm^{-1}): 3447, 2955, 2932, 2872, 1452, 1049, 1001, 633; **HRMS** (ESI) Calcd for $C_{15}H_{23}O_2$ $[M + H]^+$ 235.1698, found 235.1695.

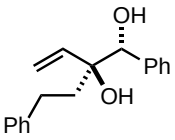

(1*R,2*S**)-2-Phenethyl-1-phenylbut-3-ene-1,2-diol (3ja):** Colorless oil (38.4 mg, 48%); R_f 0.19 (hexane/EtOAc = 4/1); 7:1 dr (determined by ^{1}H NMR of the crude mixture); **^{1}H NMR** (400 MHz, $CDCl_3$) δ 7.31-7.23 (m, 7H), 7.17-7.13 (m, 3H), 5.74 (dd, *J* = 17.3, 10.8 Hz, 1H), 5.32 (dd, *J* = 17.3, 1.4 Hz, 1H), 5.28 (dd, *J* = 10.8, 1.3 Hz, 1H), 4.60 (d, *J* = 3.2 Hz, 1H), 2.75-2.68 (m, 2H), 2.59-2.50 (m, 2H), 1.97 (ddd, *J* = 13.6, 12.1, 5.2 Hz, 1H), 1.73 (ddd, *J* = 13.6, 12.4, 4.8 Hz, 1H); **^{13}C{^{1}H} NMR** (100 MHz, $CDCl_3$) δ 142.3, 139.5, 138.4, 128.4, 128.4, 127.9. 127.6, 125.7, 115.7, 80.0, 78.0, 38.6, 29.5; **FTIR** (KBr, thin film, cm^{-1}): 3441, 3061, 3026, 2928, 1603, 1495, 1454, 1194, 1126, 1047, 926, 731, 700; **HRMS** (ESI) Calcd for $C_{18}H_{21}O_2$ $[M + H]^+$ 269.1542, found 269.1539.

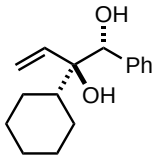

(1*R,2*R**)-2-Cyclohexyl-1-phenylbut-3-ene-1,2-diol (3ka):** The reaction was conducted without 2,2'-bipyridine in DMSO at 80 ℃ for 1 h. White solid (34.7 mg, 47%); R_f 0.34 (hexane/EtOAc = 4/1); 7:1 dr (determined by ^{1}H NMR of the crude mixture); m.p. 95-96 °C; **^{1}H NMR** (400 MHz, $CDCl_3$) δ 7.36-7.24 (m, 5H), 5.65 (dd, *J* = 17.2, 11.1 Hz, 1H), 5.14-5.08 (m, 2H), 4.87 (s, 1H), 2.60 (s, 1H), 2.09 (s, 1H), 1.99-1.96 (m, 1H), 1.82-1.60 (m, 5H), 1.31-0.99 (m, 5H); **^{13}C{^{1}H} NMR** (100 MHz, $CDCl_3$) δ 140.1, 138.3, 127.8, 127.7, 127.5, 114.8, 80.1, 75.6, 42.3, 27.8, 26.8, 26.7, 26.5, 26.3; **FTIR** (KBr, $CHCl_3$, cm^{-1}): 3455, 2932, 2853, 1452, 1045, 978, 926; **HRMS** (ESI) Calcd for $C_{16}H_{23}O_2$ $[M + H]^+$ 247.1698, found 247.1693.

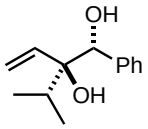

(1*R,2*S**)-2-Isopropyl-1-phenylbut-3-ene-1,2-diol (3la):** The reaction was conducted without 2,2'-bipyridine in DMSO at 80 ℃ for 1 h. White solid (31.5 mg, 51%); R_f 0.29 (hexane/EtOAc = 4/1); 11:1 dr (determined by ^{1}H NMR of the crude mixture); m.p. 76-79 °C; **^{1}H NMR** (400 MHz, $CDCl_3$) δ 7.34-7.28 (m, 5H), 5.69 (dd, *J* = 17.0, 11.2 Hz, 1H), 5.21-5.167 (m, 2H), 4.87 (s, 1H), 2.67 (br s, 1H), 2.13 (br s, 1H), 1.98 (sept, *J* = 6.8 Hz, 1H), 1.06 (d, *J* = 6.8 Hz, 3H), 0.93 (d, *J* = 7.0 Hz, 3H); **^{13}C{^{1}H} NMR** (100 MHz, $CDCl_3$) δ 140.1, 137.7, 127.8, 127.7, 127.5, 115.2, 80.2, 76.1, 32.1, 17.9, 16.7; **FTIR** (KBr, $CHCl_3$, cm^{-1}): 3422, 2965, 2936, 1470, 1452, 1387, 1368, 1098, 1086, 1047, 1001, 991, 966, 827, 702; **HRMS** (ESI) Calcd for $C_{13}H_{19}O_2$ $[M + H]^+$ 207.1385, found 207.1393.

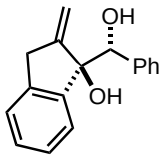

(*R)-1-((*R**)-Hydroxy(phenyl)methyl)-2-methylene-2,3-dihydro-1*H*-inden-1-ol (3ma):** Pale yellow solid (54.7 mg, 72%); R_f 0.15 (hexane/EtOAc = 4/1); 7:1 dr (determined by ^{1}H NMR of the crude mixture); m.p. 79-81 °C; **^{1}H NMR** (400 MHz, $CDCl_3$) δ 7.43 (d, *J* = 7.4 Hz, 1H), 7.32-7.22 (m, 2H), 7.15-7.11 (m, 1H), 7.07-7.03 (m,

2H), 6.97 (d, *J* = 7.0 Hz, 1H), 6.91-6.89 (m, 2H), 5.51-5.50 (m, 1H), 5.26-5.25 (m, 1H), 4.92 (s, 1H), 3.36 (br s, 1H), 3.21 (d, *J* = 19.7 Hz, 1H), 2.92 (br s, 1H), 2.44 (d, *J* = 19.7 Hz, 1H); **^{13}C{^{1}H} NMR** (100 MHz, $CDCl_3$, +; positive DEPT 135 signal, –; negative DEPT 135 signal) δ 152.3, 143.9, 141.2, 137.8, 128.9 (+), 127.2 (+), 127.1 (+), 127.0 (+), 126.8 (+), 124.2 (+), 124.1 (+), 111.0 (–), 85.0, 79.1 (+), 37.3 (–); **FTIR** (KBr, $CHCl_3$, cm^{-1}): 3418, 3065, 3030, 2920, 2887, 1661, 1607, 1452, 1418, 1049, 951, 905, 700, 665; **HRMS** (ESI) Calcd for $C_{17}H_{17}O_2$ $[M + H]^+$ 253.1229, found 253.1223.

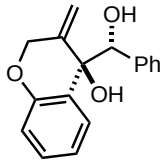

(*R)-4-((*R**)-Hydroxy(phenyl)methyl)-3-methylenechroman-4-ol (3na):** Pale yellow solid (57.3 mg, 71%); R_f 0.17 (hexane/EtOAc = 4/1); 5:1 dr (determined by ^{1}H NMR of the crude mixture); m.p. 109-112 °C; **^{1}H NMR** (400 MHz, $CDCl_3$) δ 7.58 (dd, *J* = 7.8, 1.6 Hz, 1H), 7.24-7.12 (m, 4H), 7.04-7.00 (m, 1H), 6.96-6.94 (m, 2H), 6.69 (dd, *J* = 8.2, 0.9 Hz, 1H), 5.39 (s, 1H), 5.23 (s, 1H), 5.08 (s, 1H), 4.19 (d, *J* = 13.0 Hz, 1H), 3.39 (d, *J* = 12.9 Hz, 1H), 3.30 (d, *J* = 1.8 Hz, 1H), 2.83 (s, 1H); **^{13}C{^{1}H} NMR** (100 MHz, $CDCl_3$, +; positive DEPT 135 signal, –; negative DEPT 135 signal) δ 155.1, 141.3, 138.1, 129.6 (+), 127.9 (+), 127.8 (+), 127.6 (+), 126.7 (+), 125.5, 121.1 (+), 116.7 (+), 115.1 (–), 79.3 (+), 75.0, 70.3 (–); **FTIR** (KBr, $CHCl_3$, cm^{-1}): 3443, 3061, 3030, 1605, 1485, 1456, 1449, 1047, 920, 700; **HRMS** (ESI) Calcd for $C_{17}H_{17}O_3$ $[M + H]^+$ 269.1178, found 269.1173.

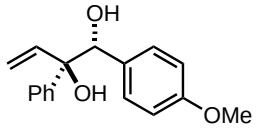

(1*R,2*R**)-1-(4-Methoxyphenyl)-2-phenylbut-3-ene-1,2-diol (3ab):** Colorless oil (63.5 mg, 78%); R_f 0.16 (hexane/EtOAc = 4/1); 13:1 dr (determined by ^{1}H NMR of the crude mixture); **^{1}H NMR** (400 MHz, $CDCl_3$) δ 7.38-7.35 (m, 2H), 7.33-7.23 (m, 3H), 7.01-6.98 (m, 2H), 6.77-6.73 (m, 2H), 6.19 (dd, *J* = 17.2, 10.8 Hz, 1H), 5.26 (dd, *J* = 17.2, 1.2 Hz, 1H), 5.19 (dd, *J* = 10.8, 1.2 Hz, 1H), 4.88 (d, *J* = 3.0 Hz, 1H), 3.75 (s, 3H), 2.82 (s, 1H), 2.63 (d, *J* = 3.5 Hz, 1H); **^{13}C{^{1}H} NMR** (100 MHz, $CDCl_3$) δ 159.1, 142.7, 139.2, 130.6, 128.9, 128.0, 127.4, 126.4, 115.5, 112.9, 79.8, 79.5, 55.1; **FTIR** (KBr, thin film, cm^{-1}): 3447, 3059, 3030, 3001, 2957, 2934, 2909, 2835, 1612, 1514, 1447,

1304, 1248, 1177, 1032, 1003, 928, 835, 756, 702, 569; **HRMS** (ESI) Calcd for $C_{17}H_{19}O_3$ $[M + H]^+$ 271.1334, found 271.1337.

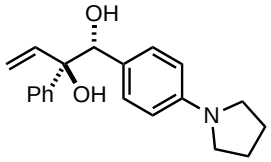

(1*R,2*R**)-2-Phenyl-1-(4-(pyrrolidin-1-yl)phenyl)but-3-ene-1,2-diol (3ac):** Pale brown oil (79.5 mg, 86%); R_f 0.20 (hexane/EtOAc = 4/1); >20:1 dr (determined by ^{1}H NMR of the crude mixture); **^{1}H NMR** (400 MHz, $CDCl_3$) δ 7.43-7.41 (m, 2H), 7.34-7.24 (m, 3H), 6.98-6.95 (m, 2H), 6.44-6.42 (m, 2H), 6.25 (dd, *J* = 17.2, 10.8 Hz, 1H), 5.27 (dd, *J* = 17.2, 1.4 Hz, 1H), 5.18 (dd, *J* = 10.8, 1.3 Hz, 1H), 4.87 (s, 1H), 3.26-3.23 (m, 4H), 2.83 (s, 1H), 2.38 (br s, 1H), 2.00-1.96 (m, 4H); **^{13}C{^{1}H} NMR** (100 MHz, $CDCl_3$) δ 147.5, 143.0, 139.7, 128.6, 127.9, 127.1, 126.4, 125.0, 115.1, 110.7, 80.1, 79.5, 47.5, 25.3; **FTIR** (KBr, thin film, cm^{-1}): 3445, 2967, 2889, 2872, 2835, 1614, 1524, 1487, 1373, 1182, 1051, 991, 924, 818, 754, 733, 702; **HRMS** (ESI) Calcd for $C_{20}H_{24}NO_2$ $[M + H]^+$ 310.1807, found 310.1811.

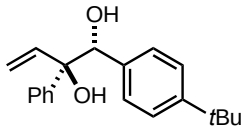

(1*R,2*R**)-1-(4-(*tert*-Butyl)phenyl)-2-phenylbut-3-ene-1,2-diol (3ad):** White solid (59.3 mg, 67%); R_f 0.26 (hexane/EtOAc = 4/1); 10:1 dr (determined by ^{1}H NMR of the crude mixture); m.p. 95-97 °C; **^{1}H NMR** (400 MHz, $CDCl_3$) δ 7.42-7.39 (m, 2H), 7.34-7.22 (m, 5H), 7.05-7.03 (m, 2H), 6.19 (dd, *J* = 17.2, 10.8 Hz, 1H), 5.24 (dd, *J* = 17.2, 1.2 Hz, 1H), 5.18 (dd, *J* = 10.8, 1.2 Hz, 1H), 4.93 (s, 1H), 2.81 (s, 1H), 2.53 (br s, 1H), 1.29 (s, 9H); **^{13}C{^{1}H} NMR** (100 MHz, $CDCl_3$) δ 150.8, 142.7, 139.4, 135.5, 128.1, 127.4, 127.4, 126.5, 124.5, 115.6, 79.9, 79.5, 34.5, 31.3; **FTIR** (KBr, $CHCl_3$, cm^{-1}): 3564, 3418, 3009, 2965, 2905, 1510, 1493, 1364, 1269, 1057; **HRMS** (ESI) Calcd for $C_{20}H_{25}O_2$ $[M + H]^+$ 297.1855, found 297.1863.

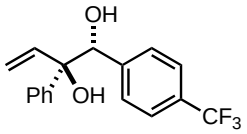

(1*R,2*R**)-2-Phenyl-1-(4-(trifluoromethyl)phenyl)but-3-ene-1,2-diol (3ae):** The reaction was conducted at 0 °C for 24 h. White solid (44.6 mg, 48%); R_f 0.25 (hexane/EtOAc = 4/1); 8:1 dr (determined by ^{1}H NMR of the crude mixture); m.p. 103-105 °C; **^{1}H NMR** (400 MHz, $CDCl_3$) δ 7.48 (d, *J* = 8.2 Hz, 2H), 7.39-7.30 (m, 5H), 7.17 (d, *J* = 8.1 Hz, 2H), 6.15 (dd, *J* = 17.2, 10.8 Hz, 1H), 5.30 (dd, *J* = 17.2, 1.1 Hz, 1H), 5.25 (dd, *J* = 10.8, 1.0 Hz, 1H), 5.00 (s, 1H), 2.78 (d, *J* = 3.0 Hz, 1H), 2.73 (s, 1H); **^{13}C{^{1}H} NMR** (100 MHz, $CDCl_3$) δ 142.5, 142.2, 138.3, 129.9 (q, $^2J_{C-F}$ = 32.2 Hz), 128.3, 128.1, 127.9, 126.5, 124.4 (q, $^3J_{C-F}$ = 3.8 Hz), 124.1 (q, $^1J_{C-F}$ = 272.0 Hz, the highest frequency peak in the quartet overlaps), 116.3, 79.8, 79.5; 20.6; **^{19}F NMR** (376 MHz, $CDCl_3$): δ –62.5; **FTIR** (KBr, $CHCl_3$, cm^{-1}): 3395, 3090, 3017, 2924, 1618, 1497, 1327, 1111, 1065, 945, 758, 698; **HRMS** (ESI) Calcd for $C_{17}H_{16}O_2F_3$ $[M + H]^+$ 309.1102, found 309.1105.

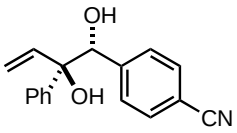

4-((1*R,2*R**)-1,2-Dihydroxy-2-phenylbut-3-en-1-yl)benzonitrile (3af):** The reaction was conducted at 0 °C for 24 h. White solid (40.8 mg, 51%); R_f 0.14 (hexane/EtOAc = 3/1); 9:1 dr (determined by ^{1}H NMR of the crude mixture); m.p. 129-130 °C; **^{1}H NMR** (400 MHz, $CDCl_3$) δ 7.49-7.47 (m, 2H), 7.37-7.29 (m, 5H), 7.17-7.15 (m, 2H), 6.14 (dd, *J* = 17.1, 10.8 Hz, 1H), 5.32 (dd, *J* = 17.1, 1.0 Hz, 1H), 5.27 (dd, *J* = 10.8, 0.9 Hz, 1H), 3.24 (d, *J* = 3.2 Hz, 1H), 2.86 (d, *J* = 3.4 Hz, 1H), 2.75 (s, 1H); **^{13}C{^{1}H} NMR** (100 MHz, $CDCl_3$) δ 143.9, 142.0, 138.0, 131.2, 128.5, 128.4, 128.0, 126.4, 118.7, 116.5, 111.4, 79.7, 79.4; **FTIR** (KBr, $CHCl_3$, cm^{-1}): 3489, 3092, 3071, 3021, 2224, 1607, 1414, 1393, 1151, 1055, 984, 926; **HRMS** (ESI) Calcd for $C_{17}H_{16}NO_2$ $[M + H]^+$ 266.1181, found 266.1186.

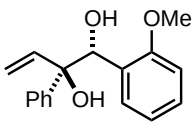

(1*R,2*R**)-1-(2-Methoxyphenyl)-2-phenylbut-3-ene-1,2-diol (3ag):** White solid (56.6 mg, 70%); R_f 0.19 (hexane/EtOAc = 4/1); 4:1 dr (determined by ^{1}H NMR of the

crude mixture); m.p. 74-77 °C; **^{1}H NMR** (400 MHz, $CDCl_3$) δ 7.44-7.42 (m, 2H), 7.32-7.28 (m, 2H), 7.25-7.20 (m, 2H), 7.08 (dd, *J* = 7.6, 1.5 Hz, 1H), 6.87 (t, *J* = 7.5 Hz, 1H), 6.80 (d, *J* = 8.2 Hz, 1H), 6.28 (dd, *J* = 17.1, 10.7 Hz, 1H), 5.28-5.23 (m, 2H), 5.07 (dd, *J* = 10.7, 1.4 Hz, 1H), 3.67 (s, 3H), 3.23 (s, 1H), 3.10 (d, *J* = 6.6 Hz, 1H); **^{13}C{^{1}H} NMR** (100 MHz, $CDCl_3$) δ 156.8, 143.1, 139.9, 129.1, 128.8, 127.9, 127.0, 126.2, 120.4, 113.9, 110.5 79.7, 76.3, 55.1; **FTIR** (KBr, $CHCl_3$, cm^{-1}): 3453, 2940, 2937, 1601, 1491, 1464, 1051, 1028, 922, 623; **HRMS** (ESI) Calcd for $C_{17}H_{19}O_3$ $[M + H]^+$ 271.1334, found 271.1327.

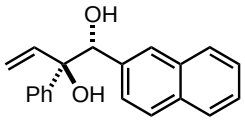

(1*R,2*R**)-1-(Naphthalen-2-yl)-2-phenylbut-3-ene-1,2-diol (3ah):** Colorless oil (70.6 mg, 81%); R_f 0.29 (hexane/EtOAc = 4/1); 8:1 dr (determined by ^{1}H NMR of the crude mixture); **^{1}H NMR** (400 MHz, $CDCl_3$) δ 7.77-7.75 (m, 1H), 7.71-7.69 (m, 1H), 7.64 (d, *J* = 8.5 Hz, 1H), 7.55 (s, 1H), 7.44-7.41 (m, 2H), 7.37-7.35 (m, 2H), 7.31-7.26 (m, 3H), 7.10 (dd, *J* = 8.5, 1.6 Hz, 1H), 6.20 (dd, *J* = 17.1, 10.8 Hz, 1H), 5.26 (dd, *J* = 17.1, 1.2 Hz, 1H), 5.17 (dd, *J* = 10.8, 1.1 Hz, 1H), 5.05 (d, *J* = 3.1 Hz, 1H), 2.87 (s, 1H), 2.84 (d, *J* = 3.6 Hz, 1H); **^{13}C{^{1}H} NMR** (100 MHz, $CDCl_3$) δ 142.6, 138.9, 136.1, 133.0, 132.6, 128.1, 128.0, 127.5, 126.9, 126.8, 126.5, 125.9, 125.8, 115.7, 80.3, 79.6; **FTIR** (KBr, $CHCl_3$, cm^{-1}): 3437, 3088, 1508, 1491, 1449, 1357, 1123, 1057, 991, 860; **HRMS** (ESI) Calcd for $C_{20}H_{19}O_2$ $[M + H]^+$ 291.1385, found 291.1376.

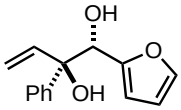

(1*S,2*R**)-1-(Furan-2-yl)-2-phenylbut-3-ene-1,2-diol (3ai):** Colorless oil (48.8 mg, 71%); R_f 0.17 (hexane/EtOAc = 4/1); 10:1 dr (determined by ^{1}H NMR of the crude mixture); **^{1}H NMR** (400 MHz, $CDCl_3$) δ 7.45-7.42 (m, 2H), 7.35-7.31 (m, 3H), 7.28-7.24 (m, 1H), 6.31-6.24 (m, 2H), 6.17 (d, *J* = 3.2 Hz, 1H), 5.34 (dd, *J* = 17.1, 1.1 Hz, 1H), 5.20 (dd, *J* = 10.8, 1.1 Hz, 1H), 4.96 (d, *J* = 5.7 Hz, 1H), 3.03 (s, 1H), 2.65 (d, *J* = 6.1 Hz, 1H); **^{13}C{^{1}H} NMR** (100 MHz, $CDCl_3$) δ 152.3, 142.1, 142.0, 139.2, 128.2, 127.4, 125.9, 115.4, 110.2, 108.9, 79.2, 74.1; **FTIR** (KBr, thin film, cm^{-1}): 3433, 3088, 3059, 2922, 1701, 1601, 1493, 1449, 1410, 1150, 1063, 1011, 924, 793, 745, 702; **HRMS** (ESI) Calcd for $C_{14}H_{15}O_3$ $[M + H]^+$ 231.1021, found 231.1020.

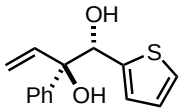

(1*S,2*R**)-2-Phenyl-1-(thiophen-2-yl)but-3-ene-1,2-diol (3aj):** Pale brown oil (54.7 mg, 74%); R_f 0.23 (hexane/EtOAc = 4/1); 16:1 dr (determined by ^{1}H NMR of the crude mixture); **^{1}H NMR** (400 MHz, $CDCl_3$) δ 7.47-7.45 (m, 2H), 7.37-7.33 (m, 2H), 7.31-7.27 (m, 1H), 7.22 (dd, *J* = 5.1, 1.1 Hz, 1H), 6.90 (dd, *J* = 5.1, 3.5 Hz, 1H), 6.75 (d, *J* = 3.4 Hz, 1H), 6.21 (dd, *J* = 17.2, 10.8 Hz, 1H), 5.30 (dd, *J* = 17.2, 1.1 Hz, 1H), 5.26 (d, *J* = 3.4 Hz, 1H), 5.22 (dd, *J* = 10.8, 1.1 Hz, 1H), 2.89 (s, 1H), 2.68 (d, *J* = 4.0 Hz, 1H); **^{13}C{^{1}H} NMR** (100 MHz, $CDCl_3$) δ 142.3, 141.8, 138.9, 128.3, 127.6, 126.4, 126.3, 126.1, 125.5, 116.1, 79.4, 76.5; **FTIR** (KBr, thin film, cm^{-1}): 3443, 3088, 3063, 1493, 1447, 1059, 1042, 989, 928, 766, 752, 700; **HRMS** (ESI) Calcd for $C_{14}H_{15}O_2S$ [M + H]$^+$ 247.0793, found 247.0790.

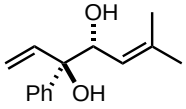

(3*R,4*R**)-6-Methyl-3-phenylhepta-1,5-diene-3,4-diol (3ak):** Colorless oil (42.7 mg, 65%); R_f 0.23 (hexane/EtOAc = 4/1); 6:1 dr (determined by ^{1}H NMR of the crude mixture); **^{1}H NMR** (400 MHz, $CDCl_3$) δ 7.51-7.49 (m, 2H), 7.35-7.31 (m, 2H), 7.27-7.22 (m, 1H), 6.29 (dd, *J* = 17.2, 10.8 Hz, 1H), 5.38 (dd, *J* = 17.2, 1.4 Hz, 1H), 5.29-5.24 (m, 2H), 4.54 (d, *J* = 9.0 Hz, 1H), 3.00 (s, 1H), 1.99 (br s, 1H), 1.70 (d, *J* = 1.0 Hz, 3H), 1.39 (d, *J* = 1.1 Hz, 3H); **^{13}C{^{1}H} NMR** (100 MHz, $CDCl_3$) δ 143.0, 139.2, 138.6, 128.0, 127.1, 126.2, 122.0, 115.8, 79.2, 74.7, 25.9, 18.2; **FTIR** (KBr, thin film, cm^{-1}): 3416, 3059, 3026, 2972, 2930, 2913, 1674, 1493, 1447, 1258, 1180, 1034, 999, 924, 851, 754, 700; **HRMS** (ESI) Calcd for $C_{14}H_{19}O_2$ [M + H]$^+$ 219.1385, found 219.1383.

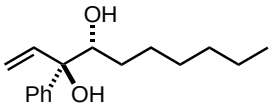

(3*R,4*R**)-3-Phenyldec-1-ene-3,4-diol (3al):** The reaction was conducted with 0.1 equiv. of 2,2'-bipyridine at 80 °C for 1 h. Colorless oil (33.4 mg, 45%); R_f 0.31 (hexane/EtOAc = 4/1); 8:1 dr (determined by ^{1}H NMR of the crude mixture); **^{1}H NMR** (400 MHz, $CDCl_3$) δ 7.50-7.48 (m, 2H), 7.38-7.34 (m, 2H), 7.29-7.25 (m, 1H), 6.27 (dd, *J* = 17.1, 10.8 Hz, 1H), 5.46 (dd, *J* = 17.1, 1.4 Hz, 1H), 5.29 (dd, *J* = 10.8, 1.4 Hz, 1H), 3.87 (d, *J* = 9.9 Hz, 1H), 2.79 (s, 1H), 1.76 (br s, 1H), 1.54-1.50 (m, 2H), 1.39-

1.19 (m, 8H), 0.86 (t, J = 6.9 Hz, 3H); **^{13}C{^{1}H} NMR** (100 MHz, $CDCl_3$) δ 143.7, 139.2, 128.4, 127.3, 126.0, 115.3, 79.4, 77.8, 31.7, 30.9, 29.2, 26.5, 22.6, 14.0; **FTIR** (KBr, thin film, cm^{-1}): 3443, 2953, 2926, 2857, 1491, 1447, 1076, 991, 924, 756, 700, 633; **HRMS** (ESI) Calcd for $C_{16}H_{25}O_2$ $[M + H]^+$ 249.1855, found 249.1857.

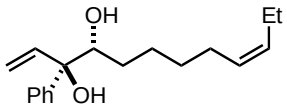

(3*R,4*R**,*Z*)-3-Phenyldodeca-1,9-diene-3,4-diol (3am):** The reaction was conducted with 0.1 equiv. of 2,2'-bipyridine at 80 °C for 1 h. Colorless oil (37.3 mg, 45%); R_f 0.31 (hexane/EtOAc = 4/1); 9:1 dr (determined by ^{1}H NMR of the crude mixture); **^{1}H NMR** (400 MHz, $CDCl_3$) δ 7.50-7.48 (m, 2H), 7.38-7.34 (m, 2H), 7.29-7.25 (m, 1H), 6.27 (dd, J = 17.1, 10.8 Hz, 1H), 5.46 (dd, J = 17.1, 1.4 Hz, 1H), 5.37-5.25 (m, 3H), 3.87 (dd, J = 9.7 Hz, 1H), 2.80 (br s, 1H), 2.03-1.94 (m, 4H), 1.78 (br s, 1H), 1.55-1.51 (m, 2H), 1.40-1.26 (m, 4H), 0.93 (t, J = 7.5 Hz, 3H); **^{13}C{^{1}H} NMR** (100 MHz, $CDCl_3$) δ 143.7, 139.1, 131.7, 128.9, 128.4, 127.4, 126.0, 115.3, 79.3, 77.7, 30.7, 29.5, 26.9, 26.1, 20.5, 14.3; **FTIR** (KBr, thin film, cm^{-1}): 3443, 2859, 2932, 2857, 1447, 1074, 993, 924, 756, 700; **HRMS** (ESI) Calcd for $C_{18}H_{27}O_2$ $[M + H]^+$ 275.2011, found 275.2018.

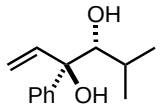

(3*R,4*R**)-5-Methyl-3-phenylhex-1-ene-3,4-diol (3an):** Colorless oil (33.6 mg, 54%); R_f 0.40 (hexane/EtOAc = 4/1); >20:1 dr (determined by ^{1}H NMR of the crude mixture); **^{1}H NMR** (400 MHz, $CDCl_3$) δ 7.50-7.48 (m, 2H), 7.37-7.33 (m, 2H), 7.27-7.23 (m, 1H), 6.26 (dd, J = 17.1, 10.8 Hz, 1H), 5.46 (dd, J = 17.1, 1.5 Hz, 1H), 5.23 (dd, J = 10.8, 1.5 Hz, 1H), 3.80 (dd, J = 4.7, 3.6 Hz, 1H), 2.86 (s, 1H), 1.94 (septet of d, J = 7.0, 3.4 Hz, 1H), 1.80 (d, J = 5.4 Hz, 1H), 0.96 (d, J = 6.8 Hz, 3H), 0.91 (d, J = 6.9 Hz, 3H); **^{13}C{^{1}H} NMR** (100 MHz, $CDCl_3$) δ 144.8, 139.5, 128.3, 127.2, 125.8, 114.2, 80.9, 79.7, 29.1, 22.2, 16.5; **FTIR** (KBr, thin film, cm^{-1}): 3447, 2963, 2874, 1709, 1470, 1447, 1410, 1391, 1368, 1169, 993, 920, 752, 702; **HRMS** (ESI) Calcd for $C_{13}H_{19}O_2$ $[M + H]^+$ 207.1385, found 207.1380.

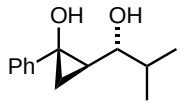

(1*R,2*R**)-2-((*R**)-1-Hydroxy-2-methylpropyl)-1-phenylcyclopropan-1-ol (4an):** White solid (major diastereomer: 15.6 mg) and colorless oil (minor diastereomer: 2.2 mg, 29% overall yield, 7:1 dr); R_f 0.56 (major diastereomer), 0.37 (minor diastereomer) (hexane/EtOAc = 3/2); m.p. (major diastereomer) 88-89 °C; **^{1}H NMR** (400 MHz, $CDCl_3$) major diastereomer: δ 7.35-7.29 (m, 4H), 7.24-7.19 (m, 1H), 3.49 (dt, *J* = 6.5, 1.7 Hz, 1H), 3.26 (br s, 1H), 2.18 (br s, 1H), 1.88 (oct, *J* = 6.7 Hz, 1H), 1.36-1.29 (m, 2H), 1.22-1.16 (m, 1H), 1.04-1.02 (m, 6H); **^{13}C{^{1}H} NMR** (100 MHz, $CDCl_3$) major diastereomer: δ 144.5, 128.3, 126.5, 124.4, 78.8, 58.8, 34.5, 31.8, 22.5, 18.7, 18.4; **^{1}H NMR** (400 MHz, $CDCl_3$) minor diastereomer: δ 7.36-7.29 (m, 4H), 7.26-7.21 (m, 1H), 3.78-3.76 (m, 1H), 2.72 (br s, 1H), 2.15 (br s, 1H), 1.90-1.79 (m, 1H), 1.33-1.27 (m, 3H), 1.02-0.98 (m, 6H); **^{13}C{^{1}H} NMR** (100 MHz, $CDCl_3$) minor diastereomer: δ 144.0, 128.4, 126.5, 124.2, 74.2, 59.6, 34.5, 31.4, 18.5, 18.4, 17.9; **FTIR** (KBr, $CHCl_3$, cm^{-1}) major diastereomer: 3433, 3065, 2963, 1466, 1458, 698; **HRMS** (ESI) Calcd for $C_{13}H_{19}O_2$ $[M + H]^+$ 207.1385, found 207.1391.

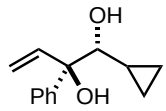

(1*R,2*R**)-1-Cyclopropyl-2-phenylbut-3-ene-1,2-diol (3ao):** Colorless oil (27.3 mg, 45%); R_f 0.28 (hexane/EtOAc = 3/1); >20:1 dr (determined by ^{1}H NMR of the crude mixture); **^{1}H NMR** (400 MHz, $CDCl_3$) δ 7.52-7.50 (m, 2H), 7.37-7.33 (m, 2H), 7.28-7.24 (m, 1H), 6.43 (dd, *J* = 17.2, 10.8 Hz, 1H), 5.42 (dd, *J* = 17.2, 1.4 Hz, 1H), 5.29 (dd, *J* = 10.8, 1.4 Hz, 1H), 3.30 (dd, *J* = 8.0, 4.0 Hz, 1H), 2.95 (s, 1H), 1.92 (d, *J* = 4.3 Hz, 1H), 1.06-0.97 (m, 1H), 0.53-0.41 (m, 2H), 0.35-0.29 (m, 1H), 0.11-0.05 (m, 1H); **^{13}C{^{1}H} NMR** (100 MHz, $CDCl_3$) δ 143.6, 139.5, 128.2, 127.2, 126.2, 115.2, 81.3, 79.5, 12.4, 4.4, 1.9; **FTIR** (KBr, thin film, cm^{-1}): 3443, 3084, 3007, 2891, 1670, 1493, 1447, 1410, 993, 760, 702; **HRMS** (ESI) Calcd for $C_{13}H_{17}O_2$ $[M + H]^+$ 205.1229, found 205.1229.

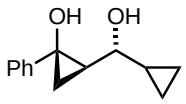

(1*R,2*R**)-2-((*R**)-Cyclopropyl(hydroxy)methyl)-1-phenylcyclopropan-1-ol (4ao):** Colorless oil (major diastereomer: 9.8 mg) and colorless oil (minor diastereomer: 4.2 mg, 23% overall yield, 2:1 dr); R_f 0.35 (major diastereomer), 0.24 (minor diastereomer) (hexane/EtOAc = 3/2); **^{1}H NMR** (400 MHz, $CDCl_3$) major diastereomer: δ 7.34-7.29 (m, 4H), 7.23-7.19 (m, 1H), 3.38 (br s, 1H), 3.13 (t, *J* = 8.3 Hz, 1H), 2.32 (br s, 1H), 1.51-1.44 (m, 1H), 1.30-1.26 (m, 1H), 1.19-1.11 (m, 2H), 0.62-0.51 (m, 2H), 0.39-0.31 (m, 2H); **^{13}C{^{1}H} NMR** (100 MHz, $CDCl_3$) major diastereomer: δ 144.3, 128.3, 126.4, 124.4, 77.4, 58.8, 33.0, 21.6, 17.5, 2.6, 2.4; **^{1}H NMR** (400 MHz, $CDCl_3$) minor diastereomer: δ 7.36-7.30 (m, 4H), 7.26-7.21 (m, 1H), 3.36 (dd, *J* = 8.4, 5.0 Hz, 1H), 3.05 (br s, 1H), 2.36 (br s, 1H), 1.46-1.37 (m, 2H), 1.31-1.27 (m, 1H), 1.19-1.10 (m, 1H), 0.61-0.50 (m, 2H), 0.43-0.33 (m, 2H); **^{13}C{^{1}H} NMR** (100 MHz, $CDCl_3$) minor diastereomer: δ 144.0, 128.4, 126.6, 124.5, 74.4, 59.9, 32.5, 18.3, 18.0, 3.2, 2.0; **FTIR** (KBr, thin film, cm^{-1}) major diastereomer: 3445, 3082, 3065, 3007, 1715, 1682, 1597, 1449, 1271, 1026, 714, 700; **HRMS** (ESI) Calcd for $C_{13}H_{17}O_2$ $[M + H]^+$ 205.1229, found 205.1225.

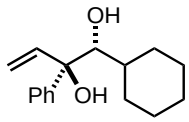

(1*R,2*R**)-1-Cyclohexyl-2-phenylbut-3-ene-1,2-diol (3ap):** White solid (33.9 mg, 46%); R_f 0.35 (hexane/EtOAc = 4/1); 16:1 dr (determined by ^{1}H NMR of the crude mixture); m.p. 103-104 °C; **^{1}H NMR** (400 MHz, $CDCl_3$) δ 7.50-7.48 (m, 2H), 7.37-7.34 (m, 2H), 7.28-7.24 (m, 1H), 6.27 (dd, *J* = 17.1, 10.8 Hz, 1H), 5.46 (dd, *J* = 17.1, 1.5 Hz, 1H), 5.25 (dd, *J* = 10.8, 1.5 Hz, 1H), 3.77 (dd, *J* = 5.2, 3.7 Hz, 1H), 2.87 (s, 1H), 1.94-1.92 (m, 1H), 1.73-1.60 (m, 5H), 1.47-1.45 (m, 1H), 1.28-1.09 (m, 5H); **^{13}C{^{1}H} NMR** (100 MHz, $CDCl_3$) δ 144.7, 139.5, 128.3, 127.2, 125.8, 114.3, 80.9, 79.7, 39.1, 32.1, 26.9, 26.5, 26.2, 26.1; **FTIR** (KBr, $CHCl_3$, cm^{-1}): 3580, 3011, 2928, 2855, 1449, 989, 924, 629; **HRMS** (ESI) Calcd for $C_{16}H_{23}O_2$ $[M + H]^+$ 247.1698, found 247.1700.

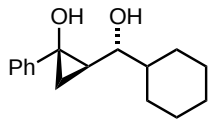

(1*R,2*R**)-2-((*R**)-Cyclohexyl(hydroxy)methyl)-1-phenylcyclopropan-1-ol (4ap):** White solid (major diastereomer: 20.5 mg) and colorless oil (minor diastereomer: 2.9 mg, 32% overall yield, 7:1 dr); R_f 0.23 (major diastereomer), 0.14 (minor diastereomer) (hexane/EtOAc = 4/1); m.p. (major diastereomer) 88-89 °C; **^{1}H NMR** (400 MHz, $CDCl_3$) major diastereomer: δ 7.33-7.25 (m, 4H), 7.22-7.18 (m, 1H), 3.50 (br s, 1H), 3.46 (dd, *J* = 8.2, 6.8 Hz, 1H), 2.38 (br s, 1H), 1.94-1.67 (m, 5H), 1.58-1.49 (m, 1H), 1.36-1.01 (m, 8H); **^{13}C{^{1}H} NMR** (100 MHz, $CDCl_3$, +; positive DEPT 135 signal, –; negative DEPT 135 signal) major diastereomer: δ 144.6, 128.3 (+), 126.4 (+), 124.4 (+), 78.0 (+), 58.7, 44.4 (+), 31.9 (+), 29.1 (–), 28.9 (–), 26.5 (–), 26.2 (–), 26.1 (–), 22.6 (–); **^{1}H NMR** (400 MHz, $CDCl_3$) minor diastereomer: δ 7.37-7.28 (m, 4H), 7.25-7.22 (m, 1H), 3.77-3.74 (m, 1H), 2.60 (br s, 1H), 2.03 (br s, 1H), 1.96-1.93 (m, 1H), 1.79-1.74 (m, 3H), 1.69-1.66 (m, 1H), 1.55-1.47 (m, 1H), 1.36-1.08 (m, 8H); **^{13}C{^{1}H} NMR** (100 MHz, $CDCl_3$) minor diastereomer: δ 144.1, 128.4, 126.5, 124.1, 73.8, 59.8, 44.6, 31.7, 28.7, 28.5, 26.5, 26.3, 26.2, 18.8; **FTIR** (KBr, $CHCl_3$, cm^{-1}) major diastereomer: 3462, 3065, 2928, 2855, 1450, 1107, 893, 698; **HRMS** (ESI) Calcd for $C_{16}H_{23}O_2$ [M + H]$^+$ 247.1698, found 247.1693.

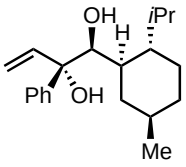

(1*R*,2*R*)-1-((1*R*,2*S*,5*R*)-2-Isopropyl-5-methylcyclohexyl)-2-phenylbut-3-ene-1,2-diol (3aq): White solid (45.5 mg, 50%); R_f 0.36 (hexane/EtOAc = 8/1); 18:1 dr (determined by ^{1}H NMR of the crude mixture); m.p. 112-114 °C; **^{1}H NMR** (400 MHz, $CDCl_3$) δ 7.50-7.47 (m, 2H), 7.37-7.33 (m, 2H), 7.27-7.23 (m, 1H), 6.25 (dd, *J* = 17.1, 10.8 Hz, 1H), 5.43 (dd, *J* = 17.1, 1.5 Hz, 1H), 5.21 (dd, *J* = 10.8, 1.5 Hz, 1H), 4.20 (d, *J* = 4.1 Hz, 1H), 2.91 (s, 1H), 2.06-1.94 (m, 2H), 1.70-1.57 (m, 4H), 1.32-1.24 (m, 2H), 1.02-0.78 (m, 9H), 0.64 (d, *J* = 6.9 Hz, 3H); **^{13}C{^{1}H} NMR** (100 MHz, $CDCl_3$) δ 145.5, 139.4, 128.4, 127.1, 125.7, 113.9, 79.8, 74.6, 43.2, 40.1, 35.0, 34.0, 32.5, 26.5, 24.3, 23.0, 21.5, 15.1; **FTIR** (KBr, $CHCl_3$, cm^{-1}): 3397, 2951, 2916, 2864, 1456, 1447, 1412, 1383, 1170, 993, 924, 702; **HRMS** (ESI) Calcd for $C_{20}H_{31}O_2$ [M + H]$^+$ 303.2324, found 303.2328. $[\alpha]^{25}_D$ = –10.4 (*c* = 1.46 in $CHCl_3$).

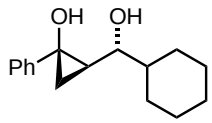

(1*R,2*R**)-2-((*S**)-1-Hydroxy-2,2-dimethylpropyl)-1-phenylcyclopropan-1-ol (4ar):** White solid (44.3 mg, 67%); R_f 0.25 (hexane/EtOAc = 4/1); >20:1 dr (determined by ^{1}H NMR of the crude mixture); m.p. 85-87 °C; **^{1}H NMR** (400 MHz, $CDCl_3$) δ 7.32-7.27 (m, 4H), 7.22-7.18 (m, 1H), 3.73 (br s, 1H), 3.41-3.35 (m, 1H), 2.45 (br s, 1H), 1.35-1.28 (m, 2H), 1.21-1.17 (m, 1H), 0.98 (s, 9H); **^{13}C{^{1}H} NMR** (100 MHz, $CDCl_3$, +; positive DEPT 135 signal, –; negative DEPT 135 signal) δ 144.7, 128.3 (+), 126.3 (+), 124.4 (+), 81.5 (+), 58.5, 35.6, 29.9 (+), 26.0 (+), 23.5 (–); **FTIR** (KBr, $CHCl_3$, cm^{-1}): 3441, 2961, 2907, 2870, 1290, 1107, 1047, 1003; **HRMS** (ESI) Calcd for $C_{14}H_{21}O_2$ $[M + H]^+$ 221.1542, found 221.1546.

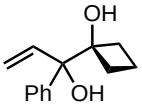

1-(1-Hydroxy-1-phenylallyl)cyclobutan-1-ol (3as): The reaction was conducted with 3 equiv. of Et_2Zn and without 2,2'-bipyridine in DMSO at 80 °C for 1 h. Colorless oil (28.9 mg, 47%); R_f 0.33 (hexane/EtOAc = 4/1); **^{1}H NMR** (400 MHz, $CDCl_3$) δ 7.58-7.55 (m, 2H), 7.37-7.33 (m, 2H), 7.29-7.25 (m, 1H), 6.52 (dd, *J* = 17.1, 10.8 Hz, 1H), 5.49 (dd, *J* = 17.2, 1.4 Hz, 1H), 5.35 (dd, *J* = 10.8, 1.4 Hz, 1H), 2.58 (s, 1H), 2.55-2.40 (m, 2H), 2.00-1.77 (m, 4H), 1.33-1.24 (m, 1H); **^{13}C{^{1}H} NMR** (100 MHz, $CDCl_3$) δ 142.1, 139.5, 128.1, 127.3, 126.6, 115.6, 80.0, 79.3, 31.3, 31.0, 12.7; **FTIR** (KBr, thin film, cm^{-1}): 3445, 3057, 2990, 2947, 1491, 1447, 1418, 1339, 1256, 1155, 1117, 995, 926, 756, 704; **HRMS** (ESI) Calcd for $C_{13}H_{17}O_2$ $[M + H]^+$ 205.1229, found 205.1225.

DFT Calculations

All the density functional theory (DFT) calculations were performed using Gaussian 16 program.[20] In view of the related DFT studies on the aldehyde allylation with allylzinc reagents reported by Houk, Marek and coworkers (which employed M05-2X/6-31G(d) level),[17, 21] geometry optimizations were performed with the M06-2X functional[22] using the 6-31G(d) basis set. Harmonic frequency calculations were performed for each stationary point to ensure that it is either an energy minimum (no imaginary frequency) or a transition state (only one imaginary frequency). The single-point energy calculations were performed with the M06-02X functional and the 6-

31+G(d,p) basis set, using the SMD model[23] (solvent = THF) to obtain energies in solution. The single-point energies corrected by the thermal correction to Gibbs free energies (TCG, obtained from frequency calculations) were used as the Gibbs free energies reported in the main text, corresponding to the reference state of 1 mol/L, 298.15 K. The 3-D structures were drawn using CYLview software.[24]

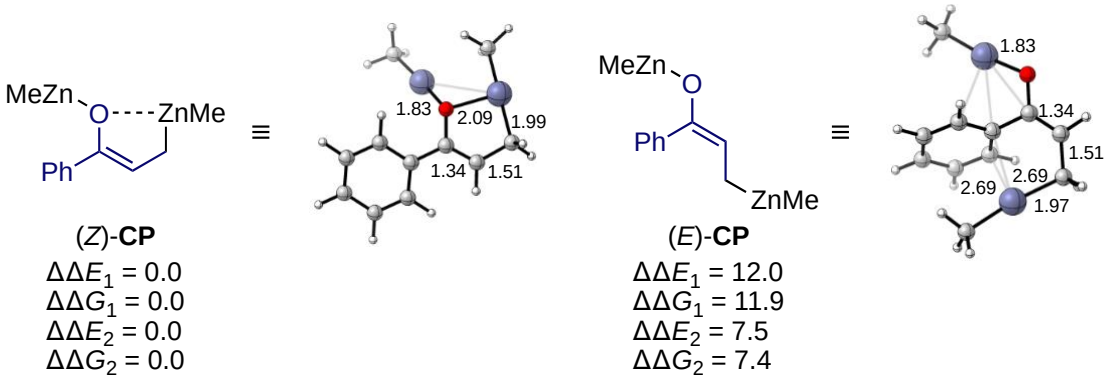

Figure 4.2. Structures of (*Z*)- and (*E*)-isomers of enolized homoenolate derived from 1-phenylcyclopropanol. Bond lengths are in Å. The definitions of the energies (kcal mol^{-1}) are as follows: E_1, electronic energy calculated at M06-2X/6-31G(d); G_1, Gibbs free energy calculated at M06-2X/6-31G(d); E_2, electronic energy calculated at M06-2X(SMD,THF)/6-31+G(d,p)//M06-2X/6-31G(d); G_2, sum of E_2 and TCG at M06-2X/6-31G(d).

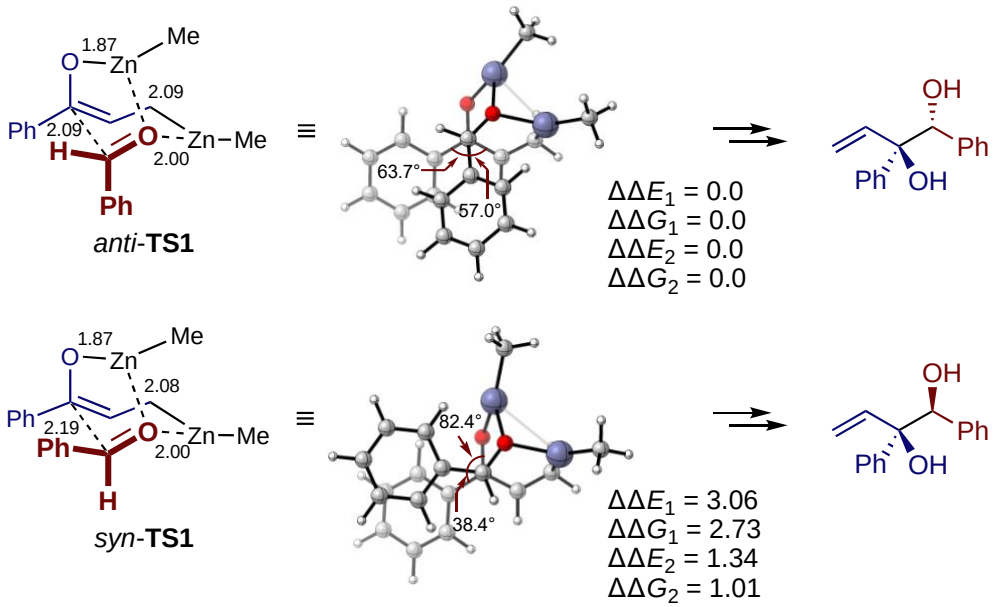

Figure 4.3. Structures of *anti*- and *syn*-TSs for the hydroxyallylation of benzaldehyde with 1-phenylcyclopropanol-derived enolized homoenolate. For the definitions of E_1,

G_1, E_2, and G_2, see the caption of Figure 4.2.

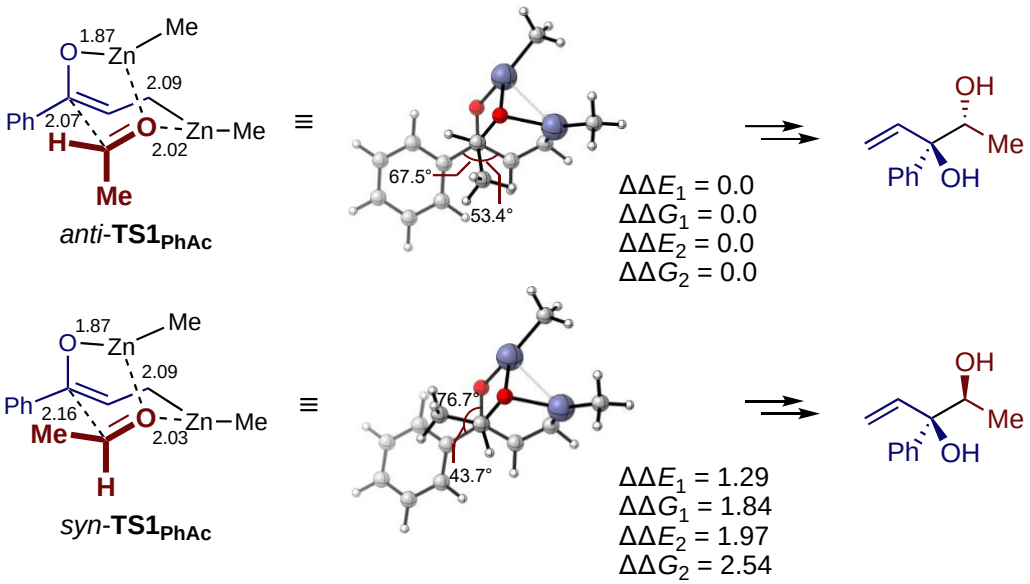

Figure 4.4. Structures of *anti*- and *syn*-TSs for the hydroxyallylation of acetaldehyde with 1-phenylcyclopropanol-derived enolized homoenolate. For the definitions of E_1, G_1, E_2, and G_2, see the caption of Figure 4.2.

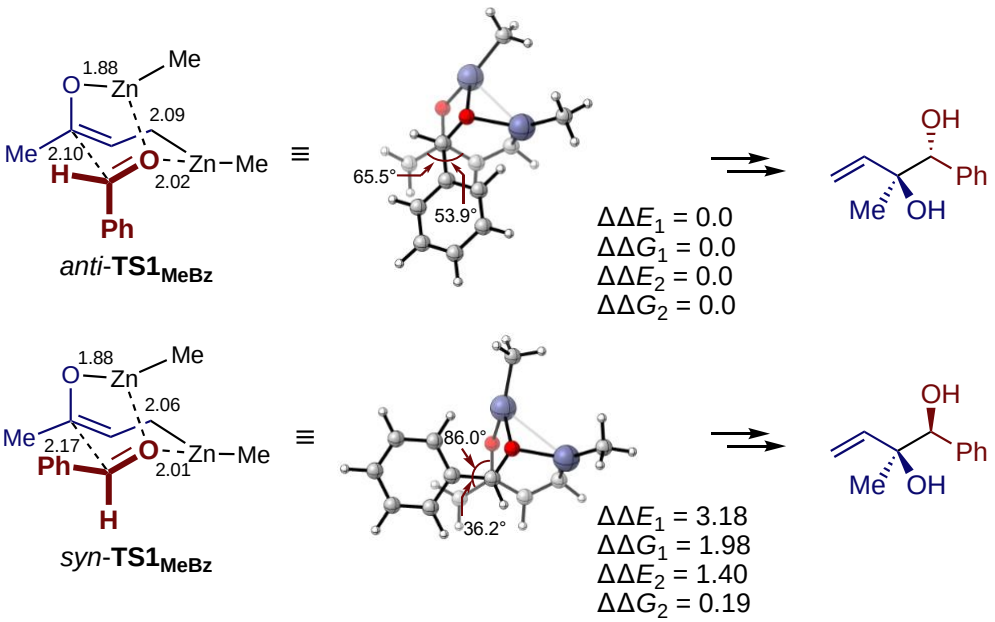

Figure 4.5. Structures of *anti*- and *syn*-TSs for the hydroxyallylation of benzaldehyde with 1-methylcyclopropanol-derived enolized homoenolate. For the definitions of E_1, G_1, E_2, and G_2, see the caption of Figure 4.2.

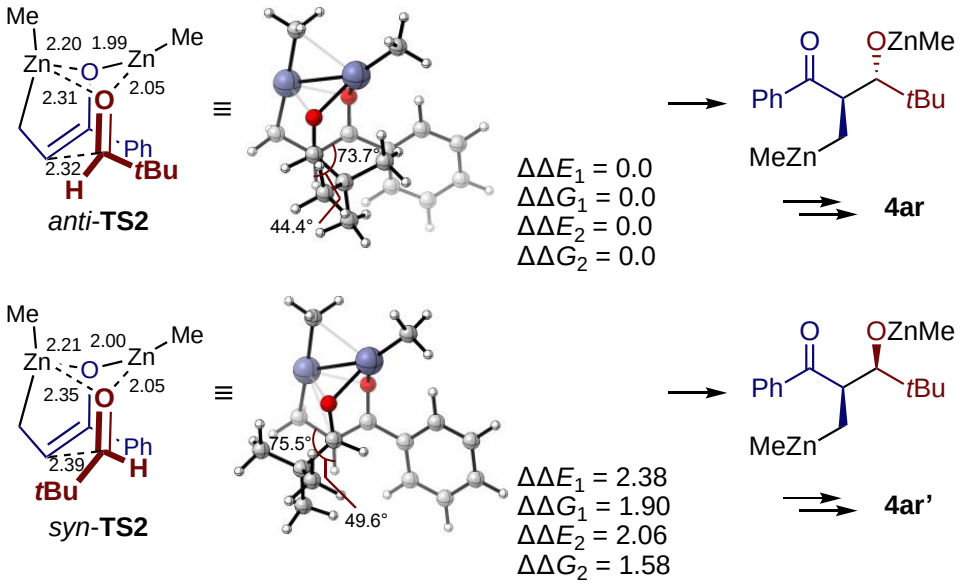

Figure 4.6. Structures of *anti*- and *syn*-TSs for the aldol reaction of pivalaldehyde with 1-phenylcyclopropanol-derived enolized homoenolate. For the definitions of E_1, G_1, E_2, and G_2, see the caption of Figure 4.2.

Table 4.2. Energy data (hartrees).

Structure	E_1[a]	TCG[b]	E_2[c]	E_2 + TCG	Imaginary Frequency
(*Z*)-**CP**	-4060.72641558	0.170030	-4060.87642005	-4060.70639005	-
(*E*)-**CP**	-4060.70737913	0.169909	-4060.86444972	-4060.69454072	-
anti-**TS1**	-4406.18503422	0.277651	-4406.34210014	-4406.06444914	255.78i
syn-**TS1**	-4406.18015521	0.277129	-4406.33996885	-4406.06283985	193.63i
anti-$\mathbf{TS1_{PhAc}}$	-4214.51473955	0.227083	-4214.66099237	-4214.43390937	244.97i
syn-$\mathbf{TS1_{PhAc}}$	-4214.51268146	0.227958	-4214.65785341	-4214.42989541	194.95i
anti-$\mathbf{TS1_{MeBz}}$	-4214.51866489	0.228772	-4214.66161208	-4214.43284008	230.80i
syn-$\mathbf{TS1_{MeBz}}$	-4214.51358994	0.226854	-4214.65938503	-4214.43253103	197.30i
anti-**TS2**	-4332.40668366	0.310711	-4332.54815356	-4332.23744256	152.82i
syn-**TS2**	-4332.40288787	0.309944	-4332.54487565	-4332.23493165	149.40i

[a]Energy of the structure optimized at M06-2X/6-31G(d). [b]Thermal correction to Gibbs free energy (1 mol/L, 298.15 K). [c]Single-point energy calculated at M06-2X (SMD, THF)/6-31+G(d,p).

Cartesian Coordinates

(*Z*)-**CP**

C	-0.065414	-2.402675	0.056680
H	0.657831	-3.197897	0.233261
C	0.410236	-1.166289	-0.168539
C	-1.542287	-2.708429	0.051014
H	-1.782747	-3.366722	-0.794620
H	-1.802768	-3.284314	0.946871
O	-0.476378	-0.166275	-0.486086
Zn	-2.384930	-0.914001	-0.065258
C	-3.212948	0.896265	0.099728
H	-3.025506	1.365706	1.077424
H	-2.843035	1.597742	-0.666869
H	-4.300872	0.908125	-0.014473
Zn	-0.473949	1.572638	0.074806
C	-0.371543	3.444442	0.535647
H	0.657529	3.811938	0.504681
H	-0.966161	4.044075	-0.159551
H	-0.760204	3.624592	1.541769
C	1.829205	-0.751965	-0.123414
C	2.247755	0.397832	-0.807160
C	2.778207	-1.456586	0.629793
C	3.572856	0.824050	-0.752427

H	1.539531	0.933069	-1.434906
C	4.100354	-1.035117	0.679840
H	2.465275	-2.326608	1.198332
C	4.504776	0.109080	-0.008176
H	3.875501	1.711282	-1.300274
H	4.818564	-1.593402	1.272623
H	5.537300	0.439864	0.040045

(*E*)-**CP**

C	-0.687722	-2.432696	-0.132218
H	-0.380241	-3.474357	-0.033373
C	0.295188	-1.533104	0.022270
C	-2.137653	-2.120965	-0.398405
H	-2.383443	-2.320388	-1.452547
H	-2.758319	-2.828360	0.165953
O	1.582926	-1.844498	0.302137
Zn	-2.603004	-0.274887	0.119894
C	-3.321250	1.434521	0.755344
H	-2.583015	1.986163	1.348248
H	-3.609739	2.089051	-0.075141
H	-4.208360	1.306705	1.384141
Zn	2.704977	-0.426344	0.086872
C	4.051819	0.944785	-0.131173

H	3.625952	1.796394	-0.671367
H	4.406624	1.315953	0.834847
H	4.922733	0.597257	-0.692428
C	0.067580	-0.056856	-0.108216
C	0.473509	0.800190	0.929927
C	-0.443896	0.511716	-1.284451
C	0.356023	2.181904	0.800915
H	0.830814	0.365432	1.862723
C	-0.553106	1.896395	-1.414173
H	-0.722271	-0.148318	-2.101958
C	-0.154364	2.732127	-0.373657
H	0.652404	2.828595	1.620922
H	-0.946351	2.322206	-2.332132
H	-0.246152	3.808513	-0.474929

anti-**TS1**

C	-0.113802	-0.207069	1.560918
H	-0.745598	0.630141	1.845489
C	-0.662512	-1.148807	0.652826
C	1.224729	-0.190242	1.959334
H	1.477084	0.476578	2.782289
H	1.735848	-1.155041	2.011063
O	0.055072	-2.196833	0.260471

Zn	2.297773	0.855752	0.395300
C	3.908124	1.980113	0.258414
H	4.693046	1.646475	0.943942
H	4.325745	1.955640	-0.753034
H	3.694618	3.027835	0.497251
Zn	1.746703	-1.867637	-0.470313
C	3.650363	-2.272858	-0.683590
H	4.269656	-1.390519	-0.478666
H	3.979569	-3.063840	-0.003891
H	3.893689	-2.593838	-1.700826
C	-0.182148	0.170281	-0.900637
O	1.130099	0.056432	-1.013648
H	-0.759924	-0.527440	-1.512388
C	-0.778629	1.510491	-0.752976
C	-2.165439	1.672719	-0.888667
C	0.004421	2.631009	-0.448587
C	-2.751491	2.914801	-0.677814
H	-2.779727	0.819157	-1.161797
C	-0.584939	3.873164	-0.238620
H	1.089659	2.562441	-0.437101
C	-1.966300	4.016725	-0.340705
H	-3.826510	3.023821	-0.782565
H	0.038697	4.732270	-0.012050

H	-2.426689	4.986184	-0.179218
C	-2.141997	-1.278985	0.501678
C	-2.626826	-2.145918	-0.485122
C	-3.063163	-0.545492	1.258032
C	-3.990140	-2.246850	-0.736869
H	-1.912732	-2.739826	-1.046277
C	-4.428663	-0.649806	1.008226
H	-2.726527	0.107855	2.055768
C	-4.898064	-1.492267	0.004467
H	-4.346367	-2.919864	-1.510921
H	-5.127184	-0.072634	1.606386
H	-5.963146	-1.571704	-0.189479

syn-**TS1**

C	0.580000	-2.041771	-0.603309
H	0.200042	-2.872566	-0.014125
C	-0.313161	-0.980447	-0.900033
C	1.937082	-2.036313	-0.950621
H	2.458187	-2.988467	-0.870007
H	2.189941	-1.458906	-1.842160
O	0.106698	0.010978	-1.664969
Zn	2.888994	-0.923640	0.592647
C	4.531529	-0.948333	1.674620

H	5.250775	-1.689920	1.315425
H	5.030646	0.025534	1.666681
H	4.307482	-1.186252	2.719904
Zn	1.296993	1.318492	-1.043280
C	2.451546	2.841022	-1.472566
H	3.512008	2.568983	-1.453349
H	2.240677	3.242768	-2.467767
H	2.319436	3.656116	-0.753810
C	0.228183	-0.219869	1.079613
O	1.379996	0.365419	0.798513
H	0.266779	-1.108076	1.718637
C	-0.943855	0.636670	1.283479
C	-2.099016	0.117635	1.884260
C	-0.958084	1.958197	0.822304
C	-3.250346	0.884837	1.979824
H	-2.093231	-0.902745	2.256613
C	-2.113448	2.727686	0.919272
H	-0.046481	2.421482	0.451562
C	-3.264955	2.190100	1.486423
H	-4.141712	0.462594	2.432868
H	-2.107694	3.753012	0.563027
H	-4.166640	2.789856	1.559309
C	-1.790463	-1.181096	-0.831762

C	-2.609686	-0.178126	-1.359751
C	-2.396743	-2.283700	-0.217403
C	-3.993646	-0.263137	-1.259076
H	-2.138415	0.670725	-1.841345
C	-3.781743	-2.370017	-0.120300
H	-1.797921	-3.089090	0.197470
C	-4.587536	-1.357129	-0.635191
H	-4.610701	0.531551	-1.667778
H	-4.232071	-3.234850	0.357872
H	-5.668205	-1.425714	-0.557068

anti-**TS1$_{PhAc}$**

C	-0.341759	-0.780327	-1.290198
H	-0.786102	-1.767816	-1.376679
C	-1.081177	0.205064	-0.606158
C	0.984959	-0.607711	-1.744251
H	1.326296	-1.368791	-2.445760
H	1.228058	0.400104	-2.094625
O	-0.618653	1.445824	-0.512583
Zn	2.298288	-0.996451	-0.112863
C	4.012728	-1.844978	0.340320
H	4.589192	-1.224890	1.034091
H	3.862582	-2.815780	0.824877

H	4.635107	-2.014212	-0.543308
Zn	1.134676	1.664843	0.112011
C	2.906432	2.497303	0.043655
H	3.703055	1.743211	0.081230
H	3.050361	3.072536	-0.875433
H	3.083392	3.175310	0.883791
C	-0.249501	-0.614445	1.101786
O	0.977737	-0.138489	1.152095
C	-0.415093	-2.096904	1.295144
H	-0.203393	-2.343482	2.342067
H	-1.433549	-2.419860	1.062343
H	0.295479	-2.658315	0.675340
H	-0.998084	0.002100	1.607559
C	-2.547635	0.037633	-0.347498
C	-3.230437	1.106999	0.241212
C	-3.259523	-1.135206	-0.628636
C	-4.583490	1.005793	0.548046
H	-2.680766	2.020304	0.438792
C	-4.611983	-1.236228	-0.318926
H	-2.774170	-1.978380	-1.110268
C	-5.280251	-0.167354	0.272948
H	-5.095661	1.849329	1.000948
H	-5.146532	-2.152516	-0.550170

H	-6.336486	-0.247132	0.510017

syn-**TS1**$_{\mathbf{PhAc}}$

C	-0.311711	-0.971652	-1.214733
H	-0.764540	-1.957864	-1.270269
C	-1.061321	0.049153	-0.605049
C	1.012476	-0.807546	-1.703230
H	1.332138	-1.598704	-2.381799
H	1.209951	0.179778	-2.134812
O	-0.607764	1.293473	-0.575649
Zn	2.377965	-1.051902	-0.120980
C	4.112105	-1.802516	0.418090
H	4.656894	-1.107261	1.064733
H	3.990240	-2.735219	0.978944
H	4.751712	-2.020792	-0.442158
Zn	1.153037	1.551578	0.013233
C	2.923701	2.378423	-0.124923
H	3.721507	1.627966	-0.052667
H	3.056717	2.899786	-1.077190
H	3.109203	3.103082	0.673389
C	-0.148883	-0.717878	1.195301
O	1.053614	-0.196868	1.160517
C	-1.103801	-0.061026	2.152326

H	-2.081884	-0.542284	2.162832
H	-0.659378	-0.123520	3.152134
H	-1.223253	0.996902	1.891295
H	-0.210463	-1.810530	1.133506
C	-2.530706	-0.118816	-0.389674
C	-3.315369	1.030770	-0.274276
C	-3.147966	-1.369901	-0.260756
C	-4.685663	0.934552	-0.046736
H	-2.829997	1.995246	-0.370964
C	-4.514522	-1.464558	-0.028083
H	-2.563455	-2.284085	-0.319963
C	-5.291265	-0.311434	0.078254
H	-5.280896	1.839067	0.034560
H	-4.974929	-2.442558	0.073936
H	-6.358861	-0.387562	0.258870

anti-**TS1$_{MeBz}$**

C	-0.219343	-0.992020	1.560152
H	-1.254662	-0.939801	1.890309
C	0.102158	-2.041467	0.671719
C	0.673678	0.034671	1.928035
H	0.357109	0.642474	2.775136
H	1.723069	-0.266526	2.008138

C	-0.785464	-3.258259	0.597878
H	-1.809734	-3.043235	0.912262
H	-0.787018	-3.668586	-0.417315
H	-0.373338	-4.027872	1.258116
O	1.335155	-2.219829	0.233973
Zn	0.684288	1.521275	0.399411
C	1.004413	3.446605	0.127293
H	1.257819	3.666195	-0.914915
H	0.125088	4.049264	0.381065
H	1.831231	3.809260	0.745964
Zn	2.211470	-0.738206	-0.510643
C	3.800154	0.379626	-0.760994
H	3.570146	1.440187	-0.599920
H	4.600498	0.112446	-0.065111
H	4.206975	0.299803	-1.773529
C	-0.623914	-0.748246	-0.816456
O	0.368000	0.101105	-1.007769
H	-0.577242	-1.658445	-1.422075
C	-1.987266	-0.212250	-0.614432
C	-3.093090	-1.072932	-0.658384
C	-2.205532	1.146027	-0.358671
C	-4.372197	-0.596016	-0.404307
H	-2.942702	-2.120694	-0.904104

C	-3.487924	1.623186	-0.102372
H	-1.388081	1.859269	-0.422946
C	-4.573714	0.753258	-0.111890
H	-5.217522	-1.276069	-0.442332
H	-3.637569	2.681291	0.088328
H	-5.573814	1.125666	0.084821

syn-**TS1**$_{\mathbf{MeBz}}$

C	-0.606670	-1.780585	1.419879
H	-0.307241	-2.818093	1.278261
C	0.438984	-0.849804	1.621669
C	-1.974561	-1.435572	1.351718
H	-2.667134	-2.269390	1.457011
H	-2.244596	-0.573248	1.967536
C	1.786063	-1.335742	2.093031
H	2.017259	-2.341815	1.731938
H	2.571229	-0.646527	1.772556
H	1.776287	-1.351420	3.187929
O	0.171913	0.411218	1.869679
Zn	-2.365022	-0.731090	-0.590343
C	-3.724624	-0.646752	-2.010101
H	-3.861937	0.377607	-2.370704
H	-3.429954	-1.253058	-2.873299

H	-4.699663	-1.009357	-1.672029
Zn	-0.500076	1.567868	0.550774
C	-1.232129	3.334052	0.131307
H	-2.298284	3.284197	-0.113060
H	-1.124758	4.029021	0.968871
H	-0.728536	3.778910	-0.732855
C	0.425638	-0.889074	-0.544481
O	-0.506354	0.016502	-0.800527
H	0.210232	-1.910645	-0.874125
C	1.829784	-0.488602	-0.733037
C	2.829251	-1.462998	-0.847528
C	2.196619	0.861173	-0.764338
C	4.163629	-1.098248	-0.963425
H	2.549904	-2.514244	-0.839041
C	3.534824	1.226709	-0.870649
H	1.434741	1.636564	-0.767975
C	4.522326	0.249926	-0.964468
H	4.926867	-1.864675	-1.054697
H	3.803994	2.277843	-0.896442
H	5.565262	0.536323	-1.053494

anti-**TS2**

C	0.284139	0.769234	-1.884902

H	1.091516	1.418471	-2.221969
C	0.627716	-0.327496	-1.112288
C	-1.055165	0.817311	-2.583278
H	-0.947848	0.327606	-3.560007
H	-1.344873	1.852306	-2.794453
O	-0.313581	-1.132191	-0.670542
Zn	-2.207913	-0.226636	-1.342688
C	-3.442902	-1.307835	-0.173421
H	-3.704743	-0.887493	0.809032
H	-3.162598	-2.357859	-0.016442
H	-4.402265	-1.351912	-0.703069
Zn	-1.228369	-0.900671	1.081686
C	-1.243668	-1.771286	2.839209
H	-1.896071	-1.241223	3.540858
H	-0.245040	-1.803605	3.288030
H	-1.607232	-2.801455	2.774630
C	-0.515501	1.833103	0.021230
O	-1.409582	1.028614	0.420332
H	-0.796014	2.531604	-0.777830
C	0.550454	2.342733	0.970357
C	2.024593	-0.688932	-0.739669
C	2.235798	-1.656607	0.250582
C	3.138949	-0.133675	-1.380735

C	3.523626	-2.025425	0.622040
H	1.375580	-2.118495	0.725868
C	4.427383	-0.503269	-1.010240
H	3.001061	0.577874	-2.188778
C	4.624823	-1.445649	-0.003568
H	3.666819	-2.771740	1.397155
H	5.279393	-0.063004	-1.518818
H	5.631075	-1.735959	0.281962
C	0.928469	1.294212	2.014349
H	1.678875	1.705429	2.697062
H	0.060360	0.997402	2.612145
H	1.362501	0.403016	1.550425
C	-0.136961	3.534390	1.676163
H	0.553203	3.965911	2.408525
H	-0.407974	4.319668	0.962249
H	-1.042158	3.210914	2.198461
C	1.774017	2.853071	0.210043
H	2.417533	3.427452	0.884220
H	2.360973	2.027061	-0.198729
H	1.477068	3.512592	-0.614025

syn-**TS2**

C	0.198462	1.157430	-1.556118

H 0.847820 2.020650 -1.666681

C 0.778895 -0.040084 -1.183378

C -1.188142 1.163816 -2.128047

H -1.130569 0.831206 -3.175513

H -1.613603 2.168339 -2.143662

O 0.026512 -1.114687 -1.075307

Zn -2.037153 -0.320995 -1.113327

C -2.985639 -1.908300 -0.295669

H -3.272693 -1.836470 0.761843

H -2.558596 -2.908485 -0.454729

H -3.941117 -1.941848 -0.834518

Zn -0.682344 -1.712089 0.700288

C -0.289846 -3.153996 1.973500

H -1.149553 -3.367900 2.615971

H 0.553041 -2.910247 2.628363

H -0.036820 -4.081640 1.449596

C -0.202038 1.206202 0.799452

H 0.848662 0.984706 1.037295

O -1.068233 0.287990 0.933865

C -0.608388 2.648222 1.060846

C 2.202027 -0.171256 -0.771843

C 2.597775 -1.307296 -0.055569

C 3.155923 0.820559 -1.037670

C	3.905441	-1.440731	0.400865
H	1.874027	-2.093820	0.132242
C	4.462336	0.684693	-0.584107
H	2.884609	1.693478	-1.622567
C	4.841384	-0.444253	0.140750
H	4.192242	-2.328356	0.956037
H	5.190642	1.458753	-0.805347
H	5.863212	-0.548811	0.491850
C	-2.091993	2.887507	0.786304
H	-2.328758	2.764273	-0.272149
H	-2.710842	2.192328	1.360144
H	-2.355323	3.909168	1.079750
C	-0.351390	2.793894	2.581047
H	0.709899	2.670527	2.822346
H	-0.658698	3.794777	2.901373
H	-0.927098	2.056073	3.147725
C	0.269757	3.657008	0.319476
H	0.173969	4.643099	0.785430
H	1.327263	3.367673	0.356636
H	-0.030411	3.748115	-0.727763

4.5 References

1. Lombardo, M.; Trombini, C., *α*-Hydroxyallylation Reaction of Carbonyl Compounds. *Chem. Rev.* **2007,** *107*, 3843-3879.

2. Schäfers, F.; Quach, L.; Schwarz, J. L.; Saladrigas, M.; Daniliuc, C. G.; Glorius, F., Direct Access to Monoprotected Homoallylic 1,2-Diols via Dual Chromium/Photoredox Catalysis. *ACS Catal.* **2020,** *10*, 11841-11847.

3. For an alternative approach to the same scaffold, see: Chen, M.; Handa, M.; Roush, W. R., Enantioselective Synthesis of 2-Methyl-1,2-*syn*- and 2-Methyl-1,2-*anti*-3-butenediols via Allene Hydroboration-Aldehyde Allylboration Reaction Sequences. *J. Am. Chem. Soc.* **2009,** *131*, 14602-14603.

4. Mejuch, T.; Botoshansky, M.; Marek, I., Combined Carbometalation-Zinc Homologation-Allylation Reactions as a New Approach for Alkoxyallylation of Aldehydes. *Org. Lett.* **2011,** *13*, 3604-3607.

5. Xiang, M.; Pfaffinger, D. E.; Ortiz, E.; Brito, G. A.; Krische, M. J., Enantioselective Ruthenium-BINAP-Catalyzed Carbonyl Reductive Coupling of Alkoxyallenes: Convergent Construction of *syn-sec,tert*-Diols via (*Z*)-*σ*-Allylmetal Intermediates. *J. Am. Chem. Soc.* **2021,** *143*, 8849-8854.

6. (a) Takai, K.; Morita, R.; Toratsu, C., Stereoselective Cross Pinacol-Type Coupling between *α,β*-Unsaturated Ketones and Aldehydes Mediated by Chromium(II) and R_3SiCl. *Angew. Chem. Int. Ed.* **2001,** *40*, 1116-1119; (b) Takai, K.; Morita, R.; Matsushita, H.; Toratsu, C., Cross-Pinacol-Type Coupling Reactions between *α,β*-Unsaturated Ketones and Aldehydes with Low-Valent Metals. *Chirality* **2003,** *15*, 17-23.

7. Yang, Y.-S.; Shen, Z.-L.; Loh, T.-P., Zn/$InCl_3$-Mediated Pinacol Cross-Coupling Reactions of Aldehydes with *α,β*-Unsaturated Ketones in Aqueous Media. *Org. Lett.* **2009,** *11*, 2213-2215.

8. Nomura, K.; Oshima, K.; Matsubara, S., Stereospecific and Stereoselective Preparation of 2-(1-Hydroxyalkyl)-1-alkylcyclopropanols from *α,β*-Epoxy Ketones and Bis(iodozincio)methane. *Angew. Chem. Int. Ed.* **2005,** *44*, 5860-5863.

9. (a) Nomura, K.; Matsubara, S., A New Zincate-Mediated Rearrangement Reaction of 2-(1-Hydroxyalkyl)-1-alkylcyclopropanol. *Chem. Eur. J.* **2010,** *16*, 703-

708; (b) Nomura, K.; Matsubara, S., Zincate-Mediated Rearrangement Reaction of 2-(1-Hydroxyalkyl)-1-alkylcyclopropanol. *Chem. Commun.* **2009**, 2212-2213.

10. (a) Sekiguchi, Y.; Yoshikai, N., Zinc-Catalyzed *β*-Functionalization of Cyclopropanols via Enolized Homoenolate. *J. Am. Chem. Soc.* **2021,** *143*, 18400-18405; (b) Hirayama, T.; Oshima, K.; Matsubara, S., Preparation of Enolate–Homoenolate Species as (*Z*)-*γ*-Siloxyallylmetal Equivalents: Sequential 1,4-Addition of Bis(iodozincio)methane to 1,4-Dicarbonylbutenes and Cyclopropanation. *Angew. Chem. Int. Ed.* **2005,** *44*, 3293-3296; (c) Huang, W.; Meng, F., Cobalt-Catalyzed Diastereo- and Enantioselective Hydroalkylation of Cyclopropenes with Cobalt Homoenolates. *Angew. Chem. Int. Ed.* **2021,** *60*, 2694-2698; (d) Ryu, I.; Nakahira, H.; Ikebe, M.; Sonoda, N.; Yamato, S.-y.; Komatsu, M., Chelation-Aided Generation of Ketone *α*,*β*-Dianions and Their Use as Copper Ate Complexes. Unprecedented Enolate Intervention in the Conjugate Addition to Enones. *J. Am. Chem. Soc.* **2000,** *122*, 1219-1220.

11. (a) Wildemann, H.; Dünkelmann, P.; Müller, M.; Schmidt, B., A Short Olefin Metathesis-Based Route to Enantiomerically Pure Arylated Dihydropyrans and *α*,*β*-Unsaturated *δ*-Valero Lactones. *J. Org. Chem.* **2003,** *68*, 799-804; (b) Wu, H.; Wang, Q.; Zhu, J., Organocatalytic Enantioselective Acyloin Rearrangement of *α*-Hydroxy Acetals to *α*-Alkoxy Ketones. *Angew. Chem. Int. Ed.* **2017,** *56*, 5858-5861; (c) Hopkins, M. H.; Overman, L. E.; Rishton, G. M., Stereocontrolled Preparation of Tetrahydrofurans from Acid-Promoted Rearrangements of Allylic Acetals. *J. Am. Chem. Soc.* **1991,** *113*, 5354-5365.

12. Das, P. P.; Belmore, K.; Cha, J. K., S_N2' Alkylation of Cyclopropanols via Homoenolates. *Angew. Chem. Int. Ed.* **2012,** *51*, 9517-9520.

13. Parida, B. B.; Das, P. P.; Niocel, M.; Cha, J. K., C-Acylation of Cyclopropanols: Preparation of Functionalized 1,4-Diketones. *Org. Lett.* **2013,** *15*, 1780-1783.

14. Murali, R. V. N. S.; Rao, N. N.; Cha, J. K., C-Alkynylation of Cyclopropanols. *Org. Lett.* **2015,** *17*, 3854-3856.

15. (a) Sekiguchi, Y.; Yoshikai, N., Metal-Catalyzed Transformations of Cyclopropanols via Homoenolates. *Bull. Chem. Soc. Jpn.* **2021,** *94*, 265-280; (b) Mills, L. R.; Rousseaux, S. A. L., Modern Developments in the Chemistry of Homoenolates. *Eur. J. Org. Chem.* **2019,** *2019*, 8-26; (c) Sekiguchi, Y.; Yoshikai, N., Enantioselective Conjugate Addition of Catalytically Generated Zinc Homoenolate. *J. Am. Chem. Soc.* **2021,** *143*, 4775-4781; (d) Mills, L. R.; Barrera Arbelaez, L. M.; Rousseaux, S. A. L.,

Electrophilic Zinc Homoenolates: Synthesis of Cyclopropylamines from Cyclopropanols and Amines. *J. Am. Chem. Soc.* **2017,** *139*, 11357-11360; (e) Kuwajima, I.; Nakamura, E., Metal Homoenolates from Siloxycyclopropanes. *Top. Curr. Chem.* **1990,** *155*, 1-39; (f) McDonald, T. R.; Mills, L. R.; West, M. S.; Rousseaux, S. A. L., Selective Carbon–Carbon Bond Cleavage of Cyclopropanols. *Chem. Rev.* **2021,** *121*, 3-79; (g) Cai, X.; Liang, W.; Dai, M., Total Syntheses via Cyclopropanols. *Tetrahedron* **2019,** *75*, 193-208; (h) Nikolaev, A.; Orellana, A., Transition-Metal-Catalyzed C–C and C–X Bond-Forming Reactions Using Cyclopropanols. *Synthesis* **2016,** *48*, 1741-1768.

16. Spino, C.; Godbout, C.; Beaulieu, C.; Harter, M.; Mwene-Mbeja, T. M.; Boisvert, L., *p*-Menthane-3-carboxaldehyde: A Useful Chiral Auxiliary for the Synthesis of Chiral Quaternary Carbons of High Enantiomeric Purity. *J. Am. Chem. Soc.* **2004,** *126*, 13312-13319.

17. Mejuch, T.; Gilboa, N.; Gayon, E.; Wang, H.; Houk, K. N.; Marek, I., Axial Preferences in Allylation Reactions via the Zimmerman-Traxler Transition State. *Acc. Chem. Res.* **2013,** *46*, 1659-1669.

18. Toratsu, C.; Fujii, T.; Suzuki, T.; Takai, K., Cross-Coupling Reactions between *α*,*β*-Unsaturated Ketones and Aldehydes with $CrCl_2$: Aldol Condensation and Cyclopropanol Formation. *Angew. Chem. Int. Ed.* **2000,** *39*, 2725-2727.

19. Liu, Q.; You, B.; Xie, G.; Wang, X., Developments in the Construction of Cyclopropanols. *Org. Biomol. Chem.* **2020,** *18*, 191-204.

20. Frisch, M. J.; Trucks, G. W.; Schlegel, H. B.; Scuseria, G. E.; Robb, M. A.; Cheeseman, J. R.; Scalmani, G.; Barone, V.; Mennucci, B.; Petersson, G. A.; Nakatsuji, H.; Caricato, M.; Li, X.; Hratchian, H. P.; Izmaylov, A. F.; Bloino, J.; Zheng, G.; Sonnenberg, J. L.; Hada, M.; Ehara, M.; Toyota, K.; Fukuda, R.; Hasegawa, J.; Ishida, M.; Nakajima, T.; Honda, Y.; Kitao, O.; Nakai, H.; Vreven, T.; Montgomery, Jr., J. A.; Peralta, J. E.; Ogliaro, F.; Bearpark, M.; Heyd, J. J.; Brothers, E.; Kudin, K. N.; Staroverov, V. N.; Kobayashi, R.; Normand, J.; Raghavachari, K.; Rendell, A.; Burant, J. C.; Iyengar, S. S.; Tomasi, J.; Cossi, M.; Rega, N.; Millam, N. J.; Klene, M.; Knox, J. E.; Cross, J. B.; Bakken, V.; Adamo, C.; Jaramillo, J.; Gomperts, R.; Stratmann, R. E.; Yazyev, O.; Austin, A. J.; Cammi, R.; Pomelli, C.; Ochterski, J. W.; Martin, R. L.; Morokuma, K.; Zakrzewski, V. G.; Voth, G. A.; Salvador, P.; Dannenberg, J. J.; Dapprich, S.; Daniels, A. D.; Farkas, Ö.; Foresman, J. B.; Ortiz, J. V.; Cioslowski, J.; Fox, D. J. Gaussian 09, Revision D.01, Gaussian, Inc., Wallingford CT, **2010**.

21. Gilboa, N.; Wang, H.; Houk, K. N.; Marek, I., Axial Preferences in Allylations via the Zimmerman-Traxler Transition State. *Chem. Eur. J.* **2011,** *17*, 8000-8004.

22. (a) Zhao, Y.; Truhlar, D. G., Density Functional for Spectroscopy: No Long-Range Self-Interaction Error, Good Performance for Rydberg and Charge-Transfer States, and Better Performance on Average than B3LYP for Ground States. *J. Phys. Chem. A* **2006,** *110*, 13126-13130; (b) Zhao, Y.; Truhlar, D. G., Density Functionals with Broad Applicability in Chemistry. *Acc. Chem. Res.* **2008,** *41*, 157-167; (c) Zhao, Y.; Truhlar, D. G., Applications and Validations of the Minnesota Density Functionals. *Chem. Phys. Lett.* **2011,** *502*, 1-13.

23. Marenich, A. V.; Cramer, C. J.; Truhlar, D. G., Universal Solvation Model Based on Solute Electron Density and on a Continuum Model of the Solvent Defined by the Bulk Dielectric Constant and Atomic Surface Tensions. *J. Phys. Chem. B* **2009,** *113*, 6378-6396.

24. CYLView20; Legault, C. Y. Universitéde Sherbrooke, 2020 (http://www.cylview.org).